An exploration of the function of specific components of the predicted secretome of *Fusarium graminearum* during wheat infection

Submitted by

Ana Karla de Freitas Miranda Machado

to the University of Exeter as a thesis for the degree of Doctor of Philosophy in Biological Sciences, September 2017

I certify that all material in this thesis which is not my own work has been identified and that no material has previously been submitted and approved for the award of a degree by this or any other University.

Signature:

……

Abstract

Fusarium graminearum is a major fungal pathogen of wheat and other small grain cereal crops globally, causing Fusarium ear blight (FEB) disease. Like many other plant pathogens, *F. graminearum* (*Fg*) is predicted to produce *in planta* secreted effector proteins that modulate plant metabolism to suppress or re-programme plant defences. Understanding the molecular functions of *Fg* effectors will help to elucidate the processes underlying wheat spike colonisation and fungal pathogenicity. With the aim of identifying *Fg* effector proteins that can suppress host plant defences, I selected using next generation sequencing and bioinformatic analysis, a set of small secreted proteins (SSP) to express *in planta* using the *Barley stripe mosaic virus* over-expression system (BSMV-VOX). I then tested whether expression of any of these SSPs enhanced *Fg* fungal infection of susceptible wheat spikes.

Amongst the set of *Fg* SSP tested, *FgSSP8*, which encodes a ribonuclease protein, induced strong symptoms of necrosis in *N. benthamiana* leaves when infiltrated via the BSMV:FgSSP8. Three other genes tested (*FgSSP7, FgSSP6 and FgSSP5*) enhance FEB disease formation in the majority of the experiments when overexpressed in wheat ears prior to infecting with *F. graminearum.* FgSSP6 and FgSSP7 belong to the cerato-platanin protein (CPP) family. In several other plant pathogenic fungi, CPPs have been implicated in a number of virulence and plant protection mechanisms, including induction of host plant cell death, binding specific polymers and/or expansin-like activity. FgSSP5 encodes a protein that possesses the pfam domain RALF (Rapid alkalinisation factor; PF05498.6). RALF domain-containing proteins are predominately found in plants and play a role in plant development regulating tissue expansion and/or negatively regulating pollen tube elongation. BLAST analyses identified RALF

domain containing proteins in a restricted range of different pathogen species. Based on the VOX results and biochemical tests, our hypothesis is that pre-elevated cerato-platanins (FgSSP6 and FgSSP7) levels in the apoplast/surrounding the hyphae could initially shield the hyphae from detection by the plant, but late induce an intense defence response culminating in cell death to benefit the necrotrophic phase of *Fg* by increasing nutrient availability. FgSSP5 may be a specific virulence factor that manipulates a key plant process, by alkalinising the plant environment during infection, and hijacks the same plant receptor repertoire used to recognise plant proteins. Once the mechanisms are further understood, these genes/proteins could potentially be novel intervention targets either for conventional chemistries and/or for methods such as host-induced gene silencing to achieve FEB disease and/or mycotoxin control. The characterisation of single and double gene deletion *F. graminearum* mutants is in progress.

Acknowledgements

Firstly, I would like to express my sincere gratitude to my supervisor Prof. Kim Hammond-Kosack, for the continuous support of my PhD study and for her patience, motivation, immense knowledge and for receiving me so well as her PhD student. Her guidance helped all the time during the research and writing of this thesis. I have learnt so much during all this journey. I could not have imagined having a better supervisor and mentor for my PhD study.

I would like to specially thank Dr. Wing-Sham Lee (Sam). I could not have done what I did without her training, patient and guidance during this PhD. Sam – you have been an exceptional co-supervisor and I am very grateful for that. I also would like to thank Dr. Martin Urban, for his great advice and support since the beginning. I could not have achieved all this without Kim, Sam and Martin.

I would like to thank the rest of my thesis committee: Prof. Nick Talbot and Dr. David Studholme for receiving me as a PhD student in Exeter and for supporting me during these 4 years.

Great thanks also goes out to all past and present members of the Wheat Pathogenomics Team for the stimulating discussions and cooperation in the lab, specially to Dr. Jason Rudd and Dr. Graeme Kettles for the help with protein work, Dr. Robert King for his remarkable work and help with the bioinformatics and Mrs Kirstie Halsey and Dr. Smita Kurup for their bioimaging support.

Thank you all support staff for maintaining the controlled environment facilities, equipment and the reliable supply of everything needed for the experiments. I thank the Brazilian sponsor CAPES for funding my PhD during three years. I also

thank BSPP, BMS and The Genetics Society, for providing grants to support travelling to attending various national and international conferences and workshops.

To the Brazilian crew at Rothamsted, for all the fun we have had in the last four years and for make the homesickness a bit easier; my former flatmates, specially Byoung Min, for their friendly advice and support.

Last but not the least, I would like to thank my parents, my sisters and my grandparents for supporting me spiritually throughout writing this thesis and my life in general. In special, to my fiancée Nick, for all encouragement, understanding and care during this journey.

Table of Contents

List of Figures and Tables

List of Abbreviations

µg	microgram
µl	microlitre
µM	micromolar
µm	micrometre
15-ADON	15-acetyl-4-deoxynivalenol
2-DE	two-dimensional gel electrophoresis
3-ADON	3-acetyl-4-deoxynivalenol
AGO	argonaute
Avr	avirulence gene
Bas	biotrophy-associated secreted
BLAST	Basic Local Alignment Search Tool
bp	base pairs
BSMV	*Barley stripe mosaic virus*
C	celsius
CA	carrot agar
Cas9	CRISPR associated protein 9
cDNA	complementary DNA
CEBiP	chitin elicitor binding protein
CFEM	common in fungal extracellular membranes
cm	centimetre
CML	Colecao Micologica de Lavras
Col-0	Columbia - 0
CPP	cerato-platanin protein
CRISPR	clustered regularly interspaced short palindromic repeats
Cyp51	cytochrome P450 lanosterol C14α-demethylase
DMI	demethylation inhibitor
DNA	deoxyribonucleic acid
DON	deoxynivalenol
dpi	days post inoculation
DSB	a double-stranded break (DSB)
dsRNA	double-strand RNA
EBI	European Bioinformatics Institute
EC	Enzyme Commission
ENA	European Nucleotide Achieve
ETI	effector-triggered immunity
ETS	effector-triggered susceptibility

FAD	Fusarium – Arabidopsis Disease
FAO	Food Agriculture Organization of the United Nations
FEB	Fusarium Ear Blight
FFA	free fatty acid
Fg	*Fusarium graminearum*
FGSC	*Fusarium graminearum* species complex
FgSSP	*F. graminearum* small secreted protein
Fol	*Fusarium oxysporum f. sp. lycopersici*
GFP	green fluorescent protein
h	hours
hai	hours after inoculation
HIGS	host-induced gene silencing
HPLC	high-performance liquid chromatography
hrs	hours
HYG	hygromicin
kb	kilobase pairs
KEGG	Kyoto Encyclopedia of Genes and Genomes
LB	Lysogeny broth
LC	liquid chromatography
Ler-0	Landsberg *erecta* - 0
LIC	ligation-independent cloning
LysM	lysin motif
MALDI-TOF	matrix-assisted laser desorption/ionization time-of-flight
MAMP	microbe-associated molecular pattern
MAPK	mitogen-activated protein kinase
MCS	multiple cloning site
mg	milligram
min	minutes
MIPS	Munich Information Services for Protein Sequences
ml	millilitre
mM	millimolar
mm	millimetre
MPL	maximum permitted levels
MS	mass spectrometry
n	number
NADH	nicotinamide adenine dinucleotide (NAD) + hydrogen (H)
NCBI	National Center for Biotechnology Information
NGS	next-generation sequencing

NHEJ	non-homologous end joining (NHEJ)
NIV	nivalenol
nm	nanometres
NRRL	Northern Regional Research Laboratory
NX-2	3α-acetoxy-7α,15-dihydroxy-12,13-epoxytrichothec-9-ene
OA	oxalic acid
p	p value
PAMP	pathogen-associated molecular patterns
PCD	programmed cell death
PCR	polymerase chain reaction
PCWDE	plant cell wall-degrading enzymes
PDA	potato dextrose agar
PDB	potato dextrose broth
PEG	polyethylene glycol
PHI-base	Pathogen-Host Interactions database
PLEXdb	Plant Expression Database
ppm	parts per million
PRR	pattern recognition receptors
PTI	(MAMPs/PAMPs)-triggered immunity
q-PCR	quantitative-polymerase chain reaction
QTL	quantitative trait locus
R	resistance gene
RALF	rapid alkalinisation factor
RdRp	RNA-dependent RNA polymerase
REMI	restriction enzyme-mediated integration
RNA	ribonucleic acid
RNAi	RNA interference
RNA-seq	RNA sequencing
ROS	reactive oxygen species
RT-PCR	reverse transcription-polymerase chain reaction
SA	salicylic acid
sgRNA	single guide RNA
SIX	secreted in xylem proteins
SNA	synthetic nutrient-poor agar
SNARE	SNAP (soluble NSF attachment protein) receptor
SOD	superoxide dismutase
SSP	small secreted protein
TAFC	triacetylfusarinine C

Taq	*Thermus aquaticus* polymerase
TRI	trichothecene
USA	United States of America
UTR	Untranslated region
UV	ultraviolet
VIGS	virus-Induced Gene Silencing
VOX	virus-mediated overexpression
YPD	yeast peptone dextrose
ZEA	zearalenone

Chapter 1 – Introduction

1.1 The current scenario of cereals agriculture

Cereal grains are a great source of food, feed and energy. Wheat (*Triticum aestivum* L. ssp. *aestivum*) is the crop with the second biggest production worldwide after maize (*Zea mays* L.), where 733 million tonnes of wheat and durum wheat were produced in 2015 and 165 million tonnes were traded. From this production worldwide, the European Union contributed with 160 million tonnes of wheat grains (FAO, 2016).

Going forward into the future, improvement of wheat yield is necessary. In 2016/2017 the wheat production is projected to expand by 1.7%, to 742 million tonnes, however, looking at the forecasts, a decrease in production is expected in China and the European Union (FAO, 2016). Figure 1.1 shows a graph comparing the total wheat production and its domestic utilisation. It is noticeable how the production is growing, but with some reductions in certain seasons over 16 years, while the global consumption is mostly growing exponentially. The lower production years coincide mainly with reports of severe wheat disease epidemics in some parts of the world and also with weather phenomena El Niño and La Niña, which affect mainly the South hemisphere and the pacific coast. These two weather phenomena often contribute to the emergence of diseases due to higher precipitation regime and changes in temperature (Coakley et al., 1999, Chakraborty et al., 2000).

By 2050 the world's population is predicted to reach 9.1 billion, 34 percent higher than today and food production must therefore increase by 70 percent to sustain the human population (FAO, 2009). It is predicted that cereal production will need to rise to about 3 billion tonnes from 2.5 billion today.

Over the last decade, direct yield losses caused by pathogens, pests, animals and weeds, are altogether responsible for losses ranging between 20 and 40 % of global agricultural productivity (Savary et al., 2012, Oerke, 2006). Oerke and Dehne (1997) suggested that the global average of actual yield losses caused by all wheat diseases, including developed and developing countries, was about 12.4% on an annual basis. Although crop losses caused by plant disease directly affect food availability, they also affect other components (e.g. food utilisation – nutritive value, safety) directly or indirectly through the fabrics of trade, policies and societies (Zadoks, 2008).

Ways to minimise the gap between actual and attainable yields and increase food availability is by finding new strategies to control diseases, and also knowing the pathogens, their ecology, distribution, virulence patterns, and variability (Duveiller et al., 2012). Disease epidemics result from the combination of available inoculum, favourable environment, and host susceptibility (the disease triangle) (Agrios, 2005). Some economically important wheat diseases are shown in figure 1.2 and described in table 1.1

Amongst the important diseases in cereal crops, especially for wheat, is Fusarium ear blight (FEB). FEB is a main concern in the warm humid and semi-humid wheat areas where the flowering stage coincides with rainy periods. This disease is caused by several species of fungi of the genus *Fusarium*, where the most important species globally is *Fusarium graminearum* (teleomorph: *Gibberella zeae*) (Bottalico & Perrone, 2002).

Changes in cropping systems due to current increases in temperature may have serious implications in some pathogens, including those responsible for FEB (Dweba et al., 2017). In the last decade, major FEB outbreaks causing significant economic and yield losses have occurred (Kriel & Pretorius, 2008, McMullen et al.,

2012, Salgado et al., 2015). Therefore, an effective control of FEB disease is a high priority in all the major wheat-growing regions of the world and understanding the mechanisms that drive the infection is essential to the development of new alternative control strategies.

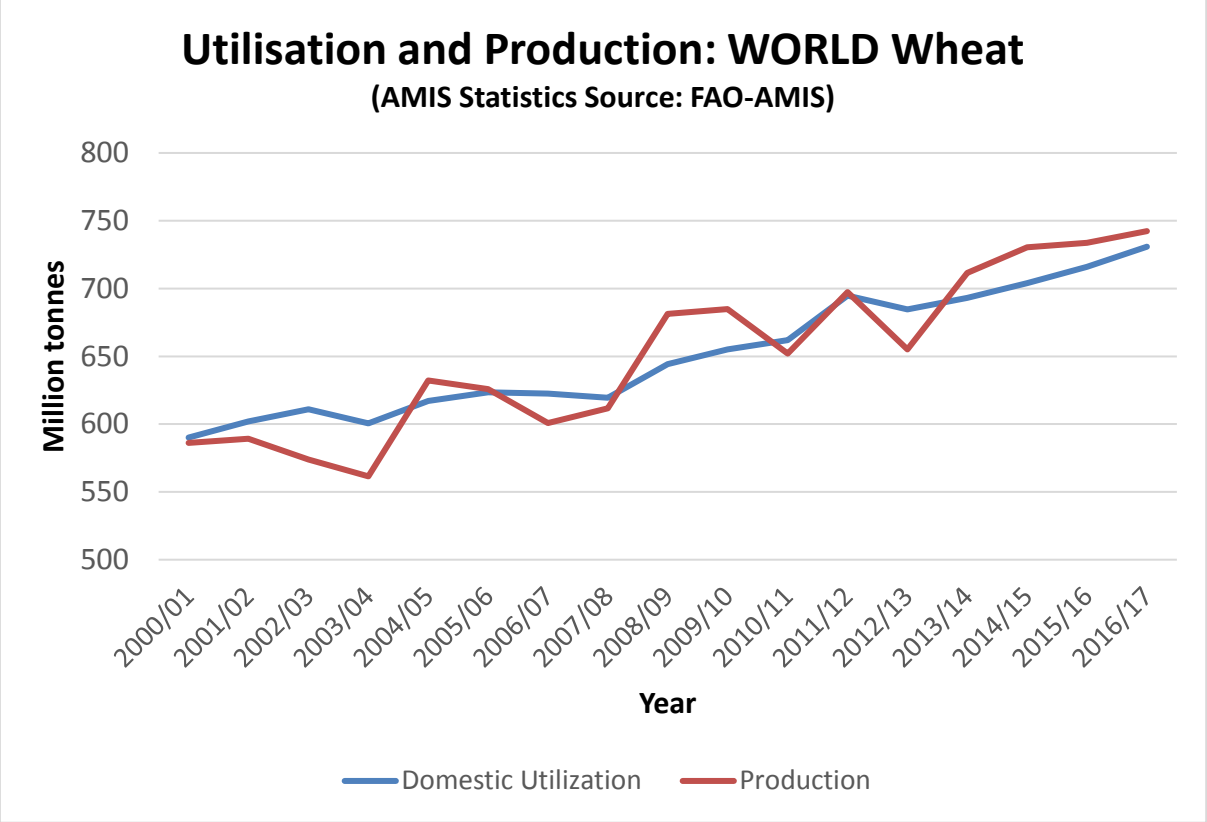

Figure 1.1 World wheat production and domestic utilisation.
(Source: http://www.fao.org/worldfoodsituation/csdb/en/)

Figure 1.2 Wheat fungal diseases. a) Take-all patches; b) yellow rust on leaves; c) Septoria leaf blotch; d) FEB in floral tissues. Photographs courtesy of Rothamsted Image database.

Table 1.1 Some economically important wheat diseases

Disease	Pathogen	Primary symptoms
Stem Rust (black rust)	*Puccinia graminis f.sp. tritici*	Pustules are dark reddish brown, and may occur on both sides of the leaves, on the stems, and on the spikes
Leaf Rust (brown rust)	*Puccinia recondita*	Pustules are circular or slightly elliptical and contain masses of orange to orange-brown urediospore. Found on the upper surfaces of leaves and leaf sheaths.
Stripe Rust (yellow rust)	*Puccinia striiformis*	Pustules contain yellow to orange-yellow urediospores, usually form narrow stripes on the leaves

Loose Smut	*Ustilago tritici*	Smut-infected heads appear earlier than normal ones and a loose, dark-coloured spore mass replaces the seed in the head.
Powdery mildew	*Blumeria graminis var. tritici*	Greyish white powdery growth appears on the leave, sheath, stem and floral parts
Leaf Blotch	*Zymoseptoria tritici*	Irregular reddish-brown spots scattered over the leaf blade. The spots, often with ashen white centres, contain many black specks (the pycnidia).
Glume Blotch	*Stagonospora (Septoria) nodorum*	Usually first noticeable on the lower leaves as small oblong lesions which are light brown with dark borders.
Tan Spot	*Pyrenophora tritici-repentis*	Present on both upper and lower leaf surfaces. At first, lesions appear as tan to brown flecks, which expand into large, irregular, oval- or lens-shaped tan blotches with a yellow or chlorotic margin.
Ear (Head) Blight or Scab	*Fusarium spp.*	Premature death or blighting of spikelets of the ear. Grain from head-blighted fields can contain sufficient mycotoxins to induce muscle spasms and vomiting in humans and certain animals.
Take-All	*Gaeumannomyces graminis var tritici*	This fungus causes rotting of the roots and lower stems. Basal stem and leaf sheath tissues, as well as roots, may turn a shiny black colour. Severely infected plants appear stunted and fail to produce any grain

1.2 Fusarium ear blight and its impact in cereal farming

Fusarium Ear Blight (FEB) is a disease that causes significant yield losses and reduces grain quality and safety in a number of cereal crops worldwide, such as wheat, barley, maize and oat. FEB was first described in England by W. G. Smith in 1884, and few years later F.D. Chester reported this disease in the United States in 1890. After these first reports, between 1910 and 1930, five major FEB epidemics events occurred in the USA (Stack, 2003). Probably due a combination of advantageous events, FEB has re-emerged in the 1980s and since then, various

epidemics events have occurred more frequently in the USA and elsewhere. These events include favourable weather conditions (warm, wet and humid) and also changes in culture practices, for example the widespread adoption of non-tillage, which may increase the inoculum availability (Shaner, 2003). West et al. (2012) developed a weather-based model with UK data and suggested that climate change affected directly the increase of FEB disease. The overall reduction to wheat crop height combined with increased compactness of the ear in high yielding genotypes have also provided more favourable conditions for FEB (Parry et al., 1995).

FEB disease is caused mainly by the ascomycete fungus *Fusarium graminearum* (Bottalico, 1998, Bottalico & Perrone, 2002, Parry et al., 1995), but also to less extent by other species within the *Fusarium* genus such as *F. culmorum*, *F. pseudograminearium*, *F. avenaceum*, *F. poae*, and more minor species belonging to a specific *F. graminearum* species complex (FGSC) found in a particular geographic region (van der Lee et al., 2015).

In the USA, yield losses due to Fusarium ear blight have been estimated at US $3 billion between the early 1990s and 2005 (Schumann & D'Arcy, 2006). In Canada, between 1993 and 1998, the losses caused also by FEB were measured in US $500 million (Gilbert & Haber, 2013).

Recurrent FEB epidemics frequently occur in the developing world. In China, the FEB is endemic in the middle-to-lower basins of the Yangtze and Huaihe Rivers. Between 1991 and 2007, two severe and seven moderate epidemics of FEB occurred in this region. In 2008, more than 95% of the wheat harvested in some Chinese provinces was contaminated with mycotoxins (Ji et al., 2014, Xiong et al., 2009). FEB is also present in parts of South America (Argentina, Brazil, Uruguay). In south of Brazil, where 90% of Brazilian wheat is grown (Del Ponte et al., 2009), average damage caused by this disease between 2000 and

2010 was 21.6%, ranging from 11.6% in 2006 up to 39.8% in 2007 (Reis & Carmona, 2013).

Climate changes may have favoured the occurrence of several epidemic years in some producing regions. For example, in South Asia, wheat flowering coincides with low relative humidity conditions and FEB is found only sporadically in the Himalayan foothills and in Bangladesh (Duveiller, 2004). However, changes of the rainfall patterns, as shown in 2005, in parts of the Punjab (India) led to a dramatic increase of FEB incidence, particularly in durum wheat (Duveiller et al., 2007).

1.3 Mycotoxins

F. graminearum as well as other species of Fusarium infecting cereals also produce trichothecene mycotoxins, including deoxynivalenol (commonly known as DON) and its acetylated forms 3-acetyl-4-deoxynivalenol (3-ADON) and 15-acetyl-4-deoxynivalenol (15-ADON), nivalenol (NIV) and zearalenone (ZEA) (Desjardins & Proctor, 2007) (Figure 1.3). These mycotoxins are also a major concern in infected grains. Once consumed, mycotoxins can be harmful to human and animal health. In addition, the mycotoxins can persist during storage and are heat resistant (Magan et al., 2010).

Recent studies have showed that environmental conditions and ecological factors can influence the population dynamics of 3-ADON and 15-ADON phenotypes (Foroud et al., 2012, Gilbert et al., 2014, Ward et al., 2008). For example, prior to 1998, 15-ADON chemotype was considered the only significant cause of FEB in North America (Foroud et al., 2012). Between 1998 and 2004, 3-ADON chemotype frequency increased more than 14-fold in western Canada, suggesting the more toxigenic 3-ADON chemotype has been replacing the dominant 15-ADON population in this region.

To protect consumers from mycotoxicosis many countries, including the European Union Member States have established maximum permitted levels (MPLs) for the most prevalent Fusarium mycotoxins in cereals and cereal products (van Egmond et al., 2007). DON has a major importance due the great number of reports of its occurrence in wheat grain at high concentrations.

The MPLs for DON concentration in wheat and grain products vary among countries (Table 1.2). Depending on the end use, processor may require a lower limit at intake than the legal limit for unprocessed cereals to ensure finished products conform to legal limits. For example, the EU regulation allows a maximum DON content in unprocessed bread wheat of 1.25 ppm, in bread and bakeries of 0.5 ppm and in baby food of 0.2 ppm (van Egmond et al., 2007). This scenario is absent in many countries, where the regulations for toxin content are not enforced and many people are likely to eat contaminated grains.

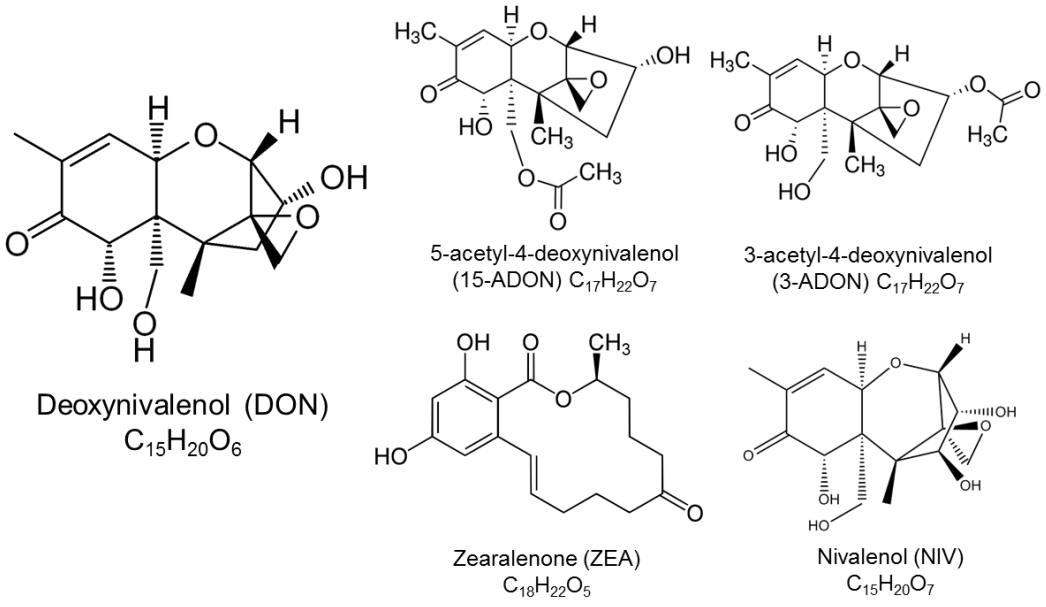

Figure 1.3 Chemical structures of the mycotoxins: DON, 3-ADON, 15-ADON, ZEA and NIV.

Table 1.2 Legal limits for mycotoxins (ppb) in grain intended for human consumption in various countries

Country	Product type[a]	Deoxynivalenol (DON) (µg/kg)
European Union[b]	Unprocessed wheat and barley	1,250
	Finished products	200-750
United States of America	Unprocessed wheat	2,000
	Processed wheat	1,000
Russia	Finished products	700
Canada	Unprocessed wheat	2,000
	Processed wheat	1,000
China	Processed wheat	1,000
Japan [c]	Wheat	1,100
India [c]	Wheat	1,000
Brazil	Unprocessed wheat	1,000
	Processed wheat	750

Sources: Agricultural and Horticulture Development Board Cereals and Oilseeds (https://cereals.ahdb.org.uk), U.S. Wheat and Barley Scab Initiative (http://scabusa.org), Anvisa (http://portal.anvisa.gov.br)

[a] Unprocessed wheat include grains and flours

[b] There is variation in the maximum permitted levels (MPLs) among countries within EU.

[c] There is no discrimination between unprocessed and processed wheat.

1.4 Available strategies to control Fusarium ear blight

Several strategies to control FEB in small grain production have been adopted. These strategies should be used in an integrated way and choice of best practices depends on environmental conditions. The methods used to try to control FEB include cultural practices, irrigation management, chemical control and genetic resistance.

The usage of tillage to bury crop residues and crop rotation with non-host species has been shown to reduce FEB intensity and DON accumulation (Dill-Macky & Jones, 2000, Schaafsma et al., 2005, Wegulo et al., 2015). A study carried out between 1995 and 1997 investigated that FEB incidence and severity was lower on moldboard ploughed plots than in chisel ploughed and no-till treatments. The same

study also verified that DON content of harvest grain in soybean-what rotation was 25% lower than wheat-wheat rotation and 49% lower than corn-wheat rotation (Dill-Macky & Jones, 2000). Schaafsma et al. (2005) showed that fields where corn was cultivated one year before to wheat with no tillage have the highest values of FEB index, DON accumulation and percentage of seeds infected with *F. graminearum.*

Another important factor that benefits FEB development and DON accumulation is moisture. When a wheat field is managed under irrigation system, irrigation management to prevent excessive moisture, mainly before, during and after anthesis can lower the risk of FEB infection. Lower percentage of kernels infected with *F. graminearum* was reduced when post-anthesis mist durations were for 0 or 10 days compared to 20 or 30 days (Cowger et al., 2009).

Choice of cultivars with agronomics traits unfavourable to FEB development can increase the chances of controlling FEB when used together with other management strategies (Wegulo et al., 2015). As the majority of FEB infections occur during flowering (Siou et al., 2014), cleistogamous (closed flowering) cultivars have been shown to have a lower risk of FEB infection than chasmogamous (opened flowering) ones (Kubo et al., 2010). Another trait that has been suggested as one of the resistance mechanisms to FEB in wheat is anther extrusion. Somes studies have showed cultivars that more anthers were retained, presented greater FEB susceptibility (Graham & Browne, 2009, Skinnes et al., 2010). Other studies suggested that shorter plants are more severely affected by FEB than taller plants (Buerstmayr & Lemmens, 2015, Mesterhazy, 1995).

So far, the most-cost effective strategy to control FEB has been genetic resistance (Wegulo et al., 2015). However, developing good resistance to FEB and minimising DON accumulation has been quite complex and slow, and in most cases resistance has been shown to be inherited in a quantitative manner. To date, only a

few cultivars appear to be moderately resistant (Gilbert & Haber, 2013). Resistance to FEB can be classified in five types: resistance to initial infection (type I), resistance to FEB spread in the host (type II), kernel size and number retention (type III), yield tolerance (type IV), and resistance to accumulation of mycotoxins (type V) (Mesterhazy, 1995, Schroeder & Christensen, 1963, Wegulo et al., 2015).

For plant breeders, the two most important types of resistance are type I and type II and some authors mention only those to classify FEB resistance (Cuthbert et al., 2006, Kubo et al., 2010, Niwa et al., 2014). Resistance type I is rarely present in cultivars and remains poorly understood, mainly because of the difficulties in screening and low frequency for this type of resistance (McMullen et al., 2012). Type II resistance is the most commonly used and a notable source of the resistance is the Chinese wheat cultivar Sumai-3. Analysis of alleles at QTL responsible for FEB resistance in Sumai-3 are located in chromosomes 3BS, 5AS and 6B (Anderson et al., 2001, Cuthbert et al. 2006). The locus on 3BS has the strongest effect on type 2 resistance, which has been named *Fhb1* (Cuthbert et al., 2006) and accordingly has been incorporated into many commercial cultivars which exhibit moderate FEB resistance. Previous study has suggested that *Fhb1* locus either encodes a DON-glucosyltransferase or regulates the expression this enzyme, which converts DON to DON-3-O-glucoside as the detoxification product. However, the specific gene (s) in *Fhb1* containing lines that is responsible for DON modification remains unknown (Lemmens et al., 2005). Additionally, recent findings have shown that there is a single gene in *Fhb1* locus that plays a major role that confers resistance to FEB. This gene encodes a pore-forming toxin-like (PFT) protein and its exact function is still unknown, but the authors demonstrated that the DON-detoxification-controlling locus is independent of *PFT,* although both are located nearby in the same genetic block (Rawat et al., 2016). The QTL on 5A (Qfhs.ifa-5A) derived from ‘Sumai-3’ appears to

be associated with resistance to fungal penetration conferring type 1 resistance rather than type 2 resistance (Buerstmayr et al., 2003). On chromosome 6BS, FEB field resistance is controlled by one gene, named *Fhb2*. The resistant allele on 6BS reduced FEB in greenhouse tests by 56% compared to lines carrying the susceptible allele (Cuthbert et al., 2007). About 20 years ago, several breeding programmes around the world started to develop cultivars partially resistance to FEB (Wegulo et al., 2015). When these programmes started, breeders and politicians had assumed the use of resistant cultivars would solve the problem of FEB by now, however this has proven not to be the case. Resistance mechanisms can be affected by the amount of initial inoculum and, mainly, by weather conditions. For example, type 2 resistance is not very effective in geographical regions where inoculum levels are continually high and where the weather conditions are optimal for infection. Therefore, other management strategies should be used with resistant cultivars to control moderate to severe FEB epidemics (McMullen et al., 2012).

Another strategy available for management of FEB is application of fungicides. The most common class of fungicide used for this purpose is the sterol demethylation inhibitor (DMI) (McMullen et al., 2012), which include the triazoles. DMI fungicides inhibit ergosterol biosynthesis by binding to the fungal cytochrome P450 lanosterol C-14α-demethylase (CYP51), which plays an essential role in mediating membrane permeability (Lepesheva & Waterman, 2007). Two studies using multivariate random-effects meta-analyses model tested the efficiency of five fungicides treatments to reduce FEB infection and DON accumulation. All fungicides tested increased grain yield, however metconazole, prothioconazole+tebuconazole, and prothioconazole had more effect to suppress FEB than tebuconazole and propiconazole (Seong et al., 2008a, Paul et al., 2010). On the other hand, fungicides belonging to the quinone inhibitor (QoI) class, also known as strobirulins are not

recommended for FEB. Application of stroburilins at early growth stages has been shown to increase DON content (Ellner, 2005).

Although DMI class of fungicides appears to reduce FEB infection, it is usually impossible to achieve complete control. This happens mainly because fungicide application must be done around the flowering period, when the susceptibility to FEB is highest. However, in large cereal fields, it is difficult to have all plants flowering evenly and multiple applications might be necessary, which may not be profitable for some farmers (Wegulo et al., 2015).

Another reason for the lack of consistency in fungicide effectiveness is the period of symptomless infection of FEB, where no visible blight is observed, but the infection has been already established. Therefore, application of fungicides at this stage will be too late to prevent disease (Brown et al., 2010).

Recently, a tebuconazole-resistant *F. graminearum* strain was discovered in the USA which was highly aggressive and toxigenic. This could be an indication that populations less sensitive to triazole fungicides are emerging (Spolti et al., 2014).

It is widely accepted that complete control of losses due to FEB is unlikely at the moment (Dean et al., 2012, Gilbert & Haber, 2013, McMullen et al., 2012, Wegulo et al., 2015). Therefore, combined efforts are needed to develop new strategies for more effective management of FEB in the future.

1.5 *F. graminearum* infection process in susceptible wheat genotypes

1.5.1 Infection cycle

Fusarium ear blight is a monocyclic disease, occurring only once during the cropping season. The infection of wheat ears is initiated during the period of anthesis, which usually occurs within a 14-day window. The fungus can grow saprophytically on

crop stubble and usually spores are disseminated through rain splash or wind. Sexual structures, called perithecia, are also observed on *F. graminearum* infected crop stubble and the ascospores can be discharged into the air (Trail & Common, 2000, Urban & Hammond-Kosack, 2013).

To infect floral tissues, the fungus initially colonises saprophytically the senescing anthers, which provide an easy source of nutrition and stimulating growth factors for disease establishment (Parry et al., 1995). Appressorium formation is not observed during infection, however, swollen structures during hyphal tip invasion have sometimes been reported (Boenisch & Schafer, 2011, Jansen et al., 2005).

Visible symptoms first appear as dark-brown spots on the glumes of infected florets. Later, entire florets become blighted, bleached and are pale brown (Brown et al., 2010, Brown et al., 2011). Infected florets often fail to produce grain, or the grain produced is poorly filled (Urban & Hammond-Kosack, 2013). Under favourable conditions in the field, the formation of asexual spores is observed at the base of bleached spikelets, resulting in the appearance of pink disease symptoms. *F. graminearum* is homothallic and black perithecia containing the sexual ascospores can also be observed in the field on fully colonised wheat ear, hence the preferred disease name in the USA Fusarium head scab. Probably due the unfavourable climatic conditions, the sexual stage is not observed in some regions, for example northwest Europe. To propagate the disease, vegetative conidial heaps as well as perithecia with ascospores can form on infected wheat ears and crop stubble. Between crops, chlamydospores and mycelia guarantee the fungal survival in the soil (Dweba et al., 2017).

1.5.2 Symptomless floral infection

During the initial phase of infection of wheat plants by *F. graminearum*, most of the wheat ear appears to be healthy at first; however, *F. graminearum* is able to establish, within the first few days of infection, a high density of both intercellular and intracellular hyphae in the spikelet and rachis tissues, resulting in a symptomless phase (Figure 1.4). For example, at 5 days' post infection of a susceptible wheat genotype, the wheat ear appears healthy, however a third of the ear may already be colonised (Brown, 2011, Brown et al., 2010). Initially the *F. graminearum* hyphae colonise the intercellular space between living wheat cells, indicating a latent period between initial infection and the onset of visible symptoms. Later, the phloem, xylem and other cell types are invaded by intracellular hyphae and the entire loss of the host cell contents. Both inter- and intracellular hyphae become abundant leading to a collapse of the host cells. At this later stage, hyphal diameters were considerably enlarged compared to those leading to the infection front. When the ear is visibly diseased, the pathogen grows predominately sideward (outwards) and accumulates below the surface of the rachis. At this point, the lignified host cell has been broken down and aerial mycelium production occurs through the epidermis rupture (Brown et al., 2010). *F. graminearum* infection progress is represented in figure 1.5.

When in association with plant tissue, *F. graminearum* hyphae can produce several different B-type trichothecene mycotoxins, including deoxynivalenol (DON), nivalenol (NIV) and the acetylated derivatives 3-acetyl and 15-acetyl deoxynivalenol (3-ADON and 15-ADON) (Hohn et al., 1998). The mycotoxin DON binds to the ribosome peptidyltransferase and inhibits protein translation (Sobrova et al., 2010). At least ten of the fifteen trichothecene biosynthesis genes are located in a single gene cluster named the trichothecene (*TRI*) gene cluster (Kimura et al., 2003).

Expression data from wheat rachis internodes inoculated with *F. graminearum* at 5 and 7 days' post inoculation shows that the *Tri* genes are upregulated in the symptomless phase of infection, reinforcing the importance of mycotoxin production for the establishment of the disease (Brown et al., 2011, Brown et al., 2010).

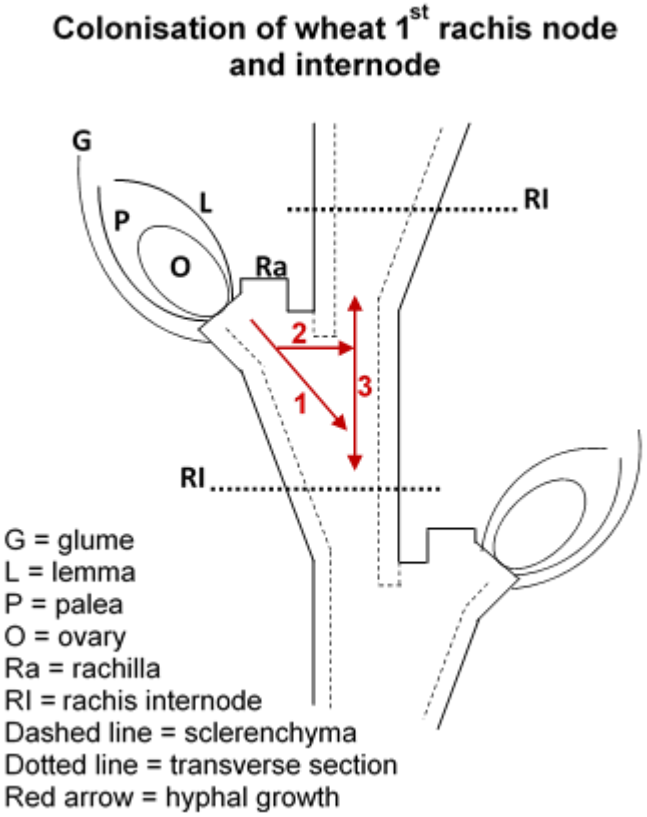

Figure 1.4 A schematic illustration of the anatomy of the wheat ear and the path of fungal infection, from the inoculated spikelet to the neighbouring spikelet. Legend: red arrow = overall direction of fungal infection, red number = stage of fungal infection described in this study. 1, vertical inter- and intracellular hyphal growth in the cortex and vasculature, down from the inoculated spikelet into the rachis. 2, lateral intracellular hyphal growth through the sclerenchyma into the rachis. 3, vertical hyphal growth up and down the rachis, intercellular colonisation of the cortex followed by intracellular colonisation of the cortex and vasculature. Adapted from Brown et al. (2010).

Figure 1.5 The macroscopic symptoms of *Fusarium graminearum* infection at 2, 6, 10 and 12 dpi following the addition of conidia into two adjacent spikelets in the middle of the ear. The black dot marking indicates each of the two inoculated spikelets. Adapted from Brown et al. (2010).

1.6 Molecular genetics of *F. graminearum* pathogenicity

1.6.1 The role of mycotoxins during virulence

Several species of *Fusarium* are known for producing trichothecenes mycotoxins. Those include *F. poae, F. sporotrichioides, F. culmorum* and *F. graminearum*. All trichothecenes-producing *Fusarium* species are destructive pathogens that can attack a wide range of plant species. In *F. graminearum*, trichothecenes are also required for the pathogenicity of specific plant hosts and tissue types. According to their structure, trichothecenes can be sub-classified into two groups: type A and type B. Type-B trichothecenes mycotoxin can be produced by *F. graminearum*, and these include deoxynivalenol (DON), nivalenol (NIV) and the acetylated derivatives 3-acetyl and 15-acetyl deoxynivalenol (3-ADON and 15-ADON) (Hohn et al., 1998). In *F. graminearum* genome, most of the genes

that participate of trichothecenes biosynthesis are found in a cluster of approximately 25 kb, named trichothecene (*TRI*) gene cluster. Allelic variation of *Tri13* and *Tri7* are associated with production of the trichothecene nivalenol (Lee et al., 2002). The structural variation in DON is attributed to DNA sequence differences in the coding region of the trichothecene biosynthetic gene *Tri8* (Alexander et al., 2011). Type A includes T-2 toxin neosolaniol, and diacetoxyscirpenol. Until 2015, type A mycotoxin had not been identified in *F. graminearum,* however, Varga et al. (2015) identified several strains in North America which produced none of the known trichothecene mycotoxins despite causing normal disease symptoms. Genetic analysis revealed a different *Tri1* allele is associated with the production of the alternative type A trichothecene NX-2.

These mycotoxins are extremely potent inhibitors of eukaryotic protein synthesis; different trichothecenes interfere with initiation, elongation, and termination stages (Cundliffe et al., 1974). Trichothecenes mycotoxins have also been shown to be required for full virulence of *F. graminearum* on wheat spikes. Whereas DON is not required for full virulence in barley, maize and Arabidopsis floral tissue (Cuzick et al., 2008, Harris et al., 1999, Proctor et al., 1995), while mutants derived from the NIV-producing strain caused less disease in maize, but did not affect *F. graminearum* infection on barley (Maier et al., 2006).

DON biosynthesis requires ~15 biochemical steps (Desjardins & Proctor, 2007). The initial committing step into the trichothecene biosynthetic pathway is catalysed by the enzyme trichodiene synthase encoded by the *Tri5* gene (Hohn et al., 1998, Proctor et al., 1995, Tag et al., 2000). The role of DON during *F. graminearum* infection in wheat was primarily determined by using a *tri5*-deficient mutant that was a non-DON producer. This mutant is able to cause only discrete eye-shaped lesions on spikelets and is unable to infect the rachis (Cuzick et al.,

2008, Jansen et al., 2005). Two wheat pathogens *Microdochium nivale* and *Fusarium poae* also cause similar eye-shaped lesion symptoms when infecting wheat. *M. nivale* is known as a non-mycotoxin producer and *F. poae* produce several mycotoxins, but is not clear why this species also produces similar symptoms to the *F. graminearum tri5* mutant (Jennings et al., 2003). These eye-shaped lesion can be defined as a central bleached lesion developed on the glumes that appear to show reduced chlorophyll content. It has been suggested that this tissue could be more susceptible to *Fusarium* attack (Cuzick et al., 2008).

DON also seems to induce production of reactive oxygen species (ROS), commonly known to be both signalling molecules and defence molecules in plants. This could lead to stimulation of programmed cell death, contributing to *F. graminearum* necrotrophic fungal growth (Desmond et al., 2008).

In addition to *tri5*, six other genes in the cluster encode biosynthetic enzymes (Alexander et al., 1998, Brown et al., 2001, Brown et al., 2002, McCormick & Alexander, 2002). Two genes encode regulatory proteins (Tri6 and Tri10) and an additional gene*, tri12*, encodes an efflux pump that functions to export the toxin outside the cell as a mean of self-protection (Alexander et al., 1999, Alkhayyat & Yu, 2014, Tag et al., 2000). The distribution of *tri* genes in *F. graminearum* genome is represented in figure 1.6.

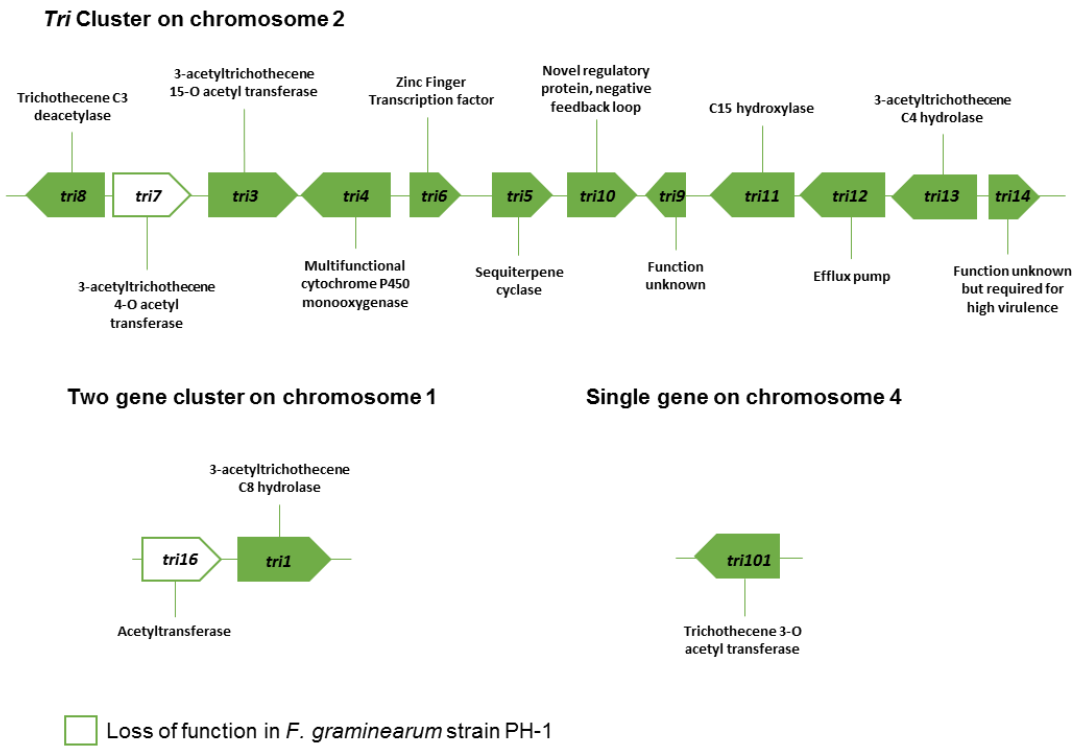

Figure 1.6 Trichothecene biosynthesis gene function and organisation in *F. graminearum.* Adapted from Brown (2011)

1.6.2 Other *F. graminearum* genes experimentally proven to contribute to virulence

Besides the *Tri* genes, numerous other genes have been described to play an important role on *F. graminearum* pathogenicity or virulence in different hosts. The Pathogen-Host Interactions database (PHI-base) (http://www.phi-base.org) (King et al., 2017b) provides a list of *F. graminearum* genes, as well as genes from ~ 260 other pathogenic species, that participate of host-pathogen interaction. The 4.3 database release (1st May 2017) gives details on a total of 185 virulence genes and 9 pathogenicity genes for *F. graminearum* that were experimentally verified in one or more pathosystem. Amongst the pathways and mechanisms responsible for loss of pathogenicity, a high proportion comprises either deletion or disruption of genes responsible for signal transduction

mechanism, including the three mitogen-activated protein kinase signalling cascades. This is mainly because these MAP kinases are involved in regulating several cellular functions and vital physiological activities (Jenczmionka & Schafer, 2005, Ramamoorthy et al., 2007, Urban et al., 2003). For example, the Gpmk1/Map1 regulates the early induction of extracellular endoglucanase, xylanolytic, and proteolytic activities. The fungus uses these enzymes to facilitate the breakdown of plant cell wall and hence to gain access to sources of nutrition. Therefore, *Gpmk1* gene disruption strongly compromised *F. graminearum* pathogenicity (Jenczmionka & Schafer, 2005, Urban et al., 2003).

Several membrane transport events have also been shown to be associated with pathogenicity in *F. graminaerum*. Zhang et al. (2016b) showed that the SNARE homologue protein FgVam7 plays a regulatory role in cellular differentiation and virulence in *F. graminearum. Vam7*-deficient mutant reduced fungal growth, sexual reproduction and virulence. SNAREs (Soluble N-ethylmaleimide-sensitive factor activating protein receptor) are membrane proteins sharing a conserved protein motif called SNARE domain. They are key components that mediate vesicle fusion (Bassham et al., 2008, Burri & Lithgow, 2004). Vam7 proteins, in several fungi species contain a PhoX homology (PX) domain and a SNARE domain, and are required for vacuolar morphology and endocytosis (Burri & Lithgow, 2004, Zhang et al., 2016b)

Table 1.3 proves a list of some of the genes included in PHI-base that affect *F. graminearum* virulence in different hosts. The genes are grouped according to their main function (modified from Urban and Hammond-Kosack (2013).

Table 1.3 Virulence genes characterised in *F. graminearum* (modified from Urban and Hammond-Kosack (2013))

FGRRES ID♦	Gene name	Protein function	Cereal hosts ‡	PHI-base ID†
Cellular communication / Signal transduction mechanism				
FGRRES_01665	*FSR1*	Putative signalling scaffold protein	B, M, W	PHI:731, PHI:1628
FGRRES_00332	*FTL1 (TBL1)*	*S. cerevisiae SIF2* (Transducin beta-subunit)	W, M	PHI:446; PHI:2348
FGRRES_09614	*GPA2*	Guanine nucleotide-binding protein alpha-3 subunit	B	PHI:1013
FGRRES_04104	*GPB1*	Guanine nucleotide-binding protein beta subunit	B	PHI:1015
FGRRES_09612	*HOG1/OS2*	*S. cerevisiae HOG1* (Osmotic stress MAPK)	W	PHI:1005
FGRRES_06385	*MAP1(GPMK1)*	*S.cerevisiae KSS1/FUS3* (mating/filamentation MAPK)	W	PHI:1189, PHI:5479
FGRRES_10313	*MGV1*	*S. cerevisiae SLT2* (Cell integrity MAPK)	W	PHI:1196
FGRRES_10114	*RAS2*	Ras GTPase	W, M	PHI:861
FGRRES_09897	*SNF1*	Sucrose nonfermenting protein kinase	B, W	PHI:1197, PHI:3862
FGRRES_16491	*STE11*	MAPKKK; hypersensitive to MsDEF1	W	PHI:1016
FGRRES_09903	*STE7*	MAPKK; hypersensitive to MsDEF1	W	PHI:1004, PHI:3377, PHI:1179
FGRRES_04982	*TEP1*	Tensin-like phosphatase 1 Phosphatidylinositol-3 kinase signalling	WC, W	PHI:2502, PHI:2325
Metabolism				
FGRRES_02506	*ADE5*	Phosphoribosylamine-glycine ligase	B	PHI:744
FGRRES_01939	*ARG2*	Acetylglutamate synthase	B	PHI:743
FGRRES_01932	*CBL1*	Cystathionine beta-lyase	W, M	PHI:443
FGRRES_05906	*FGL1*	Secreted lipase	W, M	PHI:432, PHI: 4212

FGRRES_05955	*GCS1*	Glycosylceramide synthase (sphingolipid biosynthesis)	W, M	PHI:1002
FGRRES_05658	*GzmetE*	Homoserine O-acetyltransferase	B, M	PHI:355
FGRRES_09197	*HMR1*	3-hydroxy-3-methylglutaryl-coenzyme A reductase involved in isoprenoid biosynthesis	W	PHI:1006
FGRRES_10825	*MSY1*	Methionine synthase	W, M	PHI:442
FGRRES_05593	*MT2*	Sphingolipid C-9- methyltransferase	W	PHI:2409
FGRRES_05371	*SID1*	Siderophore biosynthetic gene	W	PHI:1010
FGRRES_02549	Transposon mutant	Putative phosphoglycerate mutase family	W	PHI:1089
Energy				
FGRRES_12857_8_M	*ACL1*	ATP citrate lyase	W	PHI:2386
FGRRES_06039	*ACL2*	ATP citrate lyase	W	PHI:2387
FGRRES_00376	*NOS1*	NADH:Ubiquinone oxidoreductase	W, M	PHI:445
Protein fate				
FGRRES_10740	*ATG8*	Autophagic death protein	W, B	L. Josefsen and H. Giese, pers. comm.
FGRRES_02095	*FBP1*	F-box protein involved in ubiquitin-mediated degradation	B	PHI:733
Biogenesis of cellular components				
FGRRES_16005	*CHS2*	Chitin synthase 2	W	PHI:4661
FGRRES_10116	*CHS7*	Chitin synthase 3b	W, WC	PHI:4660
Interaction with the environment				
FGRRES_12970_M	*PAC-C*^{c}	Cys_2His_2 zinc finger transcription repressor	W	PHI:1431
FGRRES_01974	none designated	Similar to HET-C2 glycolipid transfer protein	W	PHI:1097

FGRRES_11955	*VE1*	Light-responding activator *velvet1*	W	PHI:2349
Cell transport, transport facilities and transport routes				
FGRRES_00950_M	*SYN1*	SNARE protein (transport docking and vesicle fusion)	B	PHI:2395
FGRRES_09928	*SYN2*	SNARE protein (transport docking and vesicle fusion)	B	PHI:2396
FGRRES_06629	FgVam7	Regulatory role in cellular differentiation and virulence	W	PHI:4865
FGRRES_00416	none designated	Putative major facilitator superfamily	W	PHI:1086
Cell cycle				
FGRRES_04355	*CID1*	Cyclin-C-like gene required for infection and DON production	W, M	PHI:2419, PHI:2418
Transcription and DNA modification				
FGRRES_01353	*HDF1*	*S. cerevisiae HOS2* *(*Class II histone deacetylase)	W, M	PHI:1168
FGRRES_04324	*HDF2*	*S. cerevisiae HDA1* (Class II histone deacetylase)	W, M	PHI:1169
FGRRES_10129	*STUA*	APSES transcription factor	W	PHI:1295, PHI:1290
FGRRES_06874	*TOP1*	Topoisomerase 1	W	PHI:1291
FGRRES_17309	FGSG_10057	Putative transcription factor (Zn(II)2Cys6 domain)	W	PHI:1090
FGRRES_01555	*ZIF1*	B-ZIP transcription factor	W, M	PHI:445, PHI:1320, PHI:1292
Cell rescue, defence and virulence				
FGRRES_17598 hypervirulent	Related to O-methylsterigmatocystin oxidoreductase	Cytochrome P450 monooxygenase (DON biosynthesis)	W	PHI:2393
FGRRES_10397 hypervirulent	Conserved hypothetical protein	Unknown function	W	PHI:2394

FGRRES_03747	*NPS6*	Non-ribosomal peptide synthetase for biosynthesis of extracellular siderophores	W	PHI:1007, PHI:3657
FGRRES_04111	*PTC1*	Type 2C protein phosphatase	WC	PHI:2326, PHI:2491
FGRRES_03538	*TRI10*	Regulatory protein	W	PHI:2328
FGRRES_03543	*TRI14*	Putative trichodiene biosynthesis gene	W, M	PHI:525
FGRRES_03537	*TRI5*	Trichodiene synthase	W, M	PHI:44
FGRRES_03536	*TRI6*	Transcription factor	W	PHI:439
Unclassified protein				
FGRRES_06631_M	*CPS1*	Adenylate-forming enzyme	W	PHI:304
FGRRES_16701	*MES1*	Role in cell-surface organisation	W	PHI:1078
FGRRES_02077	none designated	Conserved hypothetical protein	W	PHI:1093
FGRRES_12019	none designated	Hypothetical protein	W	PHI:1098
FGRRES_12753	none designated	Hypothetical protein	W	PHI:1092

Abbreviations: ATP (Adenosine triphosphate), APSES (100 amino acid protein domain), GTP (Guanosine triphosphate), MAPK (Mitogen-activate protein kinase), MAPKKK (Mitogen-activated protein kinase kinase kinase)

♦ FGRRES ID (*F. graminearum* locus identifier) was taken from the *F. graminearum* genome version 4.0 (King et al., 2015)

‡ Cereal hosts tested are wheat spikes (W), barley spikes (B), wheat coleoptiles (WC), maize (M).

† PHI-base ID: see PHI-base website (www.PHI-base.org)

1.7 The omics era of *Fusarium graminearum*

1.7.1 Genome analysis

The advent of whole-genome sequencing has greatly benefited the research into the biology of numerous non-pathogenic and pathogenic filamentous fungi. Due to the economic importance, *F. graminearum* was the third pathogen filamentous fungal to have the whole genome sequenced in 2007, after the genome sequence of the rice blast fungus *Magnaporthe grisea* (Dean et al., 2005) and the corn smut fungus *Ustilago maydis* (Kamper et al., 2006). The North American *F. graminearum* strain PH-1 (NRRL 31084) was used to generate the reference genome applying Sanger Sequencing Technology and then annotated by the BROAD institute (Paper et al., 2007). The resulting assembly totals 36.1 Mb and an initial set was predicted as 11,640 genes. Since then, next-generation sequencing (NGS) technologies have increased the speed and scalability of genome sequencing at a significantly reduced cost. Later, the *F. graminearum* genome sequence and annotation was improved by BROAD, and the gene models were refined by Munich Information Services for Protein Sequences (MIPS), resulting in a set of set of 13,718 annotated protein coding genes (Wong et al., 2011). This gene set was used to develop an *F. graminearum* specific Affymetrix array which has subsequently been used for many *in vitro* and *in planta* transcriptome analysis (http://www.plexdb.org) (Guldener et al., 2006) (see below).

One of the main aims of many genome sequencing projects is to identify the genic coding region of a particular genome. Thus, this information would help researchers focused on physiologic characterisation or the molecular biology of a specific cellular process. However, lately, DNA sequences that do not encode

proteins have been associated to important traits controlling life-style, adaptability and evolution of many organisms (Bickhart & Liu, 2014, Raffaele & Kamoun, 2012, Seidl & Thomma, 2014, Thomma et al., 2016). Therefore, the interest to assemble the whole genome further than the protein-coding regions has increased. Using the whole shotgun re-sequencing of the strain PH-1 to 85-fold coverage, the complete *F. graminearum* genome sequence consists of 38Mb distributed in four scaffolds assigned to the four expected chromosomes from telomere to telomere, and has been predicted to contain 14,160 protein coding genes (King et al., 2017b, King et al., 2015). These gene models have also been updated with 5' and 3' UTR annotations (King et al., 2017b).

Currently, hundreds of fungal genomes have been sequenced and are publicly available and deposited in different databases such as the European Nucleotide Archive at the EBI, GenBank at the NCBI, and the DNA Database of Japan. Table 1.4 provides information about most of the published genomes of different *Fusarium* species and strains.

The *F. graminearum* genome was found to be rich in gene diversity, measured by SNP density in the telomere proximal regions. These regions also presented elevated level of recombination (Paper et al., 2007, King et al., 2015). In addition, *F. graminearum*, distinctively, contains specific regions in the middle of each chromosome with both high sequence diversity and high recombination frequencies. It is suggested that these regions have been created by ancestral telomeric fusion events to create larger chromosomes (Paper et al., 2007). How and why these regions have maintained high genetic diversity remain unknown.

So far, only a few other few isolates of *F. graminearum* in addition to PH-1 have been sequenced and their genome studied in depth. In Canada, where both *F. graminearum* main trichothecene chemotypes: 3-ADON and 15-ADON

are present, the study carried out by Walkowiak et al. (2015) revealed that interaction between two isolates of these two chemotypes reduced trichothecene yield in culture and disease symptoms in wheat. To identify potential genes involved in this intraspecies interaction, genome and RNA sequencing analyses were performed. One of the strains sequenced by Walkowiak et al. (2015) was GZ3639, also sequenced early but at a low genome coverage by Paper et al. (2007) and used for comparison with PH-1. Later the same group compared the genome sequences of new isolates within the *F. graminearum* species complex (FGSC), which included sequencing of two more strains of *F. graminearum* and the first available genomes for *F. asiaticum* and *F. meridionale* (Walkowiak et al., 2016). They identified core genes (n= 13,470) probably responsible for the basic aspects of FGSC biology and its major phenotypic traits, and accessory genes (n= 1,827) potentially involved in niche specialisation within and between species (Walkowiak et al., 2016).

Comparative analysis of all the publicly deposited *Fusarium* genome sequences predicts 9000 genes comprise the core region due to high sequence similarity and conserved gene order (Ma et al., 2013). Alternatively, each species also contains several thousands of genes that are unique to each genome. The majority of the species specific sequences are located near to the ends of chromosomes.

Table 1.4. The set of some *Fusarium* genomes available with their genome characteristics

Species (Origin)	**Strains**	**Genes**	**Genome size (Mb)**	**Chromosomes**	**Reference**
***F. graminearum* (USA)**	PH-1	14,160	38 Mb	4	(Cuomo et al., 2007, King et al., 2017b, King et al., 2015)
***F. graminearum* (USA)**	GZ3639 (FG2)	ND	ND	4	(Cuomo et al., 2007,

					Walkowiak et al., 2015)
***F. graminearum* (Australia)**	CS3005	13,355	36.6 Mb	4	(Gardiner et al., 2014)
***F. graminearum* (Canada)**	FG1	ND	36.6 Mb	4	(Walkowiak et al., 2015)
***F. graminearum* (Canada)**	DAOM 180378	Unknown	36.4 Mb	4	(Walkowiak et al., 2016)
***F. graminearum* (USA)**	NRRL 28336	Unknown	36.7 Mb	4	(Walkowiak et al., 2016)
***F. pseudograminearum* (Australia)**	CS3220 CS3427 CS3487 CS5834	12,615 12,577 12,749 12,633	37 Mb 37 Mb 37 Mb 37.5 Mb	Unknown	(Moolhuijzen et al., 2013)
***F. pseudograminearum* (Australia)**	CS3096	ND	37 Mb	Unknown	(Gardiner et al., 2012)
***F. acuminatum* (Australia)**	CS5907	15,353	44 Mb	Unknown	(Moolhuijzen et al., 2013)
***F. incarnatum* (Australia)**	CS3069	13,743	38 Mb	Unknown	(Moolhuijzen et al., 2013)
F. oxysporum* f. sp. *lycopersici	4287	17,735	59.9 Mb	15	(Ma et al., 2010)
***F. fujikuroi* (South Korea)**	B14	14,017	44 Mb	12	(Jeong et al., 2013)
***F. fujikuroi* (UK)**	IMI58289	14,813	43.9 Mb	12	(Wiemann et al., 2013)
F. verticillioides	7600	14,179	42 Mb	11	(Ma et al., 2010)
F. solani* f. sp. *pisi	77-13-4	15,707	51 Mb	17	(Coleman et al., 2009)
***F. circinatum* (South Africa)**	FSP34	15,713	42 Mb	Unknown	(Wingfield et al., 2012)
***F. asiaticum* (Japan)**	NRRL 6101	Unknown	36.5 Mb	4	(Walkowiak et al., 2016)
***F. asiaticum* (Nepal)**	NRRL 28720	Unknown	36.4 Mb	4	(Walkowiak et al., 2016)
***F. meridionale* (Nepal)**	NRRL 28721 NRRL 28723	Unknown Unknown	36.5 Mb 36.4 Mb	4 4	(Walkowiak et al., 2016)
***F. culmorum* (UK)**	UK99	12,537	41.9 Mb	5	(Urban et al., 2016)

1.7.2 Transcriptome analysis

Genome sequencing and annotation have provided a global view of the genes present in different fungal species, however, transcriptomic and proteomic analyses have greatly accelerated the identification of fungal gene function and

helped to understand genes transcriptional and posttranscriptional regulation (Ma et al., 2010, Zhao et al., 2014).

Study of transcriptomics can be done using high-throughput techniques based on DNA microarray technology, in the case of *F. graminearum* by using the available Affymetrix array based on the Version 3 gene call (Guldener et al., 2006), or by using next-generation sequencing technology at the nucleotide level, known as RNA-Seq.

For whole genomic analyses, transcriptomics has important applications in fungal plant pathology. Analysis of gene expression can improve our understanding of fungal pathogenesis and fungal-plant interactions. As mentioned previously, many genes, comprising the core set, are very similar in different fungal species sequenced to date (Ma et al., 2013), and genomic comparison of very closely related species but that have distinct aspects of infection biology, symptom development and /or sporulation have not provided enough information to identify which genes are responsible for these underlying differences. Transcriptomics provide another type of data that can be used to explore inter-species differences. Identifying fungal genes specifically expressed during infection or under conditions that mimic infection, compared to growth *in vitro,* or on a non-host species has become a popular approach to develop candidate virulence genes lists for further investigation.

The first array experiment to monitor the fungal-pathogen interaction was carried out by Schenk et al. (2000). In order to study defence reactions in *Arabidopsis* either infected by the incompatible fungal pathogen *Alternaria brassicicola* or treated with the defence-related signalling molecules salicylic acid (SA), methyl jasmonate or ethylene, expression data was obtained. The results indicated the existence of a considerable network of regulatory interactions and

coordination of signalling pathways, which had not been observed previously in the genome analysis (Schenk et al., 2000).

Since then, global gene expression has been examined in several dozen species of filamentous fungi to address different questions related to metabolism and pathogenicity. In 2002, expression profile of the rice blast fungal *Magnaporthe oryzae* examined fungal responses in different rice lines, to identify differentially expressed genes during appressoria formation and between fungal pre- and post-penetrative stages (Rao et al., 2002, Takano et al., 2003). These findings helped with subsequent studies that identified *M. oryzae* effectors and mechanism of tissue invasion (Giraldo & Valent, 2013, Valent et al., 2013).

The Fusarium draft sequence assembly, from the two automatically predicted gene sets (The Broad Institute and MIPS) and manual annotation, was used to construct an appropriate gene set to design a custom Affymetrix GeneChip microarray. These two distinct sets of automatically predicted gene calls were used to maximise the likelihood of representing all putative genes (~14,000) on the array (Guldener et al., 2006). The first experimental application of this Fusarium array was tested on three *in vitro* cultures, with different nutritional regimes (complete media (CM), CM minus carbon, CM minus nitrogen), and in comparison with fungal growth in infected barley (Guldener et al., 2006). The Plant Expression Database (PLEXdb, http://www.plexdb.org) has been used as a public repository for expression data from this *F. graminearum* GeneChip. Currently, 17 data sets are available from this resource and an overview of the biology investigated is given in table 1.5

Mechanisms responsible for spore germination and development, or perithecia formation *in vivo* and *in vitro* were explored. Gene expression data was used to predict the cellular and physiological state of each developmental stage

for known processes. From these studies, it was found that over 10% of *F. graminearum* genes appear to be specific either to conidial germination or sexual development (Hallen et al., 2007, Seong et al., 2008a).

Other groups have explored the gene expression profile of *F. graminearum* infection during different time points and on different cereal hosts. Lysoe et al. (2011) found that a number of genes expressed up to 96 h of *F. graminearum* infection on wheat ears increased considerably. Another study using both RNA-seq and Affymetrix analysis of wheat ears rachis inoculated with *F. graminearum* at 5 and 7 days post inoculation (dpi), respectively, identified over 2000 genes upregulated in the symptomless vs symptomatic rachis comparison (Brown, 2011, Brown et al., 2017) Among the genes expressed at early stages of *F. graminearum* infection on wheat, several include genes encoding putative secreted proteins (Brown et al., 2011, Lysoe et al., 2011).

Different expression patterns were also observed in a number of host species or plant tissues. Harris et al. (2016) demonstrated that *F. graminearum* can adapt to a range of host by its genomic flexibility. Transcriptome of *F. graminearum* during early infection of barley, wheat and maize revealed considerable host-specific expression of genes (Harris et al., 2016).

Expression of specific genes was also assessed in different host tissues. Transcriptome studies of *F. graminearum* infecting wheat coleoptiles and wheat stem bases during the development of crown rot disease revealed a number of genes to be expressed solely in each tissue type (Stephens et al., 2008, Zhang et al., 2012). Particularly interesting was the identification that the *tri* cluster, responsible for DON production, which is dramatically upregulated during wheat and barley ear infection, was not upregulated in either wheat coleoptile or wheat stem base tissues. These results suggested that the mycotoxin may not play a

role on the disease establishment in either tissue. Subsequent tests with the *Tri5* mutant have revealed DON is important for *F. graminearum* virulence in wheat ears, but not for maize or Arabidopsis (Cuzick et al., 2008, Proctor et al., 1995).

Table 1.5 Expression data set generated with *F. graminearum* GeneChip. deposited in the Plant Expression Database

Experiment	Experiment factor(s)	Reference
Transcript Expression Profiles of *F. graminearum* During the Infection of Wheat and Rice	**Host species** •Wheat (ears) •Rice (panicles) **Time** •48 hai •96 hai •192 hai	none
Stage-specific expression patterns of *Fusarium graminearum* growing inside wheat coleoptiles with laser microdissection	**Time** (in wheat coleoptlile) •0 hrs •16 hrs •40 hrs •64 hrs •240 hrs •72 hrs	(Zhang et al., 2012)
Trichothecene synthesis in a *Fusarium graminearum* Fgp1 mutant.	**Genotype** •Wild type •fgp1 mutant	(Jonkers et al., 2012)
Fusarium graminearum gene expression in wheat stems during infection	**Developmental stage** (in wheat stems) •IF - vegetative hyphae •RW - wide dikaryotic hyphae •SW - perithecial initials •YP - young perithecia	(Guenther et al., 2009)
F. graminearum gene expression during wheat head blight	**Time** (in wheat ears) •0 hrs •24 hrs •48 hrs •72 hrs •96 hrs •144 hrs •192 hrs	(Lysoe et al., 2011)
DON induction media	**Growth condition** (in fungal culture) •agmatine •glutamine	(Gardiner et al., 2009)
The transcription factor FgStuAp influences spore development, pathogenicity and secondary metabolism in *Fusarium graminearum*	**Strain** •PH-1 •Δ*FgStuA* **Growth condition** •CMC media (spore production) •Wheat •Secondary metabolism	(Lysoe et al., 2011)
Fusarium graminearum gene expression during crown rot of wheat	**Time** (in wheat seedlings) •2 dpi •14 dpi •35 dpi •mycelia cultured	(Stephens et al., 2008)
Gene Regulation by *Fusarium* Transcription Factors Tri6 and Tri10	**Strain** (in wheat ears) •PH-1 wildtype •PH-1 *tri6* deletion •PH-1 *tri10* deletion	(Seong et al., 2009)

Response to trichodiene treatment in *Fusarium graminearum*	**Compound** (in fungal culture) •250 µM trichodiene •no trichodiene	(Seong et al., 2009)
Fusarium gene expression profiles during conidia germination stages	**Time** (in complete media) •0 hrs •2 hrs •8 hrs •24 hrs	(Seong et al., 2008b)
Transcript detection during in vitro sexual development of Fusarium Cch1 calcium channel deletion mutant using *Fusarium* Affy GeneChips	**Time** (sexual development induction on carrot agar) •0 hrs •96 hrs •144 hrs	(Hallen & Trail, 2008)
Fusarium transcript detection during in vitro sexual development using *Fusarium* Affy GeneChips	**Time** (sexual development induction on carrot agar) •0 hrs •24 hrs •48 hrs •72 hrs •96 hrs •144 hrs	None
Fusarium/Barley RNA dilution	**Dilution** (fungal RNA diluted with barley RNA) •original PH1 •1/10 •1/100 •1/1000 •1/10000	(Guldener et al., 2006)
Cross-species hybridisation	**Cross-species comparison** •*F. boothii* •*F. graminearum* •*F. asiaticum* •*F. pseudograminearum* •*F. oxysporum* •*F. verticillioides* •*F. culmorum*	(Guldener et al., 2006)
Expression Profiles in Carbon and Nitrogen Starvation Conditions	**Growth condition** •Complete Media •Carbon Starvation •Nitrogen Starvation	(Guldener et al., 2006)
Fusarium transcript detection on Morex barley spikes using *Fusarium* Affymetrix GeneChip	**Developmental stage** (in barley spikes) •water control •24 hours •48 hours •72 hours •96 hours •144 hours	(Guldener et al., 2006)

1.7.3 Proteomics

Due to the availability of multiple fungal genome sequences, fungal proteomics research has also increased substantially over the past 10 years. Although transcriptomics provides a useful overview of global gene expression, proteomics is often used as a complementary technique that provides a comprehensive insight into the protein profile of an organism. In addition, powerful proteomics technologies became available, for example tandem liquid

chromatography–mass spectrometry (LC-MS). This highly sensitive technique combines the physical separation capabilities of liquid chromatography (HPLC) with the mass analysis capabilities of mass spectrometry (MS) and enable high-throughput protein identification and function (Braaksma et al., 2010, Costa et al., 2010, Martin et al., 2008).

Two-dimensional gel electrophoresis (2-DE) has been used for over 20 years to dissect host–pathogen interaction and this method is still a useful tool (Kachroo et al., 1997). One of the first studies, investigated changes in the extracellular and intracellular proteomes of *Magnaporthe oryzae* when exposed to extract of resistant and susceptible rice cultivars. Specific fungal proteins were induced by susceptible rice cultivars, but due the limited availability of gene sequences at the time, these proteins could not be identified (Kachroo et al., 1997).

Proteome studies in *F. graminearum* have also been carried out. Phalip et al. (2005) investigated the exoproteome of *F. graminearum* growth in glucose and in hop (*Humulus lupulus*, L.) cell wall. These investigators used both 1-dimension and 2-DE electrophoresis followed by mass spectrometry analysis and protein identification based on similarity searches, and identified 84 unique proteins from growth in plant cell walls and 45% were implicated in cell wall degradation. Only four proteins were found both in glucose and in plant cell wall after *F. graminearum* growth. This proteome study was very helpful in verifying some of the genes bioinformatically predicted to code for small secreted proteins in the *F. graminearum* genome (Brown et al., 2012).

Wang et al. (2005) determined the proteins in resistant wheat ears induced by *F. graminearum* separately by 2-DE. Three-fold change in abundance in thirty protein spots were identified when compared with treatment without

inoculation. These proteins were further characterised using MALDI-TOF MS and the results demonstrated that proteins associated with the plant defence reactions were activated or translated shortly after inoculation.

A number of *F. graminearum* secreted proteins have also been identified using high-throughput MS/MS during fungal growth in culture and infection of wheat ears (Paper et al., 2007). Among 289 proteins identified, 49 were found only *in planta* and suggested to be promising candidates with a role in pathogenesis (Paper et al., 2007). Subsequently, some of the genes encoding these proteins were deleted and the mutant strains tested *in planta*. Some gene sequences were shown not to be required for *F. graminearum* pathogenicity, for example gene FGRRES_12973, encoding a FAD-dependent oxidoreductase (PHI:1432) (Son et al., 2011). However, other genes were shown to be important for fungal virulence, for example, gene FGRRES_05554, encoding an aminobutyrate aminotransferase (PHI:5028) (Bonnighausen et al., 2015) and gene FGSG_10825, encoding a methionine synthase (PHI:442) (Seong et al., 2005).

F. graminearum synthesises and secretes trichothecenes early in the cereal host invasion process. Another study hypothesised that expressing mycotoxins during *in vitro* conditions, proteins contributing to infection would also be induced (Taylor et al., 2008). Quantitative protein mass spectrometry using isobaric tags for relative and absolute quantification (iTRAQ) analysis confirmed that proteins potentially involved in *F. graminearum* virulence were found to be upregulated. Many of these proteins are predicted to be secreted, with no specific domains but had homology to other previously characterised fungal virulence proteins (Taylor et al., 2008).

Although proteomics studies are of great value, all three omics approaches mentioned above should be used in combination to provide more information about fungal development, physiology and pathogenicity mechanisms. Proteomics studies provide reliable information about protein production, function and localisation, however these studies suffer from a lack of sensitivity in detecting protein produced in low amounts, for example secreted fungal effectors. Therefore, currently transcriptomic data permits more inferences related to fungal-plant interaction. However, further technical developments are still needed to be able to detect small fold changes in gene expression and/or genes expressed at very low levels in a tested condition. Genome sequencing elucidates the genomic content and permit *in silico* predictions, transcriptomic and proteomic studies. In addition, the transcriptomic and proteomic data sets both refine and verify the predicted gene models.

1.8 Fungal effector proteins

One requirement for plant pathogens to establish successful infection and colonisation in the host is their ability to either not activate or overcome plant defence responses. To achieve this, bacteria, fungi, oomycetes and nematodes are now known to secrete proteins or other molecules into different cellular compartments of the plant, which are collectively known as effectors, to facilitate infection (Lo Presti et al., 2015). The interest in understanding effector functions of diverse pathogens species, and elucidate the processes that underlie host colonisation and pathogenicity have increased in the last decade (Walton et al., 2009). Usually, effectors are defined as, but not limited to, small secreted proteins (≤300 amino acids), that are also cysteine rich. The cysteine residues stabilise the protein tertiary structure by forming disulphide bridges (Lo Presti et al., 2015).

Although the generic term effector is widely used in conjunction with different fungal pathogens species, different groups of species have adopted distinct strategies to stablish infection, acquire nutrients and complete their life cycle. Biotrophic pathogens acquire sustenance for extended periods only from live plant cells. Necrotrophic pathogens are unable to occupy living plant cells and kill the host plant tissue ahead of hyphal proliferation within the host tissue. Hemibiotrophic pathogens use both biotrophic and later necrotrophic strategies to complete their life cycle. The later pathogen type initially need effectors to suppress plant defences and later need effectors that kill plant cells (Agrios, 2005, Lo Presti et al., 2015).

The interaction between a successful pathogen and its plant host relies on the loss, acquisition and modification of effectors by the pathogen, and the presence or not of host proteins that can detect these effectors either directly or indirectly. This is described by the 'zig-zag-zig' model first introduced by Jones and Dangl (2006) (Figure 1.7). Several effectors have been characterised in plant-infecting fungi that prevent the activation of microbial/pathogen-associated molecular patterns (MAMPs/PAMPs)-triggered immunity (PTI), the 'first -line' of plant defence or the subsequent effector-triggered immunity (ETI).

Due to the complexity and size of fungal proteomes, a strategy to identify proteins of interest secreted from the fungal hyphae that could potentially communicate / interact with the host is beneficial. Therefore, many research groups focus on studying a specific fraction of the proteome, called the secretome. The predicted secretome consists of the set of enzymes and other proteins which contain characteristic features, domains and motifs found in proteins experimentally proven to be secreted and / or to exhibit an effector function (Mueller et al., 2008, Espino et al., 2010, Guyon et al., 2014, Alfaro et al., 2014, Brown et al., 2012).

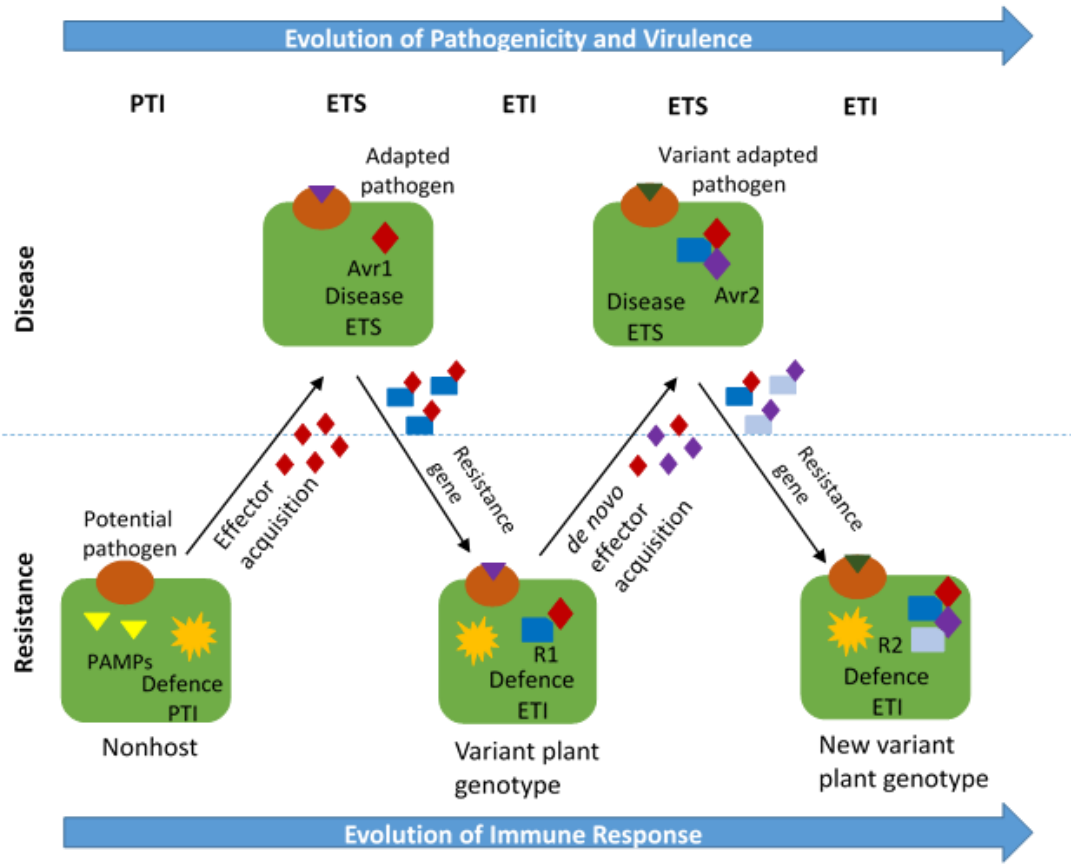

Figure 1.7 The zig-zag-zig model. Co-evolution of pathogenicity mechanisms and corresponding immune response in plants, resulting in either disease resistance or disease susceptibility. 1. PAMP recognition by the plant and PAMP-triggered immunity (PTI); 2. The pathogen acquire an effector (Avr1) that is able to overcome the PAMP recognition leading to effector-triggered susceptibility (ETS); 3. A variant plant genotype carries a resistance protein (R1) that recognises Avr1 leading to effector-triggered immunity (ETI); 4. An adapted pathogen acquire an additional effector, Avr2, resulting in ETS; 5. A new variant plant genotype carries an additional resistance protein (R2) that detects Avr2 resulting in ETI. Adapted from Brown and Hammond-Kosack (2015).

1.8.1 Biotrophic fungal pathogen effectors

The basidiomycete smut fungus *Ustilago maydis* establishes a biotrophic interaction with its host plant maize (*Zea mays*) during which the invading intracellular hyphae is surrounded by the plant plasma membrane. The *U. maydis* secretome is predicted to contain over 350 secreted proteins with a range of putatively functions that could be potential effectors (Mueller et al., 2008).

U. maydis was the first eukaryotic pathogen in which novel effectors with relevant functions for pathogenic development were discovered to be situated in small gene clusters that are transcriptionally up-regulated during infection and tumour formation. Twelve such gene clusters were identified, which all code for novel secreted proteins, and which in several instances belong to small gene families. Four of the cluster deletion mutants are significantly attenuated in virulence and show defects at different stages of pathogenic development (Kamper et al., 2006).

The most abundant protein detected in the apoplastic interaction zone of *U. maydis* was the chorismate mutase Cmu1, which has also been shown to be a virulence factor for the fungus (Djamei et al., 2011). Chorismate mutase is an enzyme that catalyses the chemical reaction for the conversion of chorismate to prephenate in the pathway to the production of phenylalanine and tyrosine, also known as the shikimate pathway (Sasso et al., 2005). The CMU1 protein is transferred into host cells during infection and is required for full virulence of the fungus *in planta*, but not for growth in culture. This enzyme is translocated from the apoplast into the cytoplasm and the chloroplast of the maize cell via an unknown mechanism. Later, Cmu1 channels chorismate into the phenylpropanoid pathway, thereby preventing its flow into the salicylic acid biosynthesis branch, thus minimising the activation of PTI (Djamei et al., 2011). Another universal effector secreted by *U. maydis* to suppress PTI is Pep1, which acts as a potent suppressor of early plant defences by inhibiting peroxidase activity (Hemetsberger et al., 2012).

During plant infection, *U. maydis* also secretes the Pit2 effector in the biotrophic interface and Pit2 accumulates in the apoplastic space around colonised maize cells (Doehlemann et al., 2011). Pit2 functions as an inhibitor of

a set of apoplastic maize cysteine proteases, and is required for *U. maydis* virulence (Mueller et al., 2013). Two cell surface-located hydrophobins, Hum3 and Rsp1, may also be considered to function as potential core effectors, although these have not yet been formally recognised as such. Deletion of both the *Hum3* and *Rsp1* genes in a single isolate severely compromises pathogenicity, causing the *U. maydis* hyphae to arrest during the early phase of infection (Muller et al., 2008).

The ascomycete *Cladosporium fulvum* (syn. *Passalora fulva*) is a biotrophic, extracellular pathogen, which colonises the existing apoplast in between plant cells and causes leaf mold disease of tomato (*Lycopersicon esculentum*). The interaction between *C. fulvum* and tomato is governed by a gene-for-gene relationship (Thomma et al., 2005). This pathogen secretes apoplastic effectors that accumulate in the tomato leaf apoplast soon after fungal hyphae have penetrated the stomata (Stergiopoulos & de Wit, 2009). To date, five avirulence (Avr) genes, Avr2, Avr4, Avr4E, Avr5 and Avr9, as well six additional extracellular proteins (Ecps), namely Ecp1, Ecp2, Ecp4, Ecp5, Ecp6 and Ecp7, have been identified. All these proteins are secreted during infection and can each trigger ETI in tomato genotypes expressing either the cognate *Cf* resistance protein or cognate *Cf-Ecp* gene, respectively (reviewed by De Wit (2016)).

One of these effectors, Ecp6, is responsible for masking *C. fulvum* from detection by the host immune system. This effector contains three LysM domains and sequesters chitin oligomers originating from the fungal cell wall before detection by plant PRRs (Figure 1.7), thereby preventing PTI (Bolton et al., 2008, de Jonge & Thomma, 2009). The *C. fulvum* Avr4 effector, which contains an invertebrate chitin-binding domain, has a similar activity and contributes to

virulence by shielding hyphae against hydrolysis by tomato chitinases (van Esse et al., 2007). While Avr4 binds directly to chitin in the fungal cell wall (van den Burg et al., 2006), Ecp6 is involved in scavenging of chitin fragments that are released from the fungal cell wall during infection by plant chitinases (Bolton et al., 2008). By contrast, the Avr2 effector inhibits extracellular tomato proteases, including Rcr3, Pip1, aleurin and TDI65, and prevents the ETI-mediated host defence. In the presence of Cf-2, Avr2 behaves as an avirulence factor, causing a HR to be triggered (van Esse et al., 2008).

C. fulvum Avr9 was one of the first avirulence genes to be characterised (Vandenackerveken et al., 1993). The 28 amino acids mature protein has six cysteines residues, which are essential for its tertiary structure and necrosis-inducing activity in Cf-9 containing tomato lines. Disruption of this gene in *C. fulvum* by homologous recombination did not affect either fungal growth *in vitro* or virulence on tomato plants. This results suggests that Avr9 is not required for full virulence (Marmeisse et al., 1993).

The exact mechanism(s) by which the other Avr proteins contribute to pathogenicity is not known yet, but heterologous *in planta* over expression studies with some of the Avr proteins have led to enhanced levels of disease when plants were challenged with *C. fulvum*, suggesting that a few may be virulence factors (Stergiopoulos & de Wit, 2009). With regard to the Ecp effectors, most of them share a little or no homology with other proteins present in public databases, with the exception of *C. fulvum* Ecp6, for which functional orthologues have now been demonstrated in other plant pathogenic fungal species, as *Magnaporthe oryzae* (the causal agent of rice blast disease*)* and *Mycosphaerella graminicola* (now referred to as *Zymoseptoria tritici* which causes Septoria blotch on wheat) (Bolton et al., 2008).

1.8.2 Hemibiotrophic fungal pathogen effectors

The ascomycete *Magnaporthe oryzae* is classified as a hemibiotrophic pathogen. This species directly penetrates plant leaf cells and appressorial formation is an absolute requirement for pathogenesis (Talbot, 2003). To generate the turgor pressure needed for the plant cell wall penetration, melanisation of the appressorium is necessary. This is achieved through ROS production and secretion of melanin by the pathogen. Targeted deletion of two *M. oryzae* genes coding for superoxide-generating NADPH oxidases, namely Nox1 and Nox2 resulted in the inability of the fungal germ tube to bring about appressorium-mediated cuticle penetration and initiation of rice blast disease (Egan et al., 2007).

After appressorium formation, *M. oryzae* invades rice tissue using specialised filamentous invasive hyphae (IH), which successively occupy living rice cells and colonise tissue extensively before the appearance of disease symptoms (Giraldo et al., 2013). The invasive hyphae (IH) are surrounded by a plant-derived extra-invasive hyphal membrane (EIHM). In addition to the formation of specialised structures during plant infection and disease induction, *M. oryzae* secretes effector proteins into host tissue to suppress immunity and support pathogen growth. One example is the small secreted protein MC69. The *mc69* mutant showed a severe reduction in blast symptoms on rice although it did not exhibit changes in saprophytic growth and conidia formation (Saitoh et al., 2012). Microscopic analysis of infection behaviour in the *mc69* mutant revealed that MC69 is dispensable for appressorium formation. However, the *mc69* mutant failed to develop invasive hyphae after appressorium formation in rice leaf

sheaths, indicating that MC69 has a critical role in *M.oryzae* interactions with host plants (Saitoh et al., 2012).

Besides the above described EIHM compartment surrounding the IH, some effectors preferentially accumulate in the biotrophic interfacial complex (BIC) (Khang et al., 2010). The BIC is a plant-derived, membrane-rich structure that initially appears adjacent to primary hyphal tips, but is later positioned subapically as IH develop within rice cells (Khang et al., 2010). Giraldo et al. (2013) demonstrated that *M. oryzae* has two distinct secretory pathways by which effectors are targeted to host tissue during plant infection. Cytoplasmic effectors, which are delivered into host cells, preferentially accumulate in the BIC. By contrast, apoplastic effectors, which do not enter host cells, are generally dispersed and retained within the EIHM compartment. These effectors are secreted by invasive hyphae into the extracellular compartment(s) via the conventional secretory pathway. Thus, the rice blast fungus has evolved distinct secretion systems to facilitate tissue invasion.

The apoplastic effectors of *M. oryzae* include the LysM protein Slp1 and several of the biotrophy-associated secreted (Bas) candidate effectors, such as Bas4. These effectors accumulate throughout an enclosed compartment that surrounds the entire IH (Khang et al., 2010, Mentlak et al., 2012). The LysM-containing Slp1 protein, which is a functional orthologue of the *C. fulvum* Ecp6 effector protein, is known to bind chitin and is required to prevent the triggering of PTI via the rice chitin elicitor binding protein (CEBiP), and is therefore essential for pathogenicity (Mentlak et al., 2012). The virulence function(s) of the Bas candidate effectors are still unknown.

Regarding the cytoplasmic effectors, the known *AVR* proteins, such as Avr-Pita1-3, Pwl1 and Pwl2, and other Bas effectors, specifically accumulate in

the BIC. When fungal transformants secreted fluorescently-tagged *PWL2* and *BAS1* proteins during epidermal cell invasion, these fluorescent proteins were observed in BICs and in the rice cytoplasm, demonstrating that that translocation across the host plasma membrane had occurred for both proteins (Khang et al., 2010). Pw1 and Pwl2 function as Avr proteins at the host species level as strains that contain these proteins are unable to infect weeping lovegrass (*Eragrostis curvula)* (Kang et al., 1995, Sweigard et al., 1995). AVR-Pita1 (Khang et al., 2008, Orbach et al., 2000), which confers avirulence toward rice containing the corresponding *R* gene *Pita*, encodes a putative zinc metalloprotease (Bryan et al., 2000).

Among the vascular wilt diseases, the best studied is the tomato wilt, which is caused by the ascomycete *Fusarium oxysporum* f. sp. *lycopersici* (*Fol*). The first *Fol* effector to be identified was called 'secreted in xylem 1' (SIX1), which is a small cysteine-rich protein required for full virulence on tomato (Rep et al., 2005). Recognition of the SIX1 protein by tomato plants carrying the resistance gene I-3 leads to disease resistance (Rep et al., 2004). Therefore, SIX1 is also called Avr3 to indicate its gene-for-gene relationship with the I-3 resistance gene.

The corresponding *R* gene that recognises the *Fol* Avr (or SIX) proteins divides the tomato genotypes into three groups. These resistance genes include *I* (for immunity), *I-1*, *I-2* and *I-3* (Huang & Lindhout, 1997), and these interact with SIX4 (Avr1), SIX3 (Avr2) and SIX1 (Avr3), respectively (Houterman et al., 2008, Houterman et al., 2009, Rep et al., 2004). However, recent findings have showed that SIX1 and SIX3 are required for full virulence on tomato (Takken & Rep, 2010, Thatcher et al., 2012). SIX4 on the other hand, is not required for full virulence on tomato cultivars lacking the corresponding *I* or *I-1* genes. SIX4 (Avr1) was found to suppress *I-2* and *I-3*-mediated disease resistance (Houterman et al., 2008,

Houterman et al., 2009). The *I* gene-mediated recognition of *FoI* infection does not cause a typical HR response, because most xylem vessels are already non-living cells. Instead ETI results in callose deposition, accumulation of phenolics and the formation of tyloses and gels in the xylem, thus minimising any further internal vascular colonisation (Brown & Hammond-Kosack, 2015)

The plant pathogen which is the focus of this PhD study, *F. graminearum*, is also a hemibiotroph. This species was initially classified as a necrotroph prior to the discovery of the symptomless apoplastic infection phase in wheat rachis tissue (Brown et al., 2010) (Figure 1.7). So far, in the wheat–*F. graminearum* interaction, no gene–for-gene relationships have been identified even though extensive host germplasm and isolate collections have been screened (Kazan et al., 2012, Lo Presti et al., 2015). No *F. graminearum* homologues were found for the *F. oxysporum* f sp. *lycopersici* (Fol) SIX genes (secreted in xylem) which activate resistance conferred by different tomato disease resistance genes (Urban & Hammond-Kosack, 2013).

The first secreted virulence molecule identified in *F. graminearum* is the DON mycotoxin, deoxynivalenol. However, it seems DON plays a role in virulence only in specific hosts and tissue types, for example required for successful colonisation of wheat ears (Proctor et al., 1997, Cuzick et al., 2008), but not required for infection of maize cobs (Maier et al., 2006) or Arabidopsis floral tissues (Cuzick et al., 2008) (see section 1.3.1 above for more details).Two other well-known and well characterised *F. graminearum* virulence genes that are secreted are the lipase encoded by *FGL1* and the siderophore triacetyl fusarinine C (TAFC). Transformation-mediated disruption of *FGL1* led to reduced extracellular lipolytic activity in culture and *fgl1* mutants displayed reduced virulence in both wheat and maize (Voigt et al., 2005). Subsequent study showed

clear evidences to suggest that FGL1 protein suppress callose biosynthesis. The inhibition of callose seems to be related to increased concentration of free fatty acid (FFA) during *F. graminearum* infection, which was strongly reduced in the Δ*fgl1* mutant strain (Blumke et al., 2014). Deletion of *Sid1* and *Nps6* genes, which encode essential enzymes in the biosynthesis of the siderophore TAFC in *F. graminearum*, resulted in reduced virulence and hypersensitivity to H_2O_2 (Oide et al., 2006). TAFC is a *F. graminearum* siderophore (low-molecular mass iron chelators) employed for iron uptake and storage. During fungal invasion, reactive iron is secreted to infection sites, mediating H_2O_2 production. The depletion of intracellular iron in the host promotes transcription of pathogenesis-related genes. These findings suggest that secreted TAFC could trigger plant defences, acting as a PAMP, benefiting the necrotrophic phase of *F. graminearum* (Greenshields et al., 2007, Haas et al., 2008, Liu et al., 2007, Oide et al., 2006).

1.8.3 Necrotrophic fungal pathogen effectors

Unlike the effectors produced by biotrophs, some effectors produced by necrotrophs should induce plant cell death. This class of effectors usually consists of toxins, secondary metabolites, cell death inducing proteins, secretion of reactive oxygen species (ROS) and plant cell wall-degrading enzymes (PCWDE), and more recently discovered, small RNAs (De Wit, 2016, Franceschetti et al., 2017).

One of the mechanisms that plants use to combat pathogen attack is the generation of reactive oxygen species that trigger a hypersensitive response leading to cell death. *Botrytis cinerea* and *Sclerotinia sclerotiorum* are examples of necrotrophic fungi that need the dead host cell to be able to develop and reproduce. Arabidopsis genotypes that accumulate less superoxide or hydrogen

peroxide were shown to be more resistant to both pathogens (Govrin & Levine, 2000). Additionally*, B. cinerea* and *S. sclerotiorum* secrete a range of PCWDEs to establish the infection (Espino et al., 2010, Heard et al., 2015). *B. cinerea* and *S. sclorotiorum* also secrete oxalic acid (OA) to induce cell death. *S. sclerotiorum* mutants that do not produce OA are unable to cause disease. Additionally, OA facilitates the breakdown of pectin layers in cell wall, alter the extracellular pH for enzymatic activity and suppresses autophagy (Kim et al., 2008, Rollins & Dickman, 2001).

Amongst the secreted proteins produced by *B. cinerea*, the enzyme Cu-Zn-superoxide dismutase BcSOD1 has been shown to be a virulence factor (Rolke et al., 2004). Another secreted protein belonging to the cerato-platanin family of proteins is one of the most abundant proteins found in the early infection secretome (Espino et al., 2010). The recombinant protein induced strong necrosis in tobacco leaves and single gene deletion mutants showed reduced virulence (Frías et al., 2011).

Recent studies have also demonstrated that *B. cinerea* is able to produce small RNAs that can silence specific Arabidopsis and tomato genes that are involved in plant defences. The presented evidence suggests that the fungal dicer protein cleaves dsRNAs into sRNAs. The Bc-sRNAs hijack the host RNA interference (RNAi) machinery by binding to Arabidopsis Argonaute 1 (AGO1) to silencing specific host immunity genes (Weiberg et al., 2013).

Some necrotrophic fungi produce host-selective toxins, which interfere with host defence pathways to induce plant programmed cell death (PCD). This approach also results in the release of nutrients and this assists pathogenesis. The secretion of small unique proteins that are internalised by host cells and interact with the host has been demonstrated for the wheat pathogens

Parastagonospora nodorum (causal agent of Stagonospora nodorum Blotch) and *Pyrenophora tritici repentis* (causal agent of tan spot). This mechanism of action by proteinaceous fungal toxins has been proposed as an inverse gene-for-gene model, i.e. when recognised by the host plant these secreted bio-molecules induce susceptibility (Oliver, 2012, Oliver & Solomon, 2010).

In the wheat leaf pathogen *P. nodorum*, a range of host selective proteinaceous toxins, ToxA, Tox1 Tox2 Tox3 and Tox4, have been recognised when the host wheat possesses the corresponding genes TSN1, SNN1, SNN2, SNN3 and SNN4. A ToxA homologue was the first host-selective toxin identified from *Pyrenophora tritici-repentis* (Friesen et al., 2007, Friesen et al., 2006)

1.9 Molecular genetic approaches to explore *F. graminearum* virulence

Characterisation of key genes responsible for *F. graminearum* virulence has proven to be a powerful tool for the development of new types of FEB control strategies. Understanding the mechanisms adopted by pathogens to overcome the plant defence response can provide solutions to develop new classes of fungicides, to find markers to assist molecular breeding approaches or to design genetic modified crop genotypes.

1.9.1 Forward genetics

Forward genetics has been shown to be a useful tool to study biological functions of many fungal genes. In forward genetics, random mutations are induced by radiation, chemical or insertional mutagenesis. In *F. graminearum*, several studies used random insertional mutagenesis approach followed by *in planta* phenotyping have been completed to characterise genes that contribute

to virulence (Baldwin et al., 2010, Dufresne et al., 2008, Han et al., 2004, Seong et al., 2005). Library of random insertion mutants for *F. graminearum* can be generated by transformation, mediated either (1) by polyethylene glycol (PEG) or (2) by *Agrobacterium tumefaciens* with a plasmid containing the *hph* gene conferring resistance to the antifungal agent hygromycin B (Baldwin et al., 2010, Han et al., 2004, Seong et al., 2005).

Seong et al. (2005) used restriction enzyme-mediated integration (REMI) approach to generate random insertional mutants of *F. graminearum*. Among 6,500 hygromycin-resistant transformants, 11 pathogenicity mutants were generated. Three disrupted genes were identified in three of the mutants that exhibited reduced virulence: a NADH: ubiquinone oxidoreductase, a putative b-ZIP transcription factor gene and the transducin beta-subunit-like gene (Seong et al., 2005).

Sometimes forward genetic approaches have led to deletion of larger chromosome region. This was the case for the disease attenuated Fusarium insertional mutant, called *daf10* in which the plasmid insertion event into the end region of chromosome 1 induced a large chromosomal deletion spanning 146 predicted genes (350 kb). The genes deleted in this mutant are suggested to have a potential role in DON production and pathogenesis while the *in vitro* growth was minimally affected (Baldwin et al., 2010, Urban et al., 2015b).

Another approach used a new transposon mutagenesis tool deploying a *F. oxysporum* transposable element to obtain knock-out mutants in *F. graminearum*. A total of 331 mutants were generated and 19 showed altered phenotype for either sexual development, radial growth or pathogenicity (Dufresne et al., 2008).

However, overall the number of novel virulence genes identified in *F. graminearum* by forward genetics has been very low and increasing reverse genetics approaches are used.

1.9.2 Reverse genetics

While forward genetic is the classical approach where a modified phenotype is investigated and then the underlying gene(s) locus/loci are identified, in a reverse genetics experiment, a genotype (e.g. based on a candidate gene or a few genes) is generated and then specific phenotypes are explored for a change from the expected wildtype phenotype (Bhadauria et al., 2009). Reverse genetics can be achieved by disruption or deletion of a gene/ a few genes, introducing mutations that make non-functional gene products and/or silencing gene expression by RNA interference (Urban & Hammond-Kosack, 2013).

The use of RNAi to silence gene expression will be discussed in more details in section 1.8.3. Therefore, I will focus here on the use of classical reverse genetics methods to generate *F. graminearum* mutants by gene deletion or disruption.

Generation of *F. graminearum* mutants was possible by using a calcium chloride/PEG mediated protoplast protocol (Proctor et al., 1995). The trichodiene synthase (Tri5) gene was disrupted using this protocol and it was the first *F. graminearum* gene shown to play a role in virulence in wheat using reverse genetics approach (Proctor et al., 1995).

After the release of 10x coverage genomic sequence of the *F. graminearum* strain PH-1 (Paper et al., 2007), targeting of *F. graminearum* specific gene became relatively easier. To target a gene of interest, a ~500bp

PCR product from the DNA coding gene can be cloned into a vector that carries a selectable marker (usually an antibiotic resistance gene). This cassette is used to disrupt a gene of interest in the fungal genome in a process that relies on a single homologous recombination events, occurring 5' and 3' of the native locus or within the coding sequencing. This gene disruption most of the times results in loss of function, however this method can sometimes lead to ectopic recombination, where the integration occurs in non-homologous regions (Watson et al., 2008).

To try to avoid problems with single homologous gene recombination, two flanking regions around the target gene are amplified and each PCR product is approximately ~1kb in length. This approach is known as double homologous recombination and the selectable marker is inserted between these two homologous region (Urban & Hammond-Kosack, 2013). Usually this method is more efficient than single homologous recombination, however the efficiency can vary depending on the target gene (Dyer et al., 2005, Urban et al., 2003).

To improve the efficiency of homologous integration, a new strategy called 'split marker' was employed. The method consists of a mixture of two DNAs fragments with overlapping truncations in the selectable marker (Fu et al., 2006, Liang et al., 2014). Each DNA fragment contains either the 3' or 5' priming ends of part of the target gene or its flanking region together with a two thirds fragment of the selectable marker gene (Catlett et al., 2003) (Figure 1.8).

Recently, the new developed RNA-guided CRISPR (clustered regularly interspaced short palindromic repeats) - Cas9 technology has been used for efficient gene editing in various organisms, including some fungal pathogens species. CRISPR/cas9 gene editing allow the accurate targeting of genes of

interest (De Wit, 2016). CRISPR/Cas9 has been shown to have 95–100% accuracy via very short (approximately 35-bp) homology arms (Zhang, 2015).

The CRISPR/Cas9 was first identified as an immune mechanism in bacteria and archaea and then has emerged as a powerful tool for genome-editing across species (Horvath & Barrangou, 2010). Basically, the system consists of two components: A Cas9 endonuclease and a single guide RNA (sgRNA) that directs the Cas9 enzyme to a site-specific target in the genome (Zhang et al., 2014). The sgRNA consist of 20 nucleotides sequence that recognise the target gene by base pairing followed by a PAM (Protospacer Adjacent Motif). PAM is 2-6 base pair DNA recognised by Cas9 and is thought to destabilise the adjacent sequence (Anders et al., 2014) and the complex can generate a double-stranded break (DSB) in the target region (Redman et al., 2016). In eukaryotic cells, in the absence of a repair template, the non-homologous end joining (NHEJ) pathway generates insertions and deletions during DSB repair. However, in the presence of a DNA template with homology to the sequences flanking the DSB location, homology-directed repair can seal the DSB in an error free manor (Iliakis et al., 2004)

The CRISPR/Cas9 system has been used efficiently in different fungal species, for example *Aspergillus fumigatus*, *Neurospora crassa*, *U. maydis*, *M. oryzae* and most recently in *F. graminearum* (Nodvig et al., 2015, Zhang et al., 2016a)

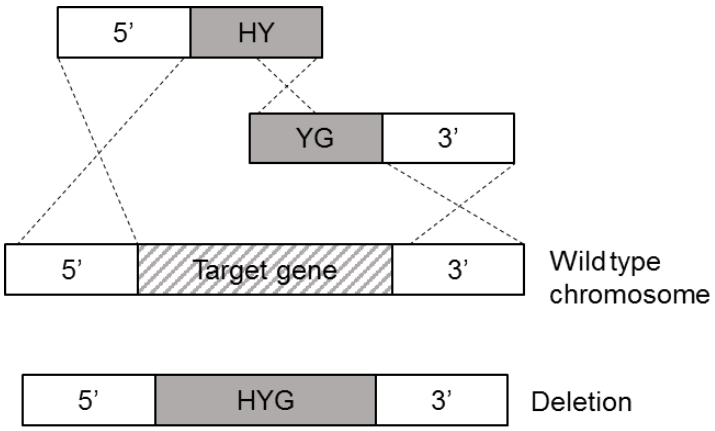

Figure 1.8 Split-marker strategy for gene deletion. Homologous recombination and gene deletion. Two separate PCR fragments (HY) and (YG) from portions of selectable marker HYG (hygromycin) fuse the flank sequences to the 5’ (HY) or 3’ (YG). The two fused fragments are used directly for transformation. Homologous recombination between the overlapping regions of the selectable marker (*HYG*), and between the flank regions and chromosomal DNA results in a directed deletion. Adapted from (Catlett et al., 2003).

1.9.3 Host induced gene silencing

Another approach to emerge in the past few years to explore gene function is the new transgene-based host-induced gene silencing (HIGS) strategy. Current evidence suggests that plants and filamentous fungi use RNA silencing to influence each other, which can be used as an alternative to develop resistant plants. Transgenic plants can generate double-strand RNA (dsRNA), in the form of hairpin, that induce the silencing of target gene transcripts via RNAi in plant pathogens during attempted infection (Nowara et al., 2010). This technique has been developed in multiple crop systems to control effectively diseases caused by insects, nematodes, fungi and oomycetes (Nunes & Dean, 2012).

In *Fusarium* species, HIGS was first demonstrated in tobacco leaf - *F. verticillioides* pathosystem and was shown to be stably inherited over six subsequent generations of the fungus (Tinoco et al., 2010). Subsequently, HIGS

was reported to control *F. graminearum* infections in Arabidopsis and barley plants (Koch et al., 2013). A stable HIGS approach was used to silence the three-membered *F. graminearum* Cyp51 gene family coding for the enzyme cytochrome P450 lanosterol C14α-demethylase required for fungal sterol production. The resulting T_1-T_3 generation GM transgenic plants exhibited strong resistance to Fusarium species (Koch et al., 2013). Chen et al. (2016) reported stable integration of RNAi constructs into the wheat genome targeting one of the *F. graminearum* chitin synthase genes required for fungal cell wall formation. This resulted in the control of *F. graminearum* infections in T_1-T_5 generation wheat plants in controlled environment experiments and in two years of field trials. In addition, stable transgenic wheat plants carrying an RNAi hairpin construct against the glucan synthase gene of *F. culmorum* has been shown to enhance FEB resistance in wheat (Chen et al., 2016).

Another recent study, curiously, established that the *F. graminearum* RNAi machinery was not involved in controlling fungal growth or responses to various abiotic stresses. Interestingly, deletion of *F. graminearum* Argonaute, Dicer or RNA-dependent RNA polymerase (RdRp) genes failed to compromise fungal pathogenicity towards wheat (Chen et al., 2015b). It appears that both a long dsRNA and siRNAs can be translocated into the fungus and induce RNAi and that processing of a long dsRNA into siRNAs depends on the fungal Dicer proteins (Koch et al., 2016, Wang et al., 2016a). However, it remains unknown how these dsRNAs are transferred from plant to fungal cells.

1.9.4 *Barley stripe mosaic virus* – mediated overexpression (BSMV-VOX)

There are a number of molecular mechanisms in living organisms to guarantee that genes are expressed at an appropriate level in different conditions. Therefore, a mutant phenotype is expected when there is a reduction of expression due a complete or partial loss of function of a target gene. In the same way, increasing expression of certain gene can also be disruptive to a cell organism (Prelich, 2012). Overexpression of target genes can, therefore, lead to a different phenotype. This approach has been explored in several pathogenic fungal species as either a complementary or as an alternative way to loss-of-function approach (Prelich, 2012).

In the last decade, the *Barley stripe mosaic virus* (BSMV) has become an increasingly popular vector for Virus-Induced Gene Silencing (VIGS) in barley and wheat (Lee et al., 2012). This is due to the availability of full-length infectious BSMV clones and a detailed knowledge of the molecular and biological functions of its various genome components. The BSMV vector can also be used for heterologous protein overexpression *in planta* (VOX - Virus-mediated Overexpression) (Figure 1.9), although there is a limitation. One caveat is predominately associated with the size of the protein that can be stably expressed form the vector (Lee et al., 2012).

The first study using BSMV:VOX involved expression of the Green Fluorescent Protein (GFP) reporter in barley (Haupt et al., 2001, Lawrence & Jackson, 2001). However, the moderately large sequence encoding GFP-(~700bp) was unstable in the viral genome. Smaller inserts within the range of 140-bp to 500-bp have been shown to be relatively more stable than larger inserts when integrated into the BSMV genome (Scofield & Nelson, 2009).

BSMV-VOX constructs overexpressing the flavin-based fluorescent reporter protein iLOV, that is approximately half the size of GFP, were shown to be more stable than GFP when expressed in *N. benthamiana* leaves (Kostya Kanyuka, personal communication). Green fluorescence is visible in *N. benthamiana* systemic leaves five days after agro infiltration under UV light.

As the majority of fungal effectors described are small, i.e. less than 200aa (corresponding to 600bp), (Stergiopoulos & de Wit, 2009), BSMV-VOX should be a viable strategy for studying the function of these proteins *in planta* (Lee et al., 2012).

Protein overexpression using BSMV as a vector has been shown in barley, wheat and tobacco leaves via overexpressing ToxA from *Pyrenophora tritici-repentis*, the causal agent of tan spot disease in wheat. ToxA is secreted in the apoplastic space and induces necrosis on cultivars that are sensitive to the toxin. In these cultivars, the ToxA protein is internalised and interacts with a chloroplast-localised protein ToxA Binding Protein 1 (ToxABP1), resulting in cell death (Manning et al., 2007). Further experimentation revealed that overexpression of ToxA without a signal peptide in plants that do not normally internalise ToxA, still resulted in cell death (Manning et al., 2010).

Other strategies to overexpress fungal proteins of interest comprise transformation of yeast or bacteria strains with vectors that permit heterologous proteins or the coating of expression vectors onto microprojectile particles for bombardment, which delivers the constructs for transient protein expression directly into plant leaf cells. However, the first approach, although useful in many plant species, does not work very efficiently in cereals. The leaves in cereals are hard and local infiltration of purified protein or cells filtrate often causes damage. In addition, the effect is only locally and the protein is not expressed systemically. Microprojectile

particle bombardment can also lead to tissue damaged that that could be confused with effector-induced cell death (Wing-Sham Lee, personal communication).

The genome of BSMV is composed of three RNAs, one of which (RNAɣ) encodes a cysteine-rich ɣb protein, involved in viral pathogenicity. The methodology consists of heterologous sequences of interest that are typically inserted directly downstream of the stop codon of the ɣb ORF. The modified RNAɣ is mixed with RNAα and RNAβ and inoculated on the host plant. To study the function of these free heterologous proteins in plant cells, a small synthetic 2A gene encoding an autoproteolytic peptide has been inserted between the 3'-terminus of the ɣb ORF and the gene sequence coding for the heterologous protein. This enables self-processing (not shown) of the ensuing ɣb fusion protein during translation of the virally-encoded proteins, which occurs very soon after the entry of BSMV to the plant cell, thus releasing the free heterologous protein (effector protein of the *F. graminearum*) (Lee et al., 2012).

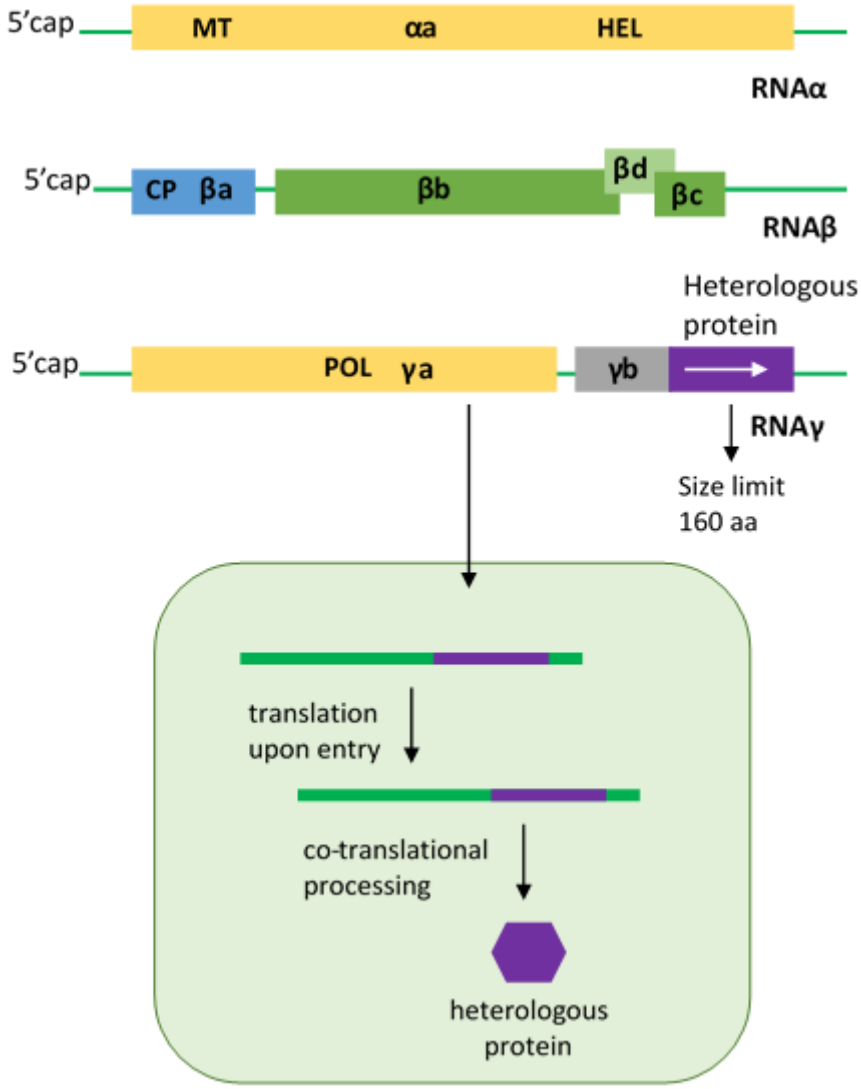

Figure 1.9 The Barley stripe mosaic virus (BSMV) genome and the mechanistic model for BSMV-VOX. Adapted from Lee et al. (2012).

1.10 Project aims, objectives and hypothesis to be tested

In this PhD project, I aimed to identify *F. graminearum* effectors that are able to suppress wheat defence responses in fully susceptible wheat cultivar infected by *F. graminearum*. The *Barley Stripe Mosaic Virus*-mediated overexpression system, BSMV-VOX, was used to identify putative *F. graminearum* effectors *in planta* (Lee et al., 2012).

During this project, the main objectives were:

- Genome sequencing of eight Brazilian *F. graminearum* strains and prediction of the core secretome.

- Selection of *F. graminearum* small secreted proteins (FgSSPs) of interest to be overexpressed *in planta* using BSMV-VOX

- Identification of FgSSPs that affect the FEB outcome (putative effectors).

- Define the mechanism(s) of action of putative *F. graminearum* effectors.

- Determine the importance and/or prevalence of these effectors in *F. graminearum* strains.

The identification of *F. graminearum* effector proteins will help us understand how *F. graminearum* induces disease, which is important for the generation of new control strategies.

The results generated in this thesis will be used to test the following hypothesis:

- *F. graminearum* genome and secretome are well conserved among different strains.

- The use of a predicted secretome in combination with early *in planta* generated transcriptome data is a powerful tool to predict putative effectors.

- BSMV-VOX is an alternative approach to study the role of putative fungal effectors during host infection.

- Proteins selected as putative effectors are able to suppress plant defence responses.

- Putative effectors that are able to suppress plant defence responses are important for fungal virulence.

Chapter 2 – General Materials and Methods

2.1 Plant material and growth conditions

Nicotiana benthamiana plants used for the preparation of BSMV sap inoculum and *F. graminearum* inoculations, and wheat plants (*Triticum aestivum*) cultivars Bobwhite, used for BSMV-VOX and *F. graminearum* inoculations, were grown in Rothamsted soil mix and grown in a controlled environment chamber (Fitotron®) at 23°C (light) and 18°C (dark), 60% relative humidity, with a 16-h light photoperiod (approximately 180µmol m^{-2} per second of light). *N. benthamiana* were sown onto 36cm^2 wide pots and 7.5cm deep, and wheat seeds were sown onto 72cm^2 wide pots and 9cm deep. *Arabidopsis thaliana* plants ecotype Landsberg erect (Ler-0), used for *F. graminearum* inoculation, were grown in Levingtons F2+S compost (Ipswich, UK) in a controlled environment chamber (Fitotron®) at 20°C (light) and 17°C (dark), 70% relative humidity, with a 16-h light photoperiod (approximately 200µmol m^{-2} per second of light). Seeds were sown onto 40 well trays (each well is 16cm^2 wide and 5cm deep). The seeds were put in the dark at 5°C for four days for stratification, and then transferred to the growth chamber.

2.2 Fungal strains

The *F. graminearum* strain used for BSMV-VOX experiments and fungal transformation was PH-1 (NRRL31084). This strain originated from the USA, is a DON/15-ADON producer (Goswami & Kistler, 2005), and is fully pathogenic on hexaploid wheat (*Triticum aestivum)* spring habit cv. Bobwhite (Urban et al., 2003) and *Arabidopsis thaliana* ecotype Landsberg (Urban et al., 2002). The eight *F. graminearum* strains used for genome sequencing were CML3064 to

CML3071 (see table 3.1). Fungal strains stored in 15% glycerol at -80ºC were grown on SNA plates (synthetic nutrient poor agar - 1 g KH_2PO_4,1g KNO_3,0.5 g $MgSO_4 7H_2O$, 0.5 g KCl, 0.2 g glucose, 0.2 g sucrose, 0.6ml NaOH (1 M), 20 g agar/l sterile distilled water). Ninety milometers diameter plastic Petri dishes were incubated at room temperature under constant illumination from one near UV-tube (Phillips 36W/08) and one white light-tube (Phillips TLD 36W/830HF). To remove old conidia and induce fresh conidia formation, 8 days-old SNA plates were washed with an overlay of TB3 (0.3% yeast extract, 0.3% Bacto Peptone, 20% sucrose) and on day 10, conidia were harvested in sterile water and adjusted to a concentration of $5x10^5$ spores.ml^{-1} water for both spray and point-inoculations (Cuzick et al., 2008). Studies with *F. graminearum* strains from Brazil, PH-1 and generated mutants were conducted under Defra licence 101948/198285/4.

2.3 *Fusarium graminearum* growth rate on PDA media

F. graminearum strains were grown on potato dextrose agar (PDA) plates in the dark at 25ºC. After three days, the diameter of fungal colonies was measured. Strains were plated in triplicate (Leslie & Summerell, 2008).

2.4 *Fusarium graminearum* perithecia production

F. graminearum strains were grown on carrot agar (CA) plates at 25ºC for 7 days under light. After one week of incubation, 0,5ml of a 2.5% Tween 60 suspension was added to the culture. The perithecia formation was assessed after 14 days (Leslie & Summerell, 2008).

DNA AND RNA MANIPULATIONS

2.5 Genomic DNA extraction

F. graminearum strains were grown in potato dextrose broth (PDB) or YPD (1% yeast extract, 2% peptone, 2% dextrose) liquid culture, with shaking at 100 rpm at 25ºC for 3 days. The fungal hyphae were vacuum filtrated (KNF Laboport®, USA), washed in sterile water, dried and stored at 4°C.

Genomic DNA was extracted using the cetyltrimethylammonium bromide (CTAB) protocol, as described previously (Xu & Leslie, 1996), using 50ml tubes with 20ml of CTAB buffer per sample (100 mM Tris-HCl [pH 8], 1.4 M NaCl, 25 mM EDTA, 2% CTAB). The purified DNA products were quantified by NanoDrop 2000c spectrophotometer (Thermo Fisher Scientific, Waltham, MA, USA).

2.6 Polymerase Chain Reaction (PCR) analyses

PCR was done using either REDTaq Ready Mix PCR reaction mix for colony PCR and confirm transformation, Phusion High Fidelity PCR Master Mix with HF Buffer (New English Biolabs, USA) where sequencing of product was required, or HotStarTaq Master Mix Kit (Qiagen) for bulk PCR. Reactions were done using a Bio-Rad T100 thermal cycler.

2.7 Gel Electrophoresis

F. graminearum genomic DNA, DNA amplified by PCR reactions and cDNA were visualised on 1% agarose gel (Fisher Scientific, UK) made using 1xTBE (Tris borate EDTA). Ethidium bromide solution (10mg/ml) was added to give a final dye concentration of 0.5µg/ml. The gels were run in a horizontal tank apparatus in 1xTBE. Typically, the gels were run at 80v for 40 minutes. After the run, the gels were visualised and photographed in UV transilluminator (Syngene, USA).

2.8 Primer design

Primers were designed using Primer3 (Koressaar & Remm, 2007, Untergasser et al., 2012) software within the Geneious programme (https://www.geneious.com/) (Biomatters Limited) and synthesised by Eurofins Genomics (Ebersberg, Germany).

2.9 RNA extraction from wheat ears

Seven days after *Fg* inoculation, seven rachis internodes below the inoculated spikelet of each ear were individually excised and frozen in liquid nitrogen. A total of 15 dissected ears were pooled as one repetition. Three repetitions were used for *F. graminearum*-infected ears treatment and one for mock-inoculated ears. Samples were grind in liquid nitrogen with mortar and pestle. Total RNA was extracted using TRIzol® reagent (Invitrogen, USA) according to the manufacturer's protocol. Total RNA was precipitated in deionised water and stored at -80ºC. The purified RNA products were quantified by NanoDrop 2000c spectrophotometer (Thermo Fisher Scientific, Waltham, MA, USA).

2.10 RT-PCR

One microgram of total RNA was treated with RQ1 RNase-free DNase I (Promega, Madison, WI, U.S.A.) and was used for random primer-generated cDNA synthesis using High Capacity cDNA reverse transcription kit (Applied Biosystems, Foster City, CA, U.S.A.) according to the manufacturer's instructions. The resulting cDNA was subsequently amplified by PCR.

BSMV-VOX EXPERIMENTS

All BSMV-VOX experiments *in planta* were carried out in containment facility level 3.

2.11 Preparation of *Barley Stripe Mosaic Virus* - mediated overexpression (BSMV VOX) constructs

The BSMV-VOX system, which comprises three T-DNA binary plasmids, namely pCaBS-α, pCaBS-β, and pCassRZ-ɣb-2A-LIC (Figure 2.1) (Yuan et al., 2011, Lee et al., 2012) was used in this study. Each construct was created by cloning each of the selected *F. graminearum* genes (FgSSP4, FgSSP5, FgSSP8, FgSSP9, FgSSP11, FgSSP6, FgSSP6-K$, which lacks the C-terminal lysine residue, FgSSP6-SP and FgSSP7-SP, both of them lack signal peptide residues) into pCassRZ-ɣb-2A-LIC using a ligation-independent cloning (LIC) strategy (Aslanidis & Dejong, 1990). Standard reverse transcription-polymerase chain reaction (RT-PCR) was used to generate cDNA clones of the selected genes from total RNA extracted from wheat cv. Bobwhite ear tissue infected with *F. graminearum* PH-1 (5 days post inoculation (dpi)). Adaptors for Ligation-Independent Cloning (LIC) site were incorporated at the 5' and 3' ends of the effector gene sequences for cloning into pCassRZ- ɣb-2A-LIC via PCR using primers listed in table 2.1.

The BSMV pCaBS-α, pCaBS-β, and pCassRZ-ɣb-2A-LIC derivatives were transformed separately into *Agrobacterium tumefaciens* strain GV3101 by electroporation (Sambrook et al., 2006). After electroporation, the cells were grown in 2-3 ml of Lysogeny Broth (LB) lennox (10g/L tryptone, 5g/L yeast extract, 5g/L sodium chloride) at 28ºC for 2 hrs and then plated on LB agar plates containing 50µg.ml^{-1} of kanamycin.

For controls, BSMV:MCS4D was used. BSMV: MCS4D has a multiple cloning site containing only non-coding sequence inserted into the BSMVγ plasmid (W-S. Lee, unpublished). This construct does not produce any protein and therefore, has no involvement or effect on the wheat - *F. graminearum* interaction. Also, it does not appear to affect either virus replication or *F. graminearum* proliferation in wheat ears (Lee, unpublished).

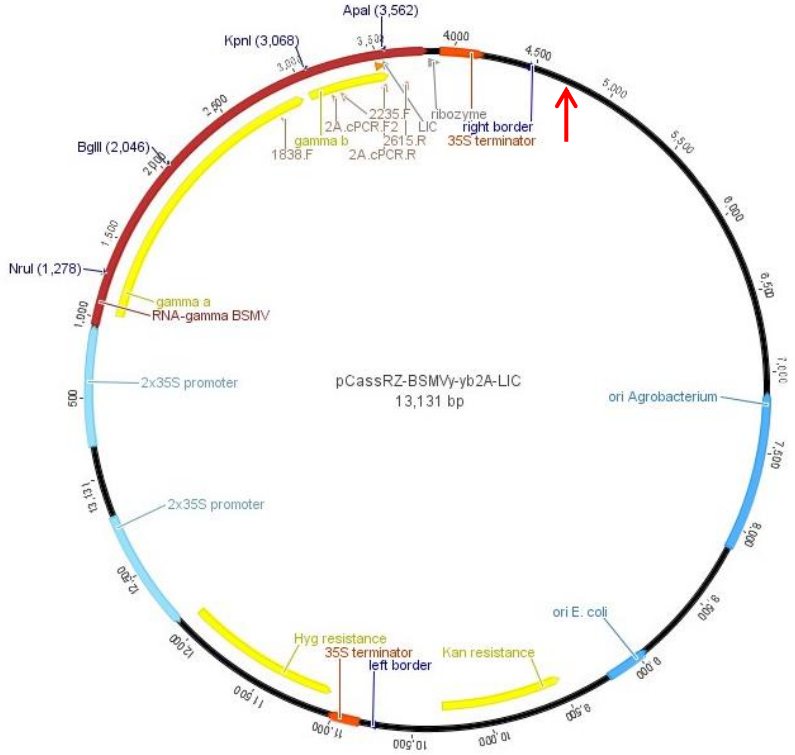

Figure 2.1 Schematic representation of the BSMV vector pCassRZ-BSMVγ-yb2A-LIC used in this study. In the schematic drawings of the vectors the main features are indicated. The red arrow indicates where the target gene sequence is inserted.

2.12 *Nicotiana benthamiana* viral inoculation

For agroinfiltration of *N. benthamiana* plants with Agrobacterium cultures carrying BSMV genome components, single colonies were grown for 20 to 22h at 28°C with constant shaking in 5ml of LB lennox (10g/L tryptone, 5g/L yeast extract, 5g/L sodium chloride) broth containing 50µg.ml^{-1} of kanamycin. Bacterial

cells were pelleted by centrifugation at 2,400 × *g* for 15 min at 4°C and re-suspended in agroinfiltration buffer [10mM $MgCl_2$, 10mM 2-(*N*-morpholino) ethanesulfonic acid (MES), pH5.6, and 0.1mM acetosyringone] to a final optical density at 600nm of 1.5 for generating viral inoculum for subsequent wheat inoculations. For experiments involving *F. graminearum* inoculation in *N. benthamiana* leaves an OD600 of 1.0 was used. After a 3-h incubation at room temperature, agrobacteria containing pCaBS-α, pCaBS-β, and the relevant pCassRZ-ɣb-2A-LIC derivative were mixed in a 1:1:1 ratio and infiltrated into the abaxial side of the leaves of 4-week-old *N. benthamiana* plants with a 1-ml needleless syringe. The infiltrated leaves were harvested at 5 days post-infiltration for subsequent wheat viral inoculation if required.

2.13 Wheat viral inoculation

For virus inoculation onto wheat leaves, *N. benthamiana* sap infiltrated with BSMV genome-transformed *Agrobacterium tumefaciens* (BSMV pCaBS-α, pCaBS-β, and pCassRZ-ɣb-2A-LIC derivatives) were used as inoculum. Wheat viral inoculation was carried out on ~ 42 days-old plants, when the main tiller was in early boot stage. The virus-containing sap was inoculated on the last two completely expanded leaves on the main tiller, which was usually the first leaf below the flag leaf (i.e. leaf 2) and the flag leaf (leaf 1).

Eight days after viral inoculation typical mild mosaic symptoms were visible, excluding the no virus inoculated plants. The treatments tested were BSMV:FgSSP2, BSMV:FgSSP4, BSMV:FgSSP6, BSMV:FgSSP6(-K$) and BSMV:FgSSP7 plus the controls (BSMV:iLOV, BSMV:MCS4D and no virus inoculation). The wheat cv. Bobwhite was used and ten replicates were used for each treatment in all experiments.

2.14 *Fusarium graminearum* wheat inoculation

For point-inoculations of wheat ears cv. Bobwhite, at the first appearance of anther extrusion, 5µl of a $5x10^5$ spores.ml^{-1} *F. graminearum* PH-1 conidial suspension was placed in the floral cavity between the palea and lemma of the outer two florets in the mid-region of the ear. Some of the no virus infected plants were inoculated with water only, as a control. The 13th and 14th spikelets (counting from the bottom of the ear) were point inoculated in each case.

Inoculated plants were placed inside transparent boxes to retain high humidity for the first 48h (with the first 24h in the dark) and were then returned to 60% relative humidity for up to 20 days. Disease progress was recorded by counting the number of visibly diseased spikelets below the inoculation points on each wheat ear. Macroscopic disease symptoms were carefully monitored after fungal inoculation every three days, until 18 days after fungal inoculation.

2.15 *Fusarium graminearum* and *Nicotiana benthamiana* inoculation

The 2nd systemically infected *N. benthamiana* leaves showing mosaic symptoms were inoculated with *F. graminearum* 6 days post-agroinfiltration by removing a single yellow anther from a non-inoculated wheat ear with the aid of fine tweezers and depositing it onto the surface of *N. benthamiana* leaves. A 1µL droplet of *F. graminearum* spore suspension (at a concentration of $5x10^5$spores.ml^{-1}) was pipetted onto each anther on the leaf surface. The controls for this experiment were water pipetted onto an anther, or *F. graminearum* spore droplets placed directly onto the leaf surface without wounding or addition of an anther. After inoculation, all the plants were kept in high humidity chambers for

three days before being returned to 60% relative humidity where they were observed for an additional 15 days for macroscopic symptom development.

2.16 Microscopy analysis of *Fusarium graminearum* inoculation in *N. benthamiana*

At 17 days post- *F. graminearum* inoculation, *N. benthamiana* leaves were detached and placed in a humid chamber for 24 hours. The lesions were visualised using a stereomicroscope (Leica) and photographed. Samples were then fixed in 1M KOH, heated to 70°C for 30min, stained with aniline blue for 5min, placed on microscope slides, observed and analysed using a Zeiss 780 laser scanning confocal microscope.

2.17 Photography

A Nikon D80 digital camera with a Sigma DC MACRO HSM 17-70mm lens was used for image capture. Plants were photographed on black velvet under growth room lighting conditions without use of flash.

2.18 Statistical analyses

GenStat (release 16.1, 2013, VSN International Ltd, Hemel Hempstead, UK) was used for the statistical analyses. The proportion of diseased wheat spikelets from ears inoculated with *F. graminearum* were analysed using generalised linear modelling (GLM) assuming a Binomial distribution with a natural logarithm link function. The variate modelled was the number of diseased spikelets as a proportion of total number of spikelets below the inoculation point accounting for individual batches as a blocking term in the model. Significance of

model terms was assessed using approximate chi-squared-tests. Calculated mean proportions of diseased ears were output with standard errors.

For the statistical analysis of all VOX experiments, generalised linear mixed model (GLMM) was used assuming a Binomial distribution with logit link function. The random factors of the model are described by batches nested within experiments. The factor treatment is the fixed effect, where the number of diseased spikelets was the explanatory variable examined.

2.19 *Fusarium graminearum* genes deletion

For deletion construct synthesis, the "split-marker" deletion strategy was applied previously developed for *Saccharomyces cerevisiae* (Fairhead et al., 1996, Fairhead et al., 1998). For the split-marker deletion method, two constructs are required per transformation, each containing a flank of the target gene and roughly two thirds of a selectable marker cassette. Homologous recombination between the overlapping regions of the selectable marker gene and between the flank regions and their genome counterparts results in a targeted gene deletion and replacement with an intact marker gene (Catlett et al., 2003).

Following the identification of target genes from *F. graminearum*, two thirds of each end (5' prime end and 3' prime end) of the selectable marker and 1kb fragment of both 5' and 3' flank regions of each gene were amplified using the primers described on table 2.1. The resulting amplicon was gel purified using Qiagen gel extraction kit QIAstock.

The purified fragments containing either the 5′ flank sequence and the two thirds of 5' prime end amplified selectable marker or 3′ flank sequence and the two thirds of 3' prime end amplified selectable marker were inserted into the EcoRV restriction site of pGEM®-T Easy Vector (Promega) using the Gibson

assembly kit (New England Biolabs,USA) according to the manufacturer's protocol.

The resulting vector was used to transform protoplasts of *F. graminearum* strain PH-1, as described previously (Hohn & Desjardins, 1992). Resistant transformants (Hygromycin or geneticin) were selected in REG medium (0.7% agarose, 0.2% Yeast Extract, 0.2% Casein-Hydrolysate (N-Z-Amine A), 0.8M sucrose) containing either 75 µg/ml of hygromycin B or 50 µg/ml of geneticin. The transformants were then screened by PCR using the primers listed in table 2.1.

Table 2.1 Primers used in this study

Primers	Sequence: 5'-3' #	Orientation	Application
LIC_FG 15123 F	CCAACCCAGGACCGTTG**ATG**A AGTTCTCTATCGCCGCC	anti-sense	Cloning FGRRES_15123 for VOX
LIC_FG 15123 R	AACCACCACCACCG**CTA**AGGA CCGGGAGGGTAACC	anti-sense	Cloning FGRRES_15123 for VOX
FOT_49-F- 5'LIC-OE	CCAACCCAGGACCGTTG**ATG**C AGTTCTCTCTCGCCACCCTT	sense	Cloning FGRRES_ 05046 for VOX
FOT_50-R- 5'LIC-OE	AACCACCACCACCG**TTA**GTTG ACTTTGGCCTGTCCAAG	anti-sense	Cloning FGRRES_05046 for VOX
FOT_51-F- 5'LIC-OE	CCAACCCAGGACCGTTG**ATG**C AGTTCTCTACTCTCACCACT	sense	Cloning FGRRES_09066 for VOX
FOT_52-R-5'LIC-OE	AACCACCACCACCG**CTA**GAGG AGCTTGACACAGTTGAG	anti-sense	Cloning FGRRES_09066 for VOX
FOT_53-F- 5'LIC-OE	CCAACCCAGGACCGTTG**ATG**A AGTTCACTGGTATCCTCTCT	sense	Cloning FGRRES_10212 for VOX
FOT_54-R-5'LIC-OE	AACCACCACCACCG**CTA**CTTC TTGAGGCCACAAGCAGA	anti-sense	Cloning FGRRES_10212 for VOX
FOT_55-F- 5'LIC-OE	CCAACCCAGGACCGTTG**ATG**T TGGCCAAGGTCTTTAGCGTT	sense	Cloning FGRRES_11047 for VOX
FOT_56-R-5'LIC-OE	AACCACCACCACCG**CTA**GCAA CGGCCACGAACCTCCTT	anti-sense	Cloning FGRRES_11047 for VOX
FOT_57-F- 5'LIC-OE	CCAACCCAGGACCGTTG**ATG**C AGCTGACCAACCTCTTCTGT	sense	Cloning FGRRES_11205 for VOX

FOT_58-R- 5'LIC-OE	AACCACCACCACCG**CTA**TTTCTTCAATCCACAGTTGCT	anti-sense	Cloning FGRRES_11205 for VOX
FOT_67-F- 5'LIC-OE	CCAACCCAGGACCGTTG**ATG**AAGACTACAATCTTTGTCACG	sense	Cloning FGRRES_ 08493 for VOX
FOT_68-R- 5'LIC-OE	AACCACCACCACCG**CTA**ACCACGCTGACGAGCGCAGCC	anti-sense	Cloning FGRRES_08493 for VOX
MLIC FG11190 VOX F	CCAACCCAGGACCGTTG**ATG**CTCTTCTTCAAGTCTATCGTC	sense	Cloning FGRRES_11190 for VOX
MLIC FG11190 VOX R	AACCACCACCACCG**CTA**TTAGCTAGTGCCAGTGCAGC	anti-sense	Cloning FGRRES_11190 for VOX
MLIC FG03599 VOX F	CCAACCCAGGACCGTTG**ATG**CAGTTCACCACCTCCTTCATC	sense	Cloning FGRRES_03599 for VOX
MLIC FG03599 VOX R	AACCACCACCACCG**CTA**AGCACAGGCAGTGCAGACG	anti-sense	Cloning FGRRES_03599 for VOX
FOT_65-F- 5'LIC-OE	CCAACCCAGGACCGTTG**ATG**AAGTTCTCCGCTGCCGTCTTC	sense	Cloning FGRRES_04583 for VOX
FOT_66-R- 5'LIC-OE	AACCACCACCACCG**CTA**TTTGGGGAGCGAAGCAGGAGC	anti-sense	Cloning FGRRES_04583 for VOX
MFG10212 VOX – KR	AACCACCACCACCG**CTA**CTTGAGGCCACAAGCAGAAGG	anti-sense	Cloning FGRRES_10212 for VOX without K$
MLIC11190VOX - SPF	CCAACCCAGGACCGTTG**ATG**AGCCCCATCCTCGAGAC	sense	Cloning FGRRES_11190 for VOX without signal peptide
MFG10212VOX - SPF	CCAACCCAGGACCGTTG**ATG**ACCACTGTCTCCTACGACAC	sense	Cloning FGRRES_10212 for VOX without signal peptide
MFG11205VOX - SPF	CCAACCCAGGACCGTTG**ATG**ATCACCGTATCCTACGACC	sense	Cloning FGRRES_11205 for VOX without signal peptide
MLICBcPepA VOXF	CCAACCCAGGACCGTTG**ATG**GTCTCCTGCTCCGACGGAAG	sense	Cloning *Botrytis cinerea* PepA[1] for VOX
MLICBcPepA VOXR	AACCACCACCACCG**CTA**GAGTCCGTTGCTTCCGTCGG	anti-sense	Cloning *Botrytis cinerea* PepA[1] for VOX
MLICBcPepB VOXF	CCAACCCAGGACCGTTG**ATG**GTCGTCGCCGGCTGGAACGA	sense	Cloning *Botrytis cinerea* PepB[1] for VOX
MLICBcPepB VOXR	AACCACCACCACCG**CTA**ACAGTTGGCATCGTTCCAGC	anti-sense	Cloning *Botrytis cinerea* PepB[1] for VOX

MLICFgPepB VOXF	CCAACCCAGGACCGTTG**ATG**ATCATCGCTGGCTGGAACTC	sense	Cloning *F. graminearum* PepB for VOX
MLICFgPepB VOXR	AACCACCACCACCG**CTA**GCAGTTGGGGGAGTTCCAGC	anti-sense	Cloning *F. graminearum* PepB for VOX
M_FgSSP6attB1 F	GGGGACAAGTTTGTACAAAAAAGCAGGCTTA**ATG**ACCACTGTCTCCTACGACACT	sense	Gateway cloning FGRRES_10212 for recombinant protein expression
M_FgSSP6attB2 R	GGGGACCACTTTGTACAAGAAAGCTGGGTA**TTA**CTTCTTGAGGCCACAAGCAGA	anti-sense	Gateway cloning FGRRES_10212 for recombinant protein expression
M_FgSSP7attB1 F	GGGGACAAGTTTGTACAAAAAAGCAGGCTTA**ATG**ATCACCGTATCCTACGACCCA	sense	Gateway cloning FGRRES_11205 for recombinant protein expression
M_FgSSP7attB2 R	GGGGACCACTTTGTACAAGAAAGCTGGGTA**CTA**TTTCTTCAATCCACAGTTGCT	anti-sense	Gateway cloning FGRRES_11205 for recombinant protein expression
PGEMt Fg55' F	CCGCGGGAATTCGATGGGGTTGAATAGAGTGAGGC	sense	5’ flank of FGRRES_15123 for gene deletion
PGEMt Fg55' R	CATAGCTGTACTGAAGAAGTAAGGGACGATTTTC	anti-sense	5’ flank of FGRRES_15123 for gene deletion
PGEMt Fg55'HY F	TTCTTCAGTACAGCTATGACCATGATTACGCC	sense	two thirds size of 5’ prime end hygromycin for gene deletion
PGEMt HY R	GCGAATTCACTAGTGATGGATGCCTCCGCTCGAAG	anti-sense	two thirds of 5’ prime end hygromycin for gene deletion
PGEMt YG F	CCGCGGGAATTCGATCGTTGCAAGACCTGCCTG	sense	two thirds of 3’ prime end hygromycin for gene deletion
PGEMt YGFg53' R	GATTCTCTCAATTGTAAAACGACGGCCAG	anti-sense	two thirds of 3’ prime end hygromycin for gene deletion
PGEMt Fg53' F	CGTTTTACAATTGAGAGAATCGCTTGTCAG	sense	3’ flank of FGRRES_15123 for gene deletion
PGEMt Fg53' R	GCGAATTCACTAGTGATTAGCACTGTGAAGACCCC	anti-sense	3’ flank of FGRRES_15123 for gene deletion
PGEMt Fg65' F	CCGCGGGAATTCGATCGTGACCATACGGGAATAGG	sense	5’ flank of FGRRES_10212 for gene deletion
PGEMt Fg65' R	CATAGCTGTGTTGACGGTTGTGGGTTTTTG	anti-sense	5’ flank of FGRRES_10212 for gene deletion
PGEMt Fg65'HY F	CCGTCAACACAGCTATGACCATGATTACGCC	sense	two thirds size of 5’ prime end hygromycin for gene deletion

PGEMt YGFg63' R	TGCAGCCGTTGTAAAACGACG GCCAG	anti-sense	two thirds of 3' prime end hygromycin for gene deletion
PGEMt Fg63' F	CGTTTTACAACGGCTGCAACTC TACGAC	sense	3' flank of FGRRES_10212 for gene deletion
PGEMt Fg63' R	GCGAATTCACTAGTGATCATGT GCTCAGAAGATGTCATAAG	anti-sense	3' flank of FGRRES_10212 for gene deletion
PGEMt Fg75' F	CCGCGGGAATTCGATACTGCA GCCGAGTATTAGCC	sense	5' flank of FGRRES_11205 for gene deletion
PGEMt Fg75' R	CATAGCTGTGTGCGATGCTTT GGGTGA	anti-sense	5' flank of FGRRES_11205 for gene deletion
PGEMt Fg75'HY F	CATCGCACACAGCTATGACCA TGATTACGCC	sense	two thirds size of 5' prime end hygromycin for gene deletion
PGEMt YGFg73' R	CAACCTTCTTGTAAAACGACGG CCAG	anti-sense	two thirds of 3' prime end hygromycin for gene deletion
PGEMt Fg73' F	CGTTTTACAAGAAGGTTGTTTG GTTGTGTTG	sense	3' flank of FGRRES_11205 for gene deletion
PGEMt Fg73' R	GCGAATTCACTAGTGATAGACT TGTCGGCTGTTGATAC	anti-sense	3' flank of FGRRES_11205 for gene deletion
PGEMt Fg65' F	CCGCGGGAATTCGATGAAGGA ATACGAGGGTTAAAGG	sense	5' flank of FGRRES_10212 for gene deletion
PGEMt Fg65' R	TTCTGTCGTTGACGGTTGTGG GTTTTTG	anti-sense	5' flank of FGRRES_10212 for gene deletion
PGEMt Fg65'Gen1 F	ACCGTCAACGACAGAAGATGA TATTGAAG	sense	two thirds size of 5' prime end geneticin for gene deletion
PGEMt Gen2Fg63' R	GTTGCAGCGCACAGGTACACT TGTTTAGAGGG	anti-sense	two thirds of 3' prime end geneticin for gene deletion
PGEMt Fg63' F	ACCTGTGCGCTGCAACTCTAC GACTTTTATG	sense	3' flank of FGRRES_10212 for gene deletion
PGEMt Fg63' R	GCGAATTCACTAGTGATATATG GGCTCGAATATGAAC	anti-sense	3' flank of FGRRES_10212 for gene deletion
GC1 (MU) R (Hyg R conf)	ACTTCTCGACAGACGTCGC	sense	5' Hygromycin for confirmation of transformation
GC2 (MU) F (Hyg F conf)	TGGCTGTGTAGAAGTACTCG	anti-sense	3' Hygromycin for confirmation of transformation
Fg5 flank5' conf F	TGACATCCAAGACTAGGCGC	sense	5' External region of FGRRES_15123 flank for confirmation of transformation

Fg5 flank3' conf R	CATCACAACACGATGCACCT	anti-sense	3' External region of FGRRES_15123 flank for confirmation of transformation
Fg7 flank5' conf F	TCAGGGCGGTAATGTAAACG	sense	5' External region of FGRRES_11205 flank for confirmation of transformation
Fg7 flank3' conf R	TGGTGCGCATTTAAACGAAC	anti-sense	5' External region of FGRRES_11205 flank for confirmation of transformation
Fgactin 61 F	ATGGTGTCACTCACGTTGTCC	sense	*Fg* Actin (FGRRES_07335) to confirm presence of the fragment
Fgactin 61 R	CAGTGGTGGAGAAGGTGTAACC	anti-sense	*Fg* Actin (FGRRES_07335) to confirm presence of the fragment
FGRRES10212_F	ACCAAGTACATCGGTGGTGTC	sense	*Fg*SSP6 (FGRRES_10212) to confirm presence of the fragment
FGRRES10212_R	CATCGAGGCCAATGTTGAAGC	anti-sense	*Fg*SSP6 (FGRRES_10212) to confirm presence of the fragment
FGRRES11205_F	AGTTTCCCTACATTGGCGGC	sense	*Fg*SSP7 (FGRRES_11205) to confirm presence of the fragment
FGRRES11205_R	GGAGAAATGTTGAAGCCCGC	anti-sense	*Fg*SSP7 (FGRRES_11205) to confirm presence of the fragment
FGRRES15123_F	CAGCAAGTCCTGTTCAGGAGAG	sense	*Fg*SSP5 (FGRRES_15123) to confirm presence of the fragment
FGRRES15123_R	TGCAACCACGAGACCAAGTATT	anti-sense	*Fg*SSP5 (FGRRES_15123) to confirm presence of the fragment

* Abbreviation. VOX = Virus-mediated overexpression

Sequences underlined are the adaptor sequences used for ligation-independent cloning

[1] Two peptides sequences from BcSpl1 (Cerato-platanin from *Botrytis cinerea*) – Frias *et al.*, 2014, *Molecular Plant Pathology*

2.20 Arabidopsis – *F. graminearum* spray inoculation

Inoculations were done as described in Urban et al. (2002). Arabidopsis plants ecotype Landsberg erecta (Ler-0) with 2-3 open flowers but no siliques (Growth stage 6) (Boyes et al., 2001) were spray inoculated with *F. graminearum* conidia suspension ($1x10^6$ spores.ml^{-1}) using 15ml spray bottles. Each plant received approximately 0.5ml of suspension. Control plants were treated with

sterile water. Inoculated plants were kept in Perspex boxes (50 x 50 x 100 cm) at 100% humidity for 7 days, with the first 24h in the dark. At 7 dpi, visible infection symptoms on the flowers and developing siliques were assessed using the Fusarium – Arabidopsis Disease (FAD) scoring system described in Urban et al. (2002) (table 2.2).

Table 2.2 Scoring of *F. graminearum* disease in Arabidopsis floral and silique tissue. Adapted from Urban et al. (2002)

Organ	***Score***	***Description of disease phenotype***
Flower (F)	0	Normal
	1	Aerial mycelium visible on flower
	3	Drying of flowers
	5	Stem constriction within flower head
Siliques (S)	0	Normal
	1	Aerial mycelium on silique surface
	3	Drying of silique surface
	5	Peduncle constriction or mycelium on peduncle or loss of siliques by disease travelling down stem
	7	Main stem constriction
Fusarium – Arabidopsis disease (FAD value) = F + S		

Chapter 3 – Inter-comparison of the genomes of *Fusarium graminearum* strains from Brazil, prediction of the core secretome and selection of genes for functional evaluation

3.1 Introduction

The *Fusarium graminearum* species complex (FGSC) comprises at least 16 recognised species (O'Donnell et al., 2008, O'Donnell et al., 2004, Sarver et al., 2011, Starkey et al., 2007, Yli-Mattila et al., 2009), of which *F. graminearum* is the most prevalent globally (Dweba et al., 2017) and the main causal agent of the FGSC-associated disease Fusarium Ear Blight (FEB).

In South America, at least six other species within the FGSC infect wheat and other cereal crops grown in Brazil, Argentina and Uruguay. These include *F. asiaticum, F. astroamericanum, F. boothii, F. brasilicum, F. cortaderiae* and *F. meridionale* (Astolfi et al., 2012, O'Donnell et al., 2004, Sampietro et al., 2011, Scoz et al., 2009, Umpierrez-Failache et al., 2013). In Brazil, a survey of more than 200 fields from two states (Parana and Rio Grande do Sul) responsible for approximately 90% of the national wheat production identified five species from the FGSC with three differential trichothecene genotypes (NIV, 3-ADON and 15-ADON) among the 671 FGSC isolates recovered from FEB - diseased wheat heads. This isolate collection comprised 83% *F. graminearum* of the 15-acetyldeoxynivalenol (15-ADON) genotype, 12.8% *F. meridionale* and 0.4% *F. asiaticum* of the nivalenol (NIV) genotype, and 2.5% *F. cortaderiae* and 0.9% *F. austroamericanum* with either the NIV or the 3-ADON genotype (Del Ponte et al., 2015). Data from the survey suggested that the FGSC composition and consequently, trichothecene contamination in wheat grown in southern Brazil is influenced by host adaptation and pathogenic fitness (Del Ponte et al., 2015). In

this region, where a humid subtropical climate and extensive no-till farming practices prevail, FEB results in extensive and significant yield loss of wheat grain (Spolti et al., 2015).

Due to the importance of this pathogen not only in South America, but also worldwide, *F. graminearum* was the first *Fusarium* species to have its genome sequenced. The strain PH-1 (NRRL 31084) originally isolated from Michigan state in North America with a 15A-DON genotype was used to generate the reference genome (Paper et al., 2007). Since selection, this strain has been used as a model for understanding *Fusarium* mycotoxin production, pathogenicity, signal transduction, transcription regulation, development, sexual and asexual reproduction, and many other biological processes and transcriptome analyses. The fully completed genome for the *F. graminearum* PH-1 strain, including fully sequenced centromeric and telomeric regions, has now been made available (King et al., 2015). The assembled supercontigs for the PH-1 genome have been assigned to four chromosomes by using information from a genetic map (Gale et al., 2005). The last re-annotation predicted a total of 14,164 gene models for PH-1 with low repetitive sequence content and an average genome size (36 Mb) for a filamentous ascomycete phytopathogen (Cuomo et al., 2007, King et al., 2015).

Currently, only a small number of other *F. graminearum* isolates have had their genomes fully sequenced, and these have originated from USA, Canada and Australia (Cuomo et al., 2007, Gardiner et al., 2014, Walkowiak et al., 2015).

Recently, in addition to whole genome sequencing of *F. graminearum* isolates, more attention has been given to predicting the secretome of this fungal species (Brown et al., 2012, Sperschneider et al., 2016). This interest is mainly

because most fungal effectors are likely to be secreted proteins, possibly with roles in shielding the fungus from the host, suppressing host immune responses, and/or manipulating host cell physiology to benefit fungal physiology (Okmen & Doehlemann, 2014, Stergiopoulos & de Wit, 2009, de Jonge et al., 2011). The broad definition of an effector is any secreted molecule that modulates the interaction between the pathogen and its host (Lo Presti et al., 2015). Therefore, understanding the role of different fungal effector proteins in disease interactions can be relevant towards discovering and developing new strategies for disease control. The identification of these putative effectors can be facilitated by predicting and inspecting the components of the candidate fungal secretome.

Fungal lifestyles and the degree of host specialisation may impact on the set of secreted proteins involved in different fungus-plant interactions. Effector identification usually includes identifying/predicting secreted proteins that also meet a defined set of different criteria. Multiple bioinformatics approaches are used to predict the effector repertoire. Usually, effectors are predicted to be small secreted proteins containing ≤300 amino acids which are rich in cysteine residues (5-10%), have disulphide bridges that form between cysteine residues are likely to stabilise their tertiary structure (Stergiopoulos et al., 2013). Therefore, these proteins may be able to maintain activity in the harsh plant apoplastic environment, as the increased efflux of H+, acidifying the apoplast or localised alkalinisation, causes stress. Another common feature of fungal effectors is the lack of identified orthologous proteins. However, these other criteria are not fully proved when defining effector proteins. Firstly, larger proteins have also been found to be effectors (Djamei et al., 2011) and some effectors are conserved between species or may possess conserved functional domains, for example the LysM domain (Marshall et al., 2011, Frias et al., 2011, Bolton et al., 2008).

Considering these uncertainties, any secreted fungal protein may potentially act as an effector and therefore the predicted repertoires of secreted proteins need to be inspected carefully.

The main aim of this study is to identify the common components of the secretome that are shared amongst the now sequenced eight *F. graminearum* strains from Brazil and the reference North American strain PH-1. This shared secretome may therefore have an important role in *F. graminearum* development and/or pathogenesis. These components will be collectively referred to as the 'core' secretome. These results were achieved by sequencing the whole genomes of eight *F. graminearum* strains isolated in Brazil during the period 2009-2011 and comparing the sequences with the *F. graminearum* reference strain PH-1 genome sequence isolated in 1996. The identified 'core' secretome was then used to narrow down the choice of putative effectors to be functionally tested using the BSMV-VOX system (Chapter 4). These results may help identify possible targets for intervention and hence new approaches to *F. graminearum* control.

3.2 Materials and Methods

3.2.1 Fungal strains

The *F. graminearum* strains used for genome sequencing are listed in table 3.1. These strains originated from Brazil and have all been verified as DON/15-ADON producers (Del Ponte et al., 2015). All eight isolates were collected in Rio Grande do Sul state in Brazil between 2009 and 2011 and provided by Professor Emerson del Ponte, from Federal University of Viçosa, Minas Gerais, Brazil. Before being sent to UK, the strains were deposited in the Coleção Micológica de Lavras (Lavras Mycological Collection) (CML) located at

the Federal University of Lavras, Minas Gerais, Brazil and permission was obtained from Professor Ludwig to export the strains. Fungal spores of each strain stored in 15% glycerol at -80ºC were grown on SNA plates (synthetic nutrient poor agar). The plates were incubated at room temperature under constant illumination from one near UV-tube (Phillips 36W/08) and one white light-tube (Phillips TLD 36W/830HF). To remove old conidia and induce fresh conidia formation, 8 days-old SNA plates were washed with an overlay of TB3 (0.3% yeast extract, 0.3% Bacto Peptone, 20% sucrose) and on day 10, conidia were harvested in sterile water and adjusted to a concentration of $5x10^5$ spores. ml^{-1} water for point-inoculation of wheat ears (Cuzick et al., 2008).

Table 3.1 The *Fusarium graminearum* strains from Brazil used for genome sequencing, *in vitro* growth and pathogenicity tests

CML code[1]	Mycotoxin genotype	Location where isolated	Year isolated	Host	Tissue of isolation	Reference
PH-1	15-ADON	USA	1996	wheat	kernels	O'Donnell et al. (2004)
CML 3064	15-ADON	Cruz Alta[2]	2007	wheat	kernels	Astolfi et al. (2012)
CML 3065	15-ADON	Panambi[2]	2009	wheat	spike	Del Ponte et al. (2015)
CML 3066	15-ADON	Ijuí[2]	2009	wheat	spike	Del Ponte et al. (2015)
CML 3067	15-ADON	Carazinho[2]	2010	wheat	spike	Del Ponte et al. (2015)
CML 3068	15-ADON	Ernestina[2]	2007	wheat	kernels	Astolfi et al. (2012)
CML 3069	15-ADON	Coxilha[2]	2010	wheat	spike	Del Ponte et al. (2015)
CML 3070	15-ADON	Santa Barbara do Sul[2]	2011	wheat	spike	Del Ponte et al. (2015)
CML 3071	15-ADON	Tapejara[2]	2010	wheat	spike	Del Ponte et al. (2015)

1. CML: Coleção Micológica de Lavras (Brazil)

2. Localised in Rio Grande do Sul state (Brazil)

3.2.2 Genome sequencing and assembly

Whole genome sequencing of Brazilian *F. graminearum* strains was conducted by The Genome Analysis Centre (TGAC – Norwich UK) using Illumina HiSeq2000 platform (short reads), 100bp paired-ends reads. The selected Brazilian reference sequence CML3066 was additionally sequenced using PacBio (long reads) with 100 smrt cells.

The *de novo* assembly was carried out using the software SOAPdenvo2 (version 2.0.4) for Illumina data for with the k-mer values of 61-99, and SMRT analysis portal for PacBio data. For the CML3066 isolate the PacBio sequence was gap filled and scaffolded using the complementary Illumina assembly. Reference sequence statistics were extracted from Geneious (version 8.1 created by Biomatters).

3.2.3 Genome annotation

The genome annotation of CML3066 was done using MAKER (version 2.30) (Cantarel et al., 2008) annotation pipeline with RepeatMasker (version 4.50) (Bedell et al., 2000).

Gene calls were generated using both AUGUSTUS (version 2.7) (Stanke et al., 2004) using *F. graminearum* species model, and GeneMark (Besemer & Borodovsky, 2005), which was trained using CML3066.

3.2.4 SNP calling

The sequencing reads of all eight Brazilian strains were aligned to *F. graminearum* [RRes v.5.0 from King et al. (2015)] or assembled CML3066 reference sequence using the software BWA (version 0.7.12-r1039), with default parameters. Alignments were converted from the sequence alignment map

(SAM) format to binary alignment map (BAM), and the BAM files were sorted and indexed using SAMtools (version 0.1.19). SNP calling was performed with SAMtools using default settings. SNP effects were predicted using snpEff (4.2 (2015-12-05)). Visualisations were done using Tablet (version 1.13.07.31). The SNP frequency for each gene were normalised by dividing by the transcript length and visualised using images generated using CIRCOS (v0.69).

3.2.5 Gene statistics, interproscan domain, GO and enzyme comparisons

Blast2GO V.3.2 was used with Decypher BLASTP search with an E-value of 0.001 against the NCBI nr database, filtered using Blast2GO annotation algorithm with settings, E-value filter 0.000001, Annotation CutOff 55, GO weight 5, Hsp-Hit Coverage CutOff 0, and GO and enzyme code annotated using a local GO database from sep/2015 with 41,436 GOs available and 4,098 Enzymes available. Interproscan results were imported into Blast2GO and the GO annotations merged.

3.2.6 Secretome identification

Blast2GO V.3.2 was used to identify signal peptide and transmembrane domains. ProtComp (Version 9.0) (ProtComp, 2011) and result columns, LocDB and PotLocDB (Rastogi & Rost, 2011) were used to exclude GPI anchored membrane proteins and other non-extracellular loci proteins. WoLfPSort (Horton et al., 2007) (extracellular score > 17, WoLfPSort) was used to predict cellular localisation and big-PI to identify GPI anchored proteins (Eisenhaber et al., 2004). Effector prediction of the secretome was carried out using EffectorP 1.0 (Sperschneider et al., 2016)

3.2.7 Identification of putative effectors

Protein domain analysis of predicted putative effectors was carried out using the Pfam database (http://pfam.xfam.org/search) (Finn et al., 2016). Blastp (https://blast.ncbi.nlm.nih.gov) was used for protein comparative analysis. An e-value threshold of 10^{-6} was used as a cut-off point to select proteins with a substantial level of similarity to proteins from one or more species.

To compare sequence similarities with previously described effectors from other pathogens, blast analysis was also conducted using the contents of PHI-base database version 4.0 (http://www.phi-base.org) (Urban et al., 2015a).

Comparisons at the 3D protein structure level of the *F. graminearum* effector subset to a protein database were made using the remote homology recognition software Phyre2 (Kelley et al., 2015a). For Phyre2, confidence and identity thresholds of 70% and 13%, respectively, were used.

The number of cysteine residues and the presence of consecutive cysteine residues, within the predicted mature peptide, were computed manually for each amino acid sequence.

To inspect the position of individual genes on the four *F. graminearum* chromosomes, the Fgra3Map tool was used according to methods described by Antoniw et al. (2011).

3.3 Results

Note: The genome assembly, annotation, circus plots and part of the bioinformatics predictions were done by Dr. Robert King, bioinformatician in the Computational & Systems Biology department at Rothamsted Research

3.3.1 Phenotypic tests *in vitro* and *in planta*

Before whole genome sequencing (WGS), the *F. graminearum* Brazilian isolates (Table 3.1) were inspected for phenotypic regarding *in vitro* mycelium growth and perithecia production, and pathogenicity on wheat ears. The *F. graminearum* strain CML3070 was not included in these analyses because it was initially misidentified as *F. meridionale*. Even though the strain CML3070 was not included in the phenotypic analysis due the initial misidentification, this isolate was send for WGS because it would be useful for another project with the aim of sequencing additional species within the Brazilian FGSC. Therefore, after genome sequencing, CML3070 was confirmed to be *F. graminearum* and then it was posteriorly included in the genome comparison analysis. To compare the *in vitro* growth between the different strains, the seven *F. graminearum* Brazilian strains and PH-1 were grown on nutrient-rich potato dextrose agar (PDA) plates in the dark at 25ºC. After three days, the diameter of the colonies was measured. When grown on PDA media, most of the seven imported Brazilian isolates grew at a similar diameter (~60-70 mm over three days) and had a similar appearance to PH-1 (Figure 3.1 and 3.2). The exceptions were CML3067 and CML3069. CML3067 had a growth of only ~35 mm over three days. CML3069 presented sectoring when cultured on PDA with differing visible characteristics, one sector grew slowly, in a similar fashion to CML3067, whilst the other sector grew at a similar extent to the other six strains under study (Figure 3.2)

The strains were also tested for the formation of perithecia on Carrot Agar (CA). All strains produced viable perithecia and therefore are homothallic as expected for *F. graminearum* (data not shown).

FEB disease progression in wheat ears of cultivar Bobwhite inoculated with *F. graminearum* strains from Brazil was assessed over 21 days. The strains

varied in the severity and extent of symptom development (Figure 3.3 and 3.4). Strains CML3064, CML3065 and CML3066 induced visible disease symptoms at a similar rate of progress to that of PH-1. These strains were classified together as the 'fully virulent' group. CML3068 and CML3071 induced reduced visible disease when compared to PH-1, and were classified as the intermediate virulent group. CML3067 and CML3069 were able to infect ears but spikelets below the inoculated florets developed fewer visible disease symptoms. With these isolates, disease was restricted to the inoculated spikelet or to those immediately below the inoculation points. CML3067 and CML3069 were classified as the weakly virulent group. It is notable that these two isolates also had reduced growth on PDA plates when compared to the remaining five Brazilian isolates or PH-1.

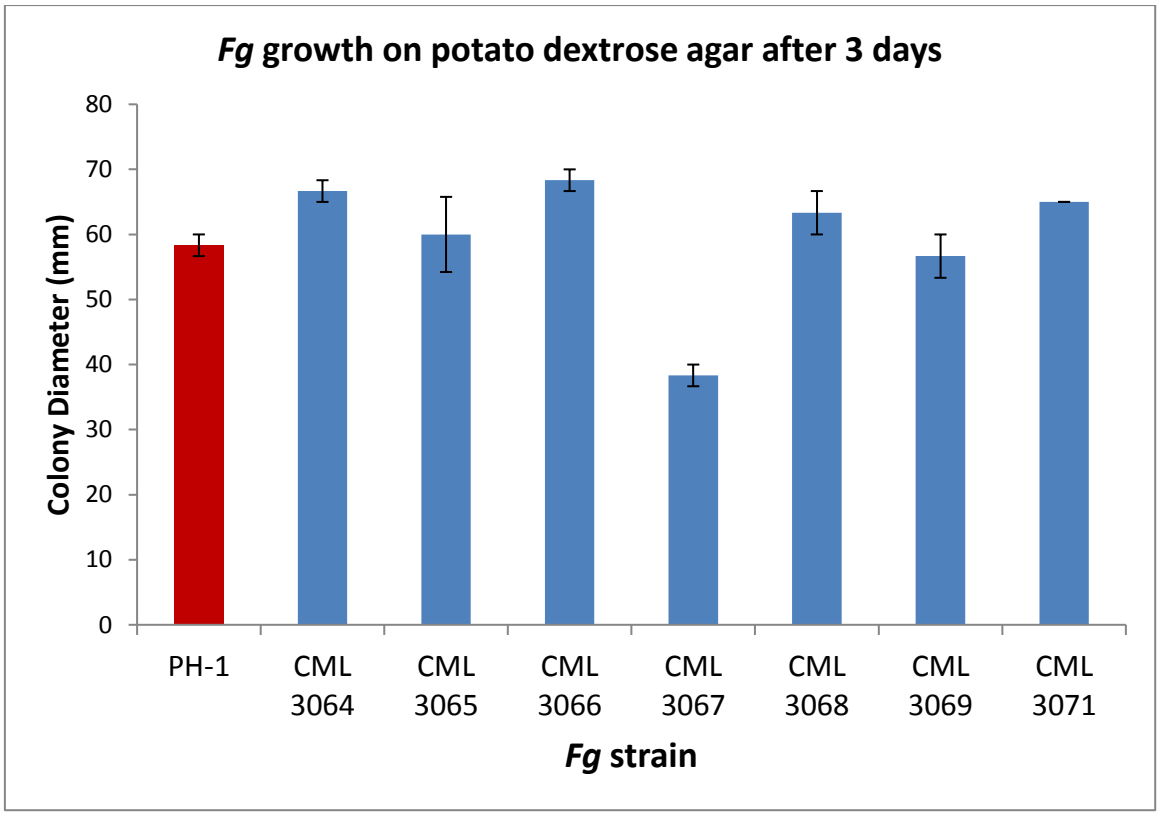

Figure 3.1 Mean colony diameters of *F. graminearum* strains grown on nutrient-rich agar (PDA). Growth of isolates originating from Brazil were compared to that of the reference isolate PH-1. Error bars represent mean ± s.e.m. of 3 replicates.

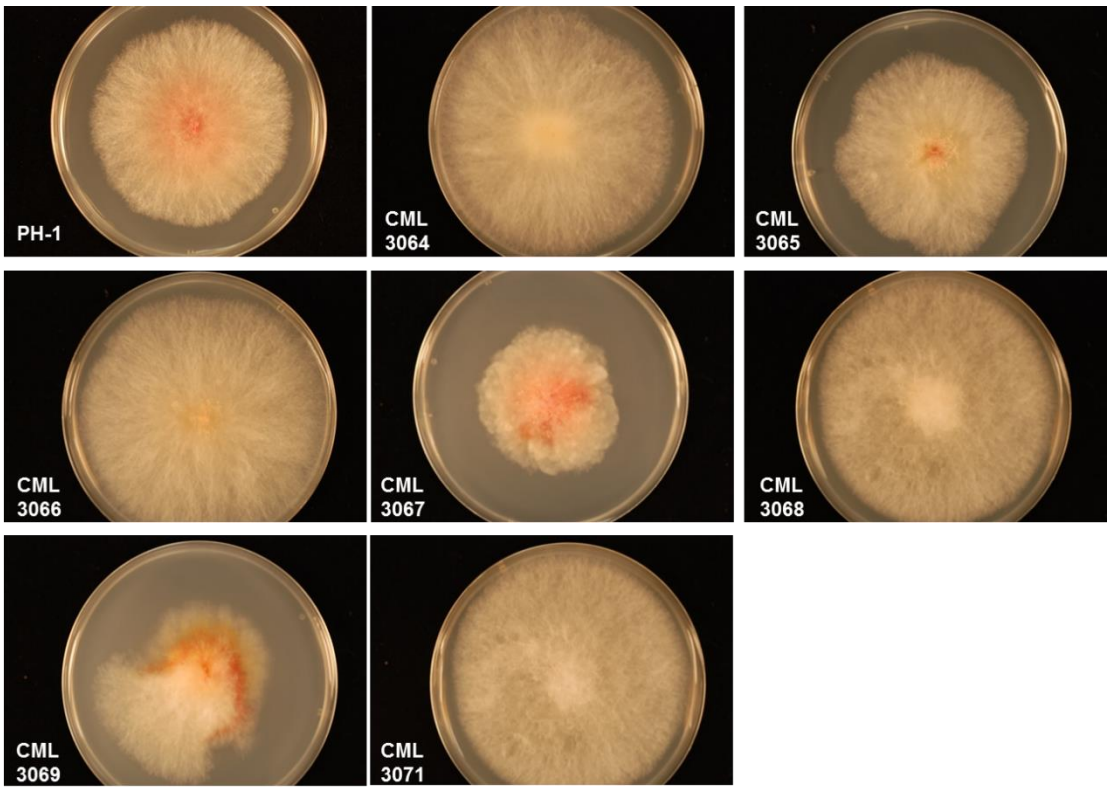

Figure 3.2 Representative colony growth in PDA after 3 days for PH-1 and seven *F. graminearum* strains from Brazil.

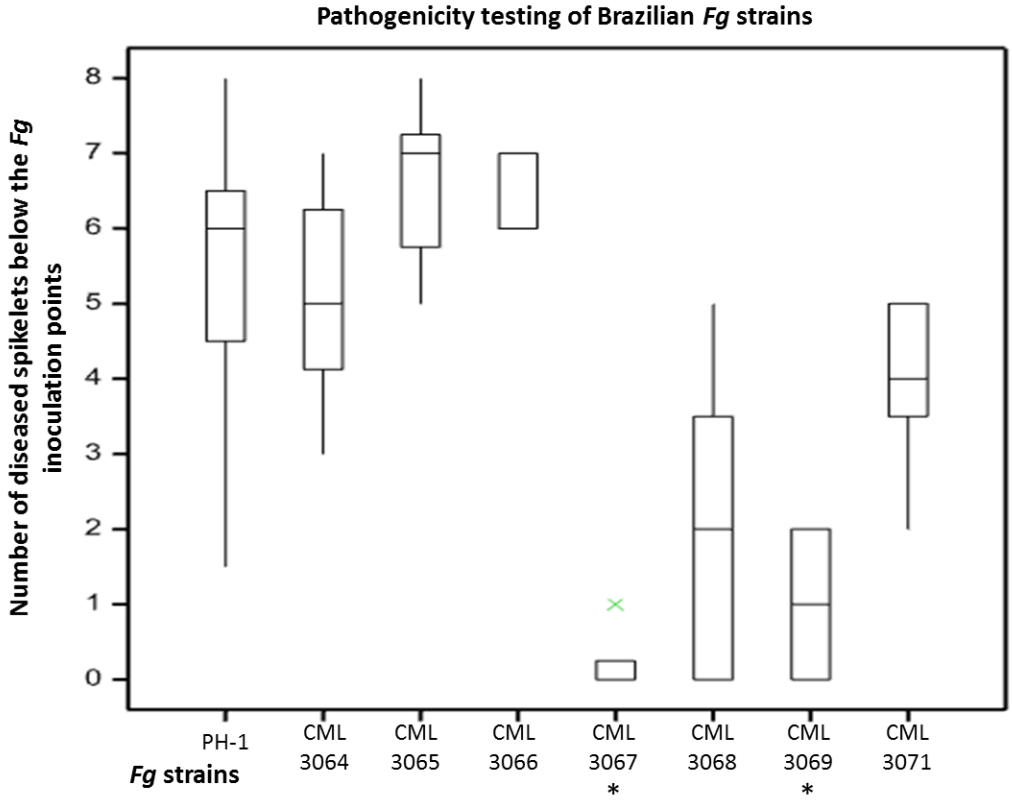

Figure 3.3 Box-plots representing the number of visibly diseased spikelets below those point-inoculated with Fusarium spores in *F. graminearum*-inoculated wheat ears (cv. Bobwhite) at 12 dpi. Five ears per treatment were analysed. Stars (*) denote treatments

in which statistically significant differences in number of diseased spikelets, relative to that on the reference PH-1 infected ears, were observed ($p < 0.05$, GLM analysis). In the box plot, the central rectangle spans the first quartile to the third quartile. A segment inside the rectangle shows the median and "whiskers" above and below the box extend to the upper (upper quartile + 1.5 x the interquartile range) and lower (lower quartile – 1.5 x the interquartile range). Outliers beyond the range of the whiskers are displayed by a green cross.

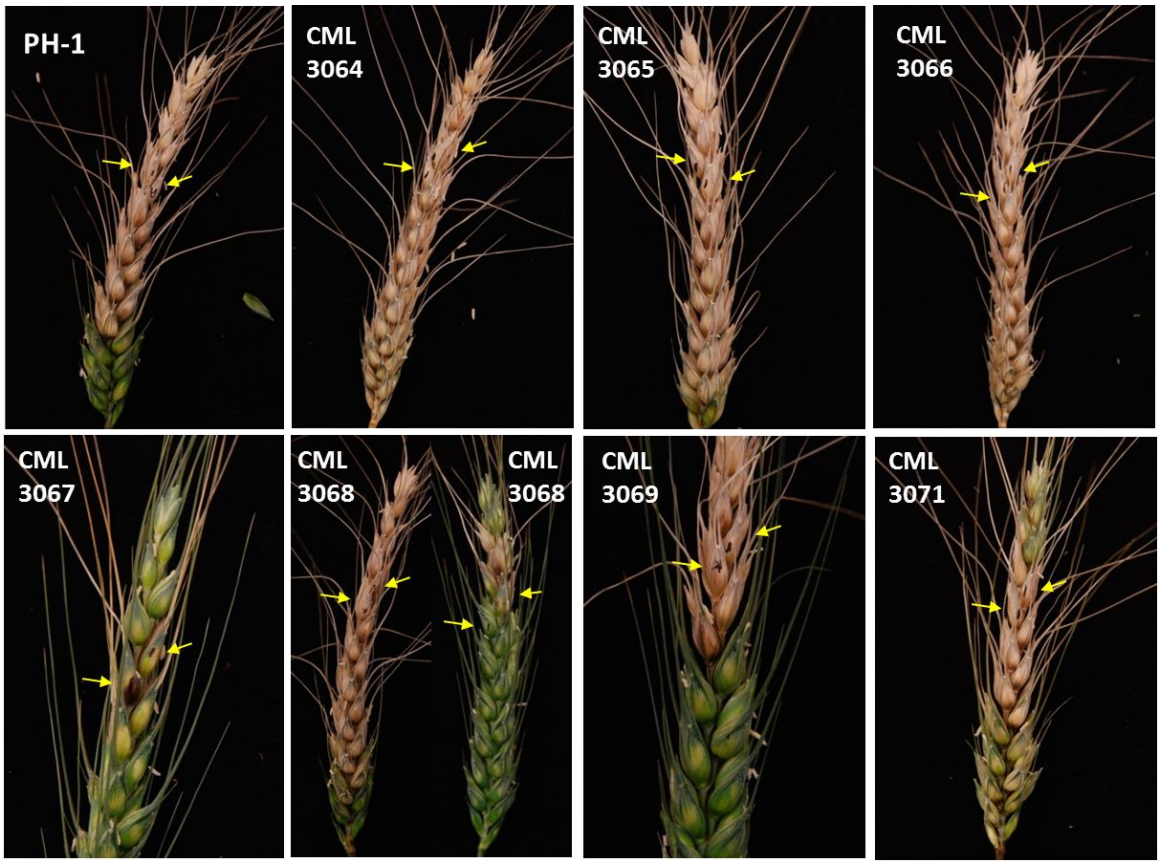

Figure 3.4 Representative disease symptoms on ears of wheat plants (cv. Bobwhite) point-inoculated with the reference *F. graminearum* strain PH-1 or one of seven *F. graminearum* strains originating from Brazil. Control plants point-inoculated with water only developed no disease symptoms (not shown). Wheat spikelets were inoculated when the plants were 60 (±5) days-old and the ears were in anthesis. The spikes of representative plants were photographed 21 days post inoculation. Yellow arrows indicate the inoculated spikelets (point of inoculation).

3.3.2 Genome sequencing analysis and selection of Brazilian reference strain

The eight Brazil-originated *F. graminearum* strains (Table 3.1) had their genome sequenced using Illumina HiSeq2000 platform with 100bp paired-end reads. The whole genome assemblies have been deposited in the European Nucleotide Archive (ENA) (ENA project accession PRJEB12819). CML3066 was selected to be the "Brazilian reference strain" because this isolate had the greatest genome coverage with regards to sequencing data (Table 3.2) and because it shows a similar phenotype to PH-1 in *in vitro* and *in planta* phenotypic tests (see section 3.3.1). CML3066 was further sequenced using SMRT sequencing on PacBio platform which produced higher-quality genomic sequence with longer reads. A summary of some features of the CML3066 versus PH-1 sequenced genomes are presented in Table 3.3 (King et al., 2015). The two genomic sequences have a similar size (approximately 37 Mb) and GC content (~48%) (Table 3.3).

The genome of the remaining seven Brazil-originated *F. graminearum* strains were compared to those of CML3066 and PH-1 first by mapping the reads from each of the seven strains to the PH-1. The percentage of reads mapped was calculated for each of the seven Brazilian strains with PH-1 genome. A cut-off value of 80% of reads mapped to the length of the genes was used to consider a gene present or absent.

Among 14,188 genes predicted in CML3066, 286 are not present in the PH-1 genome and therefore, a total of 13,902 predicted genes are shared between the Brazilian reference strain and PH-1. A total of 106 predicted genes appear to be new gene calls that have not been predicted previously, where 97

of them have no annotation. In total, 13,555 predicted genes shared 70% identity between these two strains.

Of the 13,902 predicted genes present in both PH-1 and CML3066, 178 are not present in at least one of the seven other Brazilian strains sequenced. Hence, a total of 13,724 genes comprise the core shared genome of all eight strains (Table 3.4), which is more than 96% of the genes conserved in all nine genomes of *F. graminearum.*

Regarding to the SNPs frequency along all four chromosomes of both CML3066 and PH-1 compared to the other strains, as demonstrated previously (Paper et al., 2007, King et al., 2015, Brown et al., 2012), all telomere proximal regions displayed the majority of the highest SNP density windows. In addition to the chromosome ends, three chromosomes (Chrom 1, 2 and 4) were found to have one or two large interstitial regions with a high SNP density (Figure 3.5 and 3.6).

Table 3.2 Summary of the number of reads and calculated coverage from genome sequencing of *F. graminearum* strains in this study

Strain ID	Total reads	Length (bp)	Calculated Coverage
CML3064	25,877,191	126	88
CML3065	24,633,038	126	84
CML3066	26,626,480	126	91
CML3067	25,432,225	126	87
CML3068	26,914,921	126	92
CML3069	29,726,889	126	101
CML3070	23,783,966	126	83
CML3071	20,002,864	126	68

Table 3.3 The genome sequence assemblies for *F. graminearum* strains PH-1 and CML3066 utilised in this study

	PH-1[1]	**CML3066**
Genome size (bp)[2]	36,663,736	36,908,675
Chromosomes	4	4
GC (%) content[3]	48.2 (48.0[4])	47.9 (47.9[4])
Spanned gaps	0	0
Predicted Genes	14,145	14,188
Repetitive (%)	0.99	1.17
Transposable elements (%)	0.28	0.43

Data generated by Robert King

[1] Reannotated genome (King et al., 2015)

[2] Including all scaffolds, N bases, and the mitochondria but excluding the large repetitive sequence at the carboxyl end of chromosome 4

[3] Excluding N's and mitochondria

Table 3.4 Comparison of genome of *F. graminearum* strains PH-1 and CML3066 and the remaining seven Brazilian strains

Chromosome	**Number of genes PH-1**	**Number of genes CML3066**	**Genes in the core genome***
1	4390	4429	4289
2	3648	3667	3507
3	3087	3079	3000
4	3022	3013	2928

*Genes present in all the eight Brazilian and PH-1 genome sequences

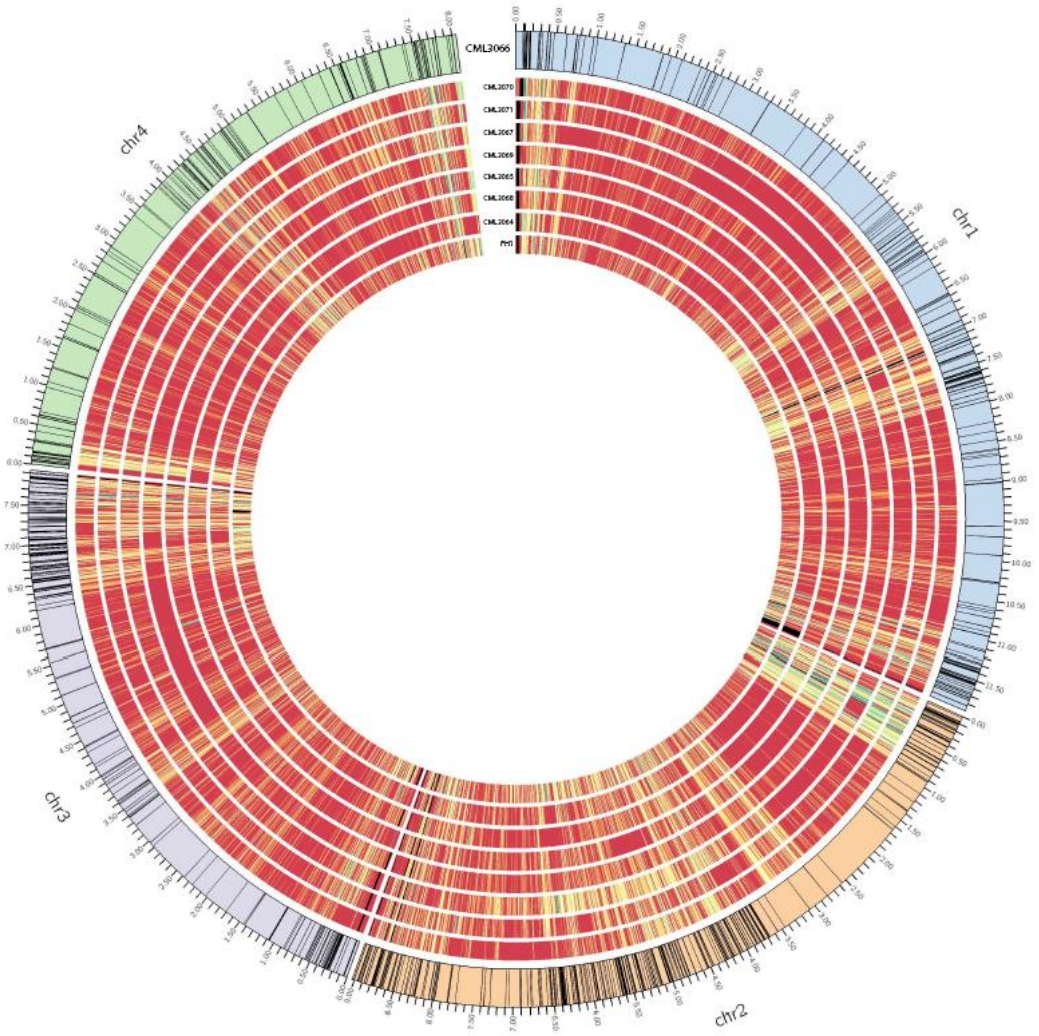

Figure 3.5 Distribution of genes in the predicted secretome for strain CML3066 across the entire *F. graminearum* CML3066 genome. A Circus plot is shown which visualises the four *F. graminearum* chromosomes followed by SNPs frequency for this strain against the other seven Brazilian strains and the reference strain PH-1 For the eight inner rings the red lines mean low SNP frequency (low polymorphic regions) and yellow to green lines mean high SNP frequency (normalised to 1000bp of cds sequence)]. On each SNP frequency ring, the blacked out lines are absent regions.

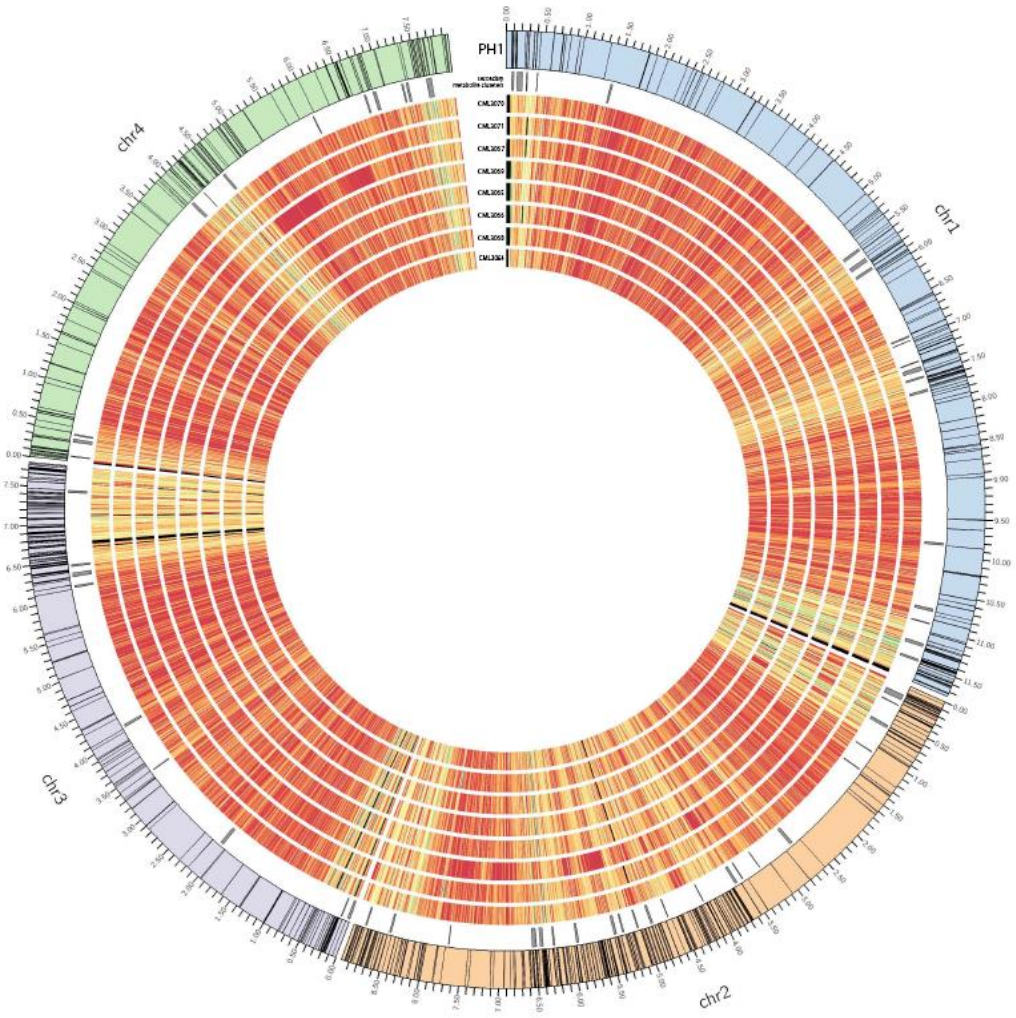

Figure 3.6 Distribution of genes in the predicted secretome for strain PH-1 across the entire *F. graminearum* PH-1 genome. A Circus plot is shown which visualises the four *F. graminearum* chromosomes followed by SNPs frequency for this strain against the other eight Brazilian strains [Red lines mean low SNP frequency (low polymorphic regions) and yellow to green lines mean high SNP frequency (normalised to 1000bp of cds sequence)]. On each SNP frequency ring, the blacked out lines are absent regions. Second band with black lines are secondary metabolites clusters.

3.3.3 The predicted *Fusarium graminearum* CML3066 and PH-1 secretome

The secretome of PH-1 has been predicted in the past (Brown et al., 2012), however in this study, a new analysis was carried out using the following pipeline.

This study initially used SignalP and TargetP (Emanuelsson et al., 2000, Petersen et al., 2011) in combination to predict the total secretome. These two tools predict the presence of signal peptide at the N-terminus of the peptides, indicating that the proteins are destined towards the secretory pathway. Within this gene set, GPI anchored membrane predicted proteins and the proteins predicted to locate to other non-extracellular loci (e.g. organelle-targeted proteins or Golgi / ER – retained proteins) were excluded.

The second stage of the analysis used a more rigorous set of prediction tools. All sequences that started with a methionine were utilised in a WolF-PSort analysis, with an extracellular score >17, which indicates higher probability that these proteins are indeed extracellularly secreted. This resulted in the prediction of the total secretomes for PH-1 and CML3066 to be 870 and 874 protein-encoding genes, respectively, which represents approximately 6% of the two predicted proteomes.

In addition, two analyses were done to further subset the secretome; big-PI (Eisenhaber et al., 2004) was used to further identify GPI anchored proteins and EffectorP for effector prediction (Sperschneider et al., 2016). In total, 182 and 183 effectors encoding-genes were predicted in CML3066 and PH-1, respectively; and 97 encoding GPI anchored proteins in both strains.

The resulting CML3066 secretome encoding genes were mapped onto the genome using CIRCOS software (Naquin et al., 2014). The entire secretome showed genes distributed in all four chromosomes preferentially located within subtelomeric regions and regions with a high recombination frequency (Figure 3.5). A similar distribution pattern was present in PH-1, as it has been showed in this study (Figure 3.6) as well as in previous publications (Brown et al., 2012, Cuomo et al., 2007, King et al., 2015).

3.3.4 Physical distribution of the secretome-encoding genes across CML3066 genome

In total, 450 of these genes were annotated as either hypothetical protein or unnamed protein product, representing 52% of CML3066 secretome, while 48% have some annotated function. Within this overall pattern, the annotated genes and the unannotated genes present in the CML3066 secretome were equally represented in the high and low recombination regions of the genome. Using effector-oriented analyses, 183 effector candidate genes were identified and 46 have some annotated function.

3.3.5 Identification of 'core' secretome

To identify the secretome encoding genes common in all eight Brazilian-originated strains and PH-1, the predicted total secretome for PH-1 and CML3066 generated in this study were used as a starting point. Genes from the two predicted secretomes that are not shared among all strains with at least 80% of reads mapped across the length of the transcript were removed from further consideration. This left 844 genes from the PH-1 predicted secretome and 843 genes from the CML3066 predicted secretome. The next step was to select the genes that were present in both secretomes, of which there were a total of 800 genes, now defined to comprise the 'core' secretome. The genes that were not present in all strains were mostly located within subtelomeric regions and regions with a high recombination frequency.

The core secretome was analysed in more detail to identify potential gene clusters. In some genomes, as in the smut fungus, *Ustilago maydis*, many genes encoding secreted proteins reside in clusters of three or more genes, of which

many have a role as effector (Kamper et al., 2006, Mueller et al., 2008, Muller et al., 2008). First, I checked if the 16 gene clusters identified by Brown et al. (2012) were present in the core secretome and thus conserved between the strains in this study. Then, I analysed for the presence of new clusters based on physical sequence location where three or more sequences were located directly next to each other. Among the 16 clusters described by Brown et al. (2012), all the genes present in 14 clusters were found to be present in the core secretome (Table 3.5). The exceptions are clusters C-1 and C-6, where FGSG_10594 was not present in two of the nine strains and FGSG_11094, annotated as a pectate lyase, was present in all nine strains, but not within the predicted secretome of CML3066. The clusters C-1 and C-6 are therefore not considered to be part of the core secretome. In addition to the genes previously predicted to be in each cluster, several additional genes have been predicted to be in seven of the 16 previously identified cluster. These include new gene calls that were identified between two previously predicted genes within the cluster, or a conserved predicted transcription factor-encoding genes located next to a cluster (Table 3.5). Two clusters (C-9, gene FGRRES_11231, and C-VII, gene FGSG_04741) have genes that previously were not predicted to be secreted but after re-analysis in this study, are now included in the predicted secretome.

One of the clusters, C-VII, is of special interest because six genes predicted to code for secreted proteins are located directly next to each other, in a region which spans 13.5 Kb This cluster includes two putative transcription factor domain-containing genes and several proteins with related predicted functions or domains. This includes a predicted RALF-like protein (Rapid alkalinisation factor) encoding gene in close proximity to a predicted alkaline ceramidase encoding gene. Alkaline ceramidases require an alkaline pH for

optimal activity, including regulation of cell growth, differentiation, apoptosis, and exocytosis (Mao & Obeid, 2008). There are also two genes in this cluster that encode predicted secreted proteins with a chitin-binding domain.

Fifteen newly predicted gene clusters were identified (Table 3.5). In the small gene cluster C-c on chromosome 1 there resides a LysM containing protein, FGRRES_10563_M, next to a chitinase, FGRRES_10561. These may be important for infection because LysM domain containing effector proteins are involved in suppressing chitin-mediated plant defences. Cluster C-g also contains genes predicted to code for secreted proteins that may be implicated in fungal pathogenesis including a CFEM domain (FGRRES_03599) and a sialidases domain(FGRRES_03598). In summary, 14% of the genes (n = 115 genes) coding for the *F. graminearum* 'core' secretome appear to reside in a total of 31 small, varied sequence, gene clusters, across all four *F. graminearum* chromosomes.

Table 3.5. Description of the 31 gene clusters members from the *F. graminearum* 'core' secretome

Cluster	Gene ID	Annotation	Interpro domain
C-1*	FGRRES_10592	small secreted protein	noIPR
	FFGRRES_10593**	hypothetical protein	noIPR
	FGRRES_10594_M**	hypothetical protein	noIPR
	FGRRES_10595	alkaline protease	IPR015500 Peptidase S8, subtilisin-related family
C-2*	FGRRES_03598	bnr asp-box repeat domain protein	IPR011040 Sialidases domain
	FGRRES_03599	hypothetical protein	IPR008427 Extracellular membrane protein, CFEM domain
	FGRRES_12411**	hypothetical protein	noIPR
	FGRRES_03600	hypothetical protein	noIPR
	FGRRES_03601	hypothetical protein	IPR002018 Carboxylesterase, type B domain
C-3*	FGRRES_03612	hypothetical protein	IPR001087 GDSL lipase/esterase domain
	FGRRES_03613**	hypothetical protein	noIPR
	FGRRES_03614	gpi anchor protein	noIPR

	FGRRES_03615**	hypothetical protein	IPR007867 Glucose-methanol-choline oxidoreductase, C-terminal domain
	FGRRES_03616	6-hydroxy-d-nicotine oxidase	IPR012951 Berberine/berberine-like domain
C-4*	FGRRES_03628	endoglucanase type b	IPR016288 1, 4-beta cellobiohydrolase family
	FGRRES_03629	alpha-glucuronidase precursor	IPR029018 Chitobiase/beta-hexosaminidase domain 2-like domain
	FGRRES_03630**	hypothetical protein	noIPR
	FGRRES_03631_M**	unnamed protein product	IPR018958 SMI1/KNR4-like domain
	FGRRES_03632	murein transglycosylase	IPR005103 Glycoside hydrolase, family 61
C-5*	FGRRES_11046	hypothetical protein	noIPR
	FGRRES_11047	hypothetical protein	noIPR
	FGRRES_11048	arabinogalactan endo- -beta-galactosidase	IPR011683 Glycosyl hydrolase family 53
	FGRRES_11049	acetylxylan esterase a	IPR010126 Esterase, PHB depolymerase family
	FGRRES_11050**#	light induced alcohol dehydrogenase bli-4	IPR002347 Glucose/ribitol dehydrogenase family
	FGRRES_11051_M**#	unnamed protein product	IPR007219 Transcription factor domain, fungi domain
C-6*	FGRRES_11094**	pectate lyase	IPR004898 Pectate lyase, catalytic domain
	FGRRES_11095	carbonic anhydrase	IPR001148 Alpha carbonic anhydrase domain
	FGRRES_17479**	unnamed protein product	noIPR
	FGRRES_11097	hypothetical protein	IPR013994 Carbohydrate-binding WSC, subgroup domain
C-7*	FGRRES_11163	pectate lyase	IPR002022 Pectate lyase/Amb allergen domain
	FGRRES_20314**#	unnamed protein product	noIPR
	FGRRES_11164	trypsin precursor	IPR001314 Peptidase S1A, chymotrypsin-type family
	FGRRES_15637**	unnamed protein product	noIPR
	FGRRES_17464**	hypothetical protein	IPR010730 Heterokaryon incompatibility domain
	FGRRES_11166	hypothetical protein	noIPR
C-8*	FGRRES_11204	hypothetical protein	IPR023296 Glycosyl hydrolase, five-bladed beta-propellor domain
	FGRRES_11205	epl1 protein	IPR010829 Cerato-platanin family

	FGRRES_11206	hypothetical protein	IPR010621 Domain of unknown function DUF1214
	FGRRES_15639**	hypothetical protein	noIPR
	FGRRES_17454**	hypothetical protein	IPR002110 Ankyrin repeat
	FGRRES_11208#	xyloglucanase	noIPR
C-9*	FGRRES_11225	hypothetical protein	noIPR
	FGRRES_17448**	unnamed protein product	IPR000028 Chloroperoxidase
	FGRRES_11227	lipase b	IPR029058 Alpha/Beta hydrolase fold
	FGRRES_11228	gmc oxidoreductase	IPR012132 Glucose-methanol-choline oxidoreductase family
	FGRRES_15635**	alcohol dehydrogenase	IPR016040 NAD(P)-binding domain
	FGRRES_11229	hypothetical protein	IPR013830 SGNH hydrolase-type esterase domain
	FGRRES_11230**	hypothetical protein	noIPR
	FGRRES_11231	mosc domain-containing protein mitochondrial	IPR005303 MOSC, N-terminal beta barrel domain
	FGRRES_11232	hypothetical protein	IPR023753 FAD/NAD(P)-binding domain
C-I*	FGRRES_00011**#	hypothetical protein	IPR001138 Zn (2)-C6 fungal-type DNA-binding domain
	FGRRES_00009	hypothetical protein	noIPR
	FGRRES_11647	hypothetical protein	noIPR
	FGRRES_11646**	hypothetical protein	noIPR
	FGRRES_11645	hypothetical protein	noIPR
C-II*	FGRRES_03121	pectin lyase precursor	IPR002022 Pectate lyase/Amb allergen domain
	FGRRES_09297**#	aat family amino acid transporter	IPR002293 Amino acid/polyamine transporter I family
	FGRRES_07017**#	dak2 domain-containing protein	noIPR
	FGRRES_03122	hypothetical protein	IPR006626 Parallel beta-helix repeat
	FGRRES_03123	hypothetical protein	IPR021054 Cell wall mannoprotein 1 family
C-III*	FGRRES_03526	parallel beta-helix repeat protein	noIPR
	FGRRES_03527**	hypothetical protein	IPR023214 HAD-like domain
	FGRRES_03528**	hypothetical protein	IPR029018 Chitobiase/beta-hexosaminidase domain 2-like
	FGRRES_03529	glycosyl hydrolase family 17	IPR000490 Glycoside hydrolase family 17
	FGRRES_03530_M	rhamnogalacturonan acetyltransferase	IPR013830 SGNH hydrolase-type esterase domain
	FGRRES_03531	hypothetical protein	IPR002227 Tyrosinase copper-binding domain
	FGRRES_03532	trichothecene c-15 esterase	IPR029058 Alpha/Beta hydrolase fold domain

C-IV*	FGRRES_03583	triacylglycerol lipase fgl5	IPR029058 Alpha/Beta hydrolase fold domain
	FGRRES_03584	ricin b lectin	noIPR
	FGRRES_03585	hypothetical protein	noIPR
C-V*	FGRRES_03892**#	sucrose utilization protein suc1	IPR001138 Zn (2)-C6 fungal-type DNA-binding domain
	FGRRES_03893	amidohydrolase family protein	IPR011059 Metal-dependent hydrolase, composite domain
	FGRRES_03894_M	hypothetical protein	noIPR
	FGRRES_17621**	hypothetical protein	noIPR
	FGRRES_03896	hypothetical protein	noIPR
C-VI*	FGRRES_03901	hypothetical protein FGSG_03901	IPR029058 Alpha/Beta hydrolase fold domain
	FGRRES_03902**	cut9-interacting protein scn1	IPR001130 TatD family
	FGRRES_03903**	hypothetical protein FG05_03903	noIPR
	FGRRES_03904	probable beta-galactosidase	IPR001944 Glycoside hydrolase, family 35
	FGRRES_03905	hypothetical protein	IPR023296 Glycosyl hydrolase, five-bladed beta-propellor domain
	FGRRES_03906**	class i alpha-mannosidase 1b	IPR001382 Glycoside hydrolase family 47
	FGRRES_03907**	hypothetical protein	IPR008979 Galactose-binding domain-like
	FGRRES_03908	pectate lyase plyb	IPR002022 Pectate lyase/Amb allergen domain
C-VII*	FGRRES_16407	transforming growth factor-beta-induced protein ig-h3	IPR000782 FAS1 domain
	FGRRES_04738	alkaline ceramidase	IPR031331 Neutral/alkaline non-lysosomal ceramidase, C-terminal
	FGRRES_04739	hypothetical protein	IPR011658 PA14 domain
	FGRRES_15123	protein ralf-like 33	IPR008801 Rapid ALkalinization Factor family
	FGRRES_04740	hypothetical protein	IPR003609 PAN/Apple domain
	FGRRES_04741	hypersensitive response-inducing protein	noIPR
	FGRRES_04742_M**	unnamed protein product	noIPR
	FGRRES_04743	alpha-l-rhamnosidase c	IPR008902 Bacterial alpha-L-rhamnosidase domain
	FGRRES_04744	hypothetical protein	noIPR
	FGRRES_04745	antifungal protein	IPR023112 Antifungal protein domain
	FGRRES_04746**#	hypothetical protein	IPR022085 Protein of unknown function DUF3632
	FGRRES_04747**#	hypothetical protein	IPR001138 Zn (2)-C6 fungal-type DNA-binding domain

	FGRRES_04748**#	isoflavone reductase family protein	noIPR
	FGRRES_04749**#	related to integral membrane protein pth11	noIPR
	FGRRES_04750**#	related to parasitic phase-specific protein psp-1	IPR007568 RTA-like protein family
	FGRRES_12602**#	hypothetical protein	IPR021858 Fungal transcription factor family
	FGRRES_16408#	hypothetical protein	IPR001002 Chitin-binding, type 1 domain
	FGRRES_04752_M#	unnamed protein product	IPR001002 Chitin-binding, type 1 domain
C-a	FGRRES_00111	hypothetical protein	noIPR
	FGRRES_00112	hypothetical protein	noIPR
	FGRRES_15688**	hypothetical protein	noIPR
	FGRRES_00114	hypothetical protein	noIPR
C-b	FGRRES_02255	hypothetical protein	noIPR
	FGRRES_12105**	von willebrand factor	noIPR
	FGRRES_15958	d-arabinono- -lactone oxidase	IPR006094 FAD linked oxidase, N-terminal domain
	FGRRES_12107**	hypothetical protein	IPR006583 PAN-3 domain
	FGRRES_02257	hypothetical protein	
	FGRRES_15959	probable fusarubin cluster-esterase	IPR029059 Alpha/beta hydrolase fold-5 domain
C-c	FGRRES_10560	hypothetical protein	noIPR
	FGRRES_10560**	hypothetical protein	noIPR
	FGRRES_10561	glycosylhydrolase family 18-6	IPR011583 Chitinase II domain
	FGRRES_10562**	hypothetical protein	noIPR
	FGRRES_10563_M	hypothetical protein	IPR018392 LysM domain domain
C-d	FGRRES_17430**	hypothetical protein	IPR001138 Zn (2)-C6 fungal-type DNA-binding domain
	FGRRES_10675	hypothetical protein	IPR013658 SMP-30/Gluconolactonase/LRE-like region domain
	FGRRES_10676	agglutinin-like protein 2	IPR018871 GLEYA adhesin domain
	FGRRES_10677	peroxisomal amine oxidase (copper-containing)	IPR000269 Copper amine oxidase family
C-e	FGRRES_02909_M	unnamed protein product	noIPR
	FGRRES_02910_M	unnamed protein product	noIPR
	FGRRES_02911**	hypothetical protein	noIPR
	FGRRES_12554	hypothetical protein	noIPR
	FGRRES_02913**	unnamed protein product	noIPR
	FGRRES_02914	hypothetical protein	noIPR
	FGRRES_02915_M**	hypothetical protein	noIPR
	FGRRES_02916**	hypothetical protein	noIPR

	FGRRES_02917	related to cellobiose dehydrogenase	noIPR
	FGRRES_02918	pepsin a	IPR001461 Aspartic peptidase A1 family
	FGRRES_16368**	hypothetical protein	IPR001138 Zn (2)-C6 fungal-type DNA-binding domain
C-f	FGRRES_03049	related to alpha-l-arabinofuranosidase ii precursor	IPR016828 Alpha-L-arabinofuranosidase family
	FGRRES_03050	hypothetical protein	IPR012338 Beta-lactamase/transpeptidase-like domain
	FGRRES_16345**	related to cercosporin resistance protein	IPR001138 Zn (2)-C6 fungal-type DNA-binding domain
	FGRRES_03052	hypothetical protein	noIPR
C-g	FGRRES_03598	bnr asp-box repeat domain protein	IPR011040 Sialidases domain
	FGRRES_03599	hypothetical protein	IPR008427 Extracellular membrane protein, CFEM domain
	FGRRES_12411**	hypothetical protein	noIPR
	FGRRES_03600	hypothetical protein	noIPR
	FGRRES_03601	hypothetical protein	IPR002018 Carboxylesterase, type B domain
C-h	FGRRES_16234	hypothetical protein	noIPR
	FGRRES_20176	hypothetical protein	noIPR
	FGRRES_15197**	unnamed protein product	noIPR
	FGRRES_03609	hypothetical protein	IPR006710 Glycoside hydrolase, family 43
C-i	FGRRES_03971	hypothetical protein	IPR010829 Cerato-platanin family
	FGRRES_03972	hypothetical protein	IPR016169 CO dehydrogenase flavoprotein-like, FAD-binding domain
	FGRRES_16175	serum paraoxonase arylesterase 1	IPR011042 Six-bladed beta-propeller, TolB-like domain
C-j	FGRRES_10982	dipeptidyl-peptidase 4	IPR002469 Dipeptidylpeptidase IV, N-terminal domain
	FGRRES_17488**	integral membrane protein pth11	noIPR
	FGRRES_10984**	hypothetical protein	noIPR
	FGRRES_10985	hypothetical protein	noIPR
	FGRRES_10986	alcohol oxidase	IPR012132 Glucose-methanol-choline oxidoreductase family
C-k	FGRRES_10998	related to 6-hydroxy-d-nicotine oxidase	IPR016169 CO dehydrogenase flavoprotein-like, FAD-binding, domain

	FGRRES_10999	endo- -beta-xylanase 1	IPR001137 Glycoside hydrolase family 11
	FGRRES_11000_M	hypothetical protein	noIPR
C-l	FGRRES_11032	galactose oxidase precursor	IPR000421 Coagulation factor 5/8 C-terminal domain
	FGRRES_11033	hypothetical protein	noIPR
	FGRRES_13865**	aldehyde dehydrogenase	IPR016162 Aldehyde dehydrogenase N-terminal domain
	FGRRES_13864_M	hypothetical protein	noIPR
	FGRRES_11035_M	unnamed protein product	noIPR
	FGRRES_11036	feruloyl esterase c	IPR029058 Alpha/Beta hydrolase fold domain
	FGRRES_20309**	unnamed protein product	noIPR
	FGRRES_11037	murein transglycosylase	IPR002594 Glycoside hydrolase family 12
C-m	FGRRES_11358**	transcriptional regulatory protein moc3	IPR001138 Zn (2)-C6 fungal-type DNA-binding domain
	FGRRES_17566	feruloyl esterase b-2	IPR029058 Alpha/Beta hydrolase fold domain
	FGRRES_13981**	cupin	IPR013096 Cupin 2, conserved barrel domain
	FGRRES_11360	glucuronan lyase a	IPR025975 Polysaccharide lyase family
	FGRRES_11361	hypothetical protein	IPR000639 Epoxide hydrolase-like family
C-n	FGRRES_06448_M**	activator of stress proteins 1	IPR007219 Transcription factor domain, fungi domain
	FGRRES_12920**	related to stress responsive a b barrel domain protein	IPR013097 Stress responsive alpha-beta barre domain
	FGRRES_06449**	fumarylacetoacetase	IPR015377 Fumarylacetoacetase, N-terminal domain
	FGRRES_06450_M	homogentisate - dioxygenase	IPR005708 Homogentisate 1,2-dioxygenase family
	FGRRES_06451	levanbiose-producing levanase	IPR001362 Glycoside hydrolase, family 32
	FGRRES_06452	bifunctional xylanase deacetylase	IPR002509 NodB homology domain
C-o	FGRRES_16902	anter-specific proline-rich protein apg	noIPR
	FGRRES_07807	hypothetical protein	noIPR
	FGRRES_07808	isoamyl alcohol oxidase	noIPR

(*) Cluster prediction from Brown et al., 2012 (**) Genes predicted not to be in the secretome (#) New genes added in the clusters not identified by Brown et al., 2012

3.3.5 *In silico* analysis of protein functions associated with 'core' secretome genes

The predicted proteins within the *F. graminearum* 'core secretome' were analysed for function using Blast2GO. In addition of protein annotations, the analysis identified InterPro domains within proteins (IPR), InterPro families (IPS), and putative enzymes with KEGG metabolic pathways and putative EC classifications. The EC classification is a numerical classification for enzymes, based on the chemical reactions each catalysis (Webb EC 1992). More than half of the core secretome (n = 402 genes) encode annotated proteins and 507 genes are predicted to contain at least one IPR domain (Appendix 1). The most commonly identified domain, an Alpha/Beta hydrolase fold domain, was present in 30 sequences. This domain is mostly found in cell-wall degrading enzymes, for example predicted cellulases and xylanases, which are predicted to be important for the establishment of *F. graminearum* necrotrophic phase and its nutrient acquisition.

A total of 255 genes encode proteins divided among 129 InterPro families (IPS) (Table 3.6). One of the 23 glycoside hydrolase families (Family 43) is the most highly represented InterPro family in the secretome, being encoded by 13 genes distributed across the *F. graminearum* genome, predicted to have xylosidase and arabinofuranosidase activities. A number of other glycoside hydrolase families are also represented in the secretome (Table 3.6). Further well represented families include the peptidase S8, subtilisin-related (IPR015500) and aspartic peptidase A1 family (IPR001461), which in some fungal species, are secreted for saprophytic protein digestion (Sansen et al., 2004, Prasad & Suguna, 2002). About 20% of the genes in the 'core' secretome are involved in some form

of catalytic activity primarily represented by hydrolases, which targeted lipids, carbohydrates and proteins, and oxidoreductases (Figure3.7).

The predicted proteins comprising the *F. graminearum* core secretome were mapped onto the KEGG metabolic pathway (Table 3.7) and this revealed the high representation of enzymes involved in starch/ sucrose metabolism and drug metabolism. The former could be involved in the breakdown of plant polysaccharides, important mainly in the necrotrophic and saprophytic life stages. The latter could be involved in the deactivation and the excretion of xenobiotics that may come from the plant.

As mentioned before, 402 genes encode proteins that have been annotated with predicted function, of which 362 have one or more predicted Interpro domain. Many of the annotated proteins are predicted cutinases, cellulases and cellulose-binding domains, xylanases, pectin lyases, peptidases and lipases, and therefore likely to be involved in plant substrate degradation. One lipase has been shown to influence *F. graminearum* infection in wheat. The fungal disruption mutant *fgl1*, which lacks the effector lipase FGL1 (FGRRES_05906), is restricted to inoculated wheat spikelets. It has been shown that the secreted fungal lipase releases free fatty acids that inhibit callose formation during wheat ear infection (Blumke et al., 2014, Voigt et al., 2005). Given the hemibiotrophic life-style of *F. graminearum*, it is not unexpected that the hyphae would produce and secrete a large number of proteins and enzymes associated with the degradation of plant host cell components (Brown et al., 2010).

Other proteins of interest predicted in the secretome include a putative transforming growth factor-beta-induced protein ig-h3 (IPR032954), which may be involved in modulating cell adhesion (Skonier et al., 1994). There are several

predicted chitin binding proteins (IPR001002), which can potentially play a role binding to fungal cell wall chitin or chitin fragments when fragments are released by plant chitinases, thus shielding invading hyphae form the plant chitin perception machinery (Marshall et al., 2011). Studied in greater depth are given in chapter 5 on two cerato-platanin proteins and three hydrophobins encoded in the *F. graminearum* secretome. Cerato-platanins have been described as either a fungal elicitor or effector and are also suggested to play a role in fungal development (Gaderer et al., 2014, Pazzagli et al., 2014). Hydrophobins may have different roles in the fungal life cycle. Some hydrophobins play a role in fungal development and also by decreasing the surface tension of water in the first step of forming an aerial mycelium following a phase of submerged growth (Minenko et al., 2014).

There are 398 proteins within the predicted 'core secretome' that do not have any predicted annotation, however 146 of these have putative Interpro domains. The most highly represented domain is the carbohydrate-binding WSC (IPR002889), identified in six proteins. This domain contains up to eight conserved cysteine residues and may be involved in carbohydrate binding. Three other common domains found in a total of five proteins are the tyrosinase copper-binding domain (IPR002227), the alpha/beta hydrolase fold (IPR029058) and the PAN/apple domain (IPR003609). The first is involved in the formation of pigments such as melanins and other polyphenolic compounds. The second is part of a family of many related domains. Some members of this family can be inactive but others may be involved in surface recognition. The PAN/Apple domain mediate protein-protein interactions as well as protein-carbohydrate interactions.

Some proteins stand out from the other unannotated proteins because of some particular features. For example, locus FGRRES_03969 encodes a protein

of 501 amino acids that has 58 cysteine residues in the mature peptide (11.5%) and is predicted to contain five epidermal growth factor-like (EGF) domains (IPR000742). EGF-like domains are mainly found in proteins known to be secreted and is also known to be a CFEM domain in the rice pathogen *Magnaporthe oryzae* and also part of a GPCR-like receptor specific to filamentous ascomycetes (Kulkarni et al., 2005). There is also the FGRRES_20390 that encode a protein containing 42 cysteine residues among its 368 amino acids (11.4%).

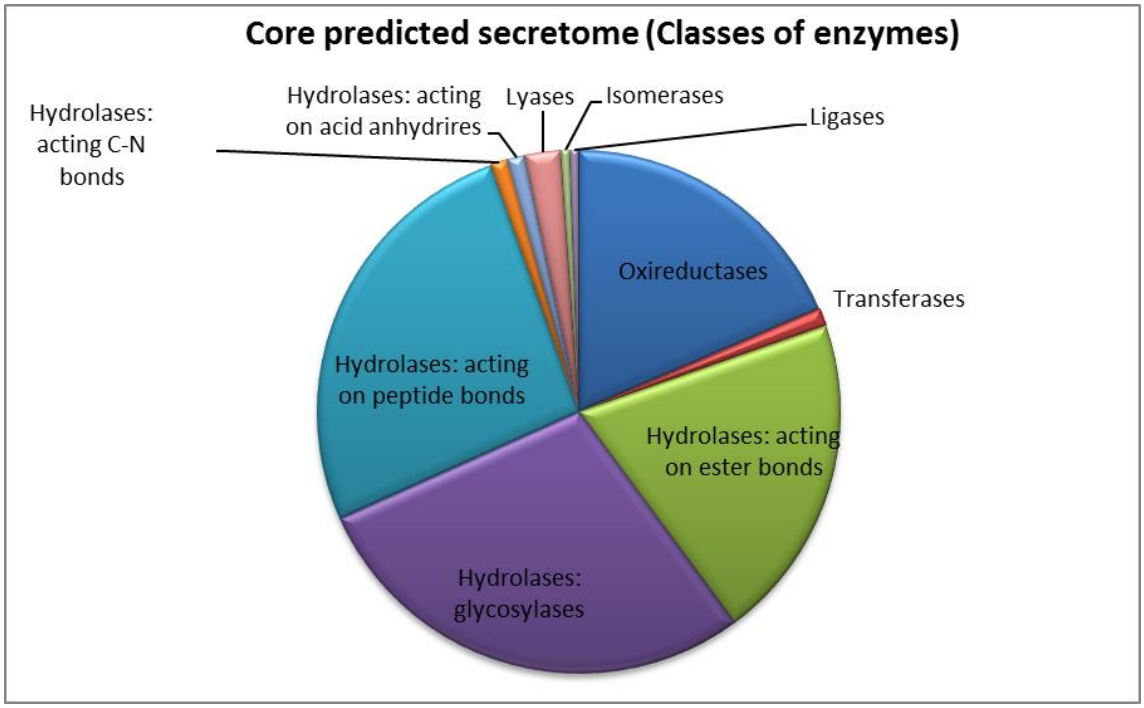

Figure 3.7 The representation of major enzyme classes in the 'core' *F. graminearum* secretome

Table 3.6 The most highly represented InterPro protein families within the *F. graminearum* 'core' secretome

InterPro Family	**N. of genes**
(IPR006710) Glycoside hydrolase, family 43	13
(IPR015500) Peptidase S8, subtilisin-related	12
(IPR001461) Aspartic peptidase A1 family	11
(IPR005103) Glycoside hydrolase, family 61	11

(IPR001563) Peptidase S10, serine carboxypeptidase	8
(IPR026892) Glycoside hydrolase family 3	8
(IPR011150) Cutinase, monofunctional	7
(IPR012132) Glucose-methanol-choline oxidoreductase	7
(IPR011118) Tannase/feruloyl esterase	6
(IPR013319) Glycoside hydrolase family 11/12	5
(IPR000743) Glycoside hydrolase, family 28	5
(IPR021476) Protein of unknown function DUF3129	4
(IPR010255) Haem peroxidase	3
(IPR008313) Uncharacterised conserved protein UCP028846	3
(IPR000120) Amidase	3
(IPR002933) Peptidase M20	3
(IPR001137) Glycoside hydrolase family 11	3
(IPR017168) Glycoside hydrolase, family 16, CRH1, predicted	3
(IPR010829) Cerato-platanin	3
(IPR010126) Esterase, PHB depolymerase	3
(IPR008701) Necrosis inducing protein	3
(IPR001568) Ribonuclease T2-like	3

Table 3.7 *F. graminearum* 'core' secreted proteins predicted to be involved in KEGG metabolic pathways.

KEGG pathway	**Seq**	**Enz**
Starch and sucrose metabolism	20	9
Drug metabolism	19	1
Amino sugar and nucleotide metabolism	17	6
Phenylpropanoid biosynthesis	11	2
Pentose and glucuronate inter-conversions	11	4
Sphingolipid metabolism	7	4
Galactose metabolism	7	4
Cyanoamino acid metabolism	6	2
Other glycan degradation	6	4

Glycerolipid metabolism	6	2
Aminobenzoate degradation	5	2
Biosynthesis of antibiotics	4	3
Bisphenol degradation	3	1
Glycosphingolipid biosynthesis—ganglio series	3	2
Glycosphingolipid biosynthesis—globo series	3	2
Glycosaminoglycan degradation	3	2
Steroid hormone biosynthesis	2	1
Purine metabolism	2	2
Glycine, serine and threonine metabolism	2	2
Tyrosine metabolism	2	2
Tryptophan metabolism	2	1
Various types of N-glycan biosynthesis	2	2
Thiamine metabolism	2	1
Glyoxylate and dicarboxylate metabolism	2	1
Arginine and proline metabolism	1	1
Methane metabolism	1	1
Phenylalanine metabolism	1	1
Fatty acid degradation	1	1
Styrene degradation	1	1
T cell receptor signalling pathway	1	1
Tropane, piperidine and pyridine alkaloid biosynthesis	1	1
Fatty acid elongation	1	1
Fatty acid biosynthesis	1	1
N-glycan biosynthesis	1	1
Alanine, aspartate and glutamate metabolism	1	1
beta-Alanine metabolism	1	1
D-Arginine and D-ornithine metabolism	1	1
Penicillin and chephalosporism biosynthesis	1	1
Isoquinoline and alkaloid biosynthesis	1	1
Ascobarte and aldarate metabolism	1	1

Ether lipid metabolism	1	1
Cysteine and methionin metabolism	1	1

Seq = number of fungal sequences, Enz = number of enzyme classes

3.3.6 Identification of functionally characterised and predicted effector motifs

The 800 proteins belonging to the 'core' secretome were inspected for the presence of known motifs that may facilitate fungal infection. Many effectors in plant infecting oomycetes and animal infecting malaria parasites retain a RXLR-dEER domain (Win et al., 2012). These two amino acids motifs exhibit the complete machinery that the pathogen needs to deliver effectors into host cells (Dou et al., 2008). Another well-known motif present in a number of pathogen effectors is the N-terminal tripeptide motif Y/F/WxC. Eight per cent of the fungal effectors upregulated during *B. graminis f. sp. hordei* infection on barley contain this conserved motif, suggesting a common functional role, although the role itself is not known (Godfrey et al., 2010). No RxLR-dEER motif encoding genes were found in the *F. graminearum* 'core' secretome. In comparison, Y/F/WxC motifs were found in 11 proteins near to the predicted signal peptide cleavage sites. Five of these proteins contain WxC motif, an endoglucanase (FGRRES_02658) and four unannotated genes encode proteins (FGRRES_13505, FGRRES_12938, FGRRES_12835 and FGRRES_02249). The FxC motif was identified in three genes encode proteins (FGRRES_03050, FGRRES_15183, FGRRES_03326) and the YxC motif in the remaining three proteins (FGRRES_00260, FGRRES_01815, FGRRES_03544). One of these genes FGRRES_03050 resides in the C-f cluster (Table 3.5), predicted to encode a protein containing a beta-lactamases domain. Beta-lactamases are enzymes were first described in bacteria and provide resistance to some antibiotics.

In the total of 800 proteins, 162 proteins were identified as putative effector using EffectorP tool (Sperschneider et al., 2016). Only 40 of these proteins have predicted annotation (Table 3.8). Of these, RALF-like and hydrophobin domain containing proteins have been implicated in plant pathogenesis in other species (Masachis et al., 2016, Beckerman & Ebbole, 1996, Talbot et al., 1996). The roles of these proteins in *F. graminearum*-wheat infection will be discussed in more detail in chapter 5 and chapter 6. The predicted effector set also includes an antifungal protein and two KP4 killer toxins, which for example, may be involved in inhibiting other potential fungal species competing with *F. graminearum* for nutrients (Gage et al., 2001, Gage et al., 2002).

Table 3.8 List of predicted annotated effectors encoded by all nine *F. graminearum* strains sequenced in this study

Gene ID	Annotation	Chromosome
FGRRES_00023	spherulin 1a precursor	Chromosome_1
FGRRES_00060	calcium channel partial	Chromosome_1
FGRRES_00061	killer kp4	Chromosome_1
FGRRES_00062	calcium channel partial	Chromosome_1
FGRRES_00783	acetylxylan esterase 2	Chromosome_1
FGRRES_01831	hydrophobin precursor	Chromosome_1
FGRRES_02181	cfem domain-containing protein	Chromosome_1
FGRRES_02977_M	pectate lyase	Chromosome_2
FGRRES_03304	cutinase 1	Chromosome_2
FGRRES_03436	sterigmatocystin biosynthesis peroxidase stcc	Chromosome_2
FGRRES_03457	cutinase 3	Chromosome_2
FGRRES_03584	ricin b lectin	Chromosome_2
FGRRES_03624	endo- -beta-xylanase 2 precursor	Chromosome_2
FGRRES_03911	phospholipase a2	Chromosome_2
FGRRES_04060	related to extracellular cellulase allergen asp f7-	Chromosome_2
FGRRES_04074	cell wall protein	Chromosome_2

FGRRES_04535	gpi anchored serine-threonine rich protein	Chromosome_2
FGRRES_04741	hypersensitive response-inducing protein	Chromosome_3
FGRRES_04745	antifungal protein	Chromosome_3
FGRRES_04848	rhamnogalacturonan acetylesterase precursor	Chromosome_3
FGRRES_04864	pectate lyase	Chromosome_3
FGRRES_04895	barwin-like endoglucanase	Chromosome_3
FGRRES_07755	pathogenicity protein	Chromosome_4
FGRRES_07784	wsc domain protein	Chromosome_4
FGRRES_07988	cell wall protein	Chromosome_2
FGRRES_08021_M	related to gegh 16 protein	Chromosome_2
FGRRES_08987	long chronological lifespan protein 2	Chromosome_4
FGRRES_09066	hydrophobin 3 precursor	Chromosome_4
FGRRES_09353	gegh 16 protein	Chromosome_4
FGRRES_09586	phosphatidylglycerol phosphatidylinositol transfer protein precursor	Chromosome_4
FGRRES_10212	probable rot1 precursor	Chromosome_1
FGRRES_10551	killer kp4 smk- partial	Chromosome_1
FGRRES_10634	cutinase precursor	Chromosome_1
FGRRES_10776_M	glutathione-dependent formaldehyde-activating enzyme	Chromosome_3
FGRRES_10999	endo- -beta-xylanase 1	Chromosome_3
FGRRES_11036	feruloyl esterase c	Chromosome_3
FGRRES_11318	related to rf2 protein	Chromosome_3
FGRRES_15123	protein ralf-like 33	Chromosome_3
FGRRES_16689	thioredoxin-like protein	Chromosome_4
FGRRES_20400	host-specific ak-toxin akt2	Chromosome_4

3.3.7 Selection of putative proteins potentially actively involved in *F. graminearum* – wheat interaction

One of the initial criteria for generating the putative effector of interest list from the core secretome was a maximum size of 160 amino acids (aa). This upper

limit of 160 aa was chosen as it is the current size limit on proteins that can be expressed using the BSMV-VOX system (Lee et al., 2012) and discussed further in chapter 4 . This selection does not exclude the fact that larger proteins may also be important effectors, however testing using in the BSMV-VOX system is not possible. Expression of the selected gene during *in planta* infection was investigated using the transcriptome (RNA-seq - Solexa) data available from *F. graminearum* infected wheat (cv. Bobwhite) tissue at 5 dpi harvested from the 2nd and 3rd rachis internode below the point-inoculated spikelets of wheat ears (Brown, 2011). At this time point of infection, no macroscopic symptoms of infection were visible in these internodes, and so these data represent the symptomless phase of *F. graminearum* infection (Brown et al., 2010).

A set of 70 proteins were the output from the analysis of these datasets. In order to narrow down the best candidates to carry forward, additional bioinformatics approaches were utilised (Figure 3.9). These included identifying *F. graminearum* proteins with similarities to known effectors from other species, although proteins with no identified similarities to other known effectors were not discounted.

A Pfam search was then used to identify candidates with previously characterised domains, and 3D protein structure was explored using the Phyre2 tool. Phyre2 allows comparisons between proteins based on predicted 3D structure, and can help to identify similarities at the protein 3D structure level when primary amino acid sequence similarity search tools may not (Kelley & Sternberg, 2009).

Blastp was used to compare the *F. graminearum* candidate proteins against eight different plant pathogenic species, namely the cereal-infecting species *F. pseudograminearum*, *F. verticillioides* and *Zymoseptoria tritici*, the

non-cereal monocot infecting species *F. oxysporum* f.sp. *cubense*, and four dicot infecting species, *F. oxysporum* f.sp*. lycopersici*, *F. solani*, *Botrytis cinerea* and *Sclerotinia sclerotiorium.* Using these tools, 12 candidate effectors were selected for further analysis (summarised in table 3.9, with information on their selection criteria)

The criteria used to select these 12 genes are outlined below: *FgSSP1*, *FgSSP2* and *FgSSP3* are among the ten most highly expressed *Fg*SSP encoding genes at the advancing infection front (rachis internode 3). Each of these genes is predicted to possess eight cysteine residues within the mature processed protein.

The small protein FgSSP4, with a full length of 54 aa, has characteristics similar to those of the MC69 effector proteins from the rice blast pathogen *Magnaporthe oryza*e and the cucumber anthracnose pathogen *Colletotrichum orbiculare* (Saitoh et al., 2012). The *M. oryzae mc69* mutant failed to develop invasive hyphae after appressorium formation in rice leaf sheath, whilst deletion of the *Mc69* orthologous gene in the plant pathogenic species *Colletrotichum orbiculare* reduced fungal pathogenicity on leaves of both cucumber (*Cucumis sativus*) and *Nicotiana benthamiana* plants (Saitoh et al., 2012).

The next gene in the list, *FgSSP5*, encodes a protein that possesses the pfam domain RALF (Rapid alkalinisation factor; PF05498.6). RALF domain-containing proteins are predominately found in plants and play a role in plant development potentially regulating tissue expansion in sugarcane and negatively regulating pollen tube elongation in tomato (Mingossi et al., 2010, Covey et al., 2010). Recently, the RALF protein in *Fusarium oxysporum* has been shown to play an important role in pathogenicity. Extracellular alkalinisation promoted by *F. oxysporum* RALF protein (F-RALF) led to infectious growth of the fungus by

stimulating phosphorylation of a conserved mitogen-activated protein kinase essential for pathogenicity. *Fusarium oxysporum* mutant strains lacking this *f-ralf* gene failed to induce host alkalinisation and showed significantly attenuated virulence on tomato plants, and induced expression of defence genes in the host (Masachis et al., 2016). This RALF domain has not been found in non-Fusarium fungal species, but a number of phytopathogens use extracellular alkalinisation by other mechanisms to improve colonisation of host tissue. One example is the phytopathogenic species of *Colletotrichum* (*C. gloeosporioides, C. coccodes* and *C. acutatum*) that elevates both the local ammonia concentration and pH in host plant tissue during infection, and this regulates expression of pectin lyase, a key virulence factor (Yakoby et al., 2000, Prusky et al., 2001, Prusky & Yakoby, 2003). In chapter 6, there will be more discussion about possible roles of this RALF-like protein in *F. graminearum* – wheat interaction.

FgSSP6 and *FgSSP7* transcripts are highly expressed in rachis internode two and three and a single cerato-platanin (CP) domain (Pfam PF07249.7) was identified in each of these two correspondent proteins. Cerato-platanins are a group of small, secreted, cysteine-rich proteins that have been implicated in virulence of certain plant pathogenic fungi (Pazzagli et al., 2014) (see also chapter 5).

FgSSP8 is annotated to have a ribonuclease domain. Ribonuclease (RNase) activities contribute to RNA processing or degradation and this activity may play an important role in gene regulation. Plant-encoded RNase IIIs include Dicer-like protein involved in RNA silencing, which mediates plant defence gene regulation as well as being an antiviral defence mechanism (Cuellar et al., 2009). Perhaps fungal RNase proteins may be able to act in siRNA from the plant to stop plant RNA silencing used as a defence mechanism.

FgSSP9 and FgSSP10 proteins belong to a family of CFEM-containing proteins. CFEM is an eight cysteine-containing domain that may function as a cell-surface receptor, signal transducer, or can aid the adhesion of the protein in host-fungi interactions (Chen et al., 2013, Kulkarni et al., 2003). A number of CFEM-containing proteins are thought to play an important role in pathogenesis. One example is the *in planta*–expressed secreted protein MoCDIP2 from *Magnaporthe oryzae*. MoCDIP2 contains a CFEM domain and has been showed to induce cell death in rice cells (protoplasts and rice calli); however, this protein was unable to induce cell death in non-host species, such as maize, Arabidopsis and *N. benthamiana* (Chen et al., 2013).

FgSSP11 is highly expressed in both rachis internodes two and three and is localised in a region with high recombination frequency in the *F. graminearum* genome (Antoniw et al., 2011). Using published RNA-seq data obtained from *F. graminearum* (PH-1 strain) conidia and mycelium samples (Zhao et al., 2014), *FgSSP11* transcript appears to have only very low expression in *F. graminearum in vitro* culture, suggesting that *FgSSP11* expression is upregulated during *in planta* infection. This could indicate that this gene potentially has a role in the plant-pathogen interaction or is important for *F. graminearum* infection.

The final protein on the list, FgSSP12, has 58% similarity at the amino acid level to a novel hypersensitive response-inducing protein elicitor (MoHrip2) secreted by *Magnaporthe oryzae*. The recombinant MoHrip2 protein induced necrotic lesions when expressed in tobacco leaves, and rice seedlings sprayed with MoHrip2 (10 μM) protein exhibited greater resistance to *M. oryzae* than control (MES sprayed) seedlings (Chen et al., 2014). One hypothesis might therefore be that overexpression of FgSSP12 in wheat ears could render the plant tissue more resistant to subsequent *F. graminearum* infection.

Of the 12 genes selected for functional characterisation by BSMV-VOX, five are located in the small gene clusters enriched for genes coding for secreted proteins (FgSSP 3, 5, 7 9 and 12). None of the selected genes had been previously selected for reverse genetics experimentation in *F. graminearum*.

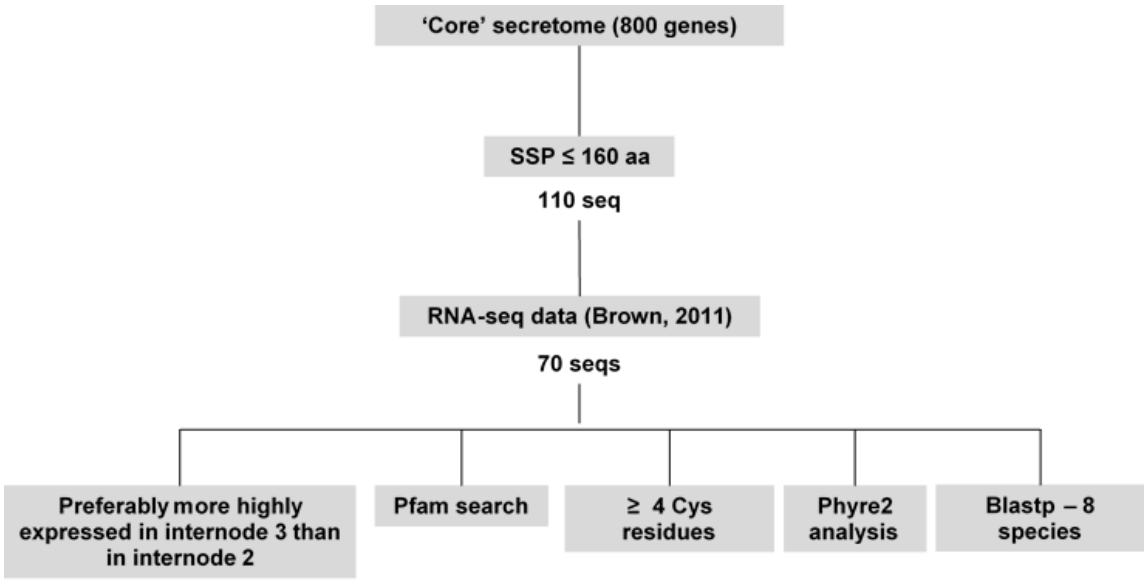

Figure 3.8 The bioinformatic pipeline used to select putative *F. graminearum* effectors for expression *in planta* using BSMV:VOX. Internode 3 had only symptomless infection (Brown, 2011).

Table 3.9 Putative effectors selected for functional analysis in the *F. graminearum*/wheat ear bioassay by BSMV:VOX

FgSSP[1]	Gene ID	Length (aa)	No. Cys[2]	Pair of Cys CC	Exp. IN3[3]	Exp. IN2[4]	Pfam domain	Pfam number	Hit info from Phyre 2	Blast hits[5]							
										Fv	*Fol*	*Foc*	*Fs*	*Fp*	*Zt*	*Bc*	*Ss*[5]
FgSSP 1	FGRRES_05046	130	8	1	8134	4706	-	-	-	x	x	x	-	x	-	-	-
FgSSP 2	FGRRES_09066	82	8	2	3802	851	-	-	structural protein	x	x	x	x	x	-	-	-
FgSSP 3	FGRRES_11047	108	8	-	2497	1339	-	-	-	x	x	x	x	-	-	-	-
FgSSP 4	FGRRES_08493	54	2	-	525	594	-	-	-	-	x	x	-	x	-	-	-
FgSSP 5	FGRRES_15123	75	4	-	269	148	RALF	PF05498.6	-	-	-	x	-	-	-	-	-
FgSSP 6	FGRRES_10212	139	4	-	1057	2564	Cerato-platanin	PF07249.7	unknown function	x	x	x	x	x	x	x	x
FgSSP 7	FGRRES_11205	138	4	-	148	1187	Cerato-platanin	PF07249.7	polysaccharide-binding protein	x	x	x	x	x	x	x	x
FgSSP 8	FGRRES_11190	132	4	-	39	39	Ribonuclease	PF00545.15	Microbial Ribonuclease	x	x	x	x	x	x	-	-
FgSSP 9	FGRRES_03599	95	10	-	18	56	CFEM Domain	PF05730.6	-	x	x	-	-	x	-	x	-

FgSSP 10	FGRRES_02181	161	8	-	9	5	CFEM Domain	PF057 30.6	-	-	x	-	-	x	-	x	-
FgSSP 11	FGRRES_04583	148	4	-	276	1614	-	-	-	x	x	x	x	x	x	-	-
FgSSP 12	FGRRES_03894	154	6	-	4	35	-	-	Antifungal protein	x	x	x	x	x	-	-	-

1. FgSSP: *F. graminearum* small secreted protein. **2.** Cys: Cysteine; **3.** Exp. IN2: fungal gene expression in the 2nd rachis internode below inoculation point during infection at 5 dpi (RNA seq data from Brown (2011)); **4.** Exp. IN3: fungal gene expression in the 3rd rachis internode below inoculation point during infection at 5 dpi; **5.** BLAST analysis against eight published predicted fungal proteomes using a cut-off value of e^{-6}. Fg: *Fusarium graminearum*; Fv: *F. verticillioides*; Fol: *F. oxysporum* f.sp. *lycopersici*; Foc: *F. oxysporum* f.sp. *cubense*; Fs: *F. solani*; Fp: *F. pseudograminearum*; Zt: *Zymoseptoria tritici*; Bc: *Botrytis cinearea*; Ss: *Sclerotinia sclerotiorum.*

3.4 Discussion

The main aim of this study was to predict the 'core' secretome among a group of *F. graminearum* isolates and select putative effector candidates for further study. The strains used for comparison are from Brazil from the wheat growing region constantly suffering from FEB disease. Although the number of strains in this study cannot represent the whole *F. graminearum* population, with this comparison it is possible to gain an indication of which gene and regions are conserved and variable in the *F. graminearum* genome and secretome. The total secretome from both *F. graminearum* strains PH-1 and CML3066 represents about 6% of each of their respective genome, while 5.6% corresponds to the 'core' secretome. Therefore, only 0.4% of the initial predicted secretome for each strain is not common between all strains sequenced here. Predicted secreted proteins shared among a number of strains provide evidences of which genes could participate of conserved molecular mechanisms. These could be good targets for future virulence interference strategies.

Often, genes in the secretome appear to be distributed within genomic compartmentalisations depending on the species (Lo Presti et al., 2015). Some pathogenic fungi (*Magnaporthe oryzae* and *Leptosphaeria maculans*) and plant pathogenic oomycetes have gene-sparse regions, which are highly enriched in repetitive elements, in which most of the secreted proteins are located (Raffaele & Kamoun, 2012). In other fungal species, such as *F. oxysporum* and *Alternaria alternata*, conditionally dispensable chromosomes are often enriched in genes encoding secreted proteins or effectors (ref). The strictly asexual plant pathogenic fungus *Verticillium dahliae*, through chromosomal rearrangements create highly dynamic regions that are lineage-specific. Such regions are greatly enriched for in planta-expressed effector genes encoding secreted proteins that

enable host colonisation (de Jonge et al., 2013). The smut fungi *Ustilago maydis* has a small genome and the genes encoding secreted proteins mostly reside in clusters of three or more genes (Mueller et al., 2008). Exploring the secretome distribution and genomic features predicted for *F. graminearum*, none of these strategies appear to be fully adopted by this species. This can be observed by the predicted low repetitive sequence content and small genome size of *F. graminearum* (King et al., 2015, Cuomo et al., 2007) and most gene clusters do not seem to have originated from gene duplications. *F. graminearum* also does not have known conditionally dispensable chromosomes and generally accessory chromosomes that are devoid of essential genes and harbour solely pathogenicity-relevant genes usually applies to species classified with races defined by virulence variation in different host cultivars (Ma et al., 2010). As *F. graminearum* species do not appear to be split into different races, it seems likely that the components of the secretome mediating fungal pathogenicity will be conserved between different strains, hence our strategy to define a 'core' secretome.

For the reasons mentioned above, *F. graminearum* putative effectors were selected based on the genes that comprise the 'core' secretome. Among the 12 genes selected, six of them are Fusarium specific. None of the putative effectors selected are among the *F. graminearum* specific one identified by King et al., 2015. In the most recent PH-1 genome annotation, 741 *F. graminearum* species specific genes have been identified. Eleven of these genes are within the PH-1 secretome predicted in this study, however two of them (FGRRES_13464 and FGRRES_20230) seems to be strains specific because these are not found in most of the additional *F. graminearum* strains sequenced. Five genes predicted to be *F. graminearum* species specific are among the 800 part of the 'core'

secretome (King et al., 2015). All five genes (FGRRES_10603, FGRRES_15183, FGRRES_15251, FGRRES_20027, FGRRES_20368) are unannotated and encode proteins smaller than 160aa and three of them predicted to be effectors (Appendix 1). These results contrasts with the *F. graminearum* secretome prediction in 2012 (Brown et al., 2012), where 25 species specific secreted proteins were identified. Probably, this is due to the fact that many other fungal species and strains have been sequenced in the last four years and when the Blast analysis was done again, some of these *F. graminearum* specific genes had homologs in other species, including the FEB causing fungus *F. culmorum*.

The low species specificity of *F. graminearum* 'core' secretome components may be explained by its lifestyle. *F. graminearum* is known as hemibiotrophic and the biotrophic phase of infection last few days. On the other hand, the necrotrophic phase is usually longer and persists for over 10 days. Therefore, it is predicted that *F. graminearum* secretes an array of PCWDE (Plant cell-wall degrading enzymes) and other enzymes (Brown et al., 2012, Cuomo et al., 2007, Soanes et al., 2007). This is probably essential for *F. graminearum* pathogenesis, once it is necessary to breakdown the plant cell to switch to the necrotrophic phase. Obligate and non-obligate biotrophic pathogens contain a higher proportion of species specific proteins. For example, *B. graminis f. sp. hordei, B. graminis f. sp. tritici* and, in particular, *U. maydis,* where two thirds of the secreted proteins are species specific (Muller et al., 2008, Kusch et al., 2014). The secretome arsenal in hemibiotrophic fungi is usually bigger and more diverse compared to biotrophic and necrotrophic species, i.e., these species initially need effectors to suppress plant defences and later need effectors that debilitate and/or kill plant cells (Lo Presti et al., 2015).

In summary, this *in silico* characterisation of *F. graminearum* 'core' secretome has provided some new information on the evolution of the F. graminearum genome. This study in particular has provided more understanding on the stability of the genes predicted to code for secreted proteins that may contribute to fungal infection. The more comprehensive analysis on identifying genes coding for secreted proteins that may be conserved in several *F. graminearum* strains could lead the discovery of new targets for disease intervention.

Chapter 4 – Analysis of the contribution of specific components of the predicted *Fusarium graminearum* core secretome to Fusarium floral infection using *Barley Stripe Mosaic Virus*-mediated overexpression.

4.1 Introduction

Like many plant pathogens*, Fusarium graminearum* is predicted to produce various secreted proteins during host plant infection and colonisation. This secreted proteins proteins, as well as secondary metabolites can modulate plant metabolism to suppress and/or re-programme plant defences (Rafiqi et al., 2012). Collectively, these secreted entities are referred to as the effector repertoire. The interaction between a successful pathogen and its plant host relies on the loss, acquisition and /or modification of effectors by the pathogen, and host proteins that can directly or indirectly detect these effectors (Lo Presti et al., 2015). Thus, understanding the molecular functions of *F. graminearum* secreted proteins will help to elucidate the processes underlying wheat spike colonisation and fungal pathogenicity.

With the aim of identifying *F. graminearum* effector proteins that can suppress host plant defences, a set of small secreted proteins (SSP) was selected using RNA-seq data analysis, inter-genome strain comparisons and various follow-on bioinformatic approaches (described in chapter 3) to be expressed *in planta* using the *Barley Stripe Mosaic Virus*-mediated over-expression system (BSMV-VOX) (Lee et al., 2012) . The effect of expressing any of these SSPs on *F. graminearum* fungal infection of susceptible wheat spikes was then analysed.

Functionally, analysing the role(s) of proteins in plant-fungal interaction by gene disruption or deletion can be challenging, and in some cases, the effect

of disrupting a particular gene may be masked by the presence of genes with similar functions, i.e. genetic redundancy occurs. For example, in *Botrytis cinerea*, deletion of four genes predicted to be involved in plant–fungus interaction did not affect virulence. This fact was attributed to functional redundancy compensatory processes (Aguileta et al., 2012). Although the lack of an altered phenotype can be disappointing to an investigator, this category highlights the major incentive for the initiation of either transient or stable overexpression studies. By this approach novel phenotypes may be observed that provide clues about the gene/protein function even when the results from gene deletion/disruption experimentation were uninformative.

Protein overexpression can be achieved using different experimental methods. For example, by replacing the promoter of the gene interest by the promoter of a gene more highly expressed *in planta* or by stably transforming the host plant with a construct the permits expression of the fungal gene of interest (Ferrari et al., 2012).

Alternatively, protein overexpression can be achieved through agro-infiltration of leaf tissue with binary vectors harbouring a sequence of interest. This method has been shown to be rapid and efficient, but it does not work well for some plant species, specially monocots (Sainsbury et al., 2009, Bos et al., 2006). Another possibility is to use a transient expression system such as virus mediated system (Manning et al., 2010). The latter approach, using a virus mediated system has been used in this study, because generating viral constructs is efficient, relatively rapid and cheap.

In wheat and barley, virus mediated expression systems are mainly used for gene silencing of host plant genes (Virus-Induced Gene Silencing - VIGS) (Lee et al., 2012). *Barley stripe mosaic virus* (BSMV) is the most commonly used vectors,

whilst in dicotyledonous species, *Tobacco rattle virus* (TRV) is a widely used vector (Senthil-Kumar & Mysore, 2011). Virus mediated protein overexpression has been used previously to study virus infection, but it is relatively new to use the virus as a vector for expressing proteins from other organisms (Lee et al., 2012). This is probably due to certain limitations with BSMV-VOX system. One constraint is predominately associated with the size of the protein that can be stably expressed from the vector. This is because, during the various virus replications *in planta*, genes that encode proteins greater than 160 amino acids can be lost more easily and the virus genome restored to its wild-type. Timing of virus inoculation is also important for the gene to be expressed in the wheat ear. If the virus is inoculated onto leaves at too early a growth stage, the virus might not be able to reach the wheat ears and overexpress the protein of interest just prior to when the plant is ready for *F. graminearum* inoculation, i.e. when the first wheat spikelets come into anthesis.

BSMV is a RNA virus with a tripartite genome. The experimental system consists of inserting the heterologous gene sequence downstream of the γb ORF in the RNAγ genome. To enable co-translational self-processing of the inserted protein to result in some free heterologous protein, a synthetic 2A gene was inserted at the 3'-terminus of the BSMV γb ORF in the RNAγ vector. 2A is a peptide sequence from a picornavirus, that is 18-amino-acid-long and has catalytic auto-proteolytic function, i.e. self-cleavage occurs, thus separating the protein of interest from the BSMV γb protein after translation (El Amrani et al., 2004) (Figure 2.1).

The candidate effectors to be tested for function *in planta* using BSMV-VOX were chosen using the pipeline shown in chapter 3. The 12 genes selected are listed in table 3.9.

4.2 Results

4.2.1 Overexpression of *F. graminearum* small secreted proteins (FgSSP) in wheat and *N. benthamiana* plants using BSMV-VOX.

The *FgSSP1 FgSSP2, FgSSP3, FgSSP6* and *FgSSP7* genes were previously cloned and were ready for expression via BSMV-VOX by Mr. Fatih Olmez, a visiting PhD student from Turkey in 2012. *FgSSP4, FgSSP5, FgSSP8, FgSSP9*, *FgSSP11* and *FgSSP12* was also cloned into BSMV-VOX constructs and then transformed into Agrobacterium strain GV3101 (Section 2.11). It was not possible to clone *FgSSP10*, possibly because it is expressed only at very low level *in planta*, and attempts to amplify the transcripts from cDNA from *F. graminearum* – infected ear tissue were unsuccessful. In hindsight, a direct gene synthesis approach could have been taken.

Seven of the BSMV-VOX constructs were then tested *in planta* (FgSSP1, FgSSP2, FgSSP4, FgSSP5, FgSSP6, FgSSP7 and FgSSP8). Before testing in wheat, the virus constructs were infiltrated in *N. benthamiana* leaves through *Agrobacterium tumefaciens* transformed cells (Section 2.12). Virus and virions accumulate in the *N. benthamiana* leaves, which were then collected 5 days after agro infiltration and the sap was utilised to inoculate wheat.

In total, eight independent BSMV-VOX experiments were carried out (VOX experiments 1-8) on susceptible wheat plants (cv. Bobwhite). The statistical analyses were carried out on the data from all experiments together at 12 days' post *F. graminearum* inoculation. Although the ears were scored for FEB symptoms every three days, the disease was well developed but had not fully bleached the whole ear at this day 12 time point. All the statistical analyses were carried out comparing the treatments with the BSMV:MCS4D control, where the only addition to the viral genome is a multiple cloning site (MCS) from pBluescript

K. Virus infection itself appears to have a slight effect on FEB disease outcome and thus virus inoculated plants are the more suitable control for comparison (Wing-Sham Lee, personal communication).

Figure 4.1 represents the number of visibly diseased spikelets below the *F. graminearum* inoculation points in wheat ears from the eight VOX experiments carried out between 2014 and 2016. Among these, three experiments tested FgSSP6 and FgSSP7, four experiments tested FgSSP5 and one experiment tested FgSSP1, FgSSP2 and FgSSP4. Typically, between 10 and 13 ears per construct were tested in each experiment.

The FgSSP1 treatment gave *F. graminearum* infection similar to the no virus treatment and was statistically different from MCS with reduced disease. However, the plants inoculated with this construct did not show visible virus symptoms and therefore none or very little protein was overexpressed. For this reason, the FEB symptom development spread through the spikelets similar to no virus infection control. This gene was one of the most highly expressed in the symptomless phase and is predicted to encode eight cysteine residues within the mature processed protein. Cysteine richness is a feature of several well characterised effectors (Lo Presti et al., 2015). It might be interesting to explore further the role(s) of this protein during infection. But as I already had other lead effector candidates at this stage in the PhD studies (see below), I did not repeat the experiment.

The FgSSP2 and FgSSP4 treatments did not induce more FEB disease and showed similar infection progress to the MCS virus control. *FgSSP2* encodes a small protein (82 amino acids) and is also highly expressed in the symptomless phase. Putative domains have not been predicted for this protein, but the results blast analysis and cysteine positions, showed high similarity with hydrophobins

(data not shown). Hydrophobins are a group of proteins expressed only by filamentous fungi. These proteins are known for their ability to form a hydrophobic coating and seem to play an important role during attachment of the fungus to the plant cuticle (Schafer, 1994). In some species, these proteins have been shown to play a role during fungal infection (Talbot et al., 1993). On the other hand, one of the *F. graminearum* hydrophobins has been reported not to have an effect in *F. graminearum* infection on wheat spikes (Martin Urban, personal communication).

FgSSP4 encodes the smallest protein in the list (54 amino acids) (Table 3.9), which is predicted to be homologous to *mc69* from *Magnaporthe oryzae. Mc69* encodes a small secreted protein and the mutant failed to form invasive hyphae (Saitoh et al., 2012). The role of this protein has not been elucidated, but this data suggests that the overexpression does not contribute to enhance disease in wheat. Nonetheless, the deletion of this gene in *F. graminearum* would confirm if it is an effector protein and has a role in wheat ear infection.

FgSSP6 and FgSSP7 encode two small secreted proteins containing a cerato-platanin domain (PFAM 07249). Proteins contained this domain are present only in fungi and have been reported in some species to play a role in pathogenicity (Pazzagli et al., 2014). At 12 dpi, about 87% of BSMV:FgSSP6 infected ears had visibly diseased spikelets whilst around 75% of the ears of BSMV:MCS4D control plants displayed typical FEB symptoms (Figure 4.1 and 4.2). Generalised linear mixed model (GLMM) analysis revealed that ears infected with BSMV:FgSSP6 are statistically more FEB diseased than ears infected with BSMV:MCS4D ($p < 0.05$) the combined analysis of the data from all experiments BSMV:FgSSP7 did not show disease enhancement. However, in one of three independent experiments, FgSSP7 overexpression did lead to

greater number of diseased spikelets compared to the control BSMV:MCS4D at 12 dpi (P = 0.05). The different results in each experiment might suggest different levels of gene overexpression had occurred. Perhaps this protein requires overexpression above a certain threshold to lead to a different disease outcome. Therefore, I decided to explore further the roles of both cerato-platanins domain proteins on wheat. These experiments are described in chapter 5.

FgSSP5, encodes a protein that possesses the pfam domain RALF (Rapid alkalinisation factor; PFAM 05498). BSMV:FgSSP5 showed slightly *F. graminearum* disease enhancement compared to BSMV:MCS4D ($p < 0.05$) (Figure 4.1 and 4.2). Interestingly in one of the VOX experiments, in the FgSSP5 treatment only, the anthers did not fully develop in the wheat ears after virus inoculation. Anthesis did not occur and the anthers remained inside the florets and contained no pollen (Figure 4.3). This phenomenon had been observed sporadically in different virus inoculated treatments in previous experiments, which would suggest this phenotype is virus associated. However, this phenotype seemed to be stronger in this specific batch and present in all plants inoculated with BSMV:FgSSP5. The same event was not observed again in the other VOX experiments when the plants had been inoculated with BSMV:FgSSP5. In the following experiments, plants inoculated with BSMV:FgSSP5 flowered normally. Additional experiments with FgSSP5 are described in chapter 6.

Sap from leaves of *N. benthamiana* plants infiltrated with BSMV:FgSSP8-carrying Agrobacterium was inoculated onto wheat plants, but the wheat plants did not develop viral symptoms and the *F. graminearum* infection on ears of these plants was similar to the non-virus inoculated plants (data not shown). When the *N. benthamiana* leaves were infiltrated with BSMV:FgSSP8, each infiltrated panel showed symptoms of necrosis at 4 dpi, and at 12 dpi the colonised leaves were

completely necrotic (Figure 4.4). Interestingly, the necrosis did not spread systematically throughout the plant. *FgSSP8* is predicted to encode a ribonuclease protein domain (PFAM 00545) and because BSMV is a RNA virus, the virus RNA may have been degraded and therefore, the virus infection stopped.

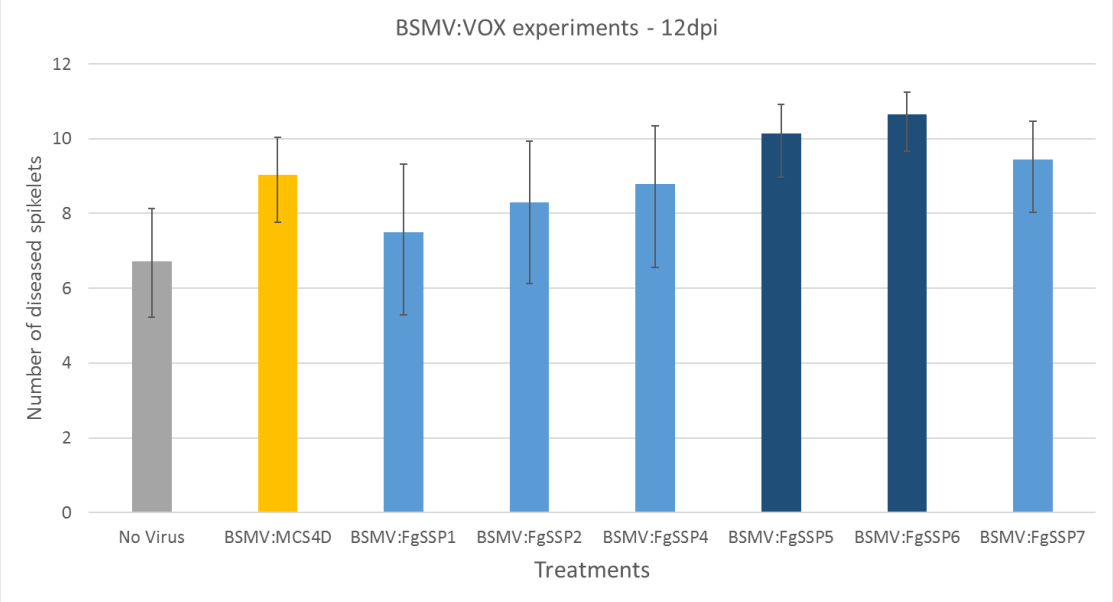

Figure 4.1 Graph representing number of visibly diseased spikelets below the *F. graminearum* inoculation points in wheat ears. A minimum of 9 ears per virus treatment were analysed. Data shown were collected at 12 days' post *F. graminearum*-inoculation. Dark blue bars denote treatments in which statistically significant differences in number of diseased spikelets, relative to BSMV:MCS4D control (yellow bar), were observed ($p < 0.05$ from GLMM analysis). This graph represents a total of eight combined experiments.

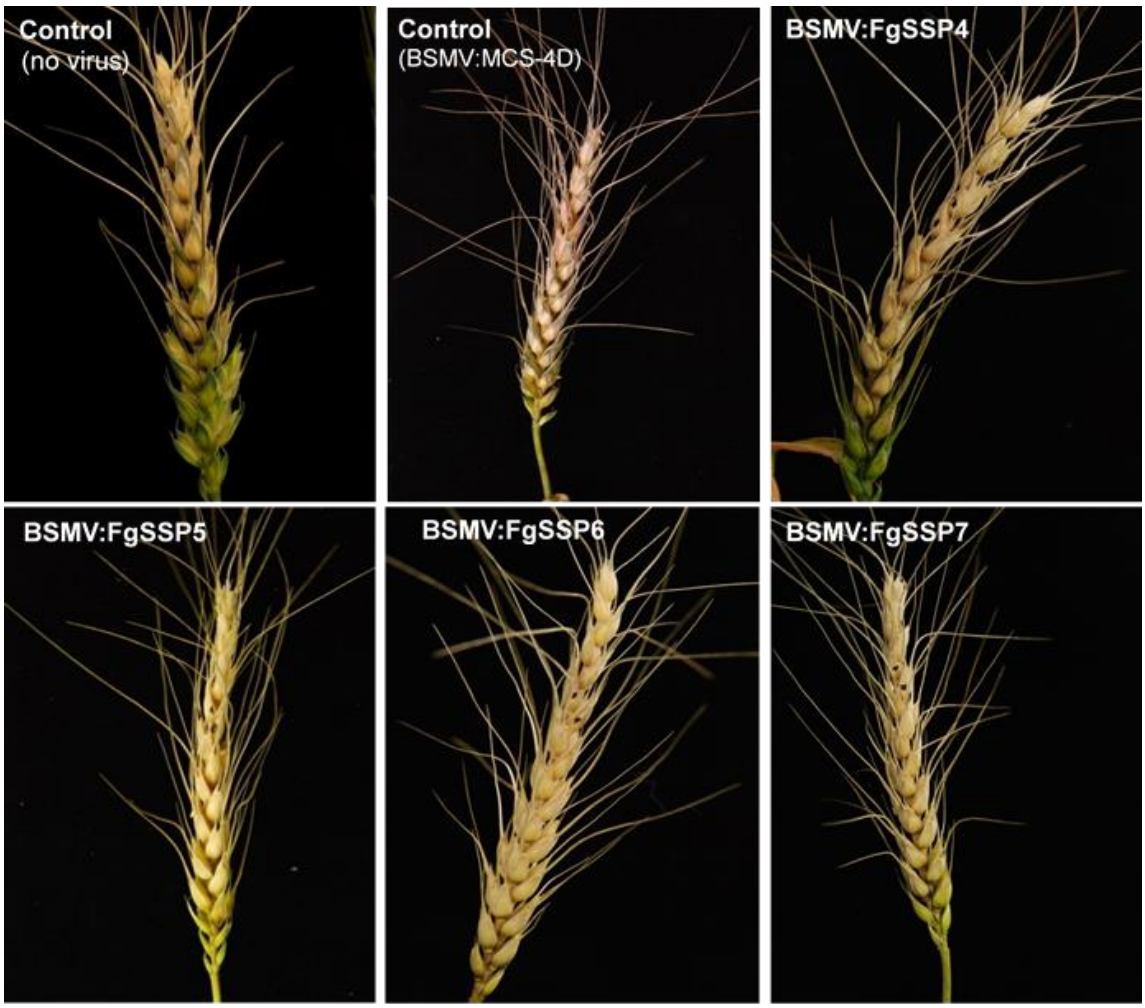

Figure 4.2 Representative *F. graminearum* disease symptoms on spikes of controls (no virus infected and BSMV:MCS4D) and BSMV:FgSSP4, BSMV:FgSSP5, BSMV:FgSSP6 and BSMV:FgSSP7 infected wheat plants. Wheat ears were point-inoculated with the *F. graminearum* strain PH-1 at anthesis, approximately 8-10 days after virus inoculation on the leaves 5 and 6. Photographs were taken at 12 days post *F. graminearum* inoculation. The two black dots on the neighbouring spikelets towards the top of each ear indicate the points of *F. graminearum* inoculation.

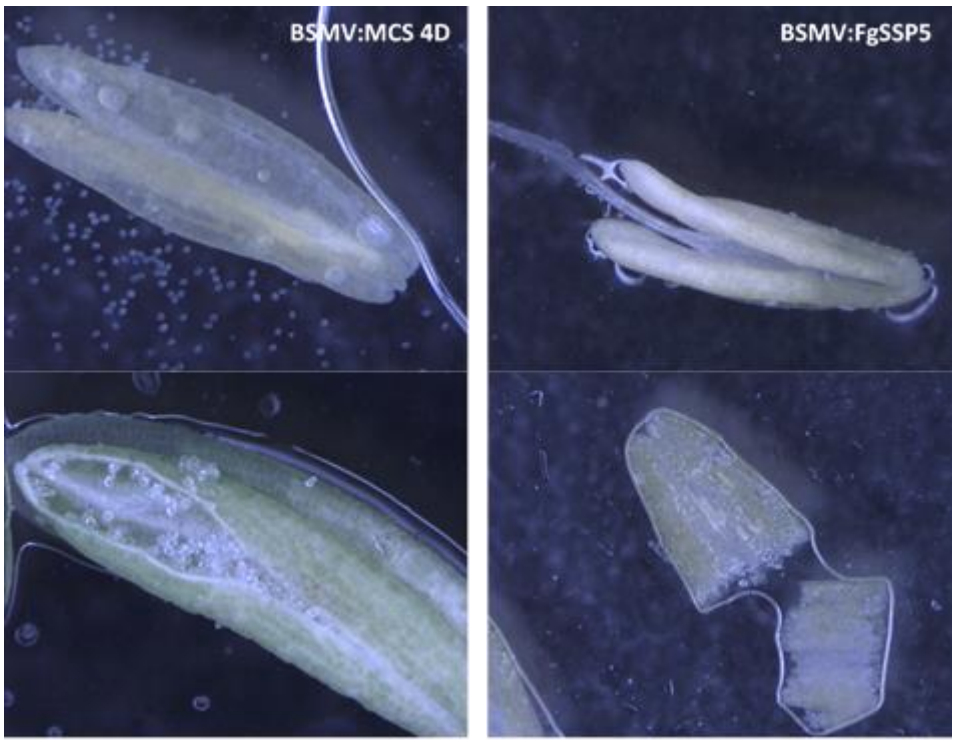

Figure 4.3 Wheat anthers development 14 days after virus inoculation with BSMV:MCS4D and BSMV:FgSSP5 in one biological repeat. Pollen formation is not observed in the BSMV:FgSSP5 inoculated plants (right hand panel) , but is abundant in the control BSMV:MCS4D inoculated plants (left hand panel) .

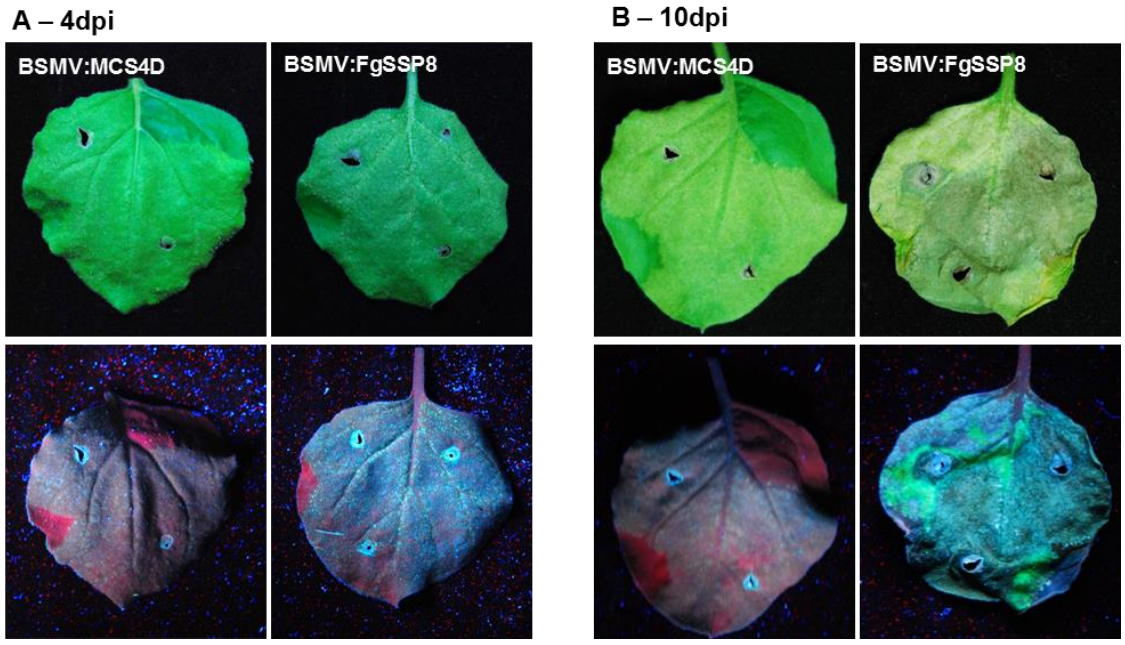

Figure 4.4. Appearance of the *N. benthamiana* leaves infiltrated with BSMV:MCS4D and BSMV:FgSSP8 at 4 dpi (A) and 10 dpi (B) viewed under white light (top) and UV light (bottom). In the lower panel, the red colour indicated chloroplast autoflourescence where the leaf tissue is still alive, whereas the green autoflourescence visible at day 10 is associated with dead leaf tissue.

4.3 Discussion

The results from the BSMV:VOX experimentation done in adult wheat plants between growth stages 37 and 42 (Zadoks, 1985) suggest that this experimental system works efficiently to explore the function of *F. graminearum* proteins that may be involved in this host-pathogen interaction. Amongst a set of 12 FgSSPs selected to be tested in the BSMV-VOX -*F. graminearum* wheat ear bioassay, seven have been tested, and four of them require further studies. Due the fact that more experiments than anticipated had to be repeated for the interesting candidates, I did not have time to test the other five genes. However, the role these proteins during *F. graminearum* – wheat interaction should still be explored.

Two of these constructs, BSMV:FgSSP6 and BSMV:FgSSP7, correspond to *F. graminearum* genes encoding cerato-platanins proteins (CPPs). The CPPs family represents a large group of proteins that contain four cysteines. The CPPs family is present in numerous fungal species and is unique to filamentous fungi. CPPs possibly exert several role(s) in the pathogenicity process, that are not yet fully understood (Gaderer et al., 2014).

Overexpression of the cerato-platanin protein (CPP) FgSSP6 consistently enhanced FEB disease symptoms development in wheat ears following point inoculation (Figure 4.1). The results of BSMV:FgSSP7 treatment in two experiments contrast with the increase in visible *F. graminearum*-induced disease in BSMV:FgSSP7 infected ears observed in the first VOX experiment. It is possible that FgSSP7 does not have as strong an effect on the disease interaction as FgSSP6. Another possibility is *FgSSP7* expression from the virus construct was at an insufficiently high level in the other two VOX experiments.

Perhaps there is a threshold of gene or protein expression level which is required for an effect of *F. graminearum* disease development to be observed.

The studies carried out so far in other fungal species to try to understand the role of CPPs in the plant have revealed intriguing properties for this family of proteins. CpCP from *Ceratocystis platani* and MpCP2 from *Moniliophtora perniciosa* showed expansin activity *in vitro* experiments. Both proteins have the ability of loosening the cellulose in a non-enzymatic way (Baccelli et al., 2014a, Barsottini et al., 2013). Other studies demonstrated that some CPPs (*Trichoderma atroviride* EPL1, *C. platani* CP, and *M. perniciosa* MpCP1-5) also have the ability to bind to chitin polymers (N-acetylglucosamine subunits) and / or chitin oligomers (Baccelli et al., 2014a, Barsottini et al., 2013, de Oliveira et al., 2011, Frischmann et al., 2013). The specific roles of *Fg* cerato-platanin in wheat have been studied in greater detail and are presented and discussed in chapter 5.

Another of the overexpressed FgSSPs, BSMV:FgSSP8, induced necrosis on its own in *N. benthamiana*, which indicates that this proteins could activate cell death in leaves of dicotyledonous plants. FgSSP8 encodes a protein containing a guanine-specific ribonuclease N1 domain (PFAM 00545). The role of fungal ribonucleases during infection is still not clear. Recent work has explored the role of a ribonuclease-like protein in the obligate biotrophic powdery mildew fungi *Blumeria graminis* f. sp. *hordei* (Pennington et al., 2016, Pliego et al., 2013). Using host-induced gene silencing, a ribonuclease-like protein BEC1054 was shown to contribute to fungal infection in barley. Recent findings suggest that BEC1054 target barley proteins responsible to trigger plant defences, contributing with the fungal biotrophic life style (Pennington et al., 2016).

FgSSP8 orthologues genes are also found in other plant pathogens. For example, wheat leaf infecting fungus *Zymoseptoria tritici*, where the gene has been named Zt6 (Kettles et al., 2017). Overexpression of Zt6 using a pEAQ vector (Sainsbury et al., 2009) in *N. benthamiana* also induce strong cell death. Further studies with the purified Zt6 purified protein demonstrated that the protein is toxic to other species of bacteria and fungi, but not to *Z. tritici.* These finding could suggest that this class of ribonuclease has an anti-fungal and anti-bacteria activity, helping the pathogen to establish infection and 'ward off' potential competitors (Kettles et al., 2017).

The role of FgSSP8 protein during *F. graminearum* – wheat infection should be explored further. However, due the difficulties to produce FgSSP8 purify protein because of its high toxicity and the limited time, additional intended studies were not I carried out during this PhD project, but could be done in the future.

Both *N. benthamiana* and wheat plants infected with BSMV:FgSSP1 did not show virus symptoms. This was intriguing and two hypotheses could be speculated: the first one is that some technical problem happen during the agroinfiltration and the constructs were not viable. The other possibility is that this protein may have triggered an extreme defence response in *N. benthamiana* and wheat plants, that led to impairment of virus infection. Because I had other FgSSP to investigate as my leads, I was not able to repeat the experiment with BSMV:FgSSP1. This interaction will be explored further by another PhD student through assessment of *N. benthamiana* defence genes expression. If there is a strong plant defence response that reduces virus infection, a different method could be the use of stable overexpression of this protein in Arabidopsis, followed by *F. graminearum* floral tissue inoculation.

The other FgSSP protein that led to a subtle disease enhancement when overexpressed was FgSSP5, which is a RALF domain-containing protein (PFAM 05498). RALF proteins are mainly found in plants and are responsible for *in planta* extracellular alkalinisation. This protein is known to interact with the plant receptor-like kinase FERONIA (Li et al., 2016). Although, both RALF and FERONIA are required for plant development, recent studies have showed that fungal RALF can be required for plant pathogenesis (Masachis et al., 2016, Thynne et al., 2017). This function for fungal RALF proteins been described in several Fusarium species. In plants, the FERONIA receptor can form a complex with BAK1 and is responsible for the initiation of the MAP kinase signalling response (Li et al., 2015, Stegmann et al., 2017). Roles of the RALF protein in plants and fungi will be discussed further in chapter 6.

In this chapter, the first report of the successful use of the BSMV-VOX system in combination with *F. graminearum*-wheat spike infections to identify novel candidate *F. graminearum* effectors is given. So far, we do not know which mechanism(s) drives the disease enhancement. Future work will test the hypothesis that there is also a trans-kingdom interaction, where overexpression of certain fungal proteins could favour the virus infection and increase the virus titre in wheat ears. Consequently, the higher virus titre could both lead to more protein overexpression, favouring the fungal infection as well as compromise plant defences and therefore render the plants more susceptible to fungal infection. If this dual hypothesis proves to be true, it could also explain the unusual outcome from the first VOX experiment with BSMV:FgSSP5, where the wheat anthers did not fully developed and the virus symptom in wheat ears was stronger than in any of the other treatments. The next two thesis chapters will focus on exploring specific roles of three of these *F. graminearum* secreted

proteins. In conclusion, there is still a lot to be explored on the mechanisms operating in the BSMV:VOX system. However, this appears to be a promising new approach because at least four and possibly five of the seven of SSP tested gave some type of altered phenotype in either *N. benthamiana* leaves or wheat floral tissue.

Chapter 5 – Two cerato-platanin proteins FgSSP6 and FgSSP7 contribute to *Fusarium graminearum* virulence on wheat spikes.

5.1 Introduction

Of the seven *F. graminearum* putative effectors screened for function using the BSMV-VOX system so far, overexpression of FgSSP6 appeared to have the most influenced on the compatible *F. graminearum*-wheat ear interaction (see Chapter 4). Although overexpression of the closely related effector FgSSP7 (66% mature peptide identity) did not have a statistically significant effect on FEB disease development in the overall combined analysis of four BSMV-VOX experiments, overexpression of FgSSP7 appeared to enhance FEB development in two independent experiments. *FgSSP6* and *FgSSP7* encode proteins that contain the same cerato-platanin (CP) domain PFAM 07249. The results shown in figure 4.1 (Chapter 4) suggest that CP function may play a role in the *F. graminearum*-wheat ear interaction. Therefore, the function of both of these CP gene encoding proteins as well as specific aspects of their sequences were analysed in more detail.

CP family proteins are small (~12kDa), secreted proteins with four conserved cysteines that have been reported only in filamentous fungi with all types of lifestyles (Pazzagli et al., 1999) but have not been found in yeasts, oomycetes or bacteria. Belonging to a family of non-catalytic fungal proteins, CPs seem to have a role in the pathogenic process that, in many cases, is not fully understood (Gaderer et al., 2014).

The first CP identified from a phytopathogenic fungus was SnodProt1 (SP1) in *Phaeosphaeria nodorum,* which is produced by the fungus during *in vitro*

culture and during infection of wheat leaves (Hall et al., 1999). Later, a CP was identified and functionally characterised in the necrotrophic fungus *Ceratocystis platani* that infects plane trees (*Platanus spp.*). This discovery provides the origin of the name of this protein family (Pazzagli et al., 1999). Since then, cerato-platanin functions have been explored in predominantly Ascomycete fungal species, including *Magnaporthe oryzae*, *Botrytis cinerea*, *Moniliophtora perniciosa*, *Trichoderma atroviride* and *T. virens* and a number of differing functions have been suggested depending on the species studied (Barsottini et al., 2013, Chen et al., 2013, Frias et al., 2011, Frischmann et al., 2013). The main discoveries about the roles of CP in different fungal species are summarised in table 5.1. Some of the features of most relevance to the current wheat – *F. graminearum* investigations are further discussed below.

Based on high level of amino-acid identity between cerato-platanins from different species and the detected presence of some in the fungal cell-wall, various studies suggest that the primary role of cerato-platanins may be in fungal growth and development, possibly by acting as an expansin-like protein (Baccelli, 2015). Expansins are proteins found mainly in plants (Sampedro & Cosgrove, 2005), however expansin-like proteins have also been found in fungi and bacteria. These proteins are also referred to as either swolenins or loosenins (Georgelis et al., 2015). The mode of action of expansins has been suggested to be to cause disruption of non-covalent bonds in wall polysaccharides by a non-hydrolytic activity, and hence, stimulate plant cell-wall extension and stress relaxation (Sampedro & Cosgrove, 2005). Cerato-platanins from the fungal species *C. platani* (CpCP) and *Moniliophtora perniciosa* (MpCP2) have been shown to possess expansin-like activity *in vitro.* These two studies reported the

ability of both proteins to loosen cellulose in a non-enzymatic way, which include weakening of filter paper, fragmentation of crystalline cellulose and breakage of cotton fibres (Baccelli et al., 2014b, Barsottini et al., 2013). Several other fungal CPs (from *T. atroviride* Epl1, *C. platani* CP, and *M. perniciosa* MpCP1-5) have been shown to be able to bind chitin and colloidal chitin (Frischmann et al., 2013, Baccelli et al., 2014b, de Oliveira et al., 2011, Barsottini et al., 2013). The ability to bind chitin had already been reported for expansin-like proteins from fungi, although it is not clear whether these proteins cause changes in the chitin structure (Quiroz-Castaneda et al., 2011). Pazzagli et al. (2014) suggests that CP has a structural role in the fungal cell wall due the ability to bind chitin and the localisation in the fungal cell-wall.

In addition to this primary role of expansin-like activity, most of the CPs described have been shown to act either as virulence factors or elicitors of specific plant responses. Within the *B. cinerea* secretome, a cerato-platanin protein, BcSpl1, has been shown to be one of the most abundant secreted proteins. A comparative proteomic analysis of *B. cinerea* secretome using LC-MS/MS approach revealed that almost one quarter of the spectra identified in different growth conditions belong to BcSpl1, indicating that this protein is very highly expressed *in vitro* and *in planta*. Expression of the corresponding gene by Q-RT-PCR demonstrated that, although *bcspl1* is expressed in every condition studied, highest levels of expression were detected *in planta* during the late stages of infection (Frias et al., 2011, Shah et al., 2009). Purified BcSpl1 injected into leaves was able to induce necrosis in tobacco, tomato and Arabidopsis in concentration dependent manner, causing a hypersensitive response and the production of reactive oxygen species (Frias et al., 2011). In the same study,

BcSpl1 was supplemented in MS media and *in vitro* growth of Arabidopsis wild-type (Col-0) and Arabidopsis mutant carrying disrupted *bak1* gene was compared. BAK1 is a receptor-like kinase component of plant PTI required for the perception of plant elicitors (Heese et al., 2007). The receptor-like kinase SERK3/BAK1 is a central regulator of innate immunity in plants. Arabidopsis mutants *bak1* were sown in MS medium supplemented with BcSpl1 and showed reduced sensitivity to BcSpl1 compared to Arabidopsis wild-type (Col-0). These results suggest that the BAK1 signalling is required for BcSpl1 activity (Frias et al., 2011).

The genomes of the biocontrol species *T. virens* and *T. atroviride* are predicted to code for three cerato-platanin proteins, named Sm1, Sm2 and Sm3 in *T. virens*; and Epl1, Epl2 and Epl3 in *T. atroviride*. Djonovic et al. (2007) demonstrated that deletion and overexpression of *SM1* in *T. virens* transformed strains, resulted in significantly reduced and enhanced levels of disease protection in maize, respectively, compared to the wild type strain, against the leaf pathogen *Colletotrichum graminicola*. Plant overexpression of cerato-platanin from *M. oryzae* (MoSM1) also conferred enhanced resistance against *M. oryzae* and the bacteria species *Xanthomonas oryzae* pv. *oryzae* in transgenic rice (Hong et al., 2017). Similar results were achieved in Agrobacterium-mediated transient expression of MgSM1 in Arabidopsis when subsequently inoculated with *B. cinerea* or *P. syringae* (Yang et al., 2009). The single gene deletion *MoSm1* (or *Msp1*) mutants also exhibited greatly reduced virulence in rice due to impaired growth during plant infection (Jeong et al., 2007). In *T. atroviride*, Epl1 could self-assemble in air surface interfaces forming protein layers that increase the polarity of aqueous solutions and surfaces. This feature is similar to

hydrophobins, however, in contrast to hydrophobins, where the self-assembly is mostly irreversible, the Epl1 protein layers could be easily redisolved by mixing or stirring the solution, and new layers could be formed again from this protein solution upon incubation without shaking (Frischmann et al., 2013).

Sm1 and *Epl1* transcripts are both abundantly expressed during fungal growth, mainly in mycelia. Sm2 and Epl2 have been detected only in fungal spores and were less abundantly expressed than Sm1 and Epl1 during fungal growth, respectively. However, analyses with *T. virens* and *T. atroviride* cerato-platanins mutants demonstrated that Sm2/Epl2 seem to be more important than Sm1/Epl1 for the promotion of plant protection conferred by *Trichoderma.* No significant levels of expression were detected for the predicted genes Sm3/Epl3 (Gaderer et al., 2015). Although Sm1 and Epl1 are closely related (81% protein identity), Epl1 is found to readily form dimers and Sm1 is predominantly found in its monomeric form. The monomeric form has been shown to be more effective in the induction of plant defence response (Vargas et al., 2008). Monomers of cerato-platanin in *Trichoderma* species were recognized in the cell interface, defence responses were activated, and reactive oxygen species (ROS) reaction was elicited. The authors demonstrated that both Epl1 and Sm1 are susceptible to oxidative-driven dimerization and no longer active to induce induced systemic resistance. However, Sm1 is produced as a glycoprotein, and the presence of the glycosylation site does not allow the monomers to dimerize, and they remain in their active form for activating the defence responses in plants (Vargas et al., 2008).

Thus, the studies conducted so far on the role of CPs *in planta* from 10 different fungal species (*C. platani, M. perniciosa, M. oryzae, B. cinereal, S.*

nodorum, T. virens, T. atroviride, F. graminearum, L. maculans and Heterobasidion annosum) reveal intriguing properties for this protein family in both monocotyledonous and dicotyledonous species (Gaderer et al., 2014).

Recently, Brown et al. (2017) explored in detail *F. graminearum* genes expression *in vitro* and *in planta* at different spatial stages of the wheat spike infection using an FgAffmetrix analysis. In this study, FgSSP6 was found to be most highly expressed when grown in rich media (PDB) compared to any other condition tested *in vitro* and *in planta*. FgSSP7, on the other hand, was most highly expressed during *in vitro* growth on poor-nutrient media (minimal media) compared to other conditions tested. *In planta*, both *FgSSP6* and *FgSSP7* were found to be more highly expressed in the symptomatic phase of *F. graminearum* infection on wheat rachis internodes, followed by the onset of infection and less expressed during the symptomless phase (Brown et al., 2017) (Figure 5.1). This new data set supports the results obtained from the earlier RNA-seq analysis used in chapter 3 to select the effector genes for functional analysis (Section 3.3.7).

The aim of the experiments presented in this chapter was to elucidate the function(s) of the newly identified *F. graminearum* CPs FgSSP6 and FgSSP7 and to understand how these proteins enhance *F. graminearum*-induced disease when overexpressed from the BSMV-VOX vector in wheat spikes. To achieve this aim, I first analysed in more detail the predicted FgSSP6 and FgSSP7 primary and second protein structures. I then attempted to determine the levels of FgSSP6 and FgSSP7 produced by the BSMV-mediated *in planta* expression system using an immunological approach. The next step was to explore the role of other motifs and domains, (not including the CP domain), present in FgSSP6

and FgSSP7 protein sequence during *F. graminearum* infection on wheat using the BSMV-VOX approach. Then again using the BSMV-VOX system, I tested the ability of FgSSP6 and FgSSP7 to suppress plant defence responses in a host and a non-host interaction, a property not previously linked to the CP protein. Finally, *in vitro* assays using purified protein and *in planta* tests using newly generated *FgSSP7* gene deletion mutant strains were carried out to explore further the role (s) of CPs during *F. graminearum* infection.

Table 5.1 Summary table of the studies carried out up to date on fungal cerato-platanin family proteins (CPPs)

Gene names	Fungal species	Necrosis inducer (protein dose)	Fungi mutated or CPP genes phenotypes	Protein activates plant defence response	Other activity	References
BcSpl1	*Botrytis cinerea*	Yes (34µM)	*Bcspl1 gene-deletion* mutants were generated and showed reduced virulence in a variety of hosts.	Yes (34µM) triggers salicylic acid (SA) pathway	The BcSpl1-treated plant tissues showed symptoms of the hypersensitive response including induction of reactive oxygen species, electrolyte leakage, cytoplasm shrinkage.	(Frias et al., 2013, Frias et al., 2014, Frias et al., 2011)
CpCP	*Ceratocystis platani*	Yes (80µM)	ND[1]	Yes (150 µM) triggers salicylic acid (SA)- and ethylene (ET)-signalling pathways	Expansin-like activity and ability to bind chitin, formation of “ordered aggregates”.	(Baccelli et al., 2014a, Baccelli et al., 2014b, Fontana et al., 2008, Pazzagli et al., 2009)
fgcpp1-2 (=FgSSP6-7 from this study)	*Fusarium graminearum*	ND	single (Δ*fgcpp1*) and double (ΔΔ*fgcpp1,2*) knock-out mutants did not affect in virulence in wheat.	ND	Fungal growth had stronger inhibition under treatments with chitinase and β-1,3-glucanase.	(Quarantin et al., 2016)
FvCP1-3	*Fusarium virguliforme*	No (overexpression system mediated by *Soybean mosaic Virus*)	ND	ND	ND	(Chang et al., 2016)
HaCPL2	*Heterobasidium annosum*	Yes (120µM)	ND	Yes (120µM) – expression of	HaCPL2 induced phytoalexin production in tobacco Retardation of apical root growth.	(Chen et al., 2015a)

				defence related genes		
Sp1	*Leptosphaeria maculans*	No	Sp1 mutants did not affect virulence in canola.	ND	Recombinant SP1 protein induced an autofluorescence response on canola leaves.	(Wilson et al., 2002)
MgSM1 (or MSP1)	*Magnaporthe oryzae*	Yes (1.5µM)	Gene-deletion mutant compromised in pathogenicity in rice and barley	Yes (1.5µM)- expression of defence related genes	*MoSM1*-overexpressing transgenic rice lines showed an improved resistance against *M. oryzae* and *Xanthomonas oryzae* pv. *oryzae*	(Hong et al., 2017, Jeong et al., 2007, Wang et al., 2016b, Yang et al., 2009)
MpCP1, 2,3 and 5	*Moniliophthora perniciosa*	No (40µM)	ND	Yes (40µM) - expression of defence related genes	Self-assembling and the direct binding to chitin NAG tetramers MpCP2 were shown to act as expansin. MpCP5 blocked NAG6-induced defence response.	(Barsottini et al., 2013)
Snodprot1	*Parastagonospora nodorum*	ND	ND	ND	It was the first Cerato-platanin-coding gene identified in a phytopathogenic fungus.	
Epl1-2	*Trichoderma atroviride*	ND	Deletion of epl1 and epl22 (single and double mutants) lack of inducing systemic resistance in potato and maize against different pathogens	Yes (mainly monomeric form) - expression of defence related genes	Self-assembly at air/water interfaces and carbohydrate binding properties.	(Bonazza et al., 2015, Frischmann et al., 2013, Gaderer et al., 2015, Salas-Marina et al., 2015, Vargas et al., 2008)
Sm1-2	*Trichoderma virens*	No (10nM)	Deletion of sm1 and sm2 (single and double mutants) lack of inducing systemic resistance in potato and maize against different pathogens	Yes (1nmol) - expression of defence related genes	Required for the induction of systemicresistance in different hosts	(Djonovic et al., 2006, Djonovic et al., 2007, Gaderer et al., 2015, Salas-Marina et al., 2015, Vargas et al., 2008)

1. Not defined

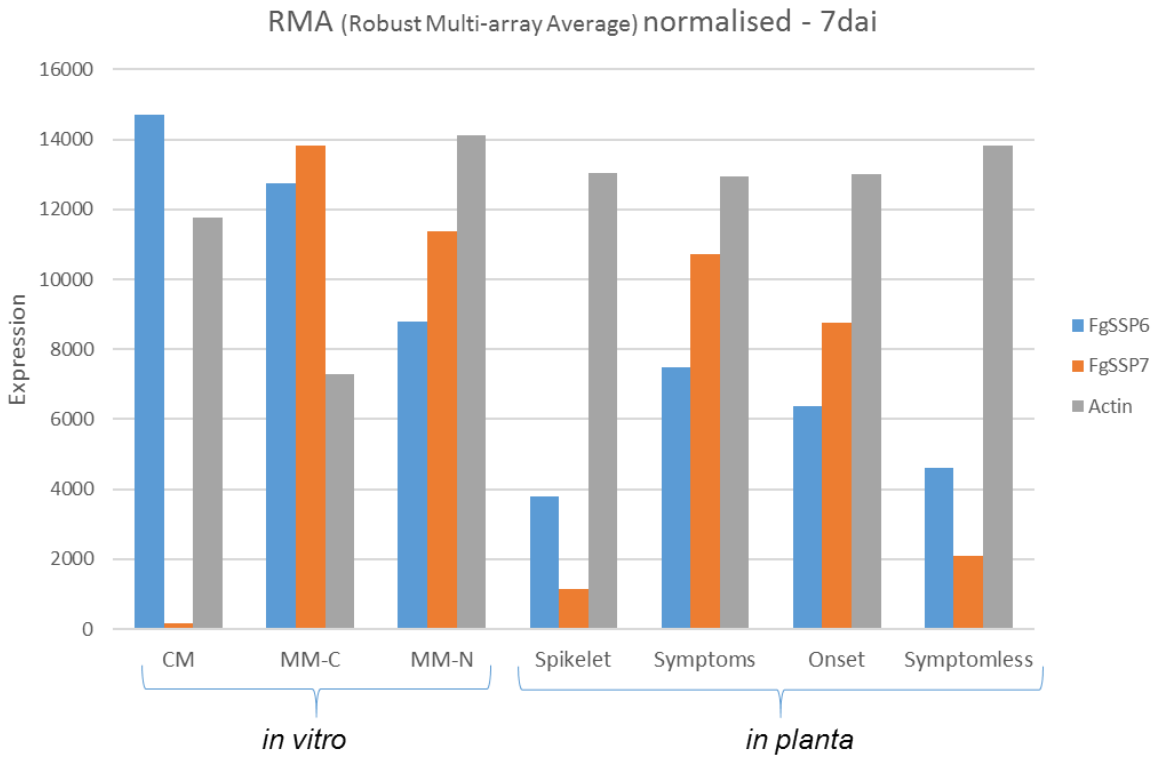

Figure 5.1 The expression pattern of FgSSP6 and FgSSP7 *in vitro* and *in planta*. *In vitro*: expression on complete media (CM), minimal media without carbon (MM-C) and minimal media without nitrogen (MM-N). *In planta*: from the point of inoculation (spikelet) through the rachis to the advancing front of infection (Brown et al., 2017, Guldener et al., 2006).

5.2 Materials and Methods

5.2.1 Synthesis of specific antibodies

Specific antibodies anti-FgSSP6 and anti-FgSSP7 were synthesised by Eurogentec Ltd. (Belgium) using their anti-peptide 28-day speedy polyclonal package. Antigen peptides sequences were generated from predicted surface exposed regions with the highest polymorphism between FgSSP6 and FgSSP7, corresponding to Ac-DTGYDDKSRPMTAVSC-NH_2 for FgSSP6 and Ac-DPGYGEAGRAMTAVSC-NH_2 for FgSSP7 (Figure 5.2).

5.2.2 Expression of recombinant FgSSP6 and FgSSP7 proteins in *E.coli*

Expression of recombinant proteins in *E.coli* was based on Gateway cloning and expression technology (Walhout et al., 2000, Hartley et al., 2000). In this study, the vector used to generate the constructs was pDEST17, which contains an N-His tag sequence. The heterologous gene was inserted downstream *att*B1 sequence (GGGGACAAGTTTGTACAAAAAAGCAGGCTTA) and upstream to *att*B2 site (GGGGACCACTTTGTACAAGAAAGCTGGGTA). As the His-tag is appended to the N-terminus (upstream of *att*B1) of the protein, predicted signal peptides at the 5' end of the sequence are not included in the construct. Expression from this vector is under the control of a T7 promoter, which is recognised by the phage T7RNA polymerase (T7RNAP). The T7RNAP, required for protein expression from the vector, is itself under the control of the lacUV5 promoter (Studier & Moffatt, 1986). Therefore, target protein expression requires the induction of T7RNA polymerase by lactose or its non-hydrolysable analogue isopropyl β-D-1-thiogalactopyranoside (IPTG).

Gateway cloning was carried out according to a previously published method (Moreland et al., 2005). Briefly, the open reading frames (ORFs) encoding FgSSP6 and FgSSP7 were amplified by PCR from a cDNA library prepared from *F. graminearum* infected wheat ears cv. Bobwhite at 5dpi. The primers used contain the attB sequence (Table 2.1). The amplified product was purified using QIAquick Gel Extraction Kit (Qiagen). A BP reaction, in which the attB-flanked PCR product was recombined with an attP substrate (pDONR207; Invitrogen) using BP Clonase (Invitrogen), was conducted to generate an entry clone. The entry clone, which contains attL sequences, was sub-cloned via a LR

reaction using LR Clonase (Invitrogen) into the attR expression vector pDEST17 (N-terminal His-tag; Invitrogen). After each of these two reactions, the vectors were cloned into the chemically competent *E. coli* strain JM109.

SHuffle® T7 Express (NEB) Competent *E. coli* B and K12 cells were transformed with the plasmid containing either of the heterologous genes *FgSSP6* or *FgSSP7.* The *E. coli* K12 strain was selected to express FgSSP6 protein and *E.coli* B for FgSSP7 expression (data not shown). The transformed *E. coli* cells with *FgSSP6* and *FgSSP7* genes were grown in LB broth overnight at 30^{o}C with shaking (250rpm). An aliquot of 1/100 of these cells were transferred to fresh LB broth and grown at 30^{o}C with shaking (250rpm) until they reached an OD600 of 0.4. IPTG was then added and the cells were grown at 16^{o}C overnight. To induce heterologous protein production, two different IPTG concentrations were used, 1mM and 0.1mM. These *E. coli* cells were harvested for protein extraction.

For extraction of total proteins, cells were harvested and homogenised in water. For extraction of soluble proteins, the cells were homogenised in water and lysed with glass beads, enabling cell membrane breakage.

To obtain purified protein, FgSSP7- and FgSSP6- transformed *E.coli* were grown in 1L of LB miller (10g/L tryptone, 10g/L NaCl, 5g/L yeast extract) with 0.1mM IPTG. After growth, *E. coli* cells were centrifuged (5,000 g for 10min), resuspended in equilibration buffer (50 mM sodium phosphate, pH 8.0, with 0.3 M sodium chloride) and lysed in sonicator. The lysate was separated by centrifugation (5,000 g for 30 min) and the supernatant recovered for recombinant protein purification using HIS-Select Nickel Affinity Gel (Sigma). Cell extracts were added to the affinity gel and mixed on an orbital shaker (175 rpm) for 15

min. The mixture was centrifuged at 5,000 g for 5 minutes and the supernatant was discarded. Ten volumes gel of wash buffer (50 mM sodium phosphate, pH 8.0, with 0.3 M sodium chloride and 10 mM imidazole) was added to the affinity gel and mixed on orbital shaker (175 rpm) for 4 minutes. The mixture was centrifuged at 5,000 g for 5 minutes and the supernatant was discarded to wash out residues that did not bind to the gel. This step was repeat two more times. To elute the protein, 2 volumes gel of elution buffer was added to the gel and protein mix (50 mM sodium phosphate, pH 8.0, with 0.3 M sodium chloride and 250 mM imidazole), mixed for 20 min on orbital shaker (175 rpm), centrifuged for 5 min and the supernatant saved. The histidine containing soluble protein will be in this fraction. Purified proteins were quantified by spectrophotometry measuring absorbance at 280 nm (A280).

5.2.3 Protein extractions from plant tissues and electrophoresis

To extract total protein from plant tissues, the selected plant tissue was homogenised in 270 µl of extraction buffer [50 mM Tris–HCl pH 7.25, 150 mM NaCl, 2 mM ethylenediaminetetraacetic acid (EDTA), 0.1% (v／v) Triton X-100]. Lysates were clarified by centrifugation and approximately 20 µl of protein-containing extracts were separated on 16% SDS-PAGE gel under reducing conditions, followed by Coomassie Brilliant Blue staining.

5.2.4 Recovery of apoplastic fluid from *N. benthamiana* leaves

The apoplast washing fluid (AWF) was obtained through the infiltration-low speed centrifugation method (O'Leary et al., 2014). *N. benthamiana* leaves were detached from the plant, submersed in distilled water to remove leaf surface

contaminants and dried gently with absorbent tissue. Each leaf was rolled into a 60ml syringe filled with distilled water until 40 ml mark. The syringe tip was covered with a piece of Parafilm and a negative pressure was created by pulling the plunger outwards to the 60ml mark and slowly releasing the plunger. The syringe tip was then uncovered to eject air, covered again and pressed further downwards on the plunger to create a modest amount of positive pressure. This process was repeated until the leaf was fully infiltrated. Leaf-filled syringes were centrifuged within a 50ml tube for 10 min, at 1,000 x g in a swinging bucket rotor, at 4 °C and a small volume of apoplastic fluid was obtained from the bottom of the centrifuge tube.

5.2.5 Acetone precipitation of soluble protein extracts

Six volumes of -20°C acetone was added to either crude leaf extracts or apoplastic fluids and placed at -20°C overnight. The mixture was centrifuge at 14,000 x g for 15 minutes at 4°C and the supernatant discarded. The pellet was washed 3x with -20°C acetone, following centrifugation at 14,000 x g for 15 minutes at 4°C. The precipitated was left to dry out for 2 hours and resuspended in 200µL of water.

5.2.6 Bradford assay for protein quantification

Quantification of protein extracts was carried out with the commercial Quick Start™ protein assay (Bio-Rad) based on colorimetric Bradford assay. First a calibration curve with BSA (bovine serum albumin), selected as reference protein, was obtained by serial dilution of BSA. The concentration of protein

extracts was then determined by extrapolation of the calibration curve (Bradford, 1976).

5.2.7 Western blot analysis.

To detect FgSSP6 and FgSSP7 in protein extracts from plants and *E. coli*, western blot analysis was carried out. Total and soluble protein extracts were denatured in SDS and 2-mercaptoethanol and separated on a 16% Tris–glycine SDS-PAGE gel under reducing conditions before being electro-blotted on to a nitrocellulose membrane (Hybond ECL, Amersham) using transfer buffer (20mMTris–HCl, 152mM glycine, 20% (*v*/*v*) methanol). The membrane was blocked in phosphate-buffered saline (PBS) containing 5% skimmed-milk powder and 0.025% (*v*/*v*) Tween-20 for 60min, probed in the same buffer either with 500-fold-diluted anti-six-His antibody (Santa Cruz Biotech, Santa Cruz, Calif.) or 1000-fold diluted anti-FgSSP6 or anti-FgSSP7 antibodies. Anti-rabbit horseradish peroxidase (HRP,1:10000, Cell Signaling Technology, New England Biolabs) was used as the secondary antibody for anti-FgSSP6 and anti-FgSSP7 blots. Specific antibody binding was detected using enhanced chemiluminescence western blotting detection reagents (Amersham Pharmacia Biotech Benelux).

5.3 Results

5.3.1 Structure of cerato-platanin proteins in *F. graminearum*

In *F. graminearum* genome, five putatively genes encoding proteins with at least one cerato-platanin domain have been identified (FGRRES_04471; FGRRES_17103; FGRRES_03971; FGRRES_10212; FGRRES_11205), however only two of them contain the full cerato-platanin sequence similar to the

class of SnodProt proteins (Hall et al., 1999). These two predicted proteins are FGRRES_10212 – FgSSP6 and FGRRES_11205 -FgSSP7. The genes *FgSSP6* and *FgSSP7* are located on chromosome 1 and 3, respectively and nucleotide alignment of the coding sequence reveals 63% identity between both sequences.

The predicted primary sequences and secondary structures for both FgSSP6 and FgSSP7 are typical of cerato-platanin domain-containing proteins. Protein alignment with other cerato-platanins identified in different species described in the literature reveal specific amino acids along the peptide sequence are conserved between CPs (Figure 5.2). *FgSSP6* and *FgSSP7* (FGRRES_10212 and FGRRES_11205) each consists of a single exon and encode proteins of 139 and 140 amino acid residues, respectively, with a signal peptide of 18 amino acids. Protein sequence analysis using Interpro (Finn et al., 2017) predicted two domains in both FgSSP6 and FgSSP7. The first is a RlpA-like double-psi beta-barrel domain (IPR009009), which is found mainly in plant and bacterial expansins, lytic transglycosylases (LTs), endoglucanases, formate dehydrogenase H, dimethyl-sulfoxide reductase, asparticproteinases and in the plant defense protein barwin. The other domain is the well characterised cerato-platanin domain (IPR010829, PF07249), which classifies FgSSP6 and FgSSP7 within the cerato-platanin protein family (Pazzagli et al., 2006). Protein model predictions using Phyre2 (Kelley et al., 2015b) showed that the secondary structure of FgSSP6 is similar to CP from the pathogenic species *M. perniciosa* (MpCp-2) (Figure 5. 3A), while FgSSP7 appears to be more analogous to Sm1 from the saprophytic / biocontrol species *T. virens* (Figure 5.3B). These structural analyses also predicted a double-psi beta-barrel fold in both the FgSSP6 and FgSSP7 proteins (Figure 5.3). A previous study suggested the region responsible

for binding carbohydrates in CP is a shallow surface located at one side of the beta-barrel (de Oliveira et al., 2011). Monomeric forms of Sm1 and Epl1 proteins in *T. atroviride* and *T. virens* have been shown to be more effective in the induction of plant defence response. These two protein are suggested to be able to form dimers because of a tryptophan (Trp34) residue with two oxidation states (Seidl et al., 2006). However, *T. atroviride* Sm1 is predominantly found in its monomeric form because this sequence has a single glycosylation site that is not present in Epl1. This glycosylation site is defined by an Asn-29 residue in Sm1, which is replaced by Asp-29 in Epl1 (Vargas et al., 2008). In *F. graminearum* CP proteins, the same tryptophan (Trp34) residue is present. In the glycosylation motif, the Asn-29 is replaced by Asp-29 in FgSSP6 and Glu-29 in FgSSP7. Therefore, the glycosylation site is probably absent in both FgSSP proteins, which are likely to readily form dimers. These results suggest if FgSSP6 and FgSSP7 have some role in inducing plant defence responses, this role could be reduced if these proteins are found predominantly as dimers.

In addition to the main cerato-platanin domain in FgSSP6 and FgSSP7, in both proteins two consecutive amino acids were identified at the C-terminus that were not observed in other CP proteins predicted from the sequenced genomes of many other fungal species (Figure 5.2). These two C terminal lysine residues do not belong to the cerato-platanin domain. In bacteria, two lysines at end of peptide sequence comprise a small motif that plays a role in plasminogen binding *Streptococcus pyogenes* and *S. pneumoniae* α-enolase (Itzek et al., 2010). In *S. pneumoniae*, the α-enolase binding to plasminogen induces plasminogen transformation into plasmin and is thought to be a virulence factor by preventing the generation of fibrin clots and thus enabling tissue invasion

(Fontan et al., 2000). The possible role of this small motif in FgSSP6 and FgSSP7 will be discussed in greater details in section 5.2.6.

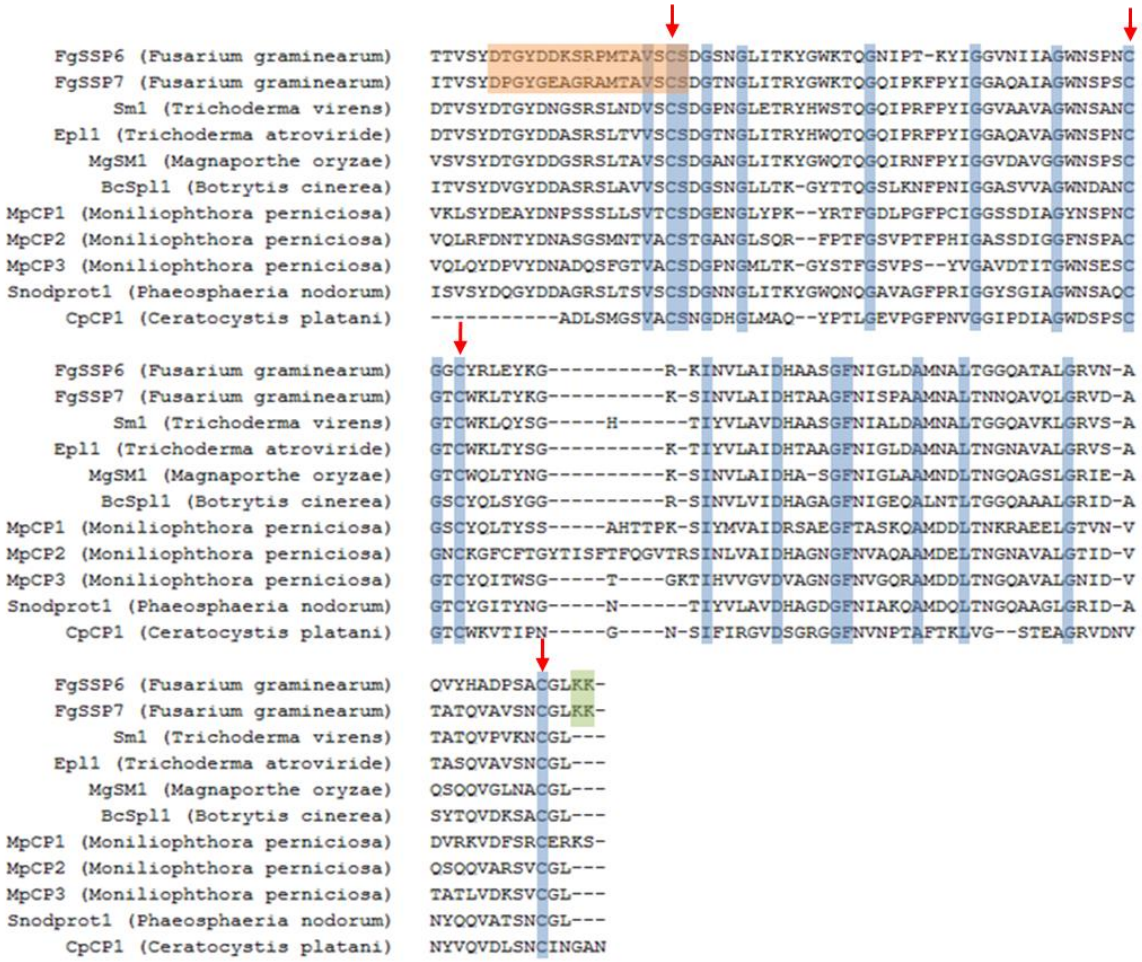

Figure 5.2 Alignment of FgSSP6 and FgSSP7 with characterised fungal CP proteins from other fungal species. Sequence alignment was carried out using Geneious software (Geneious v8.1.3, available from http://www.geneious.com). Invariant residues are shaded in light blue; red arrows indicated the cysteine residues. Amino acid sequences used for synthesis of specific antibodies of FgSSP6 and FgSSP7 are shaded in light orange; KK endings (KK$) in FgSSP6 and FgSSP7 are shaded in light green. The N-terminal secretion signal sequences of all proteins were removed to optimise the alignment.

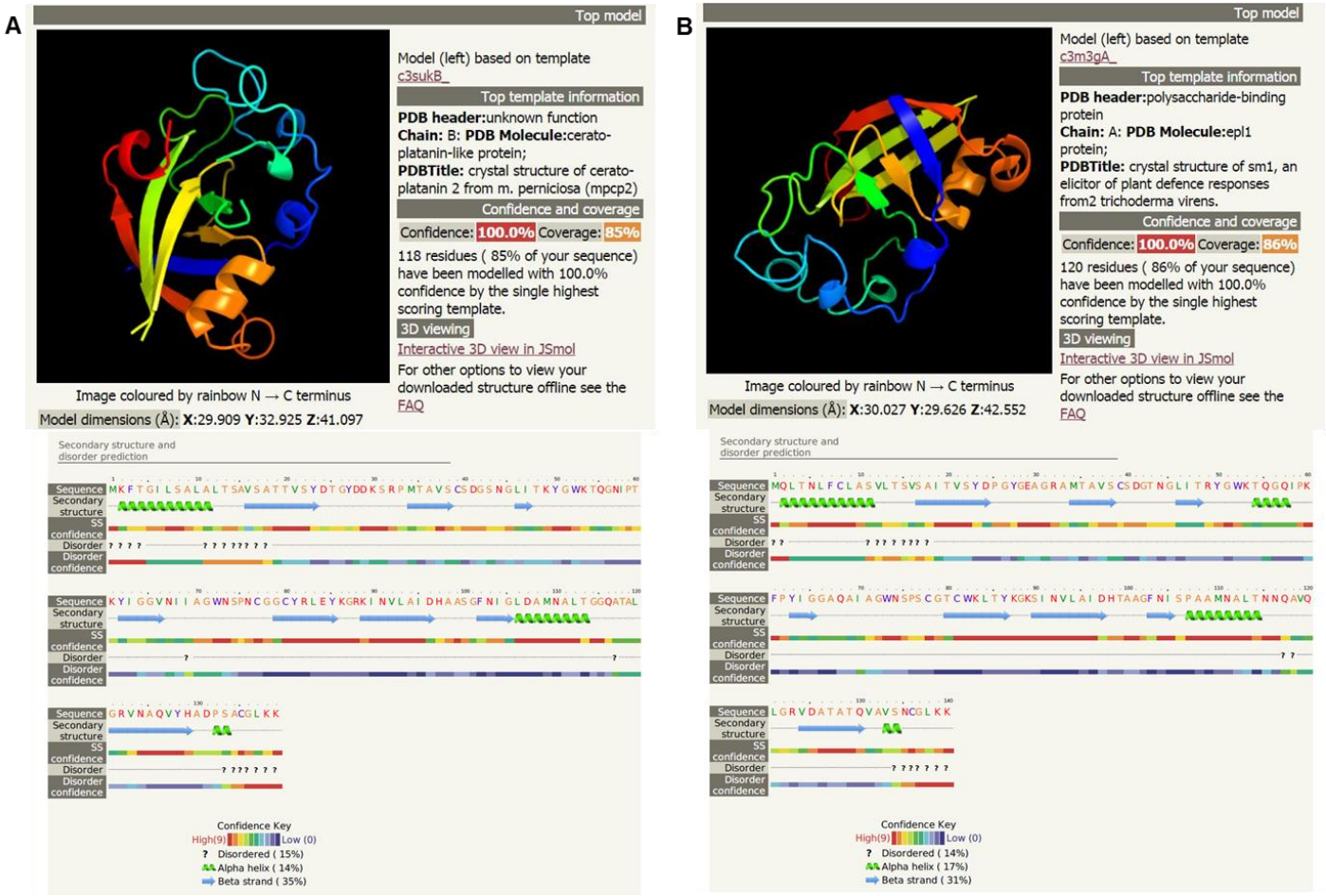

Figure 5.3 Predicted protein structure of *F. graminearum* cerato-platanins. **A.** Predicted protein structure of FgSSP6 based on crystal structure of cerato-platanin 2 from *Moniliophtora perniciosa* (mpcp2). **B.** Predicted protein structure of FgSSP7 based on crystal structure of Sm1 from *Trichoderma* virens. Protein structure prediction was done in Phyre2 (Kelley et al., 2015b).

5.3.2 Expression of recombinant FgSSP6 and FgSSP7 in *E. coli* and validation of antibodies generated against FgSSP6 and FgSSP7 using western blot analysis

Pre-expression of FgSSP6 and sometime FgSSP7 via BSMV-VOX strongly suggested a role for CP proteins during *F. graminearum* infection in wheat ears. In an attempt to detect the production of either protein from the BSMV vector during virus-infection of wheat ears, antibodies were raised against specific regions of FgSSP6 and FgSSP7. Amino acid sequences used for the synthesis of specific antibodies of FgSSP6 and FgSSP7 are shown in Figure 5.2.

The specificity of the antibodies was tested using western blot analysis against recombinant FgSSP6 and FgSSP7 proteins expressed in *E. coli.* The Gateway® destination vector pDEST17 was used for protein expression.

E. coli cells were transformed with pDEST17 carrying *FgSSP6* and *FgSSP7* gene sequences. Protein production was induced with two IPTG concentrations (1mM and 0.1mM). The cells were harvested and divided in two halves. One half was used for extraction of total proteins and the other half for extraction of soluble (i.e. not membrane bound) proteins.

The Gateway® destination vector contains an N-His tag sequence and western blot with α-HIS antibody was carried out as a control (Figure 5.4A). Bands of ~14kDa correspondent to the size of FgSSP6 and FgSSP7 in both total and soluble proteins extracts were visible on the western blot probed with α-HIS antibody (Figure 5.4A). The presence of both proteins in the soluble extract suggests that the proteins have been folded correctly and this made the

purification process easier. Insoluble proteins often need additional denaturation and refolding, which can lead to protein structure changes.

On the western blots probed with the α-FgSSP6 antibody, bands were visible in extracts from the FgSSP6-transformed *E. coli* after IPTG treatment, but not in either extract from the FgSSP7-transformed *E.coli* (+/- IPTG) (Figure 5.4B). Conversely, the α-FgSSP7 antibody only detected proteins in FgSSP7-transformed *E. coli* (+IPTG) (Figure 5.4C). These results indicate that each antibody appears to be specifically identify the correct *F. graminearum* CP.

To produce larger amounts of protein to explore the role of cerato-platanin using *in vitro* assays, FgSSP7- and FgSSP6- transformed *E. coli* was grown in 1 L of LB miller with 0.1mM IPTG at 16ºC. After growth for 12 hours, *E. coli* cells were centrifuged, resuspended in equilibration buffer and lysed in sonicator. Protein purification of lysate was done using HIS-Select Nickel Affinity Gel (Sigma).

Western blots were probed with α-FgSSP6 and α-FgSSP7 antibodies, bands were visible in extracts of FgSSP6 and FgSSP7 transformed *E. coli*, respectively from both lysate extract and purified protein (Figure 5.5). These results demonstrated that similar results were achieved when larger amounts of protein were produced and the protein purification method with HIS-Select Nickel Although, there might be presence of other protein species, affinity Gel was efficient to obtain good amounts of FgSSP6 and FgSSP7 recombinant protein.

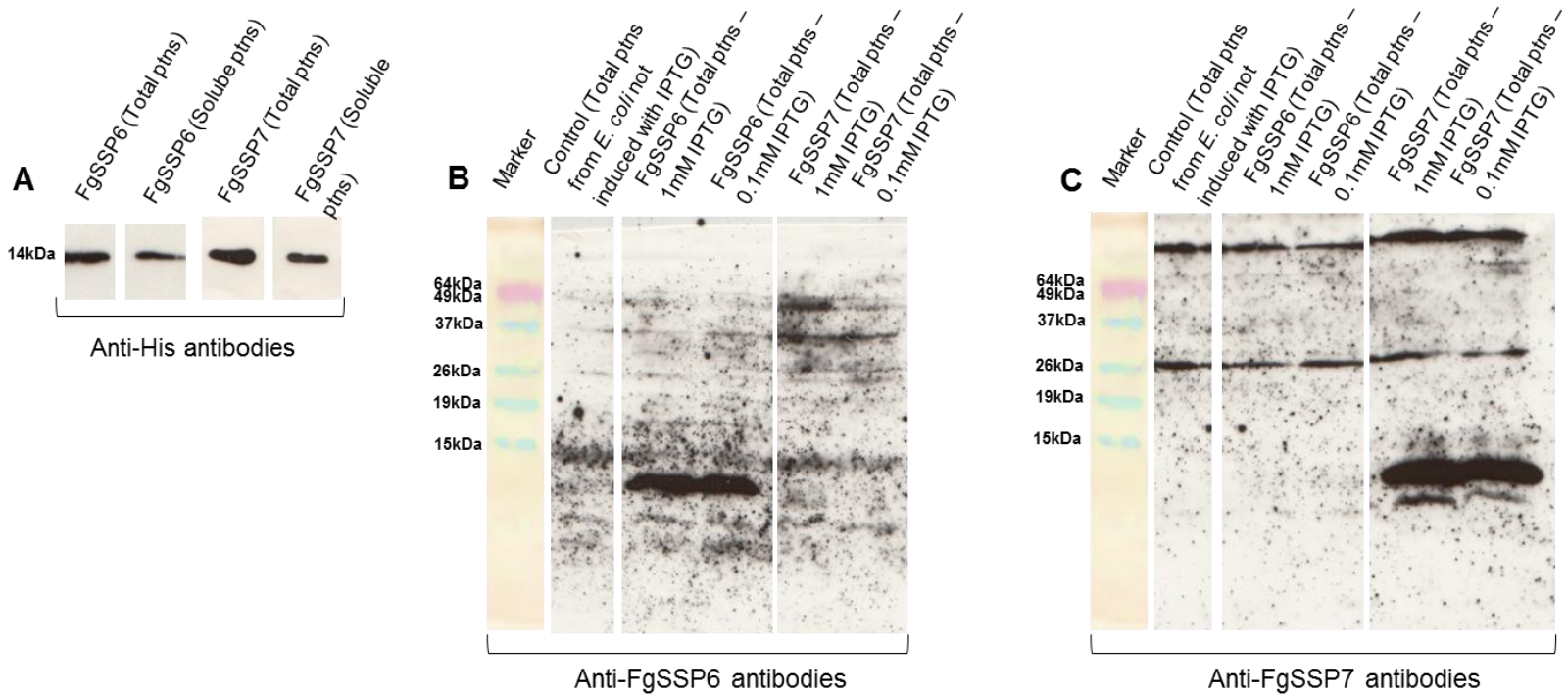

Figure 5.4 Specific detection of FgSSP6 and FgSSP7 proteins (ptns) in extracts from transformed *E. coli* using western blotting analysis. A. Total and soluble protein fractions from extracts from cultures of *E. coli* transformed with His-tagged FgSSP6 and FgSSP7, probed with α-HIS antibody (1:2000) on a western blot. B. Total protein fraction from extracts with two different IPTG concentrations (0.1mM and 1mM) from cultures of *E. coli* transformed with His-tagged FgSSP6 and FgSSP7, probed with α-FgSSP6 antibody (1:1000) on a western blot. C. Total protein fraction from extracts with two different IPTG concentrations (0.1mM and 1mM) from cultures of *E. coli* transformed with His-tagged FgSSP6 and FgSSP7, probed with α-FgSSP7 antibody (1:1000) on a western blot. The marker in A indicates estimated size of FgSSP6 and FgSSP7 of 14kDa. Contrasts in B and C were only manipulated on the markers.

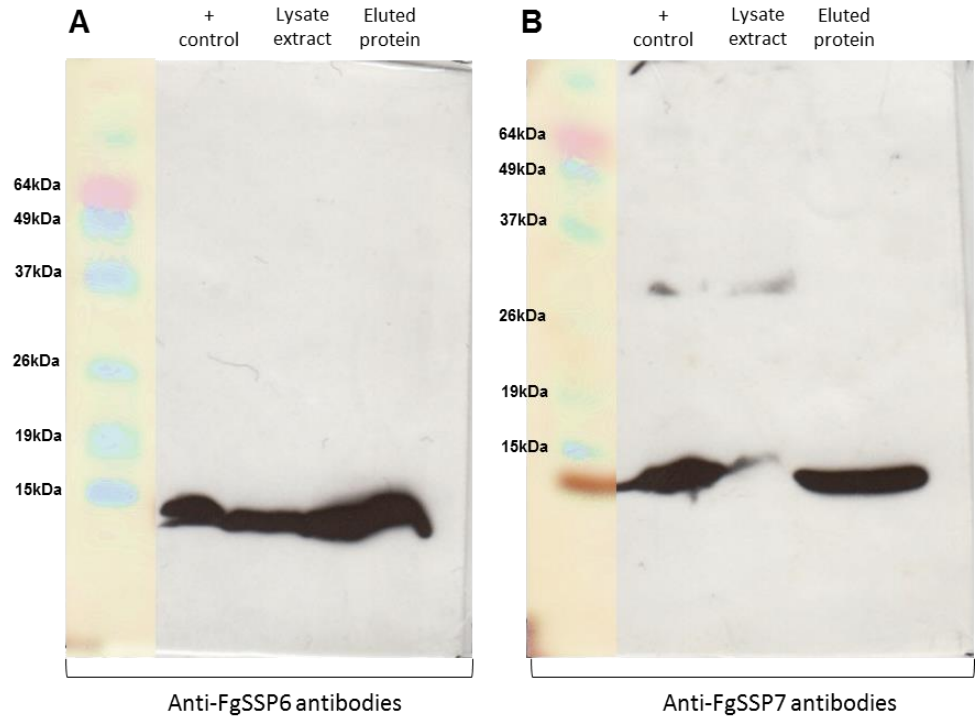

Figure 5.5. Detection of FgSSP6 and FgSSP7 in lysate cell extracts and purified protein from transformed *E. coli* using western blotting analysis. A. Lysate cell fraction and eluted protein from cultures of *E. coli* transformed with His-tagged FgSSP6, probed with α-FgSSP6 antibody (1:1000) on a western blot. B. Lysate cell fraction and eluted protein from cultures of *E. coli* transformed with His-tagged FgSSP7, probed with α-FgSSP7 antibody (1:1000) on a western blot. The marker indicates estimated size of FgSSP6 and FgSSP7 of 14kDa. Contrasts in A and B were only manipulated on the markers.

5.3.3 Detection of virus-mediated overexpressed FgSSP6 and FgSSP7 proteins in *N. benthamiana* leaves and fungal mycelia.

The α-FgSSP6 and α-FgSSP7 antibodies when tested against *E. coli* generated protein samples confirmed the desired specificity had been obtained and these two new tools could be used in other experiments. The next aim was to use the two antibodies to detect the CP proteins in BSMV:FgSSP6 and BSMV:FgSSP7 infected plant tissues, i.e. *N. benthamiana* leaves, apoplastic fluids and wheat ears. The reason that *N. benthamiana* leaves were used is

because before testing in wheat, the virus constructs were always generated by infiltrating *N. benthamiana* leaves with the three different types of *Agrobacterium tumefaciens* transformed cells. Virus-virions accumulate in the *N. benthamiana* leaves, which were then collected 5 days after agro infiltration and the sap was utilised to inoculate wheat. This protocol has been fully described in chapter 2.

Different *N. benthamiana* leaves were infiltrated with one of four treatment: The constructs BSMV:MCS 4D (negative control) , BSMV:FgSSP6 or BSMV:FgSSP7 (the two treatments) or distilled water (a 2nd negative control) . Infiltrated and systemically virus infected leaves were collected at 7 days after infiltration and ground in extraction buffer for total protein extraction. Lysates were mixed in 5x SDS loading dye and total protein was separated in 16% SDS-PAGE (Figure 5.6 A and B - top).

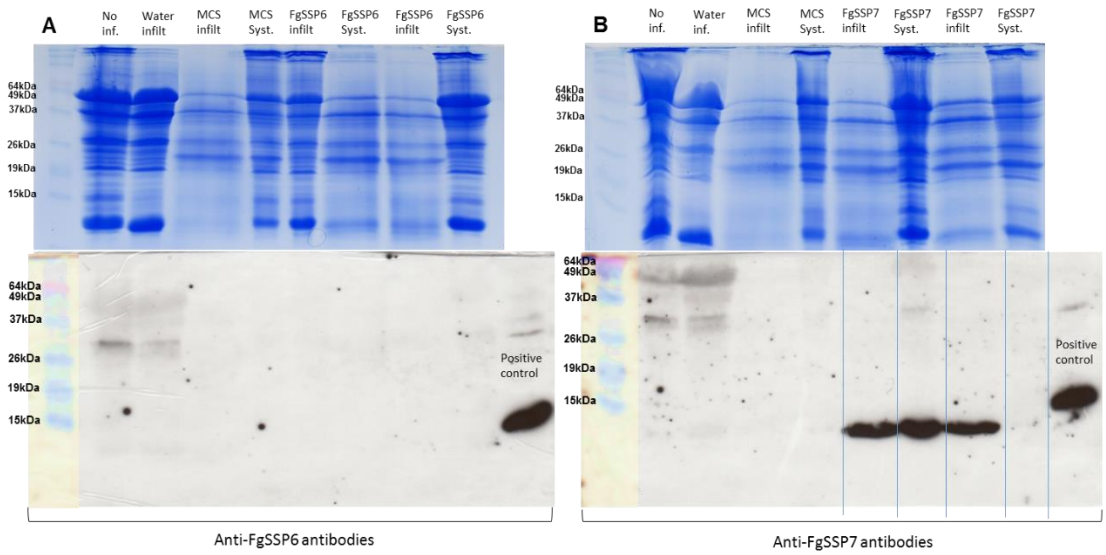

Figure 5.6 16% SDS-PAGE gel and western blotting analysis of total protein extracts from *N. benthamiana* leaves using α-FgSSP6 and α-FgSSP7 antibodies. A. Top - 16% SDS-PAGE gel of total protein extract from *N. benthamiana* leaves (lanes: non infected leaves, water infiltrated leaves, BSMV:MCS4D infiltrated leaves, BSMV:MCS4D systemically infected leaves, BSMV:FgSSP6 infiltrated leaves, BSMV:FgSSP6 systemically infected leaves, BSMV:FgSSP6 infiltrated leaves and BSMV:FgSSP6 systemically infected leaves). Bottom – western blotting analysis of total protein extract

from *N. benthamiana* leaves (lanes: same as SDS-PAGE gel above and FgSSP6 protein as positive control) probed with α-FgSSP6 antibody (1:500). B. Top - 16% SDS-PAGE gel of total protein extract from *N. benthamiana* leaves (lanes: non infected leaves, water infiltrated leaves, BSMV:MCS4D infiltrated leaves, BSMV:MCS4D systemically infected leaves, BSMV:FgSSP7 infiltrated leaves, BSMV:FgSSP7 systemically infected leaves, BSMV:FgSSP7 infiltrated leaves and BSMV:FgSSP7 systemically infected leaves). Bottom – western blotting analysis of total protein extract from *N. benthamiana* leaves (lanes: same as SDS-PAGE gel above and FgSSP7 protein as positive control) probed with α-FgSSP7 antibody (1:500). The marker indicates estimated size of FgSSP6 and FgSSP7 of 14kDa**.** Contrasts in A and B were only manipulated on the markers.

Western blots were probed with either α-FgSSP6 or α-FgSSP7 antibodies against protein extracts of leaves infected with BSMV:FgSSP6 and BSMV:FgSSP7 (infiltrated and systemically infected), respectively. For both antibodies, leaves infected with BSMV:MCS 4D (infiltrated and systemically infected), infiltrated with water and non-infected leaves were used as a negative control. Recombinants proteins produced in *E. coli* were used as positive controls (Figure 5.6).

Three ~14 kDa bands were detected in the western blot probed with the α-FgSSP7 antibody corresponding to protein extracts of *N. benthamiana* leaves infiltrated and systemically infected with BSMV:FgSSP7. This suggests that FgSSP7 protein has been successfully expressed. The three visible bands correspondent to protein extracts of infected *N. benthamiana* leaves apparently are about 1kDa smaller than the positive control. This difference is probably due the 6xHis-tag attached to the end of recombinant protein that has approximately 1kDa. One of the samples from a BSMV:FgSSP7 systemically infected leaf did not show any band. This could be because the virus titre was not high enough to

produce a detectable amount of protein or the insert had been lost from the vector (Figure 5.6B).

Unfortunately, no signal, except for the positive control, was detected from the samples of *N. benthamiana* leaves infiltrated and systemically infected with BSMV:FgSSP6 for the western blot probed with the α-FgSSP6 antibody (Figure 5.6A). Several attempts were carried out using more concentrated protein extract and longer exposure to detect FgSSP6 protein in *N. benthamiana* leaves infected with BSMV:FgSSP6. However, no signal could be detected from any of these samples (data not shown). This suggests that the predicted surface exposed region that can be detected from the *E. coli* generated samples, is either not available (i.e. cleaved) in the *in planta* generated samples or the levels of protein produced are not sensitive to this detection technique.

FgSSP6 and FgSSP7 are predicted to be secreted (Chapter 3) and may for dimers. In an attempt to detect both proteins more efficiently by western blot using specific antibodies, protein extracts were made from apoplastic fluids recovered from *N. benthamiana* leaves infected either with BSMV:FgSSP6 or FgSSP7. Detection of cerato-platanins in the apoplast would give stronger support that the prediction to be secreted was correct.

Apoplastic fluid was obtained from systemically infected *N. benthamina* leaves and non-infected leaves using vacuum infiltration and centrifugation (O'Leary et al., 2014). Leaves were infected with BSMV:FgSSP6, BSMV:FgSSP7 and BSMV:MCS 4D. For each construct (FgSSP6 and FgSSP7), two leaves were used and the total protein was also extracted from remaining leaf tissue after apoplastic fluid recovering.

Due to the lack of detection of FgSSP6 in the total soluble protein fraction of leaf tissue, total protein was also extracted from fungal mycelia (YPD) and conidia (PDA). Previous analyses have reported the *FgSSP6* gene was highly expressed during *in vitro* mainly in mycelia when grown in high-nutrient media. *FgSSP7* is low expressed in those conditions, but demonstrated to be expressed in fungal conidia when grown in low-nutrient media (Brown et al., 2017, Zhang et al., 2012).

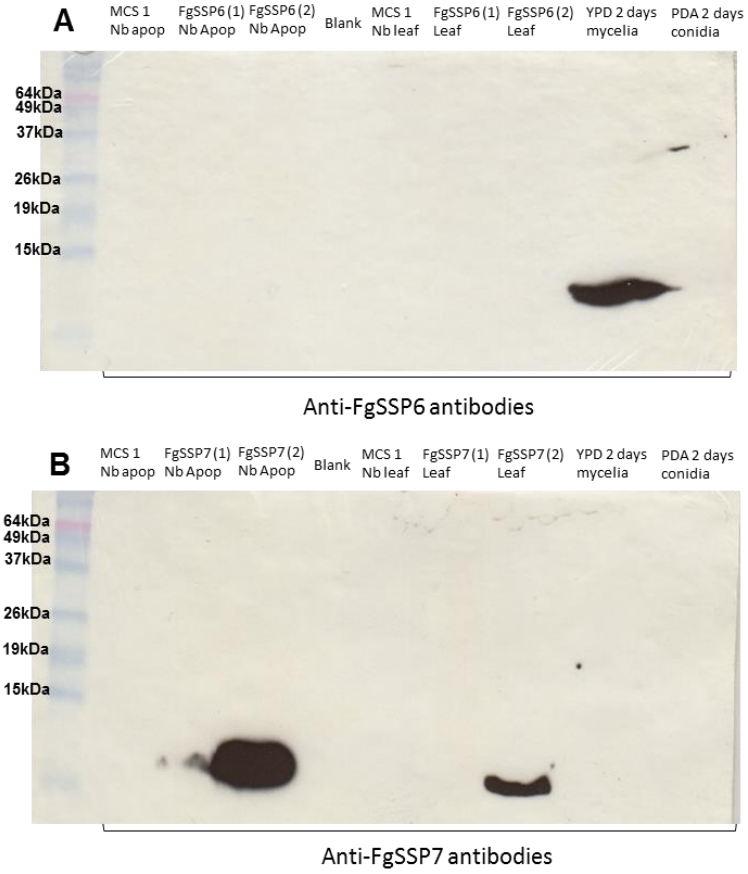

Figure 5.7 Detection of FgSSP6 and FgSSP7 from total protein extracts using western blotting analysis A. western blotting analysis of total protein extract from *N. benthamiana (Nb)* leaves and *F. graminearum (Fg)* mycelia and conidia (lanes: BSMV:MCS4D *Nb* leaf apoplastic fluid, BSMV:FgSSP6 *Nb* leaf 1 apoplastic fluid, BSMV:FgSSP6 *Nb* leaf 2 apoplastic fluid, blank lane, BSMV:MCS4D *Nb* leaf tissue, BSMV:FgSSP6 *Nb* leaf 1 tissue, BSMV:FgSSP6 *Nb* leaf 2 tissue, *Fg* PH-1 mycelia growth in YPD for 2 days, *Fg* PH-1 conidia growth in PDA for 2 days) probed with α-FgSSP6 antibody (1:500). B. western blotting analysis of total protein extract from *Nb* leaves and *Fg* mycelia and

conidia (lanes: BSMV:MCS4D *Nb* leaf apoplastic fluid, BSMV:FgSSP7 *Nb* leaf 1 apoplastic fluid, BSMV:FgSSP7 *Nb* leaf 2 apoplastic fluid, blank lane, BSMV:MCS4D *Nb* leaf tissue, BSMV:FgSSP7 *Nb* leaf 1 tissue, BSMV:FgSSP7 *Nb* leaf 2 tissue, *Fg* PH-1 mycelia growth in YPD for 2 days, *Fg* PH-1 conidia growth in PDA for 2 days) probed with α-FgSSP7 antibody (1:500).

In one of *N. benthamiana* leaves systemically infected with BSMV:FgSSP7, α-FgSSP7 antibody detected a ~14kDa band from both the apoplastic fluid and intact leaf tissue extracts, indicating the production of FgSSP7 by the BSMV and suggesting the protein is secreted. Whereas no bands were detected in the apoplastic collected other leaf samples extracted following the same BSMV:FgSSP7 treatment. This could be due the fact that not enough protein was produced to be visualised by western blotting and / or most of the protein was bound within the plant environment to either insoluble polymers or proteins and could not be routinely recovered (Figure 5.7B).

A third attempt to detect FgSSP6 using α-FgSSP6 was unsuccessful and no bands were visualised in the apoplastic fluid and leaf tissue extracts of any *N. benthamiana* leaf tissue infected with BSMV:FgSSP6. However, FgSSP6 could be detected in protein extract from *F. graminearum* mycelia growing in rich media for three days (Figure 5.7A). The α-FgSSP6 is able to detect FgSSP6 produced by *F. graminearum* or *E. coli*. However the assay or the antibody is not sensitive enough to detect the low amounts of protein in *N. benthamiana* leaves infected with BSMV:FgSSP6. As hypothesised for FgSSP7, FgSSP6 could be bound to insoluble polymers and could not be recovered.

Detection of FgSSP6 and FgSSP7 using specific antibodies was also attempted in wheat ears 10 days after infection with the corresponding BSMV constructs and relevant controls. No signal was detected in any of the western

blots (Appendix 3). Increasing the concentration of protein extract by using more ear tissue and an acetone precipitation was also tried, but no signal was detectable by western blotting.

5.3.4 Detection *FgSSP6* and *FgSSP7* transcripts in virus infected wheat ears.

It was not possible to detect the FgSSP6 protein in *N. benthamiana* leaves and neither FgSSP6 or FgSSP7 in wheat ears by western blotting, when infected with BSMV:FgSSP6 and BSMV:FgSSP7, respectively. Therefore, to provide some evidence that these proteins are being produced in wheat ears, an alternative approach was adopted. In the last BSMV-VOX experiment where BSMV:FgSSP6 and BSMV:FgSSP7 were tested, a separated batch of wheat plants were inoculated with BSMV constructs. Just before ears were ready for *F. graminearum* inoculation (~10 days after virus inoculation), the ears were collected and RNA was extracted using the Trizol method (Simms et al., 1993). A PCR analyses from the resulting cDNAs was carried out using primers that specifically amplify 150bp fragment of *FgSSP6* and *FgSSP7*. No virus infected ears and BSMV:MCS4D infected ears were used as a negative control. *F. graminearum* genomic DNA was used as positive control.

Amplification of *FgSSP6* using specific primers was observed from cDNA samples of plants infected with BSMV:FgSSP6, but not for cDNA of no virus infected and BSMV:MCS4D infected plants. The same was observed when cDNA was amplified from samples of plants infected with BSMV:FgSSP7 using *FgSSP7* specific primers. Figure 5.8 shows the PCR results from three independently generated samples from *in planta* derived cDNA for each construct. These results

could show some evidence that FgSSP6 and FgSSP7 transcripts are expressed in wheat ears infected with the respective virus constructs, but considering the fact that BSMV has an RNA genome and cDNA synthesis was performed using random primers, it is not possible to confirm that the amplification of FgSSP6 and FgSSP7 reflects the presence of the respective transcripts. Considering the difficulties encountered to detect the presence of the both proteins in wheat ear, another approach should be considered, as for example, a MALDI (matrix-assisted laser desorption/ionization) -TOF (time of flight) -MS (mass spectrometry) analysis.

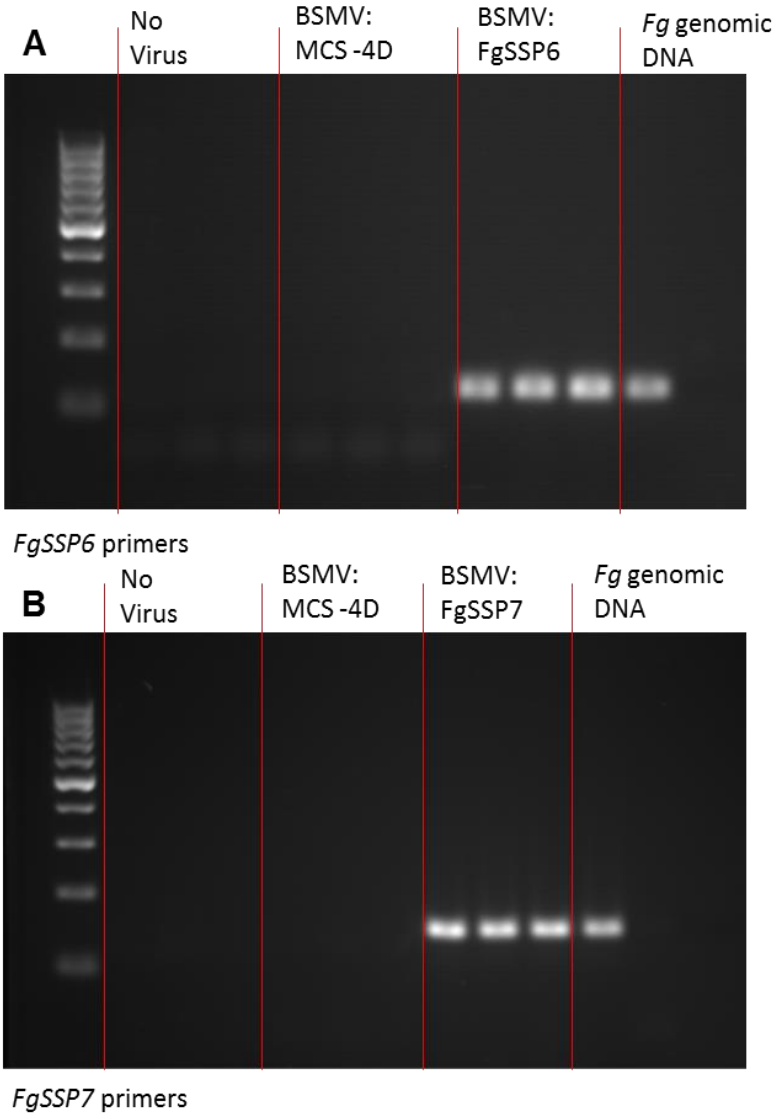

Figure 5.8 Detection of *FgSSP6* and *FgSSP7* from cDNA of virus infected wheat ears. A. Electrophoresis gel of *FgSSP6* amplified fragments from cDNA of BSMV:FgSSP6 infected wheat ears using *FgSSP6* specific primers. *FgSSP6* amplification was not observed in cDNA of no virus and BSMV:MCS4D infected wheat ears. *F. graminearum* genomic DNA was used as positive control. B. Electrophoresis gel of *FgSSP7* amplified fragments from cDNA of BSMV:FgSSP7 infected wheat ears using *FgSSP7* specific primers. *FgSSP7* amplification was not observed in cDNA of no virus and BSMV:MCS4D infected wheat ears. *F. graminearum* genomic DNA was used as positive control.

5.3.5 The signal peptides of FgSSP6 and FgSSP7 are important for their role during *F. graminearum* infection in wheat.

Based on signal peptide prediction and protein localisation tools, FgSSP6 and FgSSP7 proteins are predicted to contain a signal peptide (18 amino acids), and therefore predicted to be secreted or localised to the extracellular space. Therefore, I questioned whether the presence of signal peptide in the FgSSP6 and FgSSP7 amino acid sequences is important to enhance FEB disease when these proteins are overexpressed in wheat (reported in section 4.2).

BSMV-VOX constructs of FgSSP6 and FgSSP7 lacking signal peptide were synthesised as described in Chapter 2 – Section 2.11. When FgSSP6 and FgSSP7 constructs lacking the signal peptide (BSMV:FgSSP6-SP and BSMV:FgSSP7-SP) were pre-infected in wheat ear, the number of FEB diseased spikelets were similar to the BSMV:MCS4D negative control ($P<0.05$, $n=10$), This additional result suggests that the presence of signal peptide in the protein sequence is important for protein function(s) during infection (Figure 5.9)

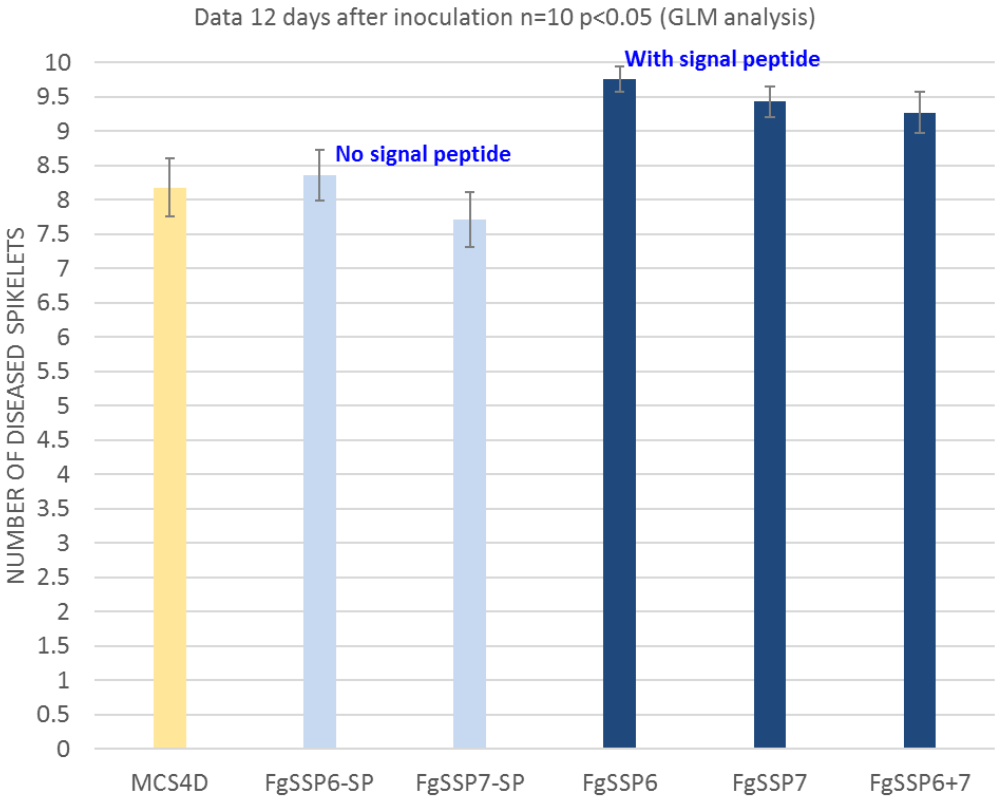

Figure 5.9 Graph representing number of visibly diseased spikelets below the *Fg* inoculation points in *Fg* inoculated wheat ears. A minimum of 10 ears per virus treatment were analysed. Data shown were collected at 12 days post *Fg*-inoculation. Dark blue bars denote treatments in which statistically significant differences in number of diseased spikelets, relative to BSMV:MCS4D control (yellow bar), were observed (p value < 0.001 from GLM analysis). FgSSP6-SP and FgSSP7-SP represent the constructs without signal peptide.

5.3.6 Exploring the role of the KK motif located at the C terminus of FgSSP6 using the BSMV-VOX expression system and wheat ear infections by *F. graminearum*

Alignment of FgSSP6 and FgSSP7 amino acid sequences with characterised CP proteins from other fungal species show that the *F. graminearum* CPs have two lysine residues (KK) at the C-terminal end ($) outside the CP domain (Figure 5.2).This KK$ is unusual within the CP family of proteins because this motif was only found in CP proteins encoded by some *Fusarium*

species closely related to *F. graminearum*, namely *F. pseudograminearum*, *F. oxysporum* and *F. sambucinum,* but not in other Fusarium species or any other fungal species with a sequenced genome deposited in the public domain. In bacteria human pathogenic bacteria *Streptococcus pyogenes* and *S. pneumoniae*, the presence of KK$ motif in proteins contribute as a determinant of virulence (Ruhanen et al., 2014). If FgSSP6 and FgSSP7 have as one of their main roles an expansin-like activity, I hypothesise that the presence of this motif could either help or be required for CP adhesion to plant and/or fungal cells.

To study the contribution of the KK$ motif to *F. graminearum* CP function, a BSMV:FgSSP6 construct in which the C-terminal lysine was omitted [BSMV:FgSSP6(-K$)] was generated and used to inoculate wheat plants (Chapter 2).

Between 10 and 13 plants per treatment were assessed per experiment, where only one ear in the main tiller was inoculated with *F. graminearum* spores. The ears were assessed every three days by scoring the number of spikelets visually diseased below the point of *F. graminearum* inoculation. Statistical analyses were carried out with data collected at 12 days post inoculation, when FEB disease was present in much of the control ears.

There was no statistically significant difference between *F. graminearum* disease progression in BSMV:FgSSP6 and BSMV:FgSSP6(-K$) pre-infected wheat ears (Figure 5.10). Thus, FEB disease is also increased by overexpression of FgSSP6(-K$) despite the removal of the C-terminal lysine, compared to control treated ears. Therefore, it is unlikely that this motif is linked to enhanced Fusarium susceptibility.

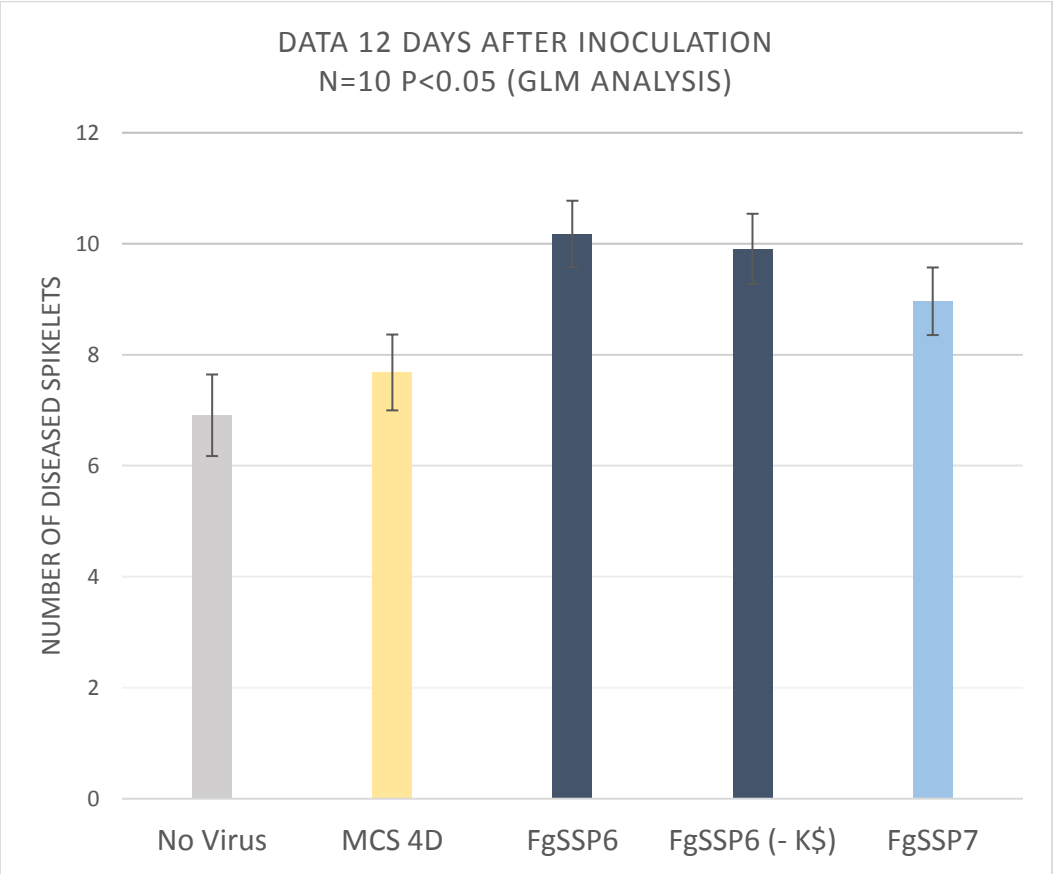

Figure 5.10 Graph representing number of visibly diseased spikelets below the *Fg* inoculation points in wheat ears. A minimum of 10 ears per virus treatment were analysed. Data shown were collected at 12 days' post *Fg*-inoculation. Dark blue bars denote treatments in which statistically significant differences in number of diseased spikelets, relative to BSMV:MCS4D control (yellow bar), were observed (p value < 0.001 from GLM analysis). FgSSP6 (-K$) represents the constructs lacking the last lysine in peptide sequence.

5.3.7 Virus-mediated overexpression of FgSSP6 and FgSSP7 cerato-platanin proteins during infection does not modify the interaction outcome when a non-DON producing *F. graminearum* mutant strain is inoculated onto wheat ears.

Several previous studies have revealed DON plays an important role during *F. graminearum* infection in wheat ears (See chapter 1). Deletion of *tri5* gene stops DON production by *F. graminearum* during infection and leads to a

strong reduction of fungal virulence. Symptoms are restricted to only the two inoculated spikelets and the fungus do not spread to the rachis (Cuzick et al., 2008, Proctor et al., 1995).

To test whether FgSSP6 and FgSSP7 overexpression enable FgPH-1Δ*tri5* to overcome the wheat immunity to a non-DON producing strain of *F. graminearum*, a BSMV-VOX experiment was carried out using BSMV:FgSSP6 and BSMV:FgSSP7 constructs and controls (No Virus and MCS 4D). If overexpression of cerato-platanins is able overcome the host defences responses triggered by wheat infected by *F. graminearum* non-DON producing strains, it is a strong indication that FgSSP6 and FgSSP7 are able to suppress plant defence responses. PH-1Δ*tri5* was point inoculated onto virus infected ears at 10 days later/at anthesis. Disease symptoms were restricted to the inoculated spikelets in all treatments, similarly as previously described in the literature (Cuzick et al., 2008). These results suggest that ectopic expression FgSSP6 and FgSSP7 was not able to help *F. graminearum* overcome wheat immunity to this fungus in the absence of DON (Figure 5.11).

Figure 5.11 Representative *Fg* disease symptoms on spikes of controls (no virus infected and BSMV:MCS 4D) and BSMV:FgSSP6 and BSMV:FgSSP7 infected wheat plants. Wheat ears were point-inoculated with the *Fg* strain PH-1Δ*tri5* at anthesis, approximately 8-10 days after virus inoculation on the 5th and flag leaves. Photographs were taken at 12 days post *Fg* inoculation. The two black dots on the neighbouring spikelets towards the top of each ear indicate the points of *F. graminearum* inoculation.

5.3.8 Effect of pre-infiltrating BSMV:FgSSP6 and FgSSP7 on *Fusarium graminearum* infection in *Nicotiana benthamiana*

To explore FgSSP protein function, several assays were carried out in the non-host plant species *N. benthaminana* to determine the effect, if any, of overexpressing these proteins on non-host resistance (Saitoh et al., 2012, Frias et al., 2011, Chen et al., 2013). By overexpressing FgSSP6 and FgSSP7 using BSMV-VOX in *N. benthamiana* it would be possible to test whether *F. graminearum* would then be able to penetrate, infect and/or colonise this non-host species. This would indicate whether FgSSP6 and/or FgSSP7 might have potential ability to suppress non-host resistance, mediated by PAMP perception. A previous study has revealed that by providing an anther as an easily accessible

nutrient source for the fungus on the leaf surface, this allowed fungal growth on the surface of tobacco (*N. tabacum*) leaves, but no hyphal penetration or necrotic lesions were not observed (Urban et al., 2002). Therefore, to confirm this earlier observation, a separate batch of *N. benthamiana* plants was used in which *F. graminearum* spores were pipetted directly onto *N. benthamiana* leaves in the absence or absence of a wheat anther. *F. graminearum* growth was observed on leaves only in the presence of the wheat anther (data not shown), suggesting that the initial nutrient source provided by the anther is indeed necessary for *F. graminearum* growth initiation on *N. benthamiana* leaves.

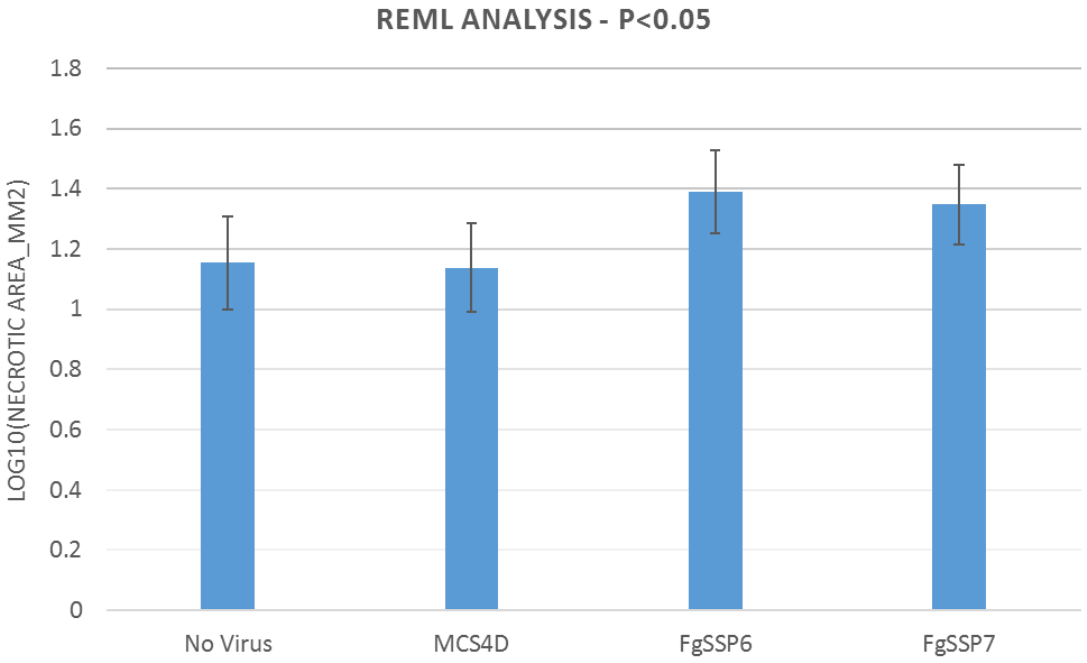

Figure 5.12 Average necrotic area of *N. benthamiana* leaves inoculated with *Fg*. A minimum of 6 leaves per virus treatment were analysed. Error bars represent mean ± s.e.m.

For the main experiment, *N. benthamiana* leaves were infiltrated with Agrobacterium strain harbouring either the BSMV:FgSSP6 construct, the BSMV:FgSSP7 construct or the control construct BSMV:MCS4D. After 6 days, *F. graminearum* (PH-1) was droplet inoculated onto a fertile wheat anther placed

on the surface of systemically virus-infected leaves of *N. benthamiana* plants. Three independent experiments were carried out. In all three experiments, leaves agroinfiltrated with either BSMV:FgSSP6 or BSMV:FgSSP7 developed bigger lesions from 10 days after *F. graminearum* inoculation when compared with control treated leaves, however statistical analysis demonstrated that these differences were not significantly different. (Figure 5.12).

In experiment 1, BSMV:FgSSP6 and BSMV:FgSSP7 infected *N. benthamiana* leaves showed larger necrotic lesions around each wheat anther compared to BSMV:MCS4D -infected leaves (Figure 5.13). Lesions were measured using transparent graph paper (0.25 cm^2) overlaid on the *F. graminearum* - inoculated leaves at 13 days post *F. graminearum* inoculation.

In experiment 2 and 3, the *F. graminearum*-inoculated leaves were photographed and necrotic leaf area analysed using ImageJ software, giving more precise measurements. BSMV:FgSSP6 and BSMV:FgSSP7 infected leaves exhibited greater necrotic area than control-treated leaves (BSMV:MCS4D) (Figure 5.14), although the area of necrosis was somewhat variable between replicates in the same treatment. Lesions of plants were compared at 13 and 17 days. There was no clear increase in lesion size between 13 and 17 days-post *F. graminearum* inoculation and photographs for ImageJ analysis were not taken until 17 days post *F. graminearum* inoculation.

In order to determine whether the necrotic lesions contained viable *F. graminearum* hyphae, indicating that the necrosis was part of the disease induced by the fungus, leaves were detached at 17 days post *F. graminearum* inoculation and placed in a humid chamber for 24 hours. The samples were fixed and stained with aniline blue to allow the lesions to be studied under a confocal microscope.

Fungal hyphae were visible inside the lesion whilst the edge of the lesion appeared brighter (Figure 5.15), resulted of cell-death. Cell-death is known to be initiated and mediated mainly by reactive oxygen species (ROS), which can lead to intracellular release of metabolites such as flavin adenine dinucleotide (FAD) or NADH from mitochondria. These metabolites have been suggested to be responsible for triggering the mechanisms auto-fluorescence (Wu et al., 2005).

Although infection of *F. graminearum* in *N. benthamiana* leaves using wheat anthers was possible, the results do not seem consistently, which is the weakness of this assay. These differences could be due to intrinsic features in each *N. benthamiana* batch as well as the amount of protein that had been overexpressed.

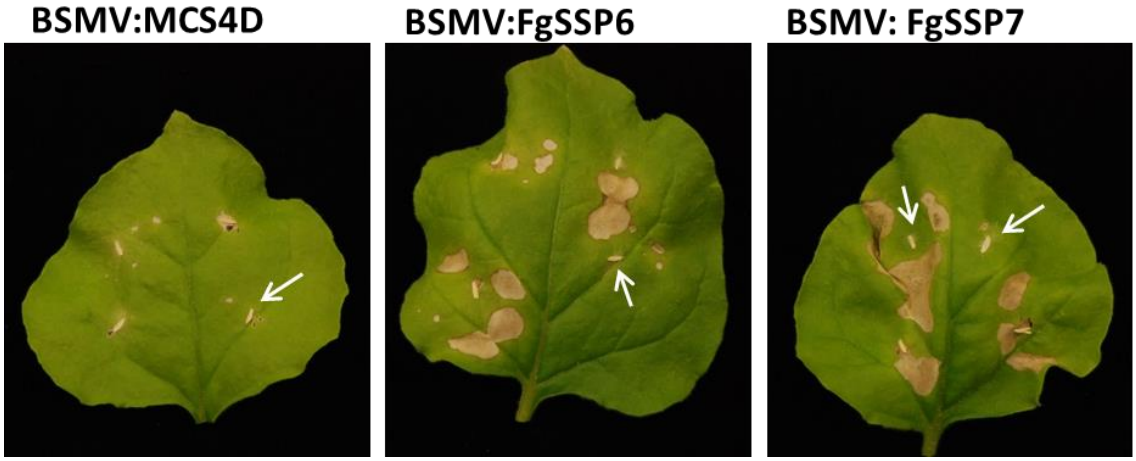

Figure 5.13 Experiment 1: Representative necrosis symptoms from *Fg* infection on *N. benthamiana* leaves systemically infected with BSMV:MCS4D (control treatment), BSMV:FgSSP6 or BSMV:FgSSP7*. N. benthamiana* leaves were agroinfiltrated with the different BSMV constructs before *Fg* inoculation. A 10µL droplet of *F. graminearum* spore suspension containing $5x10^5$spores/mL was pipetted on the top of each anther on the leaf surface. Photographs of representative leaves were taken at 13 days post *Fg* inoculation. White arrows indicate the locations of individual wheat anthers.

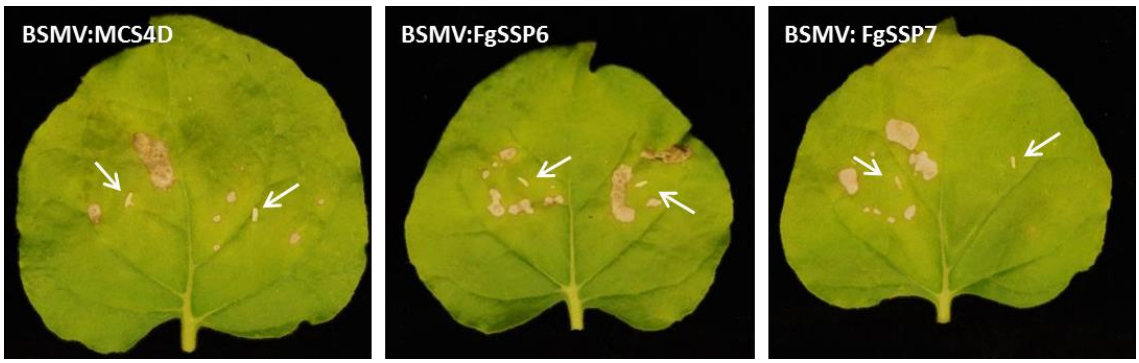

Figure 5.14 Experiment 2: Representative necrosis symptoms from *Fg* infection on *N. benthamiana* leaves systemically infected with BSMV:MCS4D (control treatment), BSMV:FgSSP6 or BSMV:FgSSP7*. N. benthamiana* leaves were agroinfiltrated with the different BSMV constructs before *Fg* inoculation. A 10µL droplet of *F. graminearum* spore suspension containing 5x10^{5}spores/mL was pipetted on the top of each anther on the leaf surface. Photographs of representative leaves were taken at 17 days post *Fg* inoculation. White arrows indicate the wheat anthers.

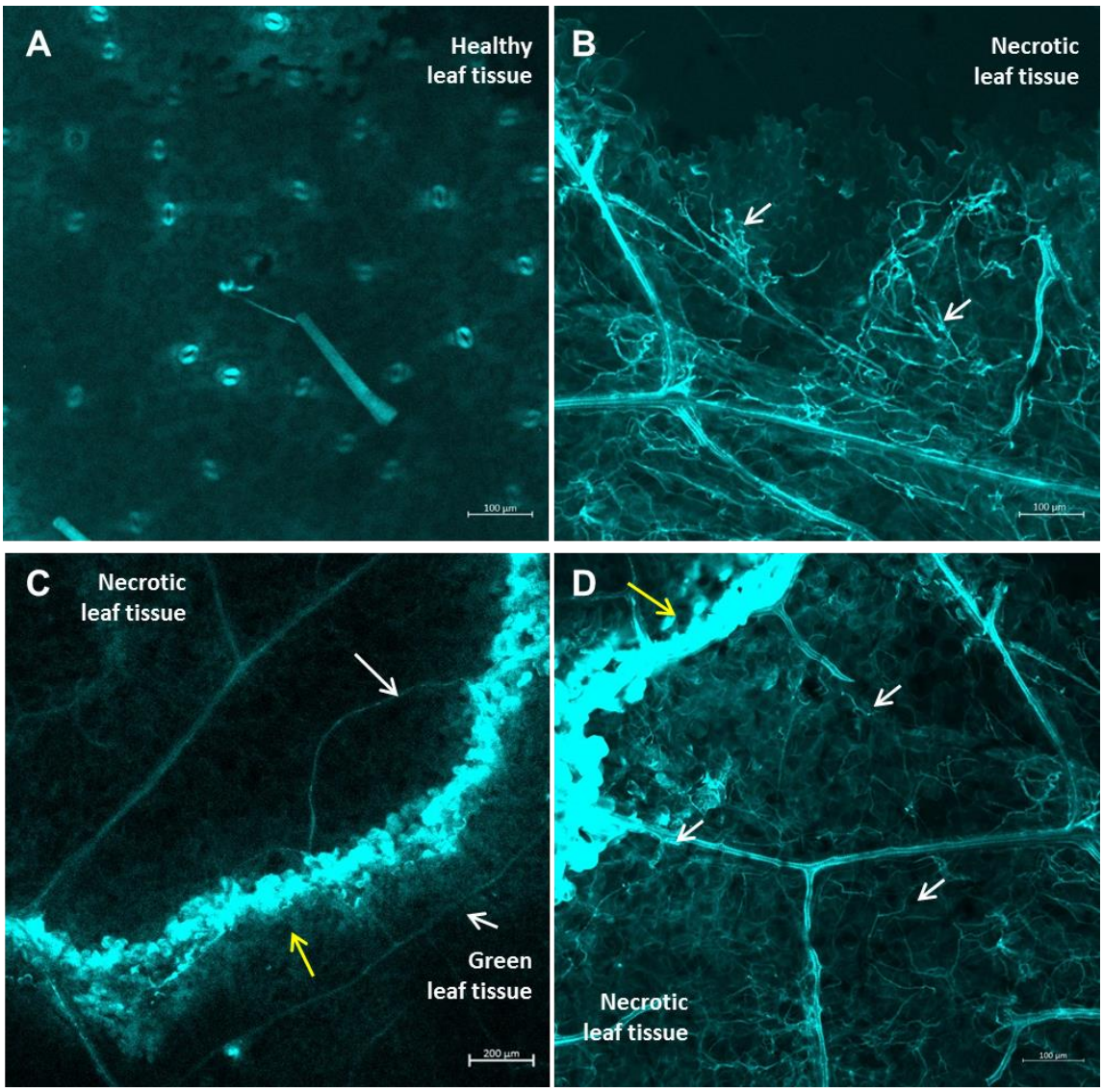

Figure 5.15 Colonisation of *N.benthamiana* leaves by *Fusarium graminearum* PH-1 stained with aniline blue at 17 dpi. A. Surface of a healthy *N. benthamiana* leaf in the absence of BSMV or *Fg* inoculation. B. Spread of *Fg* hyphae in the necrotic leaf area from non-BSMV infected plants. C and D. Green and necrotic *N. benthamiana* leaf tissue from BSMV:MCS4D infected plants. White arrows indicate *Fg* hyphae and yellow arrows indicate the edge of the lesion. Photographs were taken using Zeiss 780 laser scanning confocal microscope. Bar sizes are indicated within each figure panel.

5.3.9 Exploring possible roles of cerato-platanins during *Fusarium graminearum* infection on wheat spikes.

Using BSMV-VOX, there is already evidence that *F. graminearum* cerato-platanins have some role during wheat infection. It is known that cerato-platanin

can have multiple and distinctive activities in different fungal species (Table 5. 1). However, the function of CP proteins has not been explored in *F. graminearum*. Therefore, some experiments were carried to investigate further the role(s) of *F. graminearum* cerato-platanins.

F. graminearum cerato-platanins are able to bind different plant and fungal cell wall components

Cerato-platanins from different fungal species have been shown to primarily exhibit expansin-like activity, and also be able to bind specially chitin oligomers (Pazzagli et al., 2014). Therefore, it has been speculated that an affinity for chitin fragments by CP proteins could potentially be advantageous to the pathogen, to avoid the activation of chitin-induced plant defence responses (i.e. PTI). This role has been demonstrated previously in 3-Lysine content motif effectors in several fungal pathogens (Bolton et al., 2008, Marshall et al., 2011). Another hypothesis is that cerato-platanins are part of fungal cell-wall and therefore able to bind to chitin, the main component of fungal cell-wall. In *B. cinerea*, there are evidences that cerato-platanin is attached the fungal cell wall during hyphae growth *in vitro* and *in planta* (Frias et al., 2014).

To test whether FgSSP6 and FgSSP7 have the ability to bind chitin oligomers, purified proteins, generated in recombinant *E. coli*, were incubated with insoluble polysaccharides and affinity was evaluated via pull-down assay, i.e. by separating soluble and insoluble fractions and then assessing where the proteins were present (supernatant or pellet). The pull-down assays were performed against chitin resin, chitin from shrimp shells, chitosan, xylan and cellulose. The FgSSP6 and FgSSP7 proteins were successfully pulled-down by

each of the polysaccharides tested (Figure 5.16 A and B). BSA was used as the negative control and it was shown not to have ability by both chitin resin and chitosan (Figure 5.16C). The experiment was done twice and these results suggest that *F. graminearum* cerato-platanin has affinity for both fungal and plant polysaccharides in a non-specific way. This ability could suggest an association to an expansin-like activity and role in fungal growth and development.

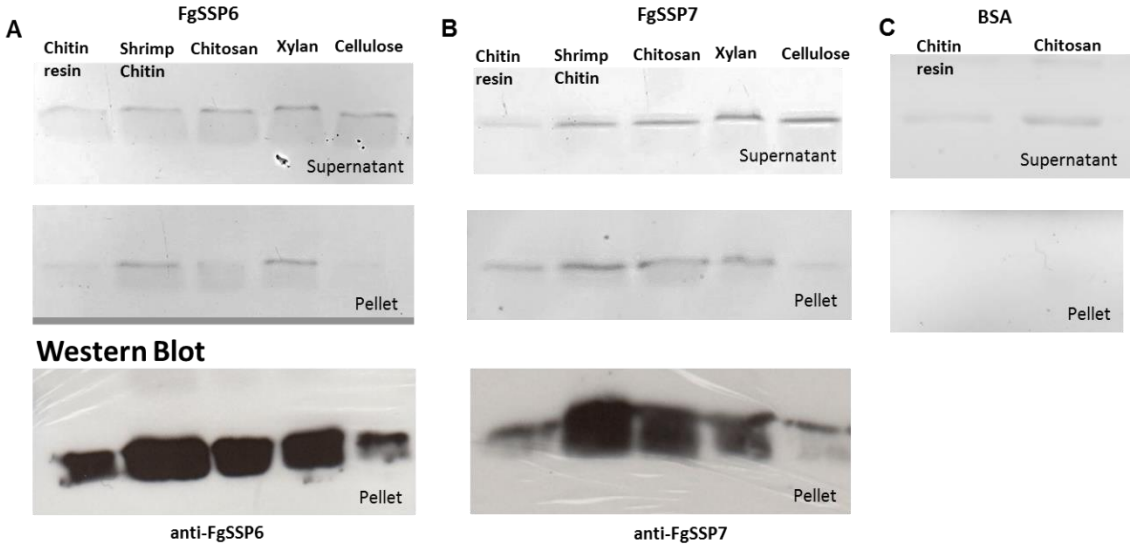

Figure 5.16 Polysaccharide binding assays. A. FgSSP6 (soluble form) tested was pulled-down by fungal and plant cell wall polymers, demonstrated by detection of 14kDa band in the pellet fraction in SDS page 16% gel, and western blotting analysis using α-FgSSP6 antibody (1:500). B. FgSSP7 (soluble form) tested was pulled-down by fungal and plant cell wall polymers, demonstrated by detection of 14kDa band in the pellet fraction in SDS page 16% gel, and western blotting analysis using α-FgSSP7 antibody (1:500). C. BSA (negative control) present only in the supernatant detected by in SDS page 16% gel and not in the pellet fraction when incubated with chitin-resin and chitosan.

F. graminearum cerato-platanins are able to induce necrosis in *N. benthamiana* leaves but not in wheat leaves

It is known that BcSpl1 from *B. cinerea* is able to induce necrosis in Arabidopsis, tomato and tobacco leaves by inducing a hypersensitive response

(Frias et al., 2013). From *T. virens*, Sm1, although not able to induce necrosis, has been shown to triggers ROS production (Djonovic et al., 2006).

Both FgSSP6 and FgSSP7 are strongly up regulated in the symptomatic phase of infection during Fusarium ear blight in wheat (Brown et al., 2017), i.e. during the *F. graminearium* necrotrophic phase. In many compatible host-pathogen interactions during the necrotrophic disease formation phase, plant defence responses are usually triggered to activate plant cell death, and therefore, contribute to fungal survival in the plant dead cell (Oliver & Solomon, 2010).

To analyse if FgSSP6 and FgSSP7 are able to induce necrosis in *N. benthamiana* and wheat leaves, 0.5 mL of purified protein (up to 30 µM) generated in *E. coli* was infiltrated into the youngest and fully expanded leaves of one-month old plants. The presence/absence of necrosis was assessed 24 hours post-infiltration under visible and UV lights. The same concentration of BSA and PBS were infiltrated separately as different negative controls. In addition, co-infiltration of 0.5 mL mixture (1:1) of FgSSP6 and FgSSP7 was carried out to check if a difference response was observed (Figure 5.17). For each treatment, six leaves were infiltrated and the experiment was done twice.

Necrosis symptoms were observed in *N. benthamiana* leaves infiltrated FgSSP6, FgSSP7 and co-infiltration of FgSSP6 and FgSSP7 at concentration of 30 µM (Figure 5.17). Co-infiltration of FgSSP6 and FgSSP7 apparently did not induce to stronger or weaker necrosis symptoms and for all treatments, necrosis remained limited to the infiltrated site and did not spread systemically. These results suggest that *F. graminearum* cerato-platanin could activate cell-death and potentially therefore even act as a PAMP during the necrotrophic phase of *F.*

graminearum infection in wheat. Infiltration of FgSSP6 and FgSSP7 in *N. benthamiana* leaves at lower concentrations (7 and 15 µM) were carried out, but necrosis was absent or not very strong (Figure 5.17).

FgSSP6 and FgSSP7 infiltration in wheat leaves did not lead to necrosis as observed in *N. benthamiana* at concentration of 30µM (Appendix 4). The absence of necrosis could be because the concentration was not high enough to induce necrosis or cerato-platanin is not recognised by wheat genes to induce cell death. A third and more plausible possibility is that plant defence genes are being upregulated and ROS production has been triggered, but visible necrosis was not induced. Induction of wheat defence genes has been carried out now by another PhD student.

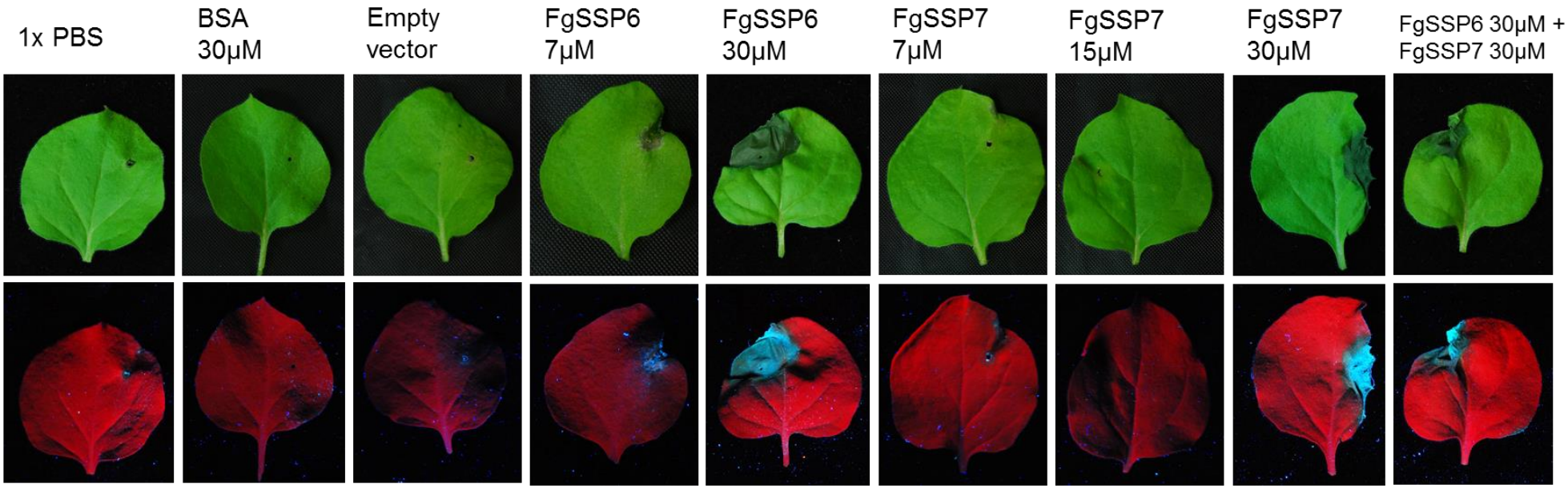

Figure 5.17 Induction of necrosis in *N. benthamiana* leaves by FgSSP6 and FgSSP7 post infiltration with purified proteins. Leaves photographed at 24 hours post-infiltration under white light (top panel) or UV light (lower panel).

5.3.10 FgSSP7 does not appear to contribute to *F. graminearum* virulence in wheat ears.

Transient overexpression of each *F. graminearum* cerato-platanins seem to contribute to infection of wheat ears. However, these results do not determine if these CP proteins are essential for *F. graminearum* virulence. To test for function, *FgSSP7* single gene deletion mutants were produced and tested *in planta.* The *F. graminearum* mutants were made at the end of this PhD. The *FgSSP6* gene deletion mutants and the *FgSSP6* and *FgSSP7* double mutants have been planned but lack of time did not permit the completion of these experiments. Three transformation attempts were unsuccessful. Single mutant of *FgSSP6* and the double mutant will still be done in the future for publication purposes.

Two ΔFgSSP7-independent mutants were selected for further analysis. The molecular characterisation the selected mutants are shown in figure 5.18. No differences were observed in fungal growth on PDA between wild type and *FgSSP7*-deleted strains (Figure 5.19).

The strains were then tested in wheat ears cv. Bobwhite and no reduction in symptoms severity was observed compared to the wild type on wheat spikes (Figure 5.20). These results suggest that the function of FgSSP7 alone does not contribute to fungal virulence.

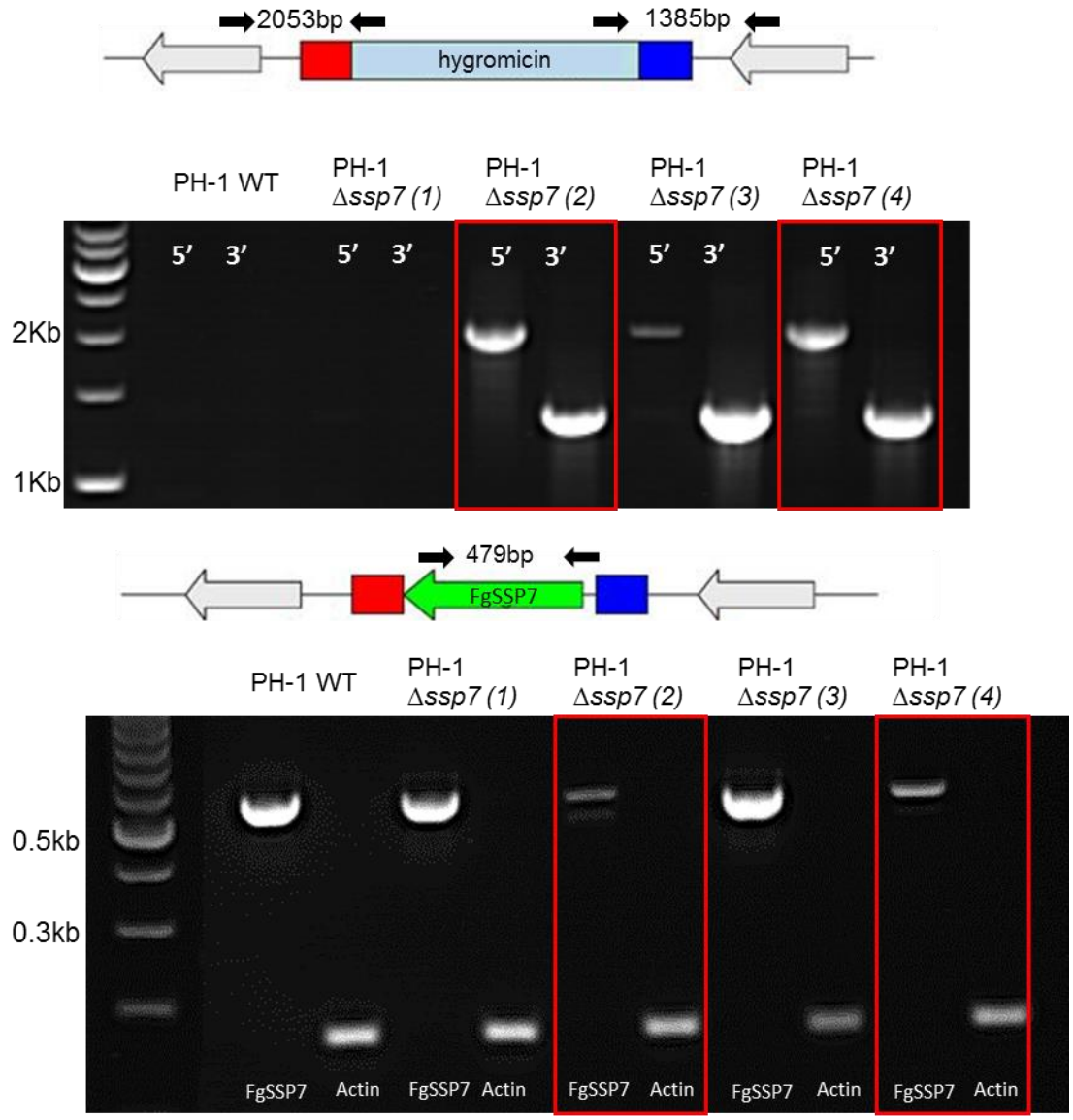

Figure 5.18 PCR analyses of four transformed *F. graminearum* strains carrying respective gene deletion constructs. Two strains were selected for analysis (with red frame). 5': PCR products from the 5′ regions of the deleted *FgSSP7* gene; 3': PCR products from the 3′ regions of the deleted *FgSSP7* gene (top). The *FgSSP7* 479 bp fragment was amplified from the 5′ and 3′ regions of the *FgSSP5* gene (bottom)

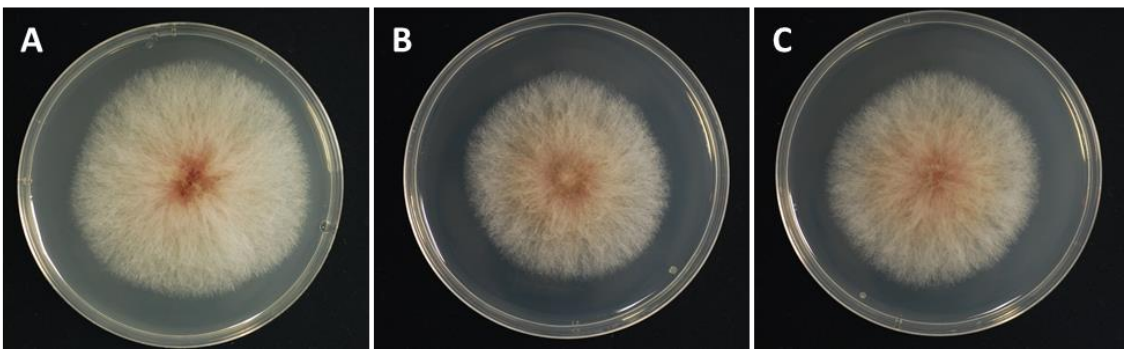

Figure 5.19 Representative colony growth in PDA after 3 days of (A) *Fg*PH-1 *wt* and two independent transformants (B) PH-1Δ*FgSSP7* (2) and (C) PH-1Δ*FgSSP7* (4).

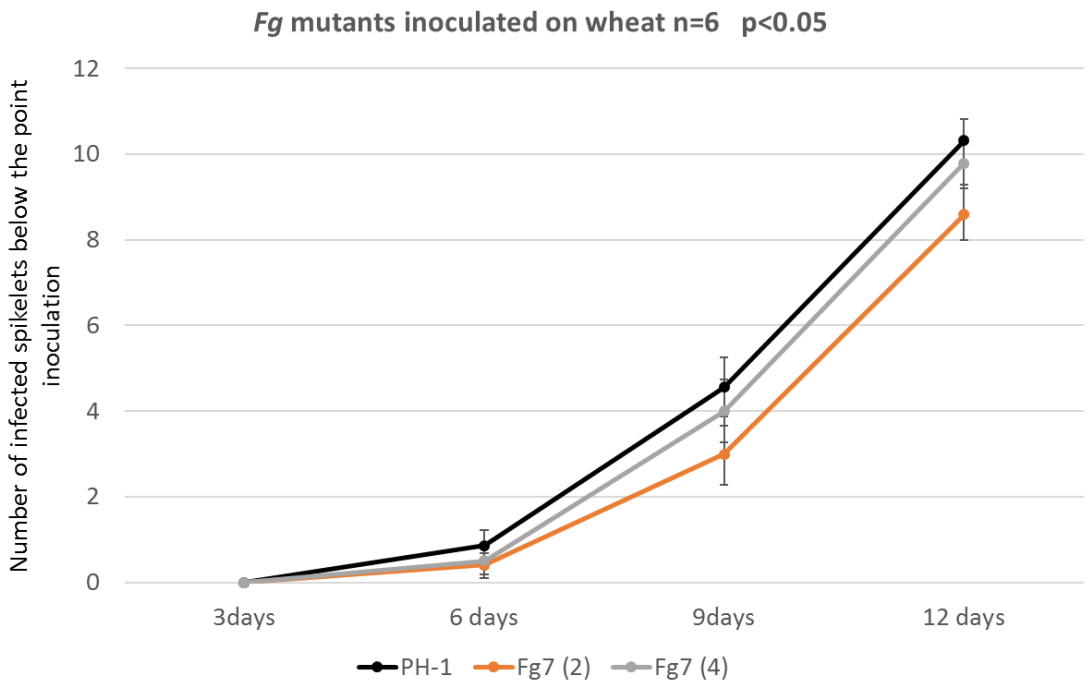

Figure 5.20 Graph representing number of visibly diseased spikelets below the *F. graminearum (Fg)* inoculation points in *Fg*PH-1 *wt,* PH-1Δ*FgSSP7(2)* and PH-1Δ*FgSSP7(4)* strains inoculated wheat ears. Infection curves are not statistically different.

5.4 Discussion

In chapter 4, I demonstrated that overexpression of the *F. graminearum* CPs FgSSP6 and FgSSP7 from BSMV enhanced development of FEB disease in wheat ears subsequently inoculated with *F. graminearum* spores (Figure 4.1 and 4.2 – Chapter 4). In this chapter, I explored further the possible roles of FgSSP6 and FgSSP7 during *F. graminearum* infection on wheat ears.

First, I tried to detect the production of both proteins by the BSMV-mediated system using specific antibodies. Unfortunately, the western blots analyses were not sensitive enough to detect FgSSP6 and FgSSP7 on virus infected wheat ears. However, a 14kDa band, correspondent size of FgSSP7,

was detected when leaf extracts and apoplastic fluid of *N. benthamiana* leaves infiltrated with BSMV:FgSSP7 were probed with α-FgSSP7 (Figure 5.7). The fact that FgSSP6 could not be detected using specific antibodies could be either due to the lower sensitivity of the α-FgSSP6, the virus expressing lower amount of FgSSP6 protein that could not be detected by western blotting or the protein was bound to insoluble components within the plant and could not be recovered. It is known from other studies that proteins produced by the plant, when present only at low concentrations, could not be detected by western blotting using specific antibodies, reinforcing the fact that the technique has sensitivity issues.

Removal of predicted signal peptide in both FgSSP6 and FgSSP7 overexpressed in BSMV led to no FEB enhancement compared to overexpression of full length peptides (Figure 5.9). Although secretion of both proteins was assumed only by prediction tools, this result support the presence of secretion and its importance for FgSSP6 and FgSSP7 functions during fungal infection. This experiment provides a 2nd independent result where a statistically significant effect of FgSSP7 on FEB disease formation has been identified. The detection of FgSSP7 by western blot in apoplastic fluid *N. benthamiana* leaves infiltrated with BSMV:FgSSP7 also reinforce the evidences that this protein is secreted in the apoplastic fluid (Figure 5.7). Live fluorescence microscopy to detect secretion of fluorescent tagged protein active at low pH, due the conditions in the apoplast, would provide stronger support of FgSSP6 and FgSSP7 secretion and function *in planta* (Djamei et al., 2011, Khang et al., 2010).

Recently, Lo Presti et al. (2017) described an assay to identify whether fungal effector proteins exhibit their activity in the plant apoplast or if they are taken up by the plant cell. The assay was used in the *U. maydis–maize* system to demonstrate effector translocation. Briefly, it is based on stable expression of

BirA (biotin-protein ligase) in maize cytoplasm and Avitagged fungal target protein. The biotinylation of the target protein is an indication of translocation to the plant cell (Lo Presti et al., 2017). We acquired these transgenic maize seeds and similar assay will be conducted to identify translocation of *F. graminearum* effector candidates. This has been done in a follow up PhD project.

The extra motif in FgSSP6 (KK$) does not appear to be essential for the role of the proteins during infection (Figure 5.10). However, after the construct was made, another publication was found showing that removal of the last lysine residue (ΔK435) (retaining the penultimate K434 residue) did not change the plasminogen-binding activity of *Streptococcus* surface enolase (SEN). However, deletion of the last two lysine residues of SEN (SEN-ΔK434-435) significantly decreased the Glu-plasminogen-and Lys-plasminogen-binding activities of mutant SEN proteins (Derbise et al., 2004). Therefore, it could be by removing both lysines at the end of the protein would lead to a different outcome in FgSSP6(-KK$) overexpression. Unfortunately, due to the limited timeframe to set up a new VOX experiment to test this new construct, this experiment could not be done during this PhD, but it is planned to be done in the future.

Neither FgSSP6 and FgSSP7 could overcome the extreme wheat immunity response induced by a non-DON producing strain of *F. graminearum* (Figure 5.11). The absence of DON during *F. graminearum* infection in wheat ears leads to very reduced diseases symptoms and the infection remains locally in the infected spikelets. This suggests that DON play a crucial role during *F. graminearum*-wheat interaction, which FgSSP6 and FgSSP7 were not able to overcome. An interesting study was done using Affymetrix microarray with PH-1Δ*tri6* and PH-1Δ*tri10* strains during infection in wheat ears (Seong et al., 2009). *Tri6* encodes a transcription factor that regulates trichothecene and isoprenoid

biosynthesis production and many other genes related to housekeeping functions, secondary metabolism and pathogenesis. *Tri10* encodes a new regulatory protein in the trichothecene pathway. Both mutants exhibit greatly reduced virulence and toxin production in wheat (Seong 2009). Although this study used gene expression from infection in the whole ear, deletion of *Tri6* or *Tri10* had no obvious effect on FgSSP6 and FgSSP7 expression (http://www.plexdb.org) (Seong et al., 2009). This suggest that *Tri6* and *Tri10*, and possibly other genes that regulate DON production as *tri5*, do not regulate expression of either *FgSSP6 or FgSSP7* during infection.

FgSSP6 and FgSSP7 purified proteins were also able to induce necrosis in *N. benthamiana* leaves (Figure 5.17). A question that could be raised from these results is why these proteins did not induce necrosis in *N. benthamiana* leaves when infected with either BSMV:FgSSP6 or BSMV:FgSSP7. This could be due the fact the necrosis is induced in a dose-dependent manner. Higher concentrations of protein need to be tested to assess if this dose–response curve is reminiscent of saturation. FgSSP6 seems to induce stronger necrosis than FgSSP7. Although the protein concentration was relatively high to test its effect *in planta*, some studies that investigate the necrotic effect of cerato-platanin in other fungal species used similar or higher protein concentrations (Chen et al., 2015a, Frias et al., 2011, Pazzagli et al., 1999). HaCPL2 from *Heterobasidion annosum* caused cell death in *N. tabacum* at a concentration of 120µM (Chen et al., 2015a). Frias et al. (2011) demonstrated that 17mmol is the minimal dose to produce noticeable necrosis in tobacco and tomato infiltrated with BcSpl1 from *B. cinerea*. The authors suggested that BcSpl1 is recognised as a PAMP and the intensity of defence response that can lead to HR and cell death depends on the presence of the right elicitor at the right concentration (Frias et al., 2011). The

fact that FgSSP6 and FgSSP7 induce cell death at higher concentrations could benefit for *F. graminearum* infection. The lower expression of FgSSP6 and FgSSP7 during the symptomless phase probably indicates that neither protein is able to induce cell death at the advancing hyphal front, thereby favouring the biotrophic phase. Whereas the higher expression at the symptomatic phase could lead to cell-death thereby assisting the necrotrophic phase (Figure 5.1) (Brown et al., 2017). The intensity of defence response activated by CPs can also be related to protein dimerisation (Vargas et al., 2008). The fact that cerato-platanins from *F. graminearum* are predicted to prone form dimers and low concentration of monomer forms will be available could explain the fact high protein concentration were necessary to activate cell-death.

FgSSP6 and FgSSP7 were also able to bind different polysaccharides that are components of either plant or fungal cell wall (Figure 5.16). This result is different of what has been found previously in few other fungal species, where CPs were able to bind only chitin oligomers. The affinity to chitin was suggested to have a role to avoid chitin recognition by plant chitin receptors (Barsottini et al., 2013, Pazzagli et al., 2014). This function has been well-studied in fugal effectors proteins containing three Lysin (LysM) domains, such as such as Ecp6 from *Cladosporium fulvum* and 3LysM from *Zymoseptoria tritici* (de Jonge & Thomma, 2009, Marshall et al., 2011). CPs, however, present a very distinct amino acid sequence and protein structure from these 3LysM effectors. The results presented on this thesis suggest these two proteins bind to different carbohydrates sources in a nonspecific way. The next step will be to repeat the same assay and include other insoluble polysaccharides that are not plant or fungal cell-wall components. So far, the data may indicate that these proteins

have an adhesive role, that could be linked to an expansin activity or to a less extent, act as a protection layer.

Unfortunately, deletion of FgSSP7 did not affect *F. graminearum* virulence in wheat heads. During the development of this PhD project, a publication testing Δf*gssp6* and the double Δf*gssp67* mutant became available and no reduction in virulence was observed compared to the wild type strain on both soybean and wheat heads (Quarantin et al., 2016). The group used a different progenitor strain but based on their results, gene deletion of FgSSP6 and double mutant are unlikely to lead to major disease phenotype changes. Tests with FgSSP6 single and double gene knock-out will be carried out to complete the datasets needed for the publication and to explore the biphasic infection phenotypes in fine detail which was not done in the published study.

In summary, *F. graminearum* cerato-platanins could have a dual role in the wheat floral interaction. Cerato-platanins could initially aid adhesion of fungal hyphal to plant cell walls (expansin activity). This role might favour *F. graminearum* infection during the early (symptomless) phase. Later on, expression data shows accumulation of cerato-platanin. These proteins could induce cell death to benefit the necrotrophic phase of *Fusarium graminearum* by increasing nutrient availability via inducing host cell death. Although not formally proven, the various data sets provided suggest that both FgSSP proteins are likely to be functioning as secreted proteins. A recent study found that cerato-platanin domains were conserved in 91 species of fungi, belonging to Pezizomycotina and Agricomycotina. Among these species, some symbionts, saprophytes and hematophagous fungi are included. However, these genes were not found in other phyla of Basidiomycota, such as Ustilaginomycotina and Pucciomycotina, were most species are considered to have a biotrophic *in planta*

lifestyle. These finds support the hypothesis that CPs may be important for the necrotrophic phase (Kim et al., 2016).

Chapter 6 – The *Fusarium graminearum* genome possesses a homologous gene of plant rapid alkalinisation factor (RALF) peptides

6.1 Introduction

The gene *FgSSP5* (FGRRES_15123) previously identified by the analyses done in Chapter 3 (Table 3.9) codes for a protein that possesses the pfam domain RALF (Rapid alkalinisation factor; PF05498.6). RALF domain-containing proteins are predominately found in plants and play a role in plant development, for example, regulating tissue expansion in sugarcane and negatively regulating pollen tube elongation in tomato (Mingossi et al., 2010, Covey et al., 2010). Although rapid-alkalinisation factor proteins are predominantly found in plants (both dicotyledonous and monocotyledonous species), this protein type is also identified to less extent in fungal species. The role of RALF proteins in fungal virulence has not yet been widely explored (see below). When I initiated this study in 2013, no publications on RALF domain containing fungal proteins existed.

Various fungal pathogens use pH sensing-response systems to adapt to their host and achieve successful colonisation. In plant pathogens, the importance of pH regulation for virulence was first demonstrated in *Colletotrichum gloeosporioides* (Yakoby et al., 2000). These studies showed elevation of local ammonia concentration and a rise in pH in host plant tissue during infection was found to regulate the expression of the cell wall degrading enzyme pectin lyase, a key virulence factor for this species (Prusky et al., 2001, Yakoby et al., 2000). To explore a nonhost interaction, *C. gloesporioides* was inoculated into apple fruit with or without the addition of ammonia and pathogenicity was enhanced in the

presence of ammonia to levels similar to those observed in a host interaction (Prusky et al., 2001).

Besides RALF, other well-known genes involved in pH sensing and regulation in fungi are the pacC and palA, B, C, F H and I, first identified and described in *Aspergillus nidulans* (Arst & Penalva, 2003, Tilburn et al., 1995). PacC plays an important role in mediating pH-dependent signalling by activating the transcription of alkaline-expressed genes and repressing transcription of acid-expressed genes (Prusky et al., 2001, Tilburn et al., 1995).

RALF proteins are found predominantly in plants and some fungal species. Thynne et al. (2017) analysed numerous fungal genomes searching for homologues of plant RALF proteins using proteins sequences from *Arabidopsis thaliana* RALF as a reference (do Canto et al., 2014). Identification of RALF homologues in other species have been named according to the similarities to members of the *A. thaliana*. In this study, 26 different species of fungi were found to possess RALF homologues from plants. Interestingly, all RALF domain containing species were plant pathogens, including Basidiomycota and Ascomycota. However, it seems *ralf* genes were acquired independently in different fungal species because phylogenetic analysis of peptide sequence similarity revealed that fungal RALF homologues are interspersed amongst the plant RALFs (Thynne et al., 2017) (Figure 6.1). The same study proposes RALF homologues diverge in four groups in *Fusarium* species, on which *F. graminearum* was placed within group III along with two other members, namely the cereal infecting species *F. pseudograminearum* and the non-cereal infecting species *F. oxysporum radicis-lycopersici* CL57 (Thynne et al., 2017) (Figure 6.2). Nevertheless, it is not known if RALF domain containing proteins share similar

functions in each group or if any correlated functions exists between the species groups.

Within group I, mutants of the tomato infecting species *Fusarium oxysporum* f.sp. *lycopersici* lacking the *f-ralf* gene have been shown to be significantly attenuated in virulence on plant roots, and also to induce expression of various defence genes in the host 2 days after inoculation (Masachis et al., 2016). By contrast, another study demonstrated that the F-RALF protein was not require for infection of *F. oxysporum f. sp. lycopersici* on tomato roots (Thynne et al., 2017). Differences on how the pathogenicity tests were carried out may account for these contrasting results. For example, Masachis et al. (2016) grew plants in vermiculite with no plant nutrients provided and scored plant survival up to 35 days. Whereas Thynne et al. (2017) grew plants in potting mix well supplied with nutrients and scored disease symptoms up to 21 days. These different growing conditions were suggested to be the main reason why divergent outcomes were reported.

While some aspects of the role of F-RALF in *F. oxysporum* f.sp. *lycopersici* – host interaction remains undetermined, both studies suggest that F-RALF-triggered plant responses are mediated by the plant's receptor-like kinase (RLK) Feronia (FER) (Masachis et al., 2016, Thynne et al., 2017).

The Arabidopsis genome potentially encodes 34 RALF family proteins and although few components of the signalling pathway have been explored, FER has been found recently to be a receptor for RALF1 (Haruta et al., 2014). RALF1 is a 120 amino acids peptide, which contains a RALF domain (PF05498) between amino acids 58-119. FER is a receptor-like kinase that contains an extracellular malectin-like protein, which is known to recognise and bind cell wall carbohydrates. RALF1 affects phosphorylation of FER and the key cell growth

regulator H^+-ATPase (Li et al., 2016). RALF1 was shown to initiate a downstream signalling cascade that lead to apoplastic alkalinisation and inhibition of cell elongation of primary root (Haruta et al., 2014). More recent studies have revealed that *Arabidopsis* mutant plants lacking FER receptor were more resistant to infection by *F. oxysporum* (Masachis et al., 2016).

As described in Chapter 4, the *F. graminearum* RALF protein, FgSSP5, appears to slightly enhance FEB disease when the protein was overexpressed using BSMV-VOX system. Therefore, I first analysed using blastp for the presence of FER receptor encoding genes within the newly available wheat genome. Then I investigated whether FgSSP5 is required for *F. graminearum* infection on wheat ears, by generating mutant strains lacking FgSSP5 and tested for virulence on wheat ears. Thirdly, with the help of a Rothamsted colleague, Dr Wing Sham Lee, a VIGS experiment was done to silence transiently all three homoeologous of the wheat *FER* gene prior to *F. graminearum* inoculation and the resulting interaction outcomes were explored in detail.

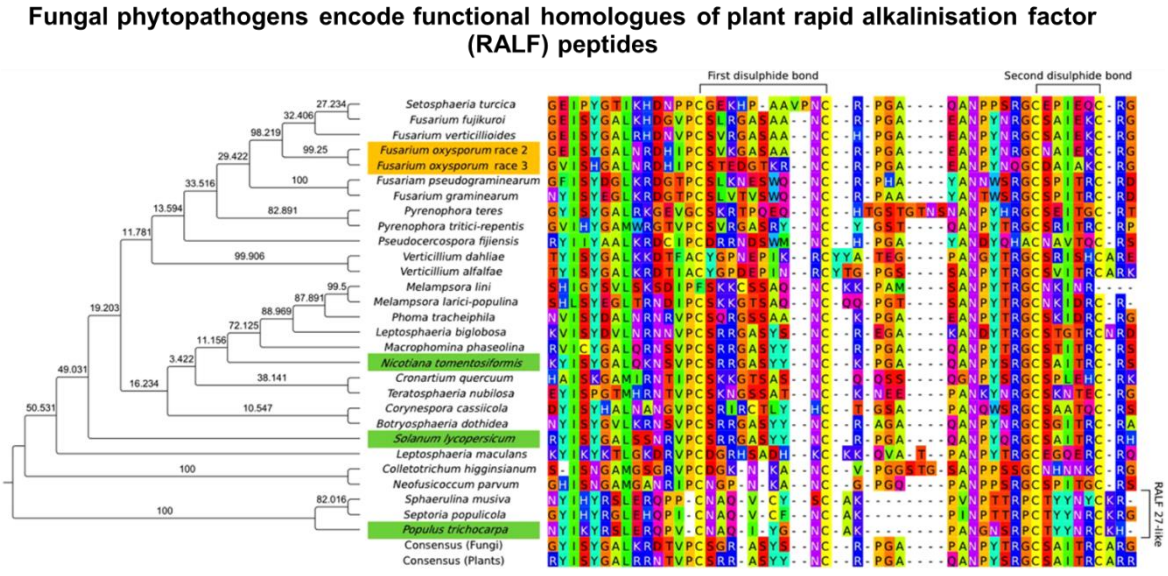

Figure 6.1 Phylogenetic analysis of the rapid alkalinisation factor (RALF) domain in fungi and selected plants proposed by Thynne et al. (2017). Figure taken from Thynne et al. (2017) - Molecular Plant Pathology 19 SEP 2016 DOI: 10.1111/mpp.12444 http://onlinelibrary.wiley.com/doi/10.1111/mpp.12444/full#mpp12444-fig-0002.

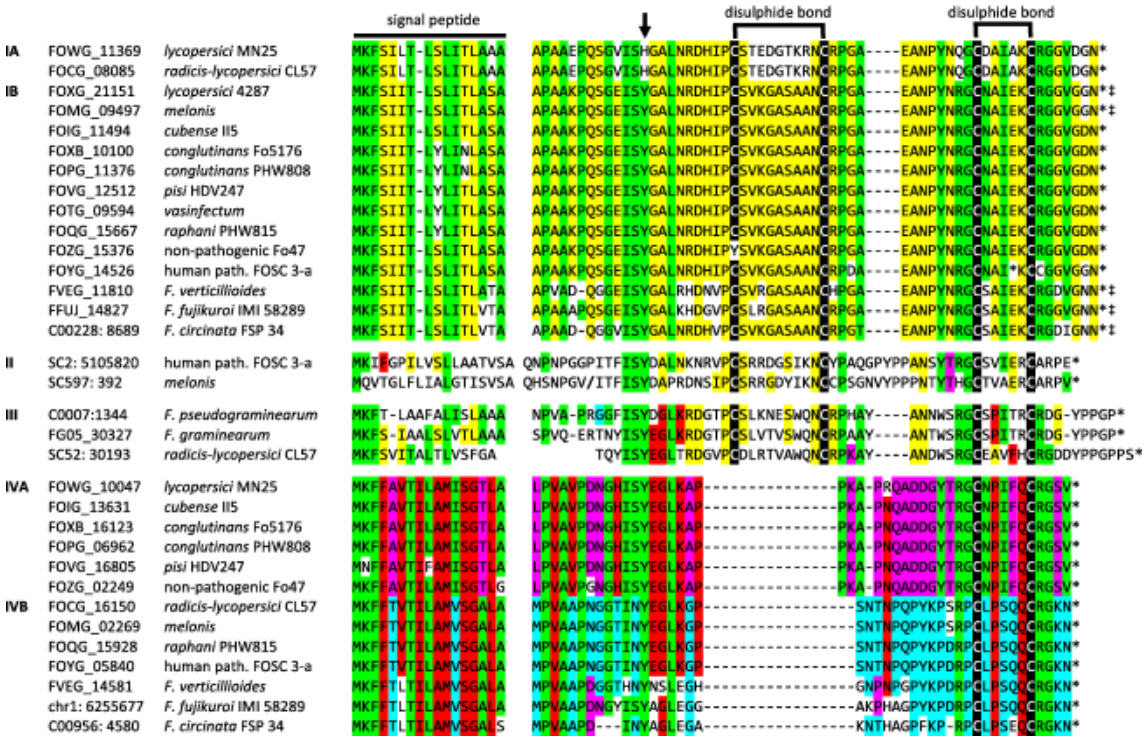

Figure 6.2 Multiple sequence alignments of *Fusarium* rapid alkalinisation factor (RALF) and RALF-like homologues. * Stop codon. Figure taken from Thynne et al. (2017) - Molecular Plant Pathology 19 SEP 2016 DOI: 10.1111/mpp.12444 - http://onlinelibrary.wiley.com/doi/10.1111/mpp.12444/full#mpp12444-fig-0003.

6.2 Materials and Methods

6.2.1 *F. graminearum* gene deletion experiments

For deletion of *FgSSP5*, the "split-marker" deletion strategy was applied (Chapter 2) (Catlett et al., 2003, Fairhead et al., 1996).

Following the identification of FgSSP5 (FGRRES_15123) from the *F. graminearum* genome, two thirds of each end (5' prime end and 3' prime end) of hygromycin and 1kb fragment of both 5' and 3' flank regions of the gene were amplified. The purified fragments containing one of the flank sequences and one of the two-thirds of amplified hygromycin were inserted into the EcoRV restriction site of pGEM®-T Easy Vector (Promega) using the Gibson assembly kit (New England Biolabs) according to the manufacturer's protocol. The resulting vector

was used to transform protoplasts of *F. graminearum* strain PH-1, as described previously (Hohn & Desjardins, 1992) and the hygromycin resistant transformants were selected.

6.2.2 Identification of putative wheat Feronia receptors.

Protein domain analysis of predicted *FER* genes in wheat was carried out using the Pfam database (http://pfam.xfam.org/search) (Finn et al., 2016). Blastn (https://blast.ncbi.nlm.nih.gov) and Blastp (https://blast.ncbi.nlm.nih.gov) was used for nucleotide and protein comparative analysis, respectively. Multiple protein sequences alignment was carried out in ClustalW, linked to Geneious 10 (Kearse et al., 2012). A tree was generated from protein alignment with Neighbour-Joining method using Jukes-Cantor distance model. Bootstrap analyses were based on 500 replicates and *A. thaliana* was used as outgroup. The wheat genome assembly used for this analysis was the TGACv1 from The Earlham Institute (http://plants.ensembl.org/Triticum_aestivum/Info/Index).

6.2.3 BSMV-VIGS

Note: BSMV-VIGS constructs were made by Dr. Wing-Sham Lee.

The BSMV-VIGS system described by Yuan et al. (2011), comprising three T-DNA binary plasmids, pCaBS-α, pCaBS-β, and pCa-γbLIC, was used. Gene-silencing constructs were created by cloning fragments of wheat *TaFER1* and *TaFER2* fragments into pCa-γbLIC in antisense orientation, using a ligation-independent cloning strategy. In silico predictions by si-Fi software were used to select the most effective gene-specific fragments for silencing, ranging from 254 to 325 bp in size, and also to ensure the selected fragments were not likely to direct off-target silencing. The cDNA fragments were generated by standard

reverse transcription-polymerase chain reaction (RT-PCR) from total RNA extracted from wheat cv. Bobwhite leaf tissue. The same BSMV:MCS4D construct used for VOX was used as a negative control construct for VIGS (Chapter 2). The BSMV pCaBS-α, pCaBS-β, and pCa-ɣbLICv derivatives were transformed separately into *Agrobacterium tumefaciens* GV3101 by electroporation. Viral inoculation of *N. benthamiana* by agroinfiltration was carried out the same way described on BSMV-VOX experiments (Chapter 2). The infiltrated *N. benthamiana* leaves were harvested at 5 days postinfiltration and ground using a mortar and pestle in 10 mM potassium phosphate buffer (pH 6.8) containing 1% celite, and the sap was used to mechanically inoculate the forth leaf of 38-day-old wheat plants.

6.3 Results

6.3.1 FgSSP5 is closely related to four putative RALF from *A. thaliana*

FgSSP5 is a small, cysteine-rich protein that contain a Rapid Alkalinisation Factor (RALF) domain (PF05498.6). However, RALF proteins are found predominately in plants. This family is most well studied in Arabidopsis and previous in silico analysis identified that this species contains 34 genes within the RALF family (Olsen et al., 2002). In order to identify which of the Arabidopsis RALF genes are more closely related to FgSSP5 in *F. graminearum*, a neighbour-joining phylogenetic tree was built. Figure 6.3 shows that FgSSP5 and other RALF proteins from different Fusarium species are more closely related to AtRALF23, AtRALF33, AtRALF22 and AtRALF1. These are well-studied RALF proteins in Arabidopsis (Stegmann et al., 2017) and their function in plant immunity will be discussed in more detail further.

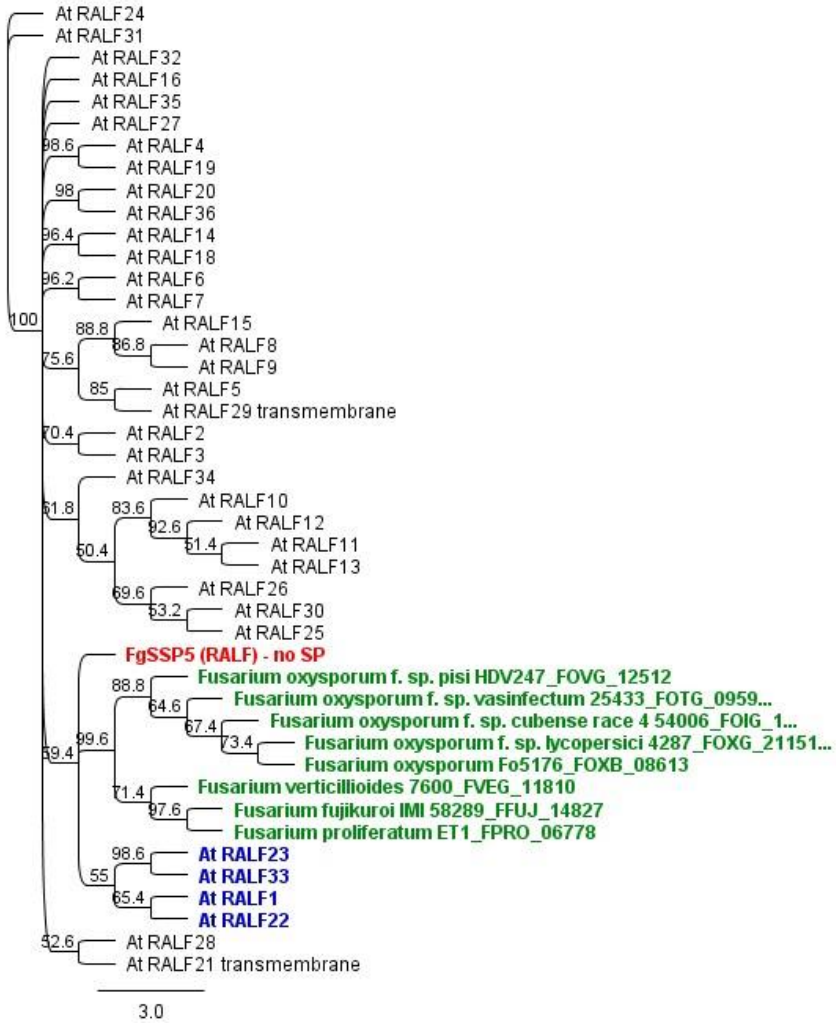

Figure 6.3 Neighbour-Joining consensus tree of RALF proteins alignment from *Arabidopsis thaliana* and selected Fusarium species. *FgSSP5* is highlighted in red; RALF genes from other Fusarium species are highlighted in green and the closely related RALF genes from Arabidopsis are highlighted in blue.

(Thynne et al., 2017) identified 26 different species of fungus that contain RALF homologues from plants. According these previous analysis, *F. pseudograminearum* also possess an orthologue of RALF, but the presence of orthologues in two *F. graminearum* closely related species has not been analysed. One is the cereal pathogenic species *F. culmorum,* and the other is the non-pathogenic species *F. venenatum*. In *F. venenatum* genome, there was no alignment hits to FgSSP5, suggesting this gene is probably absent in this

species (Figure 6.4). In chapter 3, *FgSSP5* is positioned in a cluster of predicted secreted genes in the telomere region of chromosome 3 (Table 3.5). The same cluster was identified by Brown et al. (2012). Blast analysis of this cluster within the *F. venenatum* genome (King et al., 2017a, submitted) identified that not only *FgSSP5*, but at least two more genes in the cluster are absent in *F. venenatum*.

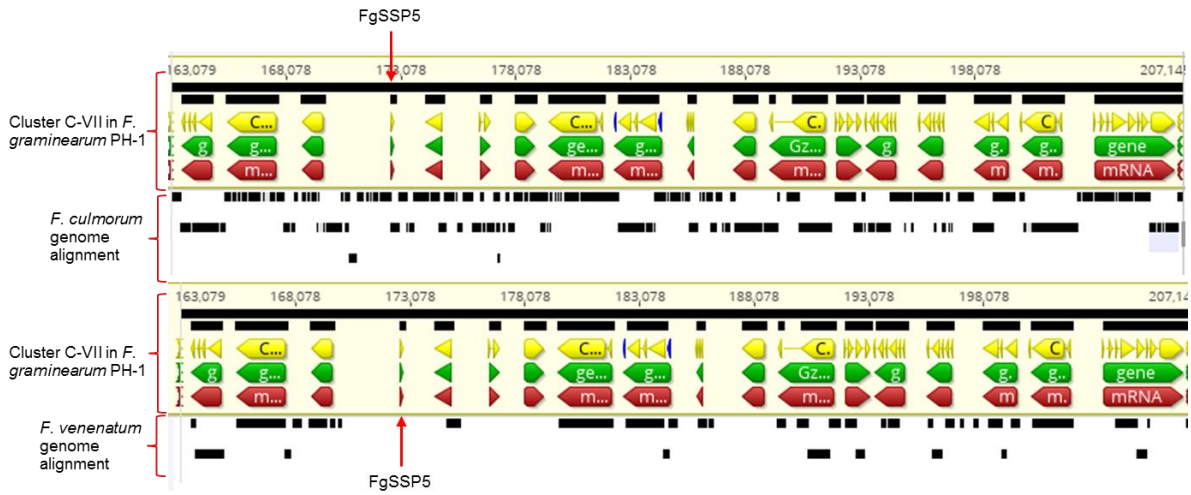

Figure 6.4 LASTZ alignment to cluster C-VII of *F. graminearum* PH-1 genome with *F. culmorum* and *F. venenatum.* Alignment was carried out in Geneious 10.

6.3.2 FgSSP5 does not appear to contribute to *F. graminearum* virulence on wheat ears.

The *in planta* overexpression of FgSSP5 via the BSMV-VOX system led to an enhancement of FEB disease (Figure 4.1). However, it is not known if this predicted secreted protein plays an essential role in *F. graminearum* virulence on wheat ears. To test the role of SSP5 in virulence, *FgSSP5* gene deletion mutants were produced and tested *in planta.* Two *PH-1ΔFgSSP5* independent mutants (1 and 8) were selected for further analysis. The molecular characterisation the selected mutants are shown in figure 6.5.

No differences were observed in in vitro fungal growth when grown on rich media (PDA) between wild type and the two *PH-1ΔFgSSP5* (1) and (8) strains (Figure 6.6). Colony colour, conidia spore morphology and germination was similar between wild-type and mutant strains.

The wild type and the two *FgSSP5*-deleted strains were tested in wheat ears cv. Bobwhite for infectivity and disease formation using the point inoculation method (Chapter 2). In two independent experiments, using six ears per strain, no reduction in initial infection or FEB symptoms development were observed compared to the wild type (Figure 6.7). In two further pathogenicity test, *F. graminearum* strain PH-1wt and *PH-1ΔFgSSP5 (1)* and *(8)* were inoculated into Arabidopsis (*Ler-0*) floral tissue using the method previously described (Urban et al., 2002). No significant differences in disease phenotype was observed (Figure 6.8). Collectively, these three results indicated that FgSSP5 is not essential for *F. graminearum* virulence on wheat floral or Arabidopsis floral tissue.

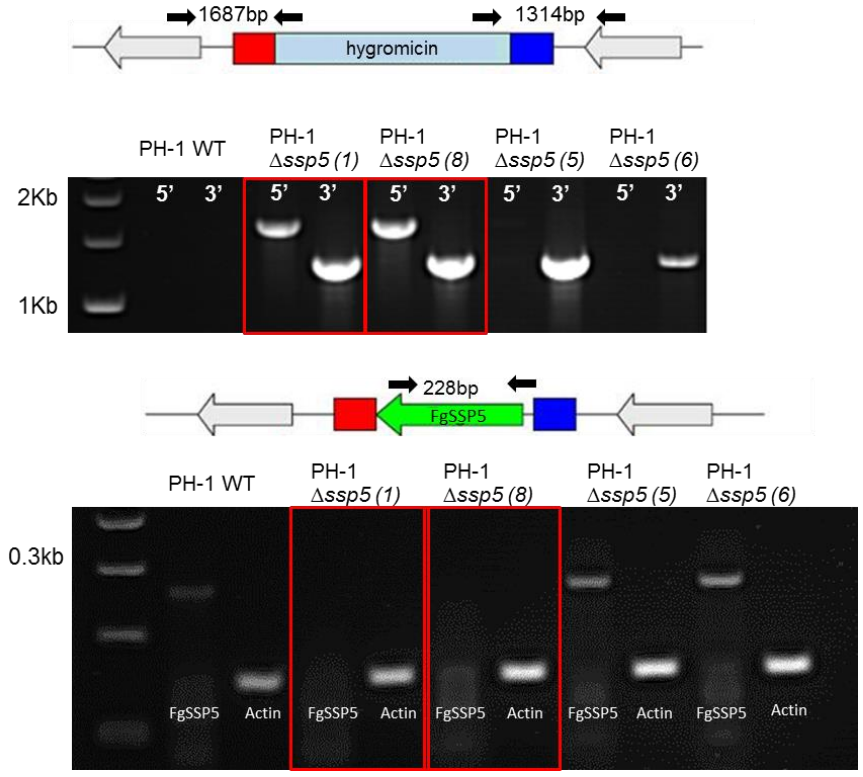

Figure 6.5 PCR analyses of four transformed *F. graminearum* strains carrying respective gene deletion constructs. Two strains were selected for analysis (with red frame). 5': PCR products from the 5′ regions of the deleted *FgSSP5* gene; 3': PCR products from the 3′ regions of the deleted *FgSSP5* gene (top). The *FgSSP5* 228 bp fragment was amplified from the 5′ and 3′ regions of the *FgSSP5* gene (bottom)

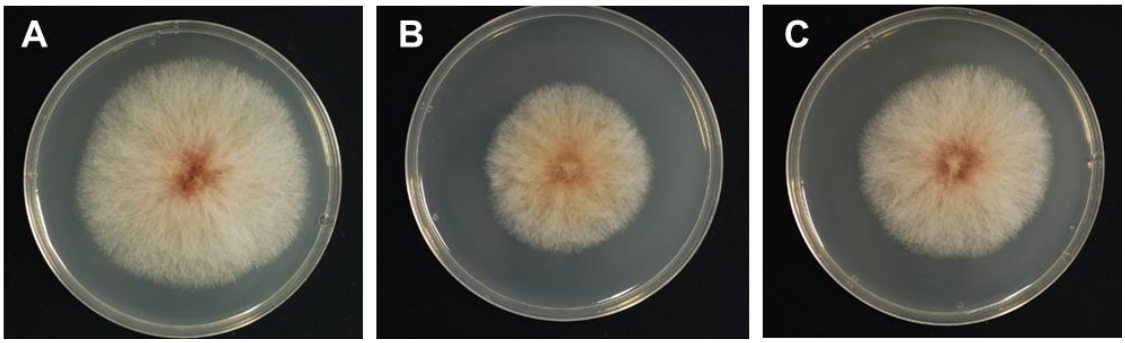

Figure 6.6 Representative colony growth in PDA after 3 days of (A) *Fg*PH-1 *wt* and two independent transformants (B) PH-1Δ*FgSSP5 strain* (1) and (C) PH-1Δ*FgSSP5* strain (8).

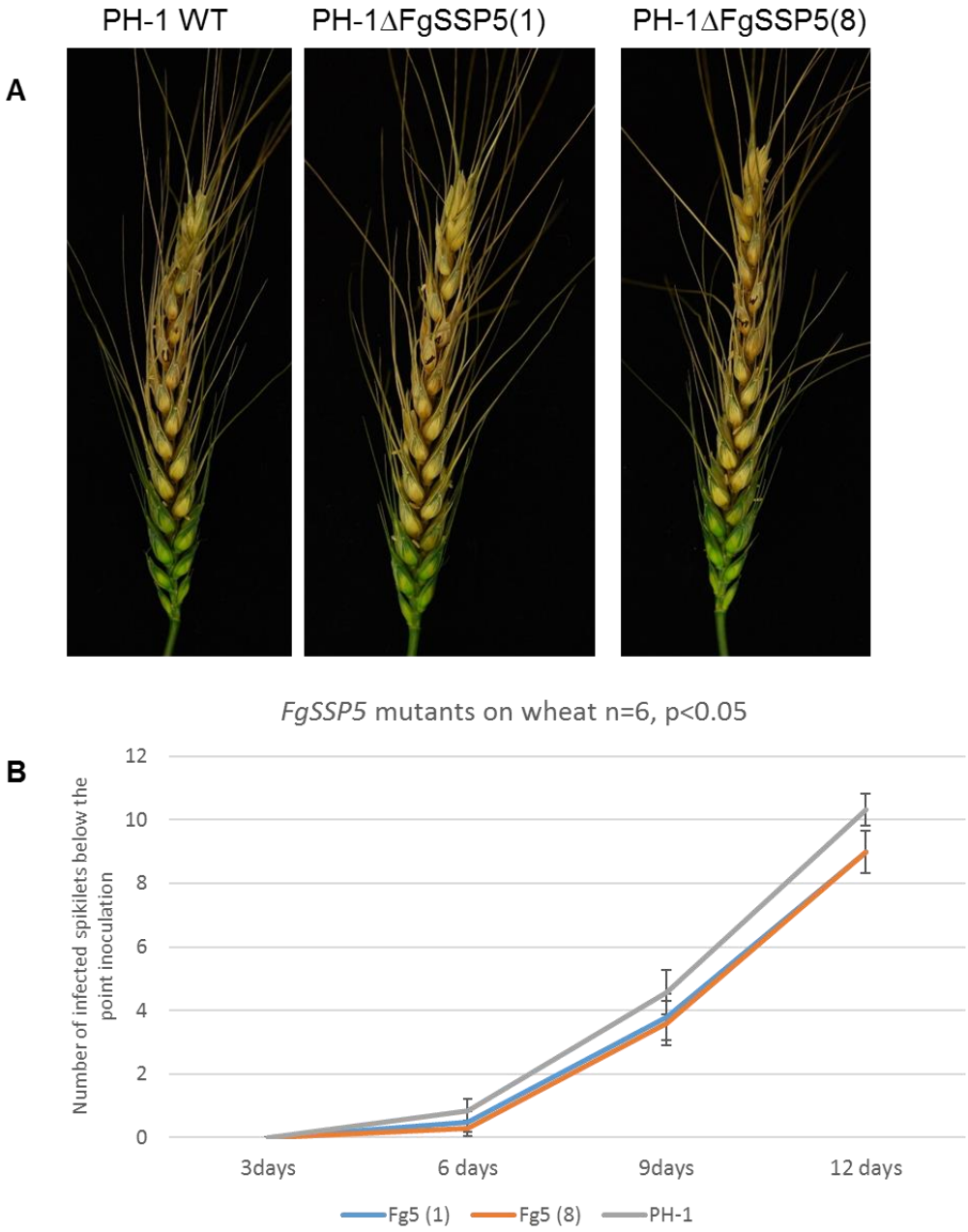

Figure 6.7 Infection of wheat spikes with *F. graminearum* wild-type and Δ*FgSSP5*. (A) Representative *Fg* disease symptoms on wheat spikes infected with PH-1 wild-type strain and PH-1Δ*FgSSP5 (1)* and *(8)* strains. Wheat ears were point-inoculated with the *Fg* strain at anthesis. Photographs were taken at 12 days post *Fg* inoculation. (B) Graph representing number of visibly diseased spikelets below the *F. graminearum (Fg)* inoculation points in *Fg*PH-1 *wt,* PH-1Δ*FgSSP5(1)* and PH-1Δ*FgSSP5(8)* strains inoculated wheat ears. Infection curves are not statistically different.

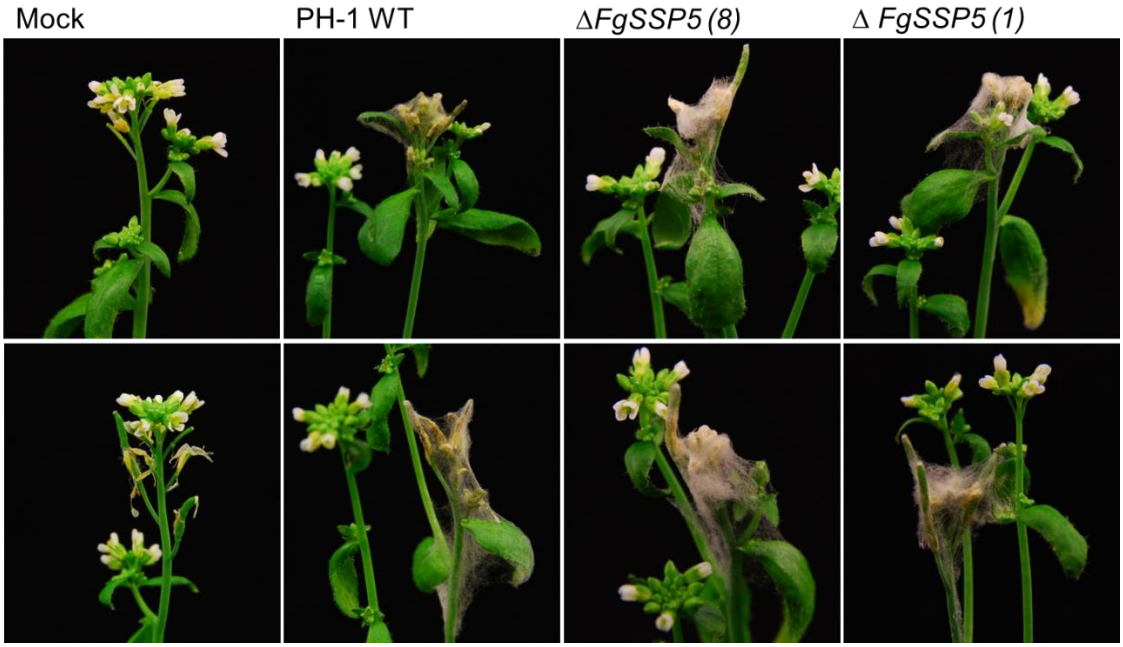

Figure 6.8 Representative images of Arabidopsis floral infection with mock sterile water control, *F. graminearum* strain PH-1 wild-type and *F. graminearum* mutants Δ*FgSSP5 (1)* and *(8)*. The ecotype used was Landsberg erecta (Ler-0).

6.3.3 The wheat genome encodes eight predicted paralogues of Feronia

Blastp analyses and the Ensembl (http://plants.ensembl.org) tool 'Plant Compara' were used to find orthologues of Arabidopsis FER gene on wheat. Eight putative candidates *FER* genes were found on wheat (*Triticum aestivum*) genome (variety Chinese Spring). The genomic and chromosome location in wheat, and similarity with the well characterised Feronia gene from *Arabidopsis thaliana* are summarised in table 6.1.

The eight wheat genes were named *TaFER1, TaFER2*, *TaFER3a, TaFER3b, TaFER4, TaFER5, TaFER6 and TaFER7*. *Triticum aestivum* is an hexaploid species and contains three copies of each gene composed of closely-related yet independently inherited homoeologous genomes termed A, B and D. Based on nucleotide alignment from the homoeologues of all three genes, there is high identity between the predicted homoeologues of *TaFER1, TaFER2* and

TaFER4 (Figure 6.9). Homoeologues of *TaFER3a, TaFER3b, TaFER5 and TaFER6* were found to be more divergent. Although some predicted TaFER genes were more divergent than others, analysis of protein domain prediction using Pfam (Finn et al., 2016) demonstrated that all eight predicted TaFER encoded proteins contain both kinase-like (PF07714) and malectin-like (PF12819) domains. The presence of these two domains in the same protein is one feature that characterise Feronia proteins. Genetic map location of putative wheat Feronia genes are represented in figure 6.10. (Note: genetic map location was done by Dr. Michael Hammond-Kosack)

Analysis of the wheat gene expression data available within the WheatExp database (https://wheat.pw.usda.gov/WheatExp/) demonstrated that all homoeologues of *TaFER1* and *TaFER2* were expressed *in planta* in all wheat tissues, with the highest expression levels present in floral spikes at early stage of development (Z32-39) and in floral spikes and grains at late stages of development (Z65-71). Whereas the expression of *TaFER3a, TaFER3b, TaFER5, TaFER6* and *TaFER7* were either absent or at very low levels in all tissue types at all stages of development (Figure 6.11). TaFER4 was more highly expressed on wheat leaves, roots and stems tissues. The identification of putative TaFER1 and 2 genes in wheat with higher expression identified in floral tissues throughout development could be an indication one or all homoeologues might be the FgSSP5 RALF receptor during *F. graminearum* infection.

Table 6.1 Genomic location and similarity to Feronia from Arabidopsis of putative Feronia coding sequences in wheat.

Gene name	Genomic location	Chrom. location[1]	% ID with AtFER[2]
TaFER1	TGACv1_scaffold_061212_1DL:152794-155418	1D	61.9
TaFER1	TGACv1_scaffold_031560_1BL:36019-38461	1B	61.7

TaFER1	TGACv1_scaffold_000346_1AL:11755-14433	1A	61.7
TaFER2	TGACv1_scaffold_343566_4DL:29013-31685	4D	62.3
TaFER2	TGACv1_scaffold_320353_4BL:238285-240918	4B	62.3
TaFER2	TGACv1_scaffold_307961_4AS:17374-20046	4A	62.7
TaFER3a	TGACv1_scaffold_328313_4BS:111040-113433	U[3]	53.8
TaFER3a	TGACv1_scaffold_457170_5DS:22565-26535	5D	55.1
TaFER3b	TGACv1_scaffold_423194_5BS:297315-300710	5B	42.5
TaFER3b	TGACv1_scaffold_362939_4DS:7851-9161	4D	53.4
TaFER4	TGACv1_scaffold_433606_5DL:63546-69028	5D	56.1
TaFER4	TGACv1_scaffold_405313_5BL:33506-37504	5B	56.2
TaFER4	TGACv1_scaffold_378245_5AL:17473-21848	5A	55.9
TaFER5	TGACv1_scaffold_272288_3DS:34,190-39,824	3D	53.8
TaFER5	TGACv1_scaffold_223903_3B:32,835-37,274	3B	57
TaFER5	TGACv1_scaffold_211867_3AS:33,940-39,187	3A	54.2
TaFER6	TGACv1_scaffold_272288_3DS:58,646-64,460	3D	56.8
TaFER6	TGACv1_scaffold_223903_3B:42,784-45,365	3B	52.5
TaFER6	TGACv1_scaffold_212160_3AS:18,556-22,670	3A	46.1
TaFER7	TGACv1_scaffold_250442_3DL:26,836-30,859	3D	52
TaFER7	TGACv1_scaffold_222397_3B:88,436-92,984	3B	53
TaFER7	TGACv1_scaffold_220955_3B:155,096-159,174	3B	53

1 Chromosome location according IWGSC

2 Percentage of identity with *Arabidopsis thaliana* Feronia genomic sequence

3 Gene assigned to the remaining unaassembled wheat contigs

Figure 6.9 Nucleotide alignment of predicted homologues of wheat Feronia coding sequences. The alignment was performed in Geneious v.10.1.13

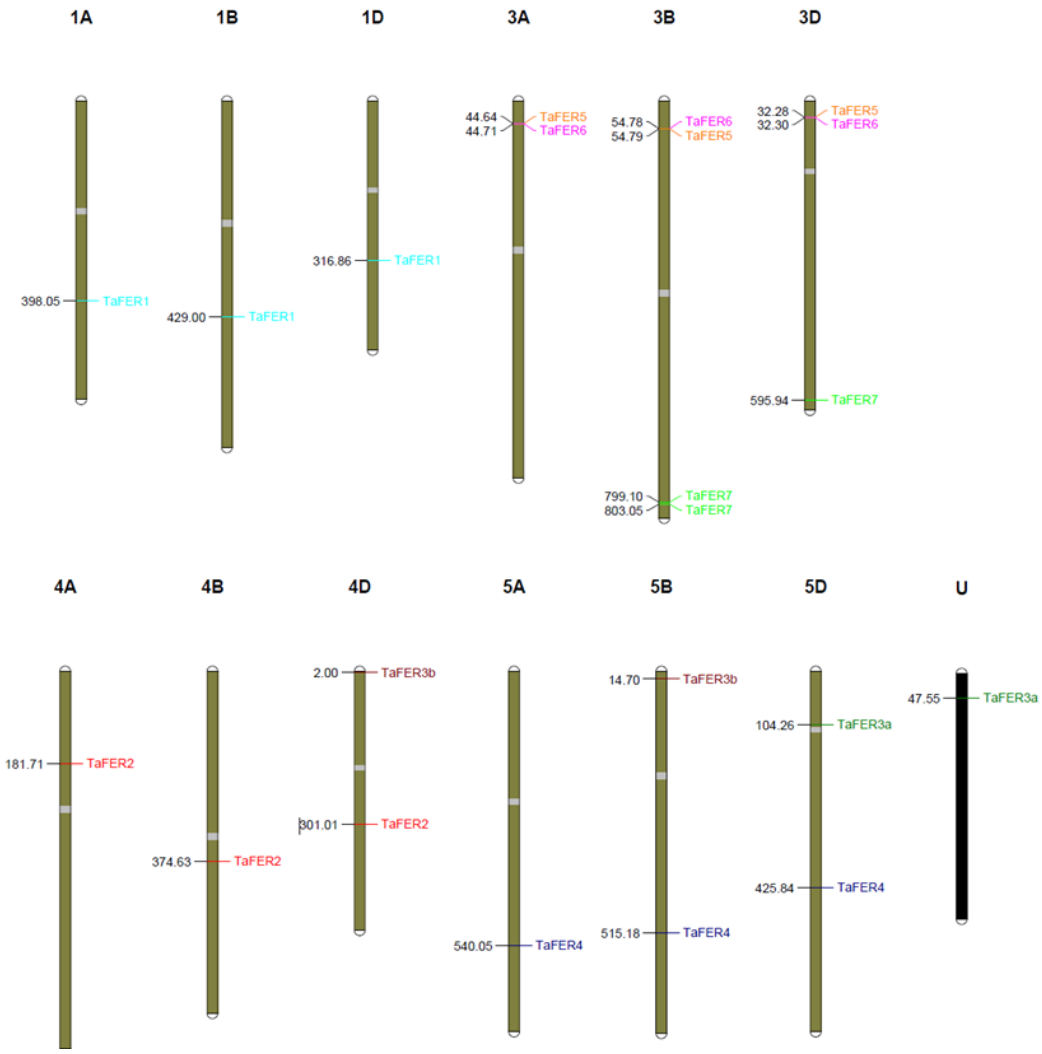

Figure 6.10 Genetic map location of putative TaFER genes in wheat chromosomes. Genetic map location performed in MapChart version 2.2 by Dr. M. Hammond-Kosack.

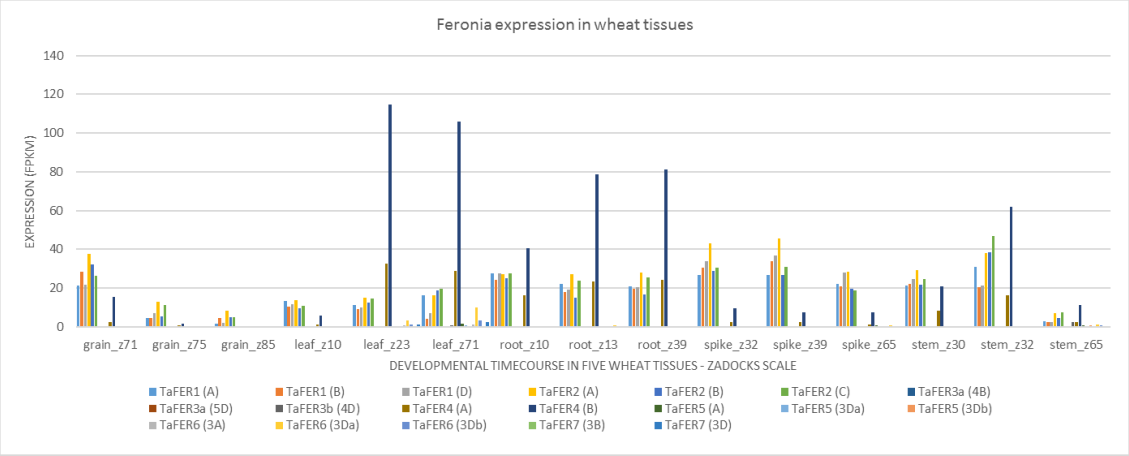

Figure 6.11 Gene expression profiles of putative TaFER genes from WheatExp database (https://wheat.pw.usda.gov/WheatExp/). Expression levels are calculated from RNA-seq datasets (FPKM) comprising multiple tissue and temporal developmental time courses.

6.3.4 BSMV- VIGS of *Feronia* genes in wheat

After I identified the putative *FER* genes in wheat, another member of the group (Dr. Wing-Sham Lee) developed a Barley stripe mosaic virus–mediated virus-induced gene silencing (BSMV-VIGS) constructs to silence these genes in wheat and later assessed the *F. graminearum* infection. In VIGS, a short fragment of a transcribed sequence of a plant gene is inserted into a cloned virus genome and the recombinant virus is then inoculated onto test plants, triggering Post-Transcriptional Gene Silencing (PTGS) (Lee et al., 2012). Five BSMV-VIGS constructs were generated: two constructs for each *TaFER1* and *TaFER2* targeting different regions in the transcripts, named TaFER1a, TaFER1b, TaFER2a and TaFER2b (Figure 6.12), and the fifth construct contains two concatenated fragments of *TaFER1* and *TaFER2* that target both sets of gene transcripts simultaneously in the same plant, name TaFER1a/2a. Off target predictions were carried out in siFi21 software (siRNA Finder, IPK-Gatersleben, Germany) (Table 6.2).

Two experiments have so far been carried. The first one was done by Dr. Wing-Sham Lee with my help during disease assessments. The second one was carried out by myself. In the first experiment, BSMV carrying VIGS constructs as(anti-sense)TaFER1a and asTaFER2a designed to silence *TaFER1* or *TaFER2* transcripts, respectively, were inoculated on wheat. About 15 days after virus inoculation, wheat ears at anthesis were inoculated with *F. graminearum* spores. Results from this experiment suggested that silencing of *TaFER1* by asTaFER1a led to a reduction of FEB symptoms compared to BSMV:MCS4D control (Figure 6.13) (Dr. Wing-Sham Lee, personal communication). Although Feronia is also involved in plant development, no visible effect on plant development were observed after silencing of either *TaFER1* or *TaFER2.*

A second BSMV-VIGS experiment was carried out to corroborate the previous results. In addition to the BSMV-VIGS constructs previously tested, the remaining three constructs were included (asTaFER1b, asTaFER2b and asTaFER1a/2a). BSMV:MCS4D was used as a virus control. Although *F. graminearum* infection pattern for the BSMV:asTaFER1a infected plants was similar to the experiment one (Figure 6.14), GLM statistical analysis did not show significant difference of MCS4D virus control treatment. This was because plants infected with virus control (BSMV:MCS4D) had also reduced *F. graminearum* infection (Figure 6.14). The second experiment was done in July 2017 and previous VIGS experiment exhibited different plant development patterns when done during the summer (Dr. Wing-Sham Lee). Although the experiments are carried out in controlled environment conditions, the air pressure changes between the seasons. This factor can interfere with the period of wheat flowering and perhaps other physiological processes. Therefore, a third VIGS experiment will be carried out during the winter season, to match the first replicate, to confirm if silencing of TaFER1 indeed leads to FEB reduction. The results from the third experiment will give further evidence to support the hypothesis that at least one of the putative *FER* genes identified in wheat could be a FgSSP5 RALF receptor during *F. graminearum* infection.

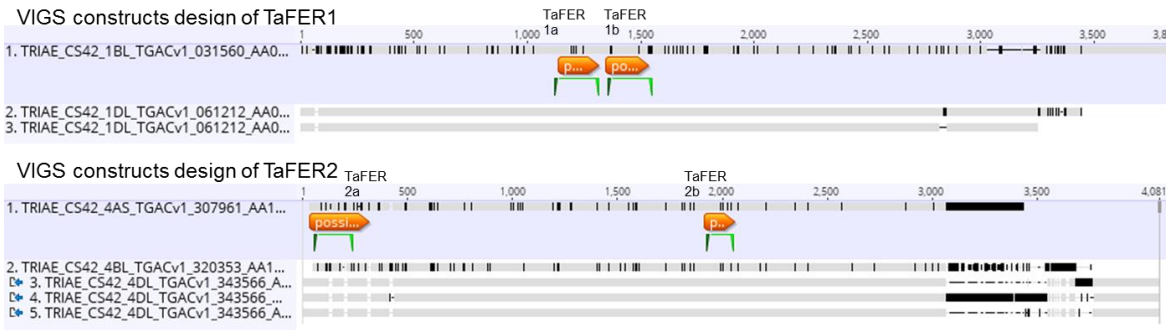

Figure 6.12 Region chosen for the design of VIGS constructs targeting TaFER1 (top) and TaFER2 (bottom) transcripts. Two anti-sense constructs were made for each gene (a and b) and the region selected for each one is underlined in green, name TaFER1a

(200bp), TaFER1b (210bp), TaFER2a (190bp), TaFER2b (140bp). *In silico* design was performed in Geneious v.10.1.13. by Dr. Wing-Sham Lee.

Table 6.2 Number of off target predictions for each of the VIGS constructs against TaFER1 and TaFER2 homoeologous. Analysis were carried in SiFi21 software (siRNA Finder, IPK-Gatersleben, Germany)

Wheat *Feronia* genes candidates	**Off target predictions**			
	asTaFER1a	asTaFER1b	asTaFER2a	asTaFER2b
TaFER1 (chr B)	93	88	0	ND[1]
TaFER1 (chr D)	65	60	0	ND
TaFER2 (chr A)	7	6	32	ND
TaFER2 (chr B)	5	2	30	ND
TaFER2 (chr D)	4	4	85	ND

[1] ND – not defined. The Sifi21 analysis failed for this construct

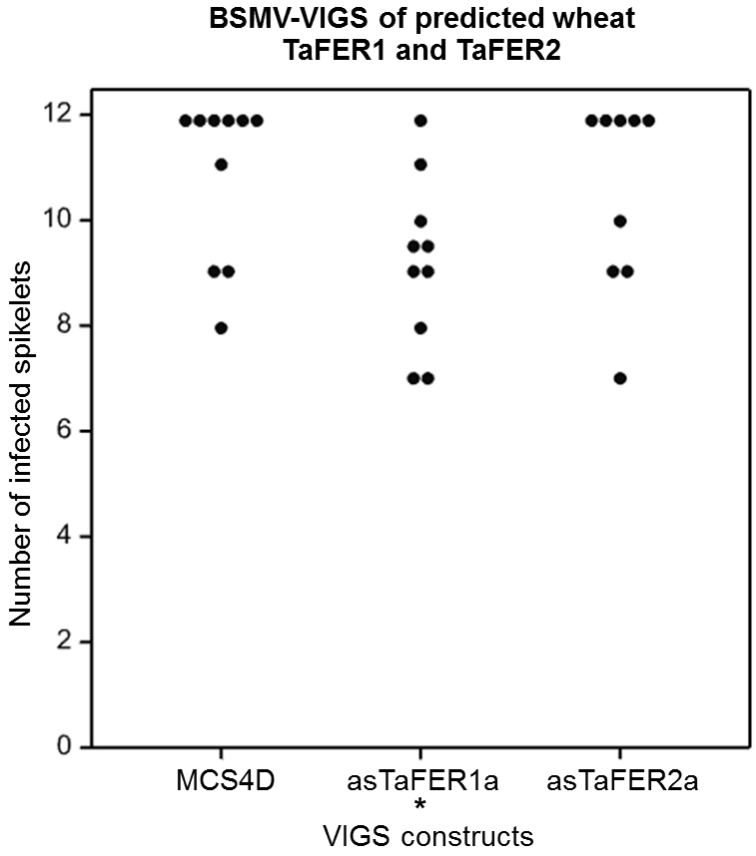

Figure 6.13 Dot-plot representing number of visibly diseased spikelets below the *F. graminearum* inoculation points in *F. graminearum* inoculated wheat ears at 15dpi. The control virus treatments (BSMV:MCS4D) and silencing constructs BSMV:asTaFER1 and BSMV:asTaFER2 were used for this experiment. Data shown were collected at 15 days' post *F. graminearum*-inoculation. Star (*) denotes the treatment in which statistically significant differences in number of diseased spikelets, relative to BSMV:MCS4D control were observed ($p < 0.05$ from GLM analysis).

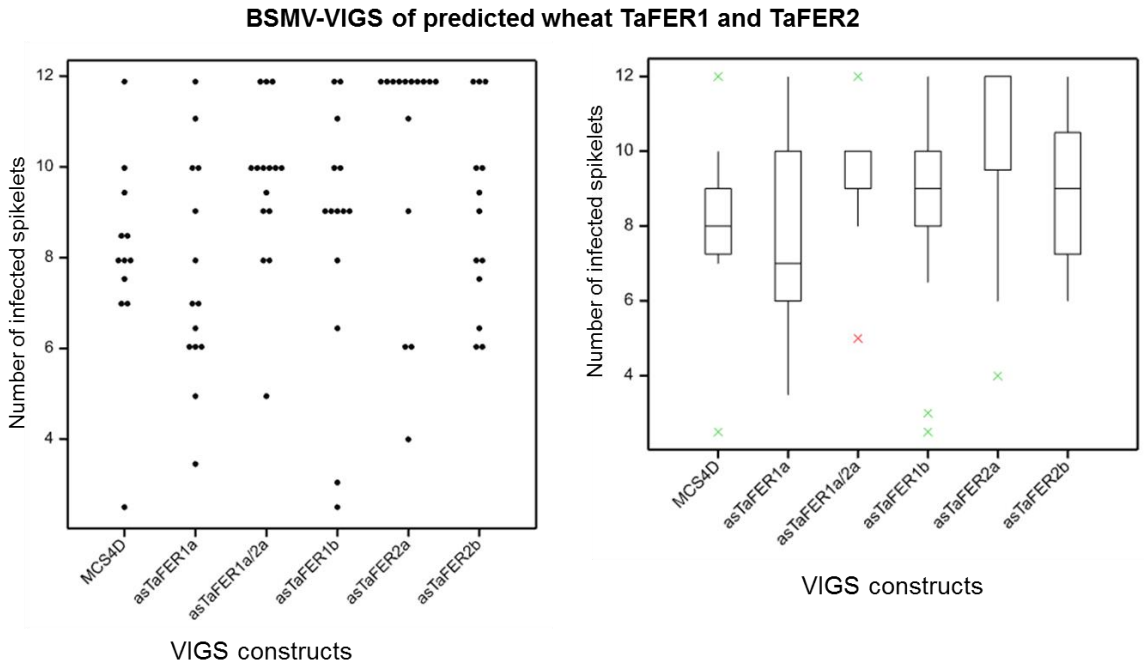

Figure 6.14 Dot-plot (left) and box-lot (right) representing number of visibly diseased spikelets below the *F. graminearum* inoculation points in *F. graminearum* inoculated wheat ears at 15dpi. The control virus treatments (BSMV:MCS4D) and silencing constructs BSMV:asTaFER1a, BSMV:asTaFER1b, BSMV:asTaFER1a/2a, BSMV:asTaFER2a and BSMV:asTaFER2b were used for this experiment. Data shown were collected at 15 days' post *F. graminearum*-inoculation. Treatments did not present statistically significant differences in number of diseased spikelets, relative to BSMV:MCS4D control ($p < 0.05$ from GLM analysis).

6.4 Discussion

The focus of this chapter was to explore whether RALF proteins may contribute to *F. graminearum* virulence. This was done in two ways, from the point of view of the pathogen and then the point of view of the host.

Based on the initial results, further analyses were also done. Firstly, I tested the effect of FgSSP5 gene deletion on *F. graminearum* virulence. Although *FgSSP5* overexpression using the BSMV-VOX system and *TaFER2* silencing via the BSMV-VIGS system influenced FEB disease formation, pathogenicity tests with two independently generated *FgSSP5* gene deletion mutants were found not to alter the FEB disease phenotype when compared to *F. graminearum* wild-type strain. My initial hypothesis 'Deletion of FgSSP5 in *F. graminearum* would result in a less virulent strain' could not be demonstrated. Nevertheless, the hypothesis this RALF protein could still contribute to *F. graminearum* infection should not be fully excluded. As mentioned in Chapter 1, the drawback of using reverse genetics approach to assess gene function is genetic redundancies (Section 1.9.2). Furthermore, by comparing the results on RALF protein analyses in *F. oxysporum f. sp. lycopersici*, the effect of *f-ralf* gene deletion mutants in fungal virulence appears to be influenced by other components, for example plant growth conditions, plant fitness and methods of disease assessment. Differences in how the pathogenicity tests were carried out in each study seemed to have led to distinct phenotype (Masachis et al., 2016, Thynne et al., 2017).

Due to the contrasting results obtained from the BSMV-VOX and FgSSP5 gene deletion experiments, I then tried to identify putative *FER* genes in wheat. Three genes were selected as putative FER receptor, however only two of them were found to be more highly expressed in wheat spikes. Within the wheat genome, a few other genes that also encode protein containing both malectin-like and protein kinase-like domains were identified, but these showed less than 45% amino acid sequence identity with the well characterised FER from Arabidopsis. In Arabidopsis, there are 16 Feronia closely related receptor-like

kinases proteins that also have the extracellular domain malectin, but are not RALF receptors (Li et al., 2016).

To further explore, the role of FER in *F. graminearum* infection, seeds of the Arabidopsis *fer-4*, the *FER* null mutants (Duan et al., 2010) were obtained and have been bulked up. These plants will be inoculated with *F. graminearum* PH-1 wild type strain and fungal infections on young floral tissue and in developing siliques will be assessed using the Arabidopsis Col-0 background as a control. I hypothesise that *F. graminearum* will be reduced in *fer-4* mutants compared to control plants. Additionally, a third BSMV-VIGS experiment will be carried out to silence TaFER1 and TaFER2 in wheat, and the silencing efficiency with the wheat ears post virus inoculation will be evaluated by q-PCR.

The exploration of the role of RALF proteins during infection of plant pathogenic fungus is very recent (Masachis et al., 2016, Thynne et al., 2017). These authors suggested that RALP genes were acquired through horizontal gene transfer. Although FgSSP5 has been shown not be required for fungal virulence, this result does not mean that its role is not important for virulence. There is the possibility that another *F. graminearum* protein could potentially undertake its role. The fact that silencing of one of the putative Feronia receptors led to less FEB disease in the first experiment could be an indication that this interaction is important for *F. graminearum* infection. Therefore, this interaction and the FER family members needs to be explored in greater detail. Further experiments will be discussed in the general discussion of this thesis (Chapter 7).

Chapter 7 – General Discussion

7.1 Key findings

This thesis has explored the roles of some putative *F. graminearum* small secreted proteins (SSPs) by overexpressing each singly during wheat infection. Barley stripe mosaic virus mediated overexpression was used as the vector to increase individual SSP levels *in planta* both prior to and during the *F. graminearum* infection process. The design of the construct should have favoured apoplastic delivery. Although the BSMV system has been described some years ago (Lee et al., 2012), very few published studies have explored the use of BSMV for protein overexpression. To select the candidate gene set, genome sequencing of eight *F. graminearum* strains and comparative analyses were carried out. Prediction of the core secretome was done followed by the detailed analysis of two early time course *in planta F. graminearum*-wheat ear transcriptome datasets. Twelve *F. graminearum* SSP encoding-genes were selected for initial characterisation in replicated BSMV-VOX experiments and four SSP sequences were taken into detailed characterisation.

Amongst the set of twelve *F. graminearum* SSP tested, *FgSSP8*, which encodes a predicted ribonuclease protein, induced strong symptoms of necrosis in *N. benthamiana* leaves when infiltrated via the BSMV:FgSSP8 construct and therefore could not be evaluated in the wheat ear system. Three other genes tested (*FgSSP7, FgSSP6 and FgSSP5*) enhance FEB disease formation in the majority of the replicated experiments when overexpressed in wheat ears prior to infecting with *F. graminearum.* The remaining eight FgSSP constructs were either not completed (n=1), made but not tested (n=4) or resulted in no change in FEB disease symptoms in the BSMV-VOX experiments (n=3).

FgSSP6 and FgSSP7 belong to the cerato-platanin protein (CPP) super family. In several other plant pathogenic fungi, CPPs have been implicated in a number of virulence and / or plant protection mechanisms, including induction of host plant cell death or expansin-like activity. The *F. graminearum* genome contains only two predicted cerato-platanins protein-encoding genes, namely FgSSP6, and FgSSP7. The enhanced FEB disease formation based on the BSMV-VOX results were encouraging but needed to be supported by other evidences. Therefore, to verify the contribution of FgSSP7 during plant infection and fungal growth, gene deletion mutants were produced but no reduction in symptom severity was observed compared to the wild-type strain on both Arabidopsis and wheat floral tissue. Due to technical difficulties and a lack of time, the SSP6 construct and the double deletions constructs are still under development. SSP6 and SSP7 were produced in *E. coli* and the purified proteins injected into *Nicotiana benthamiana* leaves were able to induce necrosis over a range of concentrations. *F. graminearum* cerato-platanins were also found to be able to bind different plant and fungal cell walls components, including chitin resin, chitin from shrimp shells, chitosan, xylan and cellulose, indicating a broad range of binding activities than reported for other for cerato-platanins (Pazzagli et al., 2014). Specific antibodies raised against either SSP6 or SSP7 indicated that FgSSP7 could be detected in leaf extracts and apoplastic fluid recovered from *N. benthamiana* leaves infiltrated with BSMV:FgSSP7, but not in wheat ears. FgSSP6 could not be detected using specific antibodies except when produced by *E. coli* or in fungal cultures. The lack of *in planta* detection could be due either to the lower sensitivity of α-FgSSP6, or because the BSMV expression system only permits low amount of FgSSP6 protein production that could not be detected by western blotting. Based on the VOX tests and the various biochemical tests,

these results appear to indicate that pre-elevated low levels of cerato-platanins (FgSSP6 and FgSSP7) in the apoplast and /or surrounding the hyphae could prevent/ reduce the initial activation of plant defences by binding know PAMPs (i.e. chitin) or DAMPs (i.e. plant cell wall fragments) whilst later on, when augmented by Fusarium produced SSPs produced by the increasing fungal biomass could induce plant defence response culminating in cell death to benefit the necrotrophic phase of *F. graminearum* colonisation. It is also formally possible that because both SSP6 and SSP7 appear to have a broader substrate binding ability that previous characterised CCPs, that over-expression of FgCCPs during the early infection phase may have increased adhesion of the Fusarium hyphae to the plant cell walls and this would have somehow assisted fungal colonisation. The *F. graminearum* infection process is now known to be biphasic in wheat floral tissue, wheat coleoptile tissue and maize stem base tissue (Brown et al., 2017, Zhang et al., 2012).

FgSSP5 encodes a protein that possesses the pfam domain RALF (Rapid alkalinisation factor; PF05498.6). RALF domain-containing proteins are predominately found in plants and play a role in plant development regulating tissue expansion and/or negatively regulating pollen tube elongation. BLAST analyses identified RALF domain containing proteins in a restricted range of different pathogenic species. In contrast to the increased disease levels arising in the BSMV-VOX *F. graminearum*-wheat inoculation experiments, the FgSSP5 gene deletion *F. graminearum* mutants showed no reduction in symptoms severity compared to the wild type strain on both Arabidopsis and wheat floral tissues. However, silencing of the putative plant RALF receptor Feronia on wheat ears using BSMV-VIGS led to reduced FEB formation. Therefore, the effector FgSSP5 may manipulate a key plant process by alkalinising the plant

environment during infection and may use the same plant receptor pathway which is usually required for endogenous signalling required for plant development.

7.2 Insights from sequencing multiple *F. graminearum* genomes

In chapter 3, eight *F. graminearum* strains originating from Brazil underwent full genome sequencing and the resulting assembled and annotated genomes were compared to the genome of the reference North American strain PH-1. The main aim of this chapter was to predict the 'core' secretome, i.e. to identify genes that encode secreted proteins present in the genome of all isolates analysed. Firstly, I tested whether all the strains were pathogenic and could cause typical FEB symptoms. Some strains were able to infect wheat ears cv. Bobwhite to levels similar to PH-1. Whereas but other strains were moderately or weakly virulent in this cultivar. As the strains varied in the severity and extent of symptom development, a detailed analysis would be interesting to identify different polymorphism between the weakly virulent and highly virulent strains genome to indicate genes that could be related to virulence. However, for a robust genome wide association generics study at least fifty fully sequenced *F. graminearum* genomes and the associated phenotyping data sets would need to be available (Dr. Gancho Slavov, Rothamsted, personal communication).

Whole genomic sequencing comparisons among all eight Brazilian strains and the reference strain PH-1 revealed that over 96% of the genes are present in all genomes. Ma et al. (2013) suggested that *Fusarium* genome is compartmentalised into core and adaptive regions. This concept is clearer in the genomes of *F. solani* and *F. oxysporum* that contain variable numbers of supernumerary chromosomes not essential for fungal survival and can undergo transfer between pathogenic and non-pathogenic strains (Ma et al., 2010).

However, this does not seem to be the case for *F. graminearum*, as the evidences from the sequenced strains suggest that there is a high conservation in the genome content. In *F. oxysporum* genome, these supernumerary chromosomes are highly enriched in transposable elements. Distinctively, the *F. graminearum* genome contains very low number of transposable elements and no evidence of supernumerary chromosomes that could be involved in pathogenicity (Cuomo et al., 2007, King et al., 2017b). Some studies demonstrated that genes unique to each Fusarium species or highly polymorphic within the same species are mainly found near the end of the chromosomes (Rep & Kistler, 2010). Whereas, *F. graminearum*, contains both sub-telomeric as well as interstitial chromosomal regions with high diversity and recombination frequencies. This can be observed in figure 3.6 (circus plot) in chapter 3. Some studies suggest that this high polymorphism in the interstitial chromosomal regions constitute the location of ancestral telomeric fusion of smaller chromosomes (Cuomo et al., 2007). A comprehensive taxonomic/ phylogenetic/genome analysis study has revealed that the more ancient Fusarium species have a higher chromosome number whereas the most recently evolving species, like *F. graminearum and F. pseudograminearum*, have the lowest number of chromosomes, at four and six, respectively (O'Donnell et al., 2013).

The interest to predict and define the fungal secretome stems mainly from the fact that secreted proteins have previously been shown to have a role in suppressing plant defence response and in shielding the fungus from the host. In addition, in the literature mostly effectors described to date for phytopathogenic fungi, oomycetes and bacteria are small secreted proteins (De Wit, 2016, Lo Presti et al., 2015). In figure 3.6 (Chapter 3), the circus plot for eight *F. graminearum* isolates reveals the distribution of the genes coding for the

secretome to be located throughout all four chromosomes in *F. graminearum.* But most of the genes encode for secreted proteins are concentrated in the most highly polymorphic regions. Although the number of strains in this study does not represent the whole *F. graminearum* population, with this limited comparison it was still possible to gain an indication of which gene and genomic regions are conserved or are more variable in the *F. graminearum* genome and secretome.

The predicted total secretome for the two reference strains PH-1 and CML3066 represents ~870 genes in each of their respective genome. Within this, a total of 800 genes corresponds to the 'core' secretome. Therefore, only 0.4% of the total genome predicted to code for the secretome of each strain is not shared between the sequenced strains. Polymorphisms in the same gene between isolates were not considered further, because of the lack of a formally described gene-for-gene, cultivar specific interaction for any *F. graminearum* isolate and wheat genotype combination (Talas et al., 2016). More detailed SNP analysis could be done to link the phenotype and genotype, but a stated above typically a detailed comparison of at least 50 isolates would be required for an informative genome wide association genetic study (Dr. Gancho Slavov, Rothamsted, personal communication). However, the 'core' secretome of these *F. graminearum* strains could be explored further, as for example, by the deletion of gene families or predicted clusters shared among all strains and/or via more detailed analysis of the available gene expression datasets.

7.2.1 Pangenome analyses as a novel analytical approach and what else is now possible via sequencing?

The development and rapid expansion in the use of Next-Generation Sequencing (NGS) technologies, both short and long reads, has created an

increase in the volume of high-throughput data for a huge array of organisms (Goodwin et al., 2016). A problem faced at this point in this study, as data from eight different *F. graminearum* strains became available, is that it is becoming more and more computationally and personally exhaustive to compare and locate similar sequences, on these genomes, by straightforward approaches (Marx, 2013, Thorisson et al., 2009). By comparing different genomes from the same species, the concept that individuals within a species all have the same genome cannot be applied anymore. Many studies are now focus in capture the entire genomic sequence present within the species, known as the species pangenome. Pangenome genes can be divided into two groups: there are variable (known also as dispensable or accessory) genes, that are present in some, but not all individuals and secondly the core genes, which are present in all individuals (Li et al., 2014, Segerman, 2012, Vernikos et al., 2015) (Figure 7.1). This concept was first introduced in 2005, when the production of the first pangenome was described for a bacterial species *Streptococcus agalactiae.* Since then, the concept of the pangenome has become increasingly popular with numerous examples available for bacteria (Tettelin et al., 2005, Tettelin et al., 2008) and more recently for some plant species (Tettelin et al., 2005, Li et al., 2014, Golicz et al., 2016b).

Pangenome analysis of fungal species has not been widely explored yet, and so far, it has been described for yeasts (Dunn et al., 2012) and to a less extent for the *F. graminearum* species complex, including strains of *F. graminearum*, *F. meridionale* and *F. asiaticum* (Walkowiak et al., 2016). The later study included two strains of wheat infecting *F. meridionale* from Nepal, two strains of *F. asiaticum* from Nepal and Japan and six strains of *F. graminearum* from North America and Australia. Additional analyses of individual species with

more isolates from other regions would be required to determine if there is gene expansion or loss in populations of this species. In this thesis, the genomes of eight *F. graminearum* strains originating from Brazil were sequenced, and then the focus was to determine the 'core' secretome. The genome and secretome comparison of these strains identified many genes present in only one or some of the strains, i.e. the variable part of the pangenome. Furthermore, another eight strains of *F. graminearum* collected from a different region in Brazil, which were not included in this thesis, have being sequenced and analysed (Robert King, Rothamsted, unpublished) Therefore, pangenome analysis of these 16 *F. graminearum* strains with the sequences publicly available from other strains, from Canada, USA and Australia (Table 1.4) will in the future provide a better understanding about variations within the species. Some urgent questions can be answered if the data available from *F. graminearum* sequences is used to produce the species pangenome. These include: How many genes are common to all individuals? How many additional genes are present within the species that are only found in one or more strains? How any additional genes from a new recovered field isolate contributes to the list of added new genes to the species pangenome derived from sequencing historic isolates?

Based on the pangenome concept, an additional approach to the 'core' secretome could be to predict the pansecretome. This will include all genes encoding secreted proteins present in all available genomes of *F. graminearum*. Preliminary data revealed that over 900 genes comprise the pansecretome (Dr. Robert King, personal communication). Compared with the 'core' secretome prediction in this thesis, there would be at least over 150 genes within the secretome that are present in only one or some *F. graminearum* strains. Further analysis on how these genes are distributed based on virulence on multiple hosts,

geographic distribution, DON production and sporulation would increase the understanding of the biology underlying different aspects of the full *F. graminearum* lifecycle

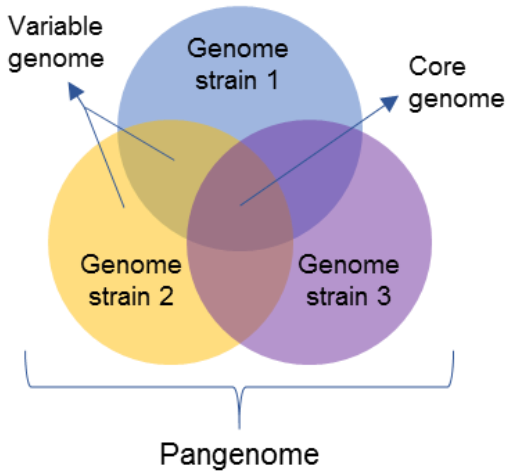

Figure 7.1 Schematic description of the pangenome. The variable genome is present only in one or some genomes and the core genome is present in all samples. Adapted from Golicz et al. (2016a).

7.3 Obtaining leads from transcriptomics approaches. A good or bad approach and how to improve the strategies going forward.

F. graminearum is a hemibiotrophic fungal. During the biotrophic phase of infection, the plant cells are still alive and plant defence responses are triggered to counteract fungal invasion. The fungus, on the other hand, is somehow able to use these alive plant cells as a source of nutrients to continue hyphal grown at about 3mm per day. At this stage, the fungal proteins produced should be able to prevent fungal recognition by the plant and/or to suppress plant defence responses. Later, during the necrotrophic phase, proteins that induce cell death and enzymes responsible to degrade the plant cell wall are likely to be produced and thereby release additional cellular nutrients to the fungal hyphae. Based on this model proposed initial by Brown et al. (2010), transcriptome

profiling has reinforced and extended the knowledge about gene functions predicted *in silico* and provided a better understanding of the potential mechanisms involved in pathogen infection and host defence. This knowledge can be utilised to develop FEB-resistant cereals. For these reason, transcriptomes of the cereal–*F. graminearum* interactions have been extensively studied during the last decade under a variety of conditions.

For this thesis, I used transcriptome data of *F. graminearum* genes expressed during early stage of wheat infection (Brown, 2011) to select the genes to be overexpressed using the BSMV-VOX system (Lee et al., 2012). Although I selected genes that were predominantly expressed during the symptomless infection phase, genes expressed particularly during the symptomatic phase could also have essential roles during *F. graminearum* infection. While the transcriptome data used for this thesis was based on the genes expressed during the symptomless phase of infection at 5-days after *F. graminearum* inoculation on wheat, recently, both symptomless and symptomatic infections were explored at the 7th day post infection time point by a genome-wide transcriptomic investigation using the species-specific Affymetrix array (Brown et al., 2017). This study also compare *F. graminearum* transcriptome under various *in vitro* conditions (nutrient-rich and nutrient-poor growth), published previously by Guldener et al. (2006), *F. graminearum* transcriptome along the continuum of wheat head infection (Brown et al., 2017). Among the 12 genes selected in chapter 3 (Table 3.9), only three of them were more highly expressed *in vitro* than *in planta*. These include FgSSP6, FgSSP7 and FgSSP12. The expression pattern of *FgSSP6* and *FgSSP7* has been shown in chapter 5 (Figure 5.1), and as discussed there, although these genes are expressed *in vitro*, they are also expressed *in planta* and upregulated in the onset and symptomatic phase of

infection. *FgSSP12* transcripts accumulate to a far higher level *in vitro* than *in planta*, suggesting that this gene may play a more important role during fungal growth. This gene encodes a protein that shows 58% similarity to a novel hypersensitive response-inducing protein elicitor (MoHrip2) secreted by *Magnaporthe oryzae* (Chen et al., 2014). This protein has not been tested using BSMV-VOX, but if FgSSP12 also has the same HR inducing function, the lower expression *in planta* could be to avoid the triggering of strong plant defence responses, which would compromise the biotrophic phase of *F. graminearum* infection. FgSSP1, 2, 3, 4, 8, 9, 10 and 11 are all upregulated *in planta* and FgSSP1, 8 and 10 were found to be upregulated specifically during symptomless phase (Brown et al., 2017). These proteins seem to have a main role during the establishment of infection, during the biotrophic phase. *FgSSP1*, in particular, is more highly expressed than *tri5* and exhibits only a low level of expression *in vitro*. The expression of this gene at 5 and 7 days post *F. graminearum* infection follows similar pattern and this high expression throughout the early stages of infection is intriguing and could suggest the protein somehow suppresses plant defence responses to favour the biotrophic phase of *F. graminearum* infection. This gene was tested in BSMV-VOX vector, but no virus symptoms were observed in wheat ears. The absence of virus symptoms could suggest a possible role for this protein in manipulating virus suppression as well. Further studies would be required to test these hypotheses. Although it is not possible to compare quantitatively gene expression from Affymetrix and RNA-seq analysis, it is possible to deduce if a gene is highly, moderately or lowly expressed by comparing with other genes in the same set. Based on this approach, interestingly, FgSSP3 was revealed to be very low expressed at 7dpi (Affymetrix data) (Brown et al., 2017, Guldener et al., 2006), which is different to the RNA-

seq data from 5dpi (Table 3.9). This could be because this gene is down regulated at 7dpi, or due a low sensitivity of the probe in the Affymetrix analysis. It was not possible to check the expression of FgSSP5 at 7dpi, because the array cover genes annotated only up to FGRRES_14100, and the FgSSP5 annotated gene is FGRRES_15123 (Guldener et al., 2006).

The *F. graminearum* interaction with various cereal species is one of the most widely studied via transcriptomic analyses of any plant–microbe interaction (Kazan & Gardiner, 2017). With the large collection of transcriptomic data available, over 20 experiments using a single platform, Guo et al. (2016) reconstructed the global *F. graminearum* gene regulatory network (GRN) using Bayesian network inference. The network model connects the expression levels of key regulators and their potential targets genes and was divided into eight distinct functional modules based on these key regulators (Kazan & Gardiner, 2017). They are cell cycle and development; detoxification and secondary metabolism; cytochrome P450-mediated detoxification processes; metabolism and RNA processing; protein synthesis; transcription and cell transport; stress response and cell differentiation; and carbohydrate metabolism and detoxification. The key regulators are predicted to modulate the expression of others *F. graminearum* genes within the same module. The modules predicted to be substantially correlated with disease phenotypes were modules B (57% of the regulators), H (70% of regulators) and C (100% of regulators) (Guo et al., 2016). Among the 12 selected genes to be tested using BSMV-VOX (Table 3.9), 11 of them are in this network (with exception of FgSSP5) and eight are in either module, B, C or H. A comparative analysis could be done to determine which modules the genes predicted to code for the core secretome are localised and if this distribution correlates with and known differences in disease phenotypes.

According to these *in silico* analysis, although all modules contain predicted effector genes, B and C have the highest ratio of predicted effector genes per module (Guo et al., 2016).

In summary, transcriptomic analyses of *F. graminearum* can be very useful to identify genes expressed *in planta* during FEB and increase the understanding of infection-related fungal processes, by exploring the expression profile either at a given time point or at a different spatial position in the infection. Therefore, by combining the transcriptome dataset available for *F. graminearum* with other approaches, valuable information can be gathered. For example, the key regulators identified (i.e. the hubs) could be potential targets for FEB control (Kazan & Gardiner, 2017).

7. 4 Use of "effectoromics" to study plant-pathogen interactions

To achieve successful infection and colonisation in the host, bacteria, fungi, oomycetes and nematodes are now known to secrete proteins or other molecules into different cellular compartments of the plant, collectively known as effectors, to facilitate infection (De Wit, 2016, Franceschetti et al., 2017). The interest in identifying effector proteins and their function in eukaryotic filamentous plant pathogens has increased massively in the last few years. Effectors are defined as small secreted proteins (≤300 amino acids), usually cysteine rich, that modulate the host cell to facilitate infection.

Performing *in silico* prediction of putative effectors is a challenge, because in most species these proteins lack unified sequence features such as conserved N-terminal sequence motifs or specific domains. To select putative effectors for this thesis, I used the predicted *F. graminearum* core secretome to select small size and cysteine-rich proteins. To select the best effectors candidates, I used *in silico* prediction together with transcriptome analysis, which provided more robustness on

the prediction. Recently, a concept of effectoromics has been introduced to define a set of proteins predicted to exhibit an effector function (Vleeshouwers et al., 2011, Ellis et al., 2009).

Effectoromes are commonly predicted from fungal secretomes using evidence such as small size, a high number of cysteines, genomic location and/or the presence of diversifying selection (Sperschneider et al., 2016). Although these criteria seem to be helpful to narrow down effectors candidates, some caveats need to be taken into consideration. Some fungal effector experimentally verified lack cysteines in their protein sequence. The small size and cysteine content criteria are often manually set by researchers. The selection of effectors based on genomic location might capture only a subset of the effector repertoire (Rafiqi et al., 2012). More recently, a tool described as EffectorP has been introduced to predict fungal effectors from secretome (Sperschneider et al., 2016). EffectorP eliminates the reliance on manually thresholds such as small size and cysteine content through a machine learning method. However, the authors emphasise that EffectorP is a powerful tool when combined with *in planta* expression data to predict effector candidates (Sperschneider et al., 2016).

Although I have included the putative effectors predicted by EffectorP in chapter 3, when I completed the selection of small proteins to be tested using the BSMV-VOX system, this tool was not available. From twelve genes selected, only one has been predicted as an effector by EffectorP prediction (FGRRES_02181 – FgSSP10). Therefore, although effectoromics could be helpful to narrow down possible effectors candidates, the whole secretome and even the whole genome should be taken in consideration. This is because some effectors do not possess the main features considered to be required for a possible candidate effector function. One example is the chorismate mutase Cmu1 in *Ustilago maydis*, which is an enzyme

from the primary metabolism (Djamei et al., 2011). *Magnaporthe oryzae* presents a set of structurally similar but sequence divergent effectors termed MAX effectors (*Magnaporthe* AVRs and ToxB like) (de Guillen et al., 2015). These effector family are suggested to be important during the biotrophic infection of *M. oryzae*. Another *M. oryzae* effector was also shown to adopt the MAX fold (Maqbool et al., 2015), but this was not predicted by the *in silico* analysis. These exceptions in the literature and the results obtained in this PhD thesis indicate that the study of effector often require an integration of different approaches, that combine next generation of machine-learning tools, gene expression data, structural biology, genomic organisation and promoter analysis, in order to increase the reliability of *in silico* prediction of putative effectors (Varden et al., 2017).

7.5 Is BSMV-VOX a suitable system to study the function of fungal secreted proteins *in planta*?

Seven *F. graminearum* genes were tested using the BSMV-VOX system. From this set of genes tested, four showed promising results to be studied further (FgSSP5, FgSSP6, FgSSP7 and FgSSP8). Although, a different phenotype was observed either in *N. benthamiana* leaves (FgSSP8) or wheat (FgSSP5, FgSPP6 and FgSSP7), these results on their own are not enough to determine the precise role(s) of each protein during FEB disease formation on wheat. One of the reasons the role(s) of these proteins cannot be determined is because their potential function was revealed through overexpression. A disease enhancement was observed, but how and why more rapid development of disease symptoms occurred is currently not known. Secondly, the disease enhancement observed due to protein overexpression was a subtle phenotype and at least three independent experiments each with a large number of plants/treatment were

necessary to confirm this enhancement. Furthermore, in BSMV-VOX, virus symptoms are usually observed in the ears and it is not known if BSMV activates the same plant defence signalling pathway activated by Fusarium hyphae.

A recent study carried out a RNA-seq analyses of *Brachypodium distachyon* infected with two BSMV strains. The selected Brachypodium line was resistant to the BSMV wild-type strain, but susceptible to a BSMV double mutant strain. The results showed that in the compatible interaction, where Brachypodium was infected with the double mutant strain, some components of salicylic acid (SA) signalling was activated, and several genes in the jasmonate and ethylene responses were down-regulated (Wang et al., 2017). It is already known that SA contributes to the response of wheat spikelets and Arabidopsis floral tissues to *F. graminearum* infection (Brewer & Hammond-Kosack, 2015) Genes coding for components of SA signalling were upregulated in fungus-inoculated spikelets (Ding et al., 2011). Although the RNA-seq study of BSMV infection was carried out in Brachypodium, this species is used as a model for cereal-pathogen interactions (Fitzgerald et al., 2015), and the results could suggest that the BSMV infection of wheat could by itself trigger some defence response that alter the outcome of *F. graminearum* infection. For this reason, the BSMV carrying a multiple cloning site (MCS 4D) insert is considered the best negative control in a VOX experiment. Using this virus control, the effect from virus symptoms can be subtracted from the *F. graminearum* VOX infection outcome.

Although BSMV-VOX system comes with some limitations, it is still a valuable tool for screening *F. graminearum* proteins that could play a role during infection *in planta*. For example, to have produced and fully evaluated transgenic wheat plants over-expression each FgSSP would have taken considerably more,

space, and money. In this thesis, the assessment of protein overexpression was done by assessing FEB disease on wheat plants inoculated with different BSMV constructs. This is one just one possible way to explore the use of BSMV-VOX to study plant-pathogen interaction. Currently, another PhD project in the wheat pathogenomics team is focusing in deciphering the defence mechanism triggered by *F. graminearum* small secreted proteins expressed in *N. benthamiana* through BSMV-VOX. The results coming from this study will indicate which *F. graminearum* proteins can lead to up or down regulation of plant defence-related genes and /or changes in the associated titres of the BSMV coat protein detected immunologically (Catherine Walker, unpublished). Another approach is to over-express individual FgSSPs into Arabidopsis plants and assess floral susceptibility, and then take forward the most promising candidate SSP into a BSMV -VOX experiment.

As stated previously, another limitation of BSMV-VOX is the size limit of the inserted sequence which restricts expression to proteins up to ~ 150 amino acids in length. This is to maintain the stability of the construct and to ensure correct viral packaging required for systemic movement. To circumvent this issue, another virus vector was designed to mediate protein overexpression of larger inserted sequences. A Foxtail mosaic virus (FoMV) vector was created and it is able to infect both wheat and maize and overexpress proteins up to 600 amino acids in length (Bouton et al., 2017, submitted).

7.6 Further work

7.6.1 What is the role of a putative ribonuclease during *F. graminearum* infection

One of the genes tested with BSMV-VOX was FgSSP8, which encodes a putative ribonuclease protein (Chapter 4), more specifically a predicted guanine-specific ribonuclease N1/T1/U2 (IPR000026). This specific ribonuclease seems to be exclusive to fungi and bacteria (Lacadena et al., 2007). RNase T1 is the best-known representative of a large family of ribonucleolytic proteins secreted by fungi, mostly *Aspergillus* and *Penicillium* species, although this gene sequence is present in many other Ascomycete fungi species.

FgSSP8 encodes a ribonuclease protein of 132 amino acids, with residues 1-19 corresponding to a secretion signal peptide (SP) predicted using SignalP and TargetP. The predicted guanine-specific ribonuclease N1/T1/U2 domain represents most of the mature protein sequence and is characterised by a histidine-glutamic acid-histidine (HEH) catalytic triad at amino acid positions 66, 84 and 117, respectively. Blastp analysis of FgSSP8 protein sequence did not identify any paralogous protein in *F. graminearum*, but showed that homologous of FgSSP8 are present in many *Fusarium* species as well as other Ascomycetes. The mature FgSSP8 contains four cysteines residues. Some species contain a 2-cysteine form of secreted ribonuclease, such as *Pseudocercospora musae* and *Zymoseptoria tritici* (Kettles et al., 2017). HHowever many plant pathogens including other Fusarium species encode a secreted ribonuclease containing four cysteines. How the cysteine content may alter the protein folding is not known.

Analysis of expression of FgSSSP8 in PLEXdb (http://www.plexdb.org) from different experiments and conditions revealed that this gene is upregulated *in planta*. Overall, FgSSP8 is expressed either in barley and wheat infected with *F. graminearum* and is down regulated during *in vitro* conditions (Dash et al.,

2012). Data from this database reinforce the hypothesis that this gene could be important during *F. graminearum* infection.

During BSMV-VOX experiments, the BSMV:FgSSP8-carrying *Agrobacterium* was infiltrated in *N. benthamiana* leaves and within 4 days, necrotic spots were observed in infiltrated leaves. Systemic leaves did not show either virus symptoms or necrosis. Most likely during *N. benthaminana* infection, expression of FgSSP8 degraded the BSMV genome, which is a RNA virus. Therefore, no virus symptoms could be observed in *N. benthamiana* leaves and the wheat inoculation experiment was unsuccessful.

In plant pathogen interactions, the role of ribonuclease-like proteins has been explored in several *formae speciales* of *Blumeria graminis*. In *B. graminis* f.sp. *hordei*, host induced gene silencing of two ribonuclease-like effectors led to a decrease of pathogen development (Pliego et al., 2013). One of these effectors, BEC1054, is suggested to play a central role in fungal virulence by targeting several barley proteins that are key players of defence and response to pathogens (Pennington et al., 2016). In *B. graminis* f.sp. *tritici*, ribonuclease-like protein (SvrPm3a1/f1) is involved in suppressing ETI mediated by AvrPm3a2/f2-Pm3a/f interaction (Bourras et al., 2015, Parlange et al., 2015). SvrPm3a1/f1 showed structural similarities to ribonuclease F1 from the rice pathogen fungus *Fusarium fujikuroi*, of unknown. AvrPm2 is another ribonuclease-like protein, conserved among cereals mildews and recognised by the resistance protein Pm2, which is a NLR protein (nucleotide-binding domain and leucine-rich repeat containing). Structure prediction tools identified that AvrPm2 is more structurally similar to ribonuclease T1 from *Aspergillus phoenicis* (Praz et al., 2017). Although these proteins have been characterised in *B. graminis* as effectors in several hosts, the roles of ribonuclease-like proteins during infection in this species have

just started to be elucidated (Pennington et al., 2016). It is known that they are structurally similar to ribonucleases, but present a non-functional ribonuclease activity that still have a role in host immunity manipulation through the binding of host RNA molecules (Pliego et al., 2013).

More recently, Kettles et al. (2017) characterised a secreted ribonuclease (Zt6) in the fungus *Zymoseptoria tritici*. The authors demonstrated that Zt6 possesses potent cytotoxic activity (ribotoxin-like) against plants as well as against several prokaryotic and eukaryotic microbes, but found to be non-toxic to *Z. tritici* itself. The production of ribonucleases therefore potentially are a mechanism of self-protection, but the details remain to be revealed. Zt6 is suggested to play a dual role during infection by contributing to the execution of plant cell death to benefit the necrotrophic phase, and secondly, acting in antimicrobial competition and niche protection (Kettles et al., 2017).

Zt6 has the same predicted domain as FgSSP8 (pfam 00545) and both appear to be structurally similar. The two sequences share 64% identity in the mature peptide, but Zt6 contains two cysteines residues which are not predicted to form a disulphide bridge (Kettles et al., 2017), while FgSSP8 contains four cysteines residues and two of these are predicted to form one disulphide bridge (DiANNA) (Ferre & Clote, 2005).

Amongst the structural predictions suggest for FgSSP8, several display some similarity to the RNAse T1 from *A. oryzae* (Phyre2), which is the best characterised representative of a large family of ribonucleolytic proteins secreted by fungi. Ribotoxins stand out among RNAses because of their cytotoxic characteristics. Although FgSSP8 induced cell death in *N. benthamiana,* more experiments are needed to identity if this protein can be classified as a ribotoxin. In *Z. tritici*, *Zt6* was expressed in *N. benthamiana* leaves and induced strong cell

death, however the mode of action of this protein appears to be different from ribotoxins. Constructing and testing a *F. graminearum* Δfgssp8 mutants would also reveal if this protein is important for fungal virulence. Unfortunately, due the time frame of this PhD, the role of this protein could not be explored further, but the findings from FgSSP8 overexpression in *N. benthamiana* provided leads for a follow up project that could focus entirely on defining the role(s) of FgSSP8 in *F. graminearum* during infection of various plant tissues in wheat and other hosts.

7.6.2 The effect of cerato-platanins on FEB infection and disease development

In chapter 4, overexpression of the *F. graminearum* cerato-platanins (CPs) FgSSP6 and FgSSP7 from BSMV enhanced development of FEB disease in wheat ears subsequently inoculated with *F. graminearum* spores. In chapter 5, the possible roles of FgSSP6 and FgSSP7 during *F. graminearum* infection on wheat ears were further explored. Although some extra experiments are needed, the results from both chapters suggest that *F. graminearum* cerato-platanins could have a dual role in the wheat floral interaction. Initially cerato-platanins could initially aid adhesion of fungal hyphal to plant cell walls (expansin activity), as well as bind chitin fragments released through the action of plant chitinases and thereby minimise the activation of PAMP triggered plant defences (i.e. PTI). Collectively these two early roles may favour *F. graminearum* infection during the symptomless biotrophic phase. Later on, expression data shows accumulation of cerato-platanin in addition to the SSP6 or SSP7 protein delivered via BSMV expression. These two proteins could induce cell death to benefit the necrotrophic phase of *Fusarium graminearum* by increasing overall nutrient availability.

One of the questions that has arisen relates to the results from the various *in vitro* assays. This is whether the protein expressed in *E. coli*, which is a prokaryotic expression system would be appropriate for protein-encoding eukaryotic genes. We do not know if FgSSP6 and FgSSP7 produced in the *E. coli* expression system has the same conformation as the native proteins produced in *F. graminearum* cells. Nevertheless, many studies have used transient expression systems to assess the roles of cerato-platanin proteins in other fungal species, including *Pichia pastoris* and *E. coli*. *P. pastoris* is a species of yeast, and as a eukaryote, it is more likely to produce disulphide bonds and glycosylation when expressing heterologously proteins. On the other hand, protein production in *E. coli* is usually faster and with higher yields. In this study, both proteins produced in *E. coli*, were ready soluble and did not have to be resolubilised prior to their use in the various follow up experiments. Recently, Zhang et al. (2017) compared production of BcSpl1, a cerato-platanin protein from *B. cinerea*, in *P. pastoris* and *E. coli*. The study demonstrated that BcSpl1 expressed in both organisms exhibited the same activity (Zhang et al., 2017). Additionally, in the western blots of purified protein, a second band double of the size FgSSP6 or FgSSP7 was sometimes observed, which could be protein dimers (data not shown). In general, CPs have been shown to be fairly stable, with unfolding temperature up to 76ºC and preservation of secondary structure in a wide pH range (3-9) (de Oliveira et al., 2011). This feature would support the fact these proteins are secreted and act mainly in the harsh environment of the plant apoplast.

Many studies have explored the roles of CP in the plant pathogen fungus *Ceratocystis platani* (CpCP) and *B. cinereae* (BcSpl1). In CpCP, a single amino acid mutation has been shown to affect its elicitor and expansins-like activities.

The study reveals that the carboxyl group of D77 is crucial for expansin-like and PAMP activities. The same amino acid residue is found in both FgSSP7 and FgSSP6, reinforcing the hypothesis that both proteins have expansin-like activity and elicit plant defence genes (Luti et al., 2017). The phytotoxic activity of BcSpl1 has been demonstrated to reside in two regions, located on the surface-exposed loops β1-β2 and β2-β3 (Frias et al., 2014). Those two loops are highly conserved in FgSSP6 and FgSSP7. The corresponding regions span the sequences Val^{20} – Leu^{29} and Ile^{52} – Cys^{61} (Figure 5.3). Unfortunately, the current published assay to assess expansin-like activity is not particularly robust or easy to obtain quantitative results. This assay needs to be further improved.

The current hypothesis based on the results presented in this thesis can only be validated when the steps in the elicitation cascade triggered by FgSSP6 and FgSSP7 are elucidated. So far, the cerato-platanin receptor in either the pathogen or the host has not been identified in any pathosystem. The mechanism by which CPs induce plant defence responses is not known. Most recent studies suggest the more probable involvement of a "yet to be found" receptor able to recognise the structural motif created by loops β1-β2 and β2-β3 (Frias et al., 2013).

Screening for the cerato-platanin receptor could be done for example using yeast two-hybrid system, or a forward genetic screen of a full length normalised cDNA expression library in a *N. benthamiana* and dual agroinfiltation assay. Once the receptor is identified, further experiments can be done to explore its role during *F. graminearum* infection. *F. graminearum* is able to infect Arabidopsis, therefore it would be possible to produce Arabidopsis mutants lacking the correspondent gene and assess if there is any influence during fungal infection. If the receptor can also be identified in wheat, BSMV-VIGS experiments

could be carried out to test for a reduction of FEB symptoms. This would facilitate the further exploration of the *in planta* role(s) of FgSSP6 and FgSSP7, during both the early and later stages of the infection process.

Based on the studies so far in different fungal species, it is not possible to answer why so many fungal species secrete cerato-platanin proteins. It is hypothesised that this class of secreted proteins plays at least two roles in fungi: a primary role in growth and development and a secondary role, more puzzling, that explain their interaction with plants (Pazzagli et al., 2014). Although studies on CPs have been explored more in some pathosystems than others, the precise biological function(s) of this class of protein remains to be elucidated.

7.6.3 Deciphering the importance of RALF for *F. graminearum* infection

In chapter 4 of this thesis, BSMV:FgSSP5 showed slightly enhanced FEB disease compared to BSMV:MCS4D. In chapter 6, the focus was to explore whether RALF proteins may contribute to *F. graminearum* virulence. FgSSP5 is a small, cysteine-rich protein that contain a Rapid Alkalinisation Factor (RALF) domain (PF05498.6). A RALF domain-containing peptide was first isolated from tobacco leaves and shown to induce rapid alkalinisation of media with tobacco suspension cultured cells and the activation of an intracellular MAP kinase. Additionally, synthesised polypeptide caused an arrest of root growth and development in Arabidopsis (Pearce et al., 2010). Since then, homologs of RALF peptide have been isolated from several plant species (Murphy & De Smet, 2014). Recent studies have identified a malectin-like receptor-kinase, Feronia (FER), as a receptor for RALF1 from Arabidopsis (AtRALF1) and, homologues of RALF, typically AtRALF1, have also been identified within numerous fungal

phytopathogens, with these potentially acting in plant-pathogen interactions (Thynne et al., 2017). One of this includes FgSSP5 from *F. graminearum*. Therefore, by identifying Feronia homologues in wheat through a bioinformatics analysis, I was also able to explore the role of FgSSP5 during *F. graminearum* infection from the host side. The first BSMV-VIGS experiments reported in chapter 6 indicates that silencing of one of putative Feronia in wheat led to reduced Fusarium infection (Figure 6.13). The second experiment carried out did not exhibit significant difference of TaFER1 silencing constructs with MCS4D virus control because the poor *F. graminearum* infection in the controls. In addition to AtRALF1 produced by *A. thaliana*, Cao and Shi (2012) identified 36 more RALFs in the same species. Although initially FER was considered a receptor of AtRALF1, a recent study demonstrated that FER is also a receptor of AtRALF23 and suggested that FER may bind other additional RALF peptides (Stegmann et al., 2017). Therefore, it is formally possibly that the wheat Feronia protein confers responsiveness to various Fusarium effectors including FgSSP5. Previous studies demonstrated that AtRALF23 is a substrate of an Arabidopsis site-1 protease (AtS1P) (Srivastava et al., 2009). These SIP1 proteases are members of the subtilisin-like proprotein convertase family, which includes proteases that process protein and peptide precursors trafficking through regulated or constitutive branches of the secretory pathway. Homologues of S1P are present in many other organisms. Stegmann et al. (2017) found that AtS1P cleaves the RALF23 propeptide to inhibit plant immunity. Why the plant has this mechanism is not known, but the role could be to regulate very tightly the triggering of defence responses in floral tissue. This inhibition is mediated by FER. FER otherwise facilitates the ligand-induced complex formation between EFR and FLS2 with their co-receptor BAK1 to initiate immune signalling. Another

small peptide AtRALF17, on the other hand, seems to induce ROS production and this mechanism is dependent of FER. Therefore, it is suggested that FER acts as a RALF-regulated scaffold that modulates receptor kinase complex assembly. It is known that loss of At*RALF23* led to increased elf18-triggered ROS production and resistance to *Pseudomonas syringae* pv. *tomato (Pto)* (Stegmann et al., 2017). Conversely, At*RALF23* overexpression inhibited elf18-triggered ROS production and increased susceptibility to *Pto.* RALF from Fusarium species, including FgSSP5, are more closely related to AtRALF23, AtRALF33, AtRALF22 and AtRALF1 (Figure 6.3), therefore these fungal RALF proteins could regulate host immunity. A future experiment to test the hypothesis that FgSSP5 mediates host immunity would be to test if *ralf23* Arabidopsis mutant is more resistant to *F. graminearum* infection. If so, the *ralf23* mutant could be complemented with *FgSSP5* from *F. graminearum* and then tested to determine if the WT phenotype is restored during *F. graminearum* infection. Changes to *Pto* infections could also be explored. Another possibility is to overexpress FgSSP5 in Arabidopsis and test if it would increase susceptibility to *F. graminearum*. This is being done at the moment by another PhD student at Rothamsted and infection tests will be done soon.

The wheat genome contains at least eight putative FER homologues (Figure 6.10), and also contains one S1P homologue. Using the Biomart tool (Ensembl), 35 genes in wheat were predicted to encode a RALF-domain (PF05498) protein. More detailed analysis would be necessary to identify the various homoeologous and any paralogous genes. *F. graminearum* is predicted to contain only FgSSP5 as a RALF orthologous gene, and over 30 genes predicted to encode subtilisin-like proteases. More analysis would be necessary to identify if any of these genes are orthologous of *AtS1P.* If so, two hypotheses

could be considered: first, *F. graminearum* secretes FgSSP5 during infection, which are cleaved by wheat S1P and inhibit plant immunity mediated by wheat FER. This hypothesis is based on the recent studies demonstrating that FER is regulated by RALF scaffold (Stegmann et al., 2017). The question is why the plant would counter its own defence mechanism? Probably because FgSSP5 is hijacking the role of a plant RALF, usually involved in plant development to somehow assist fungal virulence. Second, *F. graminearum* has an orthologous gene to AtS1P which is upregulated during fungal infection and may cleave FgSSP5 before secretion to inhibit plant immunity hijacking the receptor FER in wheat and thereby facilitate the fungal infection process. Interestingly, FgSSP5 has orthologous in other *F. graminearum* strains and species including *F. culmorum*, *F. pseudograminearum* (Figure 6.2 and 6.4), but homologous of this sequence was not identified in the genome of the non-pathogenic species *F. venenatum* genome (Figure 6.4). *F. venenatum* is very closely related to *F. graminearum* (King et al., 2017a, submitted). The *F. graminearum* mutant strains Δ*fgssp5* did not exhibit a reduce virulence phenotype in either wheat or Arabidopsis and although only one gene is predicted to encode a protein containing RALF domain, these prediction tools could miss other genes that encode proteins with similar functions and structure. Therefore, the possibility of genetic redundancy cannot be discounted. It would be interesting to delete the entire gene cluster in *F. graminearum*, or to construct a double gene deletion strain with the best candidates of S1P homologs in *F. graminearum*. A more speculative experiment would be to insert the FgSSP5 sequence into *F. venenatum* and determine if the strain became pathogenic towards wheat. The next VIGS experiment with other predicted wheat FER genes will be done and if conclusive this will give stronger support to explore this mechanism further.

7.7 A working model for *F. graminearum* infection

F. graminearum is considered to be a hemibiotrophic fungal pathogen (Brown et al., 2010). This is because when infecting the wheat host plant, the fungal hyphae starts to advance between live host cells in the apoplastic space. During this stage, no visible disease symptoms is observed. Behind this asymptomatic infection front, disease symptoms are observed and are accompanied by the early senescence of the wheat tissue. The symptomatic phase commences with the death of wheat cells surrounded by fungal hyphae and subsequently extensive intracellular colonisation of these dead plant cells (Brown et al., 2011, Brown et al., 2010). This initial model was defined using a detailed cell biology analysis. Recently, this model has been refined by a genome-wide transcriptomic investigation that has examined the early phases of the *F. graminearum*–wheat head interaction, exploring both symptomless and symptomatic infections (Brown et al., 2017). One aspect of the model that still need to be determined is exactly when and where the invading hyphae feed.

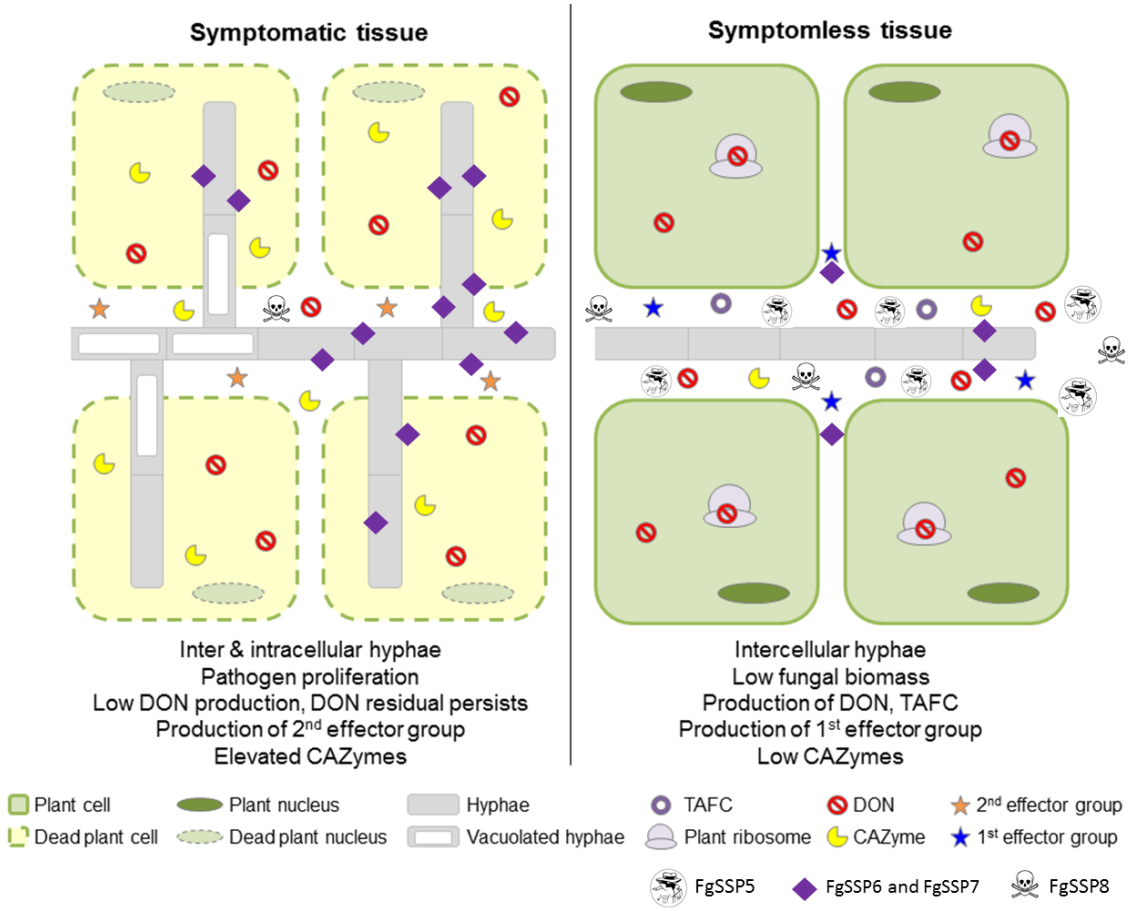

Figure 7.2 A spatial temporal model for *Fusarium graminearum* infection of wheat floral tissue adapted from Brown et al. (2017). This model suggests virulence strategies used in the symptomless and symptomatic wheat tissue during *F. graminearum* infection, based on regulation of previously characterised effectors and effectors described on this thesis (FgSSP5, FgSSP6, FgSSP7 and FgSSP8). CAZyme, carbohydrate-active enzyme; DON, deoxynivalenol; TAFC, triacetyl fusarinine C.

In chapter 3, I used a RNA-seq experiment of *F. graminearum* infecting wheat during the symptomless phase at 5dpi. This had been previously generated by Brown (2011). Although this data is very useful for screening of putative effectors, it could not be published in a journal because only one pooled set of 30 rachis internodes was sequenced. In Brown et al. (2017), the infection phase-specific *F. graminearum* transcriptome was explored at 7 dpi in rachis internode and spikelet tissues in a fully replicated experiment using the species-specific Affymetrix array.

With this new dataset, a refined FEB infection model was proposed. Some proteinaceous virulence factors and host- and non-host-specific, toxic and non-toxic metabolites that were previously known to be important for FEB disease can now be placed into a coordinated spatial temporal expression model, and provide more evidence to support the hypothesis that multiple virulence strategies are used by the *F. graminearum* hyphae during wheat rachis colonisation (Figure 7.2). For example, the sesquiterpenoid DON is known to be required for *F. graminearum* virulence on wheat (Cuzick et al., 2008, Proctor et al., 1995). Affymetrix, RNA-seq and qRT-PCR data show that the *TRI* genes, which encode for biosynthetic enzymes involved in the production of the DON mycotoxin dramatically increase in transcript abundance within the symptomlessly infected wheat tissue. It is suggested that the production of DON by *F. graminearum* during the early stages of infection may inhibit host defences, by preventing protein translation, and thereby promote the establishment of infection throughout the wheat head.

Based on this new proposed spatial temporal FEB infection model now augmented with the data generated in this thesis, a refined virulence strategy could be suggested for some of the secreted protein studied. For example, *FgSSP6* and *FgSSP7* genes (encoding cerato-platanins proteins) are expressed in *F. graminearum* during both symptomless and symptomatic infection in wheat (Figure 7.2) and also during *in vitro* growth. Therefore, a primary role in fungal development, maybe by contributing to hyphae growth, could be suggested. During infection, both genes show lower expression in the spikelet (symptomatic dead tissue) and during symptomless infection (biotrophic phase). Therefore, the low expression in the biotrophic phase could be to dampen further the plant immunity responses, and thereby keep the plant cells alive within the newly

colonised tissues. If both Fusarium proteins are proven to possess expansin-like activity then this should assist hyphal adhesion, nutrition and the invasive process through the apoplast, whilst in close contact with living plant cells. In addition, the ability of FgSSP6 and FgSSP7 to bind different components of plant and fungal cell wall, including cellulose from the plant and chitin (Figure 5.16) could function as an early protection mechanism, from either PTI or DAMP mediated plant immunity. None of the *F. graminearum* genomes sequenced to date are known to contain a homologue of the 3LysM secreted protein that has been shown to be responsible for binding chitin in three other phytopathogenic fungal species, namely *Z. tritici* (Marshall et al., 2011), *M. orzyzae* (Koharudin et al., 2011) and *Cladosporium fulvum* (Bolton et al., 2008). The upregulation of FgSSP6 and FgSSP7 during infection onset and the symptomatic phase could induce cell death to benefit the necrotrophic colonisation by *F. graminearum.* This is also the phase of pathogen proliferation related to their role in fungal development. FgSSP6 and FgSSP7 were shown to cause cell-death in *N. benthamiana*, suggesting that these proteins can induce plant defence responses. When FgSSP6 and FgSSP7 are highly expressed *in planta*, the elicited plant immune responses would include the overexpression of plant cell wall-degrading enzymes, which would produce chitin oligomers. To avoid degradation of chitin, cerato-platanins proteins bind to the fungal cell-wall to protect against plant chitinases. Therefore, plant cell-death would still occur and release cellular nutrients for the fungus, but the fungal hyphae would be protected and growth could continue. When the tissues are completely dead and plant immune responses are low, *FgSSP6* and *FgSSP7* are down regulated again (down regulation in spikelets). FgSSP6 and FgSSP7 would play a major role in the 2nd wave of effectors (Figure 7.2).

FgSSP5 is predict to be a RALF domain-containing protein. The RNA-seq data on *FgSSP5* indicated that this gene is upregulated during symptomless phase of *F. graminearum* infection at 5dai. Gene expression analysis of *FgSSP5* by qRT-PCR also demonstrated that there is an upregulation at 7dai in the symptomless stage (Catherine Walker, Rothamsted, personal communication). Data generated in this thesis indicates FEB disease enhancement when wheat ears were prior inoculated with BSMV:FgSSP5. Additionally, silencing of one of the putative wheat Feronia (AtFER1) genes led to delayed FEB development. Taken together this information with the recent findings in the literature (Stegmann et al., 2017), I suggest that FgSSP5 could aid in suppression of defence genes. This would be achieved by mimicking a plant pathway. This role would be important in the first wave of effectors (Figure 7.2), which are mainly acting at the asymptomatic stage of *F. graminearum* infection in wheat ears.

FgSSP8 is a ribonuclease domain-containing protein. A number of gene expression experiments revealed that FgSSP8 expression is upregulated *in planta* (http://www.plexdb.org). The *Fusarium graminearum* transcriptome analysis during symptomless and symptomatic wheat infection indicated that FgSSP8 was modest expression throughout the infection and it is upregulated in the symptomless phase (Brown et al., 2017). Infiltration of BSMV:FgSSP8 in *N. benthamiana* leaves induced necrosis and impaired virus systemic infection. The same expression pattern and necrosis activity was observed in Zt6, a secreted ribonuclease in *Z. tritici* (Kettles et al., 2017). Therefore, this protein could assist in the establishment of infection during the asymptomatic phase to minimise plant defences. Whether FgSSP5 has antimicrobial activity, as demonstrated for Zt6 (Kettles et al., 2017), has yet to be determined. These two roles may be importance in the first wave of effectors. Later, this protein could contribute to the

necrotrophic phase by inducing cell death in wheat, thereby contributing to the function of the second wave of effectors.

7.8 Experimental difficulties encountered and possible solutions

During the development of this thesis some challenges were encountered. One of them was that when I started, the BSMV-VOX system explorations had been limited and I needed to stablish a robust protocol. Although BSMV-VIGS is more widely used (Baulcombe, 2015, Lee et al., 2012, Yuan et al., 2011), the vector used for both approaches is the same, and therefore some differences had to considered and further optimised. When VIGS is used for testing host gene function in *F. graminearum* – wheat interaction, the aim is to silence a plant gene expressed in wheat ears. Therefore, the silencing needs to happen before the ear is fully formed and emerged. Silencing is coincident with viral spread and is usually greatest 2–3 weeks after inoculation (Burch-Smith et al., 2004). In VOX, the fungal protein is overexpressed in the wheat ear, however the longer virus replication occurs in the plant, the greater is the chance that the inserted gene in the gamma-b genome will be lost or rearranged. For this reason, the window in the VOX experiment between virus infection and *F. graminearum* inoculation needs to be no longer than the time required for the virus to reach the wheat ears, just prior to the optimum point of inoculation, i.e. anthesis. This difference in the time of the initial leaf infection with the transgenic BSMV in each approach is a key factor on the outcome and overall experimental success.

Once the best time of BSMV infection for VOX was determined (see section 2.13), some complications were faced when exploring the phenotypic changes and defence responses induced upon BSMV infection alone. Wheat ears where virus symptoms were strongly induced presented light chlorosis,

probably due to high virus accumulation. These symptoms could be confused with the early stages of *F. graminearum* infection. The spikelet infected with *F. graminearum* usually first presents FEB symptoms in the awns as a dry bleached appearance and accompanied awn bending (see figure 4.2). Therefore, by assessing the status of the awns when score FEB progress would avoid the misleading scoring of virus infected spikelets. Another possibility that could be used in the future is to assess *F. graminearum* biomass and compare between treatments. This could be done by q-PCR using the tri5, actin or tubulin genes. This has previously been done when assessing fungicide efficacy (Zhang et al., 2009). The downside of using this approach is that the material would need to be destroyed and it is not possible to follow the disease progression in a single experimental replicate. One time point would have to be chosen for quantitative biomass evaluation. Alternatively, automated analysis of high resolution digital images could be used as an accurate and non-destructive approach.

A further concern about the use of BSMV-VOX is how to demonstrate the virus is producing a heterologous protein. To detect protein production from the BSMV vector during virus-infection of wheat ears, antibodies were raised against specific regions of FgSSP6 and FgSSP7 to permit detection (see section 5.2.1). Amino acid sequences used for the synthesis of specific antibodies of FgSSP6 and FgSSP7 are shown in figure 5.2. The specificity of the antibodies was tested using western blot analysis against recombinant FgSSP6 and FgSSP7 proteins expressed in *E. coli.* The next step was to use the two antibodies to detect the CP proteins in BSMV:FgSSP6 and BSMV:FgSSP7 infected plant tissues, i.e. *N. benthamiana* leaves, apoplastic fluids and wheat ears. FgSSP7 was detected by western blotting in *N. benthamiana* infected leaves and the apoplastic fluid. However, FgSSP6 was not detectable in the same tissue. Subsequently, I tried

to detect both proteins in wheat ears infected with BSMV:FgSSP6 and BSMV:FgSSP7. Unfortunately, I was not able to detect either proteins in wheat ears tissue. Several alternative approaches were attempted, for example the use of columns to separate large and small proteins, the use of extracts from virus infected leaves and concentrate of these protein extracts. Neither approach was successful. The detection of both proteins produced in E. coli was successful, but I never attempted to mix *E. coli* generated protein with plant extracts to see if detection was still possible. The Affymetrix data revealed that FgSSP6 is also highly expressed in fungal mycelia (Figure 5.1). Therefore, I tried to detect FgSSP6 by western blotting from mycelia protein extract and a 14kDa band, as expected, was visible. This provides strong evidence that the protein could be detected when produced by fungal hyphae. I then tried to check the presence of the *FgSSP6* and *FgSSP7* transcripts in wheat ears infected with BSMV:FgSSP6 and BSMV:FgSSP7 respectively (Figure 5.8). The presence of transcripts gives an indication that protein translation is happening. It is formally possible that during plant infection, the surface exposed sequence used to raise each antibody, became bound to unknown plant protein(s) or was cleaved from the protein by unknown plant protein(s). Either scenario could have occurred prior to or during the extract phase and therefore FgSSP6 and FgSSP7 detection in wheat was not possible.

7.9 Current and future perspectives for FEB management

As discussed in chapter 1, available strategies to control FEB are limited. Although the most adopted strategy globally to control FEB is the application of fungicides, it is almost impossible to achieve complete control. This is mainly due to the inherent resistance of *F. graminearum* and the problems associated with

timing the T3 spray fungicide applications to protect all the emerging wheat ears (Fan et al., 2013). Additionally, DMI fungicides are the only class that has been shown to be more effective to control FEB. Some other classes, although reducing disease are associated with elevated DON production (Ellner, 2005). Besides the reduced grain quality and yield losses, a second but no less important problem is the contamination of the grains by mycotoxins, notably deoxynivalenol (DON) (Xiong et al., 2009). Global contamination of food and feeds with mycotoxins is an important problem, with DON and zearalenone (ZEA) being among the mycotoxins of global concerns (Dweba et al., 2017, Zain et al., 2012).

Genetic control, involving breeding for resistance have been explored since 1990's, but so far, no wheat cultivar has been identified and released with complete resistance or immunity to FEB disease (Dweba et al., 2017). Genetic analyses identified multiple QTLs responsible for wheat cv. Sumai-3 mediated FEB resistance to be located on chromosomes 3BS, 5AS and 6B (Anderson et al., 2001, Cuthbert et al., 2006). The major QTL located on 3BS, *Fhb1* (Cuthbert et al., 2006), provides good level of type II resistance and also resistance to DON (Lemmens et al., 2005). A recent study has identified a pore-forming toxin-like (*PFT*) gene residing in this *fhb1* locus that provides resistance to spread of FEB (Rawat et al., 2016). The resistance conferred by this locus appears complex, because *PFT* does not confer resistance against DON. Moreover, at least two other genes residing in the vicinity of *PFT* have also been reported to be required for FEB resistance (Ma et al., 2017, Steiner et al., 2017, Su et al., 2017). To date more than 50 QTLs for FEB resistance have been described from wheat genotypes other than Sumai-3.

Another consideration during the development of FEB resistant material is the accumulation of mycotoxins, which can occur independently of disease

severity and is expensive for the breeders to evaluate (Siou et al., 2014). Some studies have shown that plants are able to modify the chemical structure of mycotoxins to defend themselves. For example, some wheat lines, selected through plant breeding, can convert DON and ZEA into deoxynivalenol-3-glucoside and zearalenone-14-glucoside, respectively, when infected with FEB species, which are not themselves virulent factors (Berthiller et al., 2013). The extractable conjugated or non-extractable bound mycotoxins forms remain present in the plant tissue but are currently not regulated by legislation. Therefore, these forms are often referred to as masked mycotoxins. However, these masked mycotoxins might be reactivated during mammalian metabolism (Berthiller et al., 2013).

My main aim as a plant pathologist, as well as all plant pathologists I believe, is to find alternatives to control plant diseases. Based on the strategies available today, FEB can not be fully managed. The study of fungal effectors could provide evidences of possible new fungicide targets and/or targets for RNA interference (RNAi).

Some of the genes explored in this thesis were tested for importance in virulence through generation of *F. graminearum* mutants and no differences in fungal virulence were observed. Regardless of this outcome, these genes could be part of important pathway for fungal infection, that are genetically redundant. Dweba et al. (2017) in their review highlight that are a number of underlying factors influencing FEB resistance breeding, which includes the pathogen and its virulence mechanisms. If these pathways can be understood, along with the host resistance mechanisms, effective control of the disease will be easier to be achieved. Deciphering effector function is not limited to find single genes that when deleted reduce virulence. It also includes progress towards understanding

the role and level of contribution of certain protein during infection. Plant pathologists should take note of the quote from the ancient Chinese military treatise “The Art of War” as a motto:

“If you know the enemy and know yourself, you need not fear the result of a hundred battles. If you know yourself but not the enemy, for every victory gained you will also suffer a defeat. If you know neither the enemy nor yourself, you will succumb in every battle.” (Sun Tzu, The Art of War).

Understanding the mechanisms pathogens use to successful infect and colonise plant hosts is as important as understanding the host mechanisms used to fight against plant diseases. The new emerging approaches may allow us to interfere with these mechanisms at a genomic and/or transcriptomic level. One example is the use of RNAi. RNAi is sequence-specific and therefore permits the highly specific targeting of individual fungal species, or specific orders of fungal pathogens (Wang & Jin, 2017). This is preferential, and distinct, to the broad acting chemical antifungal treatments that often promote the evolution of resistance in the targeted, and non-targeted fungal populations, such as those associated with the use of azole fungicides in agriculture. This process is called Host-Induced Gene Silencing (HIGS), a transgene-based plant-mediated method to produce small-interfering RNA (siRNA) that can silence gene transcripts in fungal and/or oomycete pathogens during the infection (see section 1.9.3) (Koch et al., 2013). An alternative non-GM RNAi approach is Spray-Induced Gene Silencing (SIGS), which exploits the RNAi mechanism, through the exogenous application of double-strand RNA (dsRNA) and siRNAs (Koch et al., 2016). SIGS

was initially used as a strategy to simulate HIGS, without the need to develop stably transformed plants.

The use of both SIGS and HIGS on a commercial scale appears possible in the near future. Similar HIGS-based approaches may be developed and assessed in their efficacy to control other Fusarium borne diseases of other important crops, e.g. banana, tomato, lettuce and oil palm, or to control other problematic fungal diseases of wheat, i.e. wheat blast caused by the ascomycete fungus *Magnaporthe oryzae*. With the increased interest in the use of RNAi for fungal disease control, a greater understanding of the genes and pathways controlling the phenomena of the trans-kingdom RNAi will emerge. This new knowledge should then help to further optimise the construction, deployment and re-use of HIGS multi-gene cassettes for the sustainable control of plant diseases (Machado et al., 2017, submitted).

7.10 Conclusions.

Recent studies suggest that due to increased temperatures and global warming, major epidemics of FEB will occur more frequently, mainly in regions with high humidity conditions (Shah et al., 2014). These forecasts raise serious concerns for global food and feed security. Currently, the predominant species of FEB, *F. graminearum* is considered the fourth most important pathogen based on its scientific and economic importance (Dean et al., 2012) and yet the infection biology of *F. graminearum* and the underlying mechanisms are not fully understood.

Taken together, the results generated in this thesis provide more understanding about the mechanisms of FEB infection in wheat and the predicted secretome. Overall, the use of BSMV-VOX system in combination with the *F.*

graminearum-wheat spike infection has been showed to be an effective tool to identify novel candidate *F. graminearum* genes coding for small secreted proteins involved in the host-pathogen interaction that may not have been revealed via the classical single gene deletion reverse genetic approach.

Once the mechanisms underlying the functions of SSP8, SSP7, SSP6 and SSP5 as well as their temporal and spatial regulation are further understood, these genes/proteins could potentially be novel intervention targets either for conventional chemistries and/or for methods such as host-induced gene silencing (HIGS) to achieve FEB disease and/or mycotoxin control.

Appendices

Appendix 1 *F. graminearum* 'core' secretome

FGRRES ID	Prediction	Annotation PH-1	Chromosome
FGRRES_00028	Effector	unnamed protein product	Chromosome_1
FGRRES_00060	Effector	hypothetical protein FGSG_13628	Chromosome_1
FGRRES_00184	Effector	thioredoxin-like protein	Chromosome_1
FGRRES_15714_M	Effector	hypothetical protein FGSG_11077	Chromosome_1
FGRRES_00294	Effector	hypothetical protein FG05_30643	Chromosome_1
FGRRES_00571	Effector	LOW QUALITY PROTEIN: hypothetical protein FGSG_14020	Chromosome_1
FGRRES_00588	Effector	pathogenicity protein	Chromosome_1
FGRRES_00707	Effector	pectate lyase	Chromosome_1
FGRRES_00728	Effector	hypothetical protein FGSG_00056	Chromosome_1
FGRRES_00793	Effector	pectate lyase	Chromosome_1
FGRRES_01240	Effector	unnamed protein product	Chromosome_1
FGRRES_01607	Effector	unnamed protein product	Chromosome_1
FGRRES_01748	Effector	hypothetical protein FG05_30503	Chromosome_1
FGRRES_01754	Effector	hypothetical protein FGSG_01239	Chromosome_1
FGRRES_15917_M	Effector	cell wall protein	Chromosome_1
FGRRES_02059	Effector	hypothetical protein FGSG_12514	Chromosome_1
FGRRES_12082	Effector	hypothetical protein FGSG_05341	Chromosome_1
FGRRES_02181	Effector	cell wall protein	Chromosome_1
FGRRES_02206	Effector	hypothetical protein FGSG_12081	Chromosome_1
FGRRES_02228	Effector	hypothetical protein FG05_30242	Chromosome_1
FGRRES_15959	Effector	hypothetical protein FGSG_07221	Chromosome_1
FGRRES_02263	Effector	hypothetical protein FGSG_01660	Chromosome_1
FGRRES_02309	Effector	hypothetical protein FGSG_01674	Chromosome_1
FGRRES_02314	Effector	hypothetical protein FG05_30400	Chromosome_1
FGRRES_02337	Effector	hypothetical protein FGSG_01688	Chromosome_1
FGRRES_02339	Effector	hypothetical protein FGSG_13021	Chromosome_1
FGRRES_15971_12118_M	Effector	acetylxylan esterase precursor	Chromosome_1
FGRRES_12119	Effector	hypothetical protein FGSG_07899	Chromosome_1
FGRRES_02360	Effector	hypothetical protein FGSG_07972	Chromosome_1
FGRRES_02385	Effector	phosphatidylglycerol phosphatidylinositol transfer protein precursor	Chromosome_1
FGRRES_16018_M	Effector	hypothetical protein FPSE_02100	Chromosome_1
FGRRES_02651	Effector	hydrophobin precursor	Chromosome_1
FGRRES_02666	Effector	hypothetical protein FGSG_11647	Chromosome_1
FGRRES_02720	Effector	hypothetical protein FG05_30294	Chromosome_1
FGRRES_11602	Effector	hypothetical protein FGSG_05046	Chromosome_1
FGRRES_10176	Effector	hypothetical protein FGSG_03662	Chromosome_1
FGRRES_17344	Effector	hypothetical protein FGSG_00260	Chromosome_1
FGRRES_10341	Effector	rhamnogalacturonan acetylesterase precursor	Chromosome_1
FGRRES_10525	Effector	hypothetical protein FGSG_09126	Chromosome_1
FGRRES_10543	Effector	hypothetical protein FGSG_03674	Chromosome_1
FGRRES_10551	Effector	hypothetical protein FGSG_04624	Chromosome_1
FGRRES_10561	Effector	antifungal protein	Chromosome_1
FGRRES_10604	Effector	hypothetical protein FGSG_04735	Chromosome_1
FGRRES_17402	Effector	hypothetical protein FG05_30454	Chromosome_1

FGRRES ID	Prediction	Annotation PH-1	Chromosome
FGRRES_17424	Effector	hypothetical protein FGSG_11052	Chromosome_1
FGRRES_17425	Effector	hypothetical protein FGSG_11047	Chromosome_1
FGRRES_10659	Effector	hypothetical protein FGSG_04740	Chromosome_1
FGRRES_08115	Effector	hypothetical protein FGSG_03585	Chromosome_2
FGRRES_08150	Effector	hypothetical protein FGSG_03599	Chromosome_2
FGRRES_08175	Effector	hypothetical protein FGSG_03600	Chromosome_2
FGRRES_13412	Effector	spherulin 1a precursor	Chromosome_2
FGRRES_17022	Effector	hypothetical protein FGSG_11033	Chromosome_2
FGRRES_16958_M	Effector	wsc domain protein	Chromosome_2
FGRRES_02841	Effector	phospholipase a2	Chromosome_2
FGRRES_02888	Effector	hypothetical protein FGSG_01754	Chromosome_2
FGRRES_02917	Effector	hypothetical protein FGSG_07829	Chromosome_2
FGRRES_02933	Effector	hypothetical protein FGSG_01763	Chromosome_2
FGRRES_12547	Effector	small secreted protein	Chromosome_2
FGRRES_03017	Effector	barwin-like endoglucanase	Chromosome_2
FGRRES_03035	Effector	hypothetical protein FGSG_01815	Chromosome_2
FGRRES_03050	Effector	hypothetical protein FGSG_02110	Chromosome_2
FGRRES_03054	Effector	feruloyl esterase c	Chromosome_2
FGRRES_03123	Effector	hypothetical protein FGSG_04471	Chromosome_2
FGRRES_03156	Effector	hypothetical protein FGSG_02255	Chromosome_2
FGRRES_03194	Effector	hypothetical protein FGSG_06597	Chromosome_2
FGRRES_03212	Effector	hypothetical protein FPSE_11620	Chromosome_2
FGRRES_12486	Effector	small secreted protein	Chromosome_2
FGRRES_03274	Effector	cutinase 1	Chromosome_2
FGRRES_03326	Effector	cutinase 3	Chromosome_2
FGRRES_03331_M	Effector	hypothetical protein FGSG_10603	Chromosome_2
FGRRES_03359	Effector	hypothetical protein FGSG_02309	Chromosome_2
FGRRES_03379	Effector	hypothetical protein FGSG_08387	Chromosome_2
FGRRES_03432	Effector	endo- -beta-xylanase 2 precursor	Chromosome_2
FGRRES_03457	Effector	host-specific ak-toxin akt2	Chromosome_2
FGRRES_16258	Effector	hypothetical protein FGSG_06712	Chromosome_2
FGRRES_03569	Effector	hypothetical protein FG05_30052	Chromosome_2
FGRRES_03598	Effector	hypothetical protein FGSG_13462	Chromosome_2
FGRRES_03600	Effector	cutinase precursor	Chromosome_2
FGRRES_16234	Effector	calcium channel partial	Chromosome_2
FGRRES_03632	Effector	unnamed protein product	Chromosome_2
FGRRES_03662	Effector	hypothetical protein FGSG_02378	Chromosome_2
FGRRES_03724	Effector	hypothetical protein FGSG_00111	Chromosome_2
FGRRES_03795	Effector	hypothetical protein FPSE_08081	Chromosome_2
FGRRES_03842	Effector	hypothetical protein FGSG_12504	Chromosome_2
FGRRES_12369	Effector	hypothetical protein FPSE_02093	Chromosome_2
FGRRES_03893	Effector	glutathione-dependent formaldehyde-activating enzyme	Chromosome_2
FGRRES_03904	Effector	endo- -beta-xylanase 1	Chromosome_2
FGRRES_03908	Effector	unnamed protein product	Chromosome_2
FGRRES_03911	Effector	unnamed protein product	Chromosome_2
FGRRES_03971	Effector	hypothetical protein FGSG_02935	Chromosome_2
FGRRES_16175	Effector	unnamed protein product	Chromosome_2
FGRRES_04020	Effector	hypothetical protein FGSG_02962	Chromosome_2

FGRRES ID	Prediction	Annotation PH-1	Chromosome
FGRRES_16163	Effector	hypothetical protein FGSG_00112	Chromosome_2
FGRRES_04060	Effector	hypothetical protein FGSG_07921	Chromosome_2
FGRRES_04239_M	Effector	hypothetical protein FGSG_10560	Chromosome_2
FGRRES_04374_M	Effector	hypothetical protein FGSG_13782	Chromosome_2
FGRRES_04429	Effector	hypothetical protein FGSG_03013	Chromosome_2
FGRRES_04439	Effector	hypothetical protein FGSG_10554	Chromosome_2
FGRRES_16111_M	Effector	hypothetical protein FGSG_10549	Chromosome_2
FGRRES_16104	Effector	hypothetical protein FGSG_10543	Chromosome_2
FGRRES_04510	Effector	probable rot1 precursor	Chromosome_2
FGRRES_04563	Effector	hypothetical protein FGSG_03035	Chromosome_2
FGRRES_04661	Effector	protein ralf-like 33	Chromosome_2
FGRRES_11548	Effector	acetylxylan esterase 2	Chromosome_2
FGRRES_16407	Effector	hypothetical protein FGSG_09132	Chromosome_3
FGRRES_04738	Effector	gegh 16 protein	Chromosome_3
FGRRES_04741	Effector	hypothetical protein FGSG_00114	Chromosome_3
FGRRES_04768	Effector	hydrophobin 3 precursor	Chromosome_3
FGRRES_04841	Effector	hypothetical protein FGSG_03096	Chromosome_3
FGRRES_04848	Effector	unnamed protein product	Chromosome_3
FGRRES_16459	Effector	unnamed protein product	Chromosome_3
FGRRES_05719	Effector	hypothetical protein FGSG_11229	Chromosome_3
FGRRES_05757_M	Effector	unnamed protein product	Chromosome_3
FGRRES_05838	Effector	hypothetical protein FGSG_03156	Chromosome_3
FGRRES_05983	Effector	gpi anchored serine-threonine rich protein	Chromosome_3
FGRRES_16584	Effector	agglutinin receptor	Chromosome_3
FGRRES_06117	Effector	hypothetical protein FGSG_08210	Chromosome_3
FGRRES_16621	Effector	cfem domain-containing protein	Chromosome_3
FGRRES_10729	Effector	hypothetical protein FPSE_08081	Chromosome_3
FGRRES_10772	Effector	hypothetical protein FPSE_04628	Chromosome_3
FGRRES_10782	Effector	unnamed protein product	Chromosome_3
FGRRES_11000_M	Effector	hypothetical protein FGSG_10206	Chromosome_3
FGRRES_11006	Effector	hypothetical protein FG05_30584	Chromosome_3
FGRRES_11011	Effector	long chronological lifespan protein 2	Chromosome_3
FGRRES_11032	Effector	hypothetical protein FG05_30153	Chromosome_3
FGRRES_13864_M	Effector	hypothetical protein FGSG_00588	Chromosome_3
FGRRES_11052	Effector	ricin b lectin	Chromosome_3
FGRRES_11143	Effector	hypothetical protein FGSG_08180	Chromosome_3
FGRRES_11204	Effector	hypothetical protein FGSG_03820	Chromosome_3
FGRRES_13834	Effector	hypothetical protein FGSG_07807	Chromosome_3
FGRRES_11228	Effector	hypothetical protein FG05_30664	Chromosome_3
FGRRES_11249	Effector	hypothetical protein FGSG_13849	Chromosome_3
FGRRES_11326	Effector	hypothetical protein FG05_30188	Chromosome_3
FGRRES_11487	Effector	hypersensitive response-inducing protein	Chromosome_3
FGRRES_06443	Effector	hypothetical protein FGSG_08085	Chromosome_4
FGRRES_06452	Effector	hypothetical protein FGSG_13443	Chromosome_4
FGRRES_06465	Effector	hypothetical protein FGSG_00029	Chromosome_4
FGRRES_06469	Effector	hypothetical protein FGSG_03211	Chromosome_4
FGRRES_06592	Effector	hypothetical protein FGSG_09127	Chromosome_4
FGRRES_06605	Effector	hypothetical protein FGSG_13067	Chromosome_4

FGRRES ID	Prediction	Annotation PH-1	Chromosome
FGRRES_06610	Effector	hypothetical protein FGSG_12300	Chromosome_4
FGRRES_15003	Effector	killer kp4 smk- partial	Chromosome_4
FGRRES_13067	Effector	small secreted protein	Chromosome_4
FGRRES_07221	Effector	hypothetical protein FGSG_03334	Chromosome_4
FGRRES_07551	Effector	killer kp4	Chromosome_4
FGRRES_07569	Effector	hypothetical protein FGSG_04661	Chromosome_4
FGRRES_07608	Effector	hypothetical protein FGSG_11373	Chromosome_4
FGRRES_07625	Effector	hypothetical protein FGSG_12554	Chromosome_4
FGRRES_15448_M	Effector	calcium channel partial	Chromosome_4
FGRRES_07772	Effector	related to extracellular cellulase allergen asp f7-	Chromosome_4
FGRRES_07794	Effector	unnamed protein product	Chromosome_4
FGRRES_07807	Effector	hypothetical protein FGSG_03463	Chromosome_4
FGRRES_07899	Effector	related to gegh 16 protein	Chromosome_4
FGRRES_07918	Effector	hypothetical protein FGSG_08825	Chromosome_4
FGRRES_17592	Effector	unnamed protein product	Chromosome_4
FGRRES_09475	Effector	hypothetical protein FGSG_03640	Chromosome_4
FGRRES_09358	Effector	related to rf2 protein	Chromosome_4
FGRRES_09353	Effector	hypothetical protein FGSG_11225	Chromosome_4
FGRRES_09289	Effector	hypothetical protein FGSG_00230	Chromosome_4
FGRRES_09099	Effector	hypothetical protein FGSG_05841	Chromosome_4
FGRRES_13505	Effector	sterigmatocystin biosynthesis peroxidase stcc	Chromosome_4
FGRRES_11648_M		endopolygalacturonase 1	Chromosome_1
FGRRES_00009		acid phosphatase	Chromosome_1
FGRRES_11647		endo- -beta-glucanase	Chromosome_1
FGRRES_11645		acid phosphatase	Chromosome_1
FGRRES_00006		a chain crystal structure of gh29 family alpha-l-fucosidase from fusarium graminearum in the closed form	Chromosome_1
FGRRES_00005		chitinase 18-7	Chromosome_1
FGRRES_00023		unnamed protein product	Chromosome_1
FGRRES_00029		chitinase a1	Chromosome_1
FGRRES_15679		hypothetical protein FGSG_11136	Chromosome_1
FGRRES_00056		hypothetical protein FGSG_00602	Chromosome_1
FGRRES_00061		triacylglycerol lipase	Chromosome_1
FGRRES_00062		hypothetical protein FGSG_13505	Chromosome_1
FGRRES_00072		arabinogalactan endo- -beta-galactosidase	Chromosome_1
FGRRES_11675		endo- -beta-glucanase	Chromosome_1
FGRRES_00100		catalase-peroxidase 2	Chromosome_1
FGRRES_00111		beta-glucosidase 1 precursor	Chromosome_1
FGRRES_00112		choline dehydrogenase	Chromosome_1
FGRRES_00114		beta-glucosidase 4	Chromosome_1
FGRRES_00131		parallel beta-helix repeat protein	Chromosome_1
FGRRES_15706		hypothetical protein FGSG_11078	Chromosome_1
FGRRES_11715		serum paraoxonase arylesterase 2	Chromosome_1
FGRRES_00230		hypothetical protein FGSG_00707	Chromosome_1
FGRRES_00260		para-nitrobenzyl esterase	Chromosome_1
FGRRES_00314		hypothetical protein FGSG_12486	Chromosome_1
FGRRES_00411		hypothetical protein FGSG_00769	Chromosome_1
FGRRES_00415		subtilisin-like serine protease	Chromosome_1

FGRRES ID	Prediction	Annotation PH-1	Chromosome
FGRRES_00487		acid phosphatase	Chromosome_1
FGRRES_00569		para-nitrobenzyl esterase	Chromosome_1
FGRRES_00576		pathogenesis-related protein 1c	Chromosome_1
FGRRES_00602		pectate lyase	Chromosome_1
FGRRES_00642		hypothetical protein FGSG_08115	Chromosome_1
FGRRES_00742		unnamed protein product	Chromosome_1
FGRRES_00769		pectate lyase	Chromosome_1
FGRRES_00783		hypothetical protein FGSG_11675	Chromosome_1
FGRRES_00806		hypothetical protein FGSG_12434	Chromosome_1
FGRRES_00847		transforming growth factor-beta-induced protein ig-h3	Chromosome_1
FGRRES_00987		pectate lyase a	Chromosome_1
FGRRES_00989		unnamed protein product	Chromosome_1
FGRRES_20027		xyloglucanase	Chromosome_1
FGRRES_01179		pectate lyase b precursor	Chromosome_1
FGRRES_01239		pectate lyase l precursor	Chromosome_1
FGRRES_01283		alkaline proteinase	Chromosome_1
FGRRES_01351		unnamed protein product	Chromosome_1
FGRRES_01368		pectate lyase plyb	Chromosome_1
FGRRES_01531		unnamed protein product	Chromosome_1
FGRRES_01570		acetylornithine deacetylase	Chromosome_1
FGRRES_01588		alpha-l-arabinofuranosidase precursor	Chromosome_1
FGRRES_01603		unnamed protein product	Chromosome_1
FGRRES_01621		minor extracellular protease vpr	Chromosome_1
FGRRES_01636		hypothetical protein FGSG_00793	Chromosome_1
FGRRES_01660		hypothetical protein FGSG_00987	Chromosome_1
FGRRES_01674		pectin lyase b precursor	Chromosome_1
FGRRES_01685		hypothetical protein FGSG_13412	Chromosome_1
FGRRES_01688		hypothetical protein FGSG_01179	Chromosome_1
FGRRES_01711		unnamed protein product	Chromosome_1
FGRRES_01728		pectin lyase b precursor	Chromosome_1
FGRRES_01763		fas1 domain-containing protein precursor	Chromosome_1
FGRRES_01771		hypothetical protein FGSG_01368	Chromosome_1
FGRRES_01778		hypothetical protein FGSG_01588	Chromosome_1
FGRRES_15885		galactose oxidase precursor	Chromosome_1
FGRRES_01803		glucuronan lyase a	Chromosome_1
FGRRES_01805		feruloyl esterase b-2	Chromosome_1
FGRRES_01815		pectin lyase precursor	Chromosome_1
FGRRES_01818_M		glycoside hydrolase family 55 protein	Chromosome_1
FGRRES_01829		hypothetical protein FGSG_12251	Chromosome_1
FGRRES_01831		murein transglycosylase	Chromosome_1
FGRRES_01846		unnamed protein product	Chromosome_1
FGRRES_01872		tripeptidyl aminopeptidase	Chromosome_1
FGRRES_01982		unnamed protein product	Chromosome_1
FGRRES_01988		hypothetical protein FGSG_08074	Chromosome_1
FGRRES_01993		hypothetical protein FGSG_12591	Chromosome_1
FGRRES_02015		hypothetical protein FGSG_05846	Chromosome_1
FGRRES_02077		muc1-extracellular alpha- -glucan glucosidase	Chromosome_1
FGRRES_12067		unnamed protein product	Chromosome_1

FGRRES ID	Prediction	Annotation PH-1	Chromosome
FGRRES_15931		pectinesterase precursor	Chromosome_1
FGRRES_15937		hypothetical protein FG05_13581	Chromosome_1
FGRRES_02147		alcohol oxidase	Chromosome_1
FGRRES_02154_M		endonuclease exonuclease phosphatase family protein	Chromosome_1
FGRRES_12081		hypothetical protein FGSG_03958	Chromosome_1
FGRRES_02189_M		fad binding domain-containing protein	Chromosome_1
FGRRES_02202		pepsin a	Chromosome_1
FGRRES_02204		hypothetical protein FGSG_01636	Chromosome_1
FGRRES_02249		peptidase a4 family protein	Chromosome_1
FGRRES_02255		peroxisomal amine oxidase (copper-containing)	Chromosome_1
FGRRES_15958		hydrolase mb2248c	Chromosome_1
FGRRES_12107		beta-glucosidase m	Chromosome_1
FGRRES_02269		choline dehydrogenase	Chromosome_1
FGRRES_02328		homogentisate -dioxygenase	Chromosome_1
FGRRES_02330		triacylglycerol lipase	Chromosome_1
FGRRES_02332		choline dehydrogenase	Chromosome_1
FGRRES_02351		hypothetical protein FGSG_01728	Chromosome_1
FGRRES_02354		haloacetate dehalogenase h-1	Chromosome_1
FGRRES_02378		phosphatase dcr2	Chromosome_1
FGRRES_02381		meiotic sister chromatid recombination protein 1	Chromosome_1
FGRRES_12123		hypothetical protein FGSG_08958	Chromosome_1
FGRRES_15142		carboxypeptidase cpds	Chromosome_1
FGRRES_15982		hypothetical protein FG05_09289	Chromosome_1
FGRRES_02408		mannan endo- -beta-mannosidase c	Chromosome_1
FGRRES_02422		hypothetical protein FGSG_09094	Chromosome_1
FGRRES_02448		clock-controlled protein 6	Chromosome_1
FGRRES_12142		unnamed protein product	Chromosome_1
FGRRES_16013		feruloyl esterase	Chromosome_1
FGRRES_02616		hypothetical protein FGSG_06730	Chromosome_1
FGRRES_02658		fad-linked oxidoreductase yvdp	Chromosome_1
FGRRES_02674		unnamed protein product	Chromosome_1
FGRRES_02686		unnamed protein product	Chromosome_1
FGRRES_02721		phosphatidylinositide phosphatase sac2	Chromosome_1
FGRRES_15043		palmitoyl-protein thioesterase	Chromosome_1
FGRRES_09955		monophenol monooxygenase	Chromosome_1
FGRRES_10000		unnamed protein product	Chromosome_1
FGRRES_13692		hypothetical protein FGSG_04429	Chromosome_1
FGRRES_17314		hypothetical protein FGSG_11072	Chromosome_1
FGRRES_10125		inactive purple acid phosphatase 16	Chromosome_1
FGRRES_17328		murein transglycosylase	Chromosome_1
FGRRES_10206		hypothetical protein FGSG_03673	Chromosome_1
FGRRES_10212		hypothetical protein FGSG_07629	Chromosome_1
FGRRES_10316		related to tyrosinase precursor	Chromosome_1
FGRRES_10343		hypothetical protein FGSG_09358	Chromosome_1
FGRRES_10357		hypothetical protein FGSG_00411	Chromosome_1
FGRRES_10395		rhamnogalacturonase b precursor	Chromosome_1
FGRRES_10435		fad binding domain-containing protein	Chromosome_1
FGRRES_10495		acid phosphatase	Chromosome_1

FGRRES ID	Prediction	Annotation PH-1	Chromosome
FGRRES_10500		hypothetical protein FGSG_07698	Chromosome_1
FGRRES_10537		alpha-l-rhamnosidase c	Chromosome_1
FGRRES_13782		endo- -beta-glucanase	Chromosome_1
FGRRES_10549		dnase1 protein	Chromosome_1
FGRRES_10554		beta-glucosidase g	Chromosome_1
FGRRES_10560		2-hydroxyacylsphingosine 1-beta-galactosyltransferase	Chromosome_1
FGRRES_10563_M		beta-fructofuranosidase	Chromosome_1
FGRRES_10592		unnamed protein product	Chromosome_1
FGRRES_10595		glucoamylase precursor	Chromosome_1
FGRRES_10598		beta-glucosidase g	Chromosome_1
FGRRES_10603		hypothetical protein FGSG_03748	Chromosome_1
FGRRES_10607_M		endoglucanase-4 precursor	Chromosome_1
FGRRES_10609		l-sorbosone dehydrogenase	Chromosome_1
FGRRES_10611		hypothetical protein FG05_10204	Chromosome_1
FGRRES_20104		chitinase	Chromosome_1
FGRRES_10634		kelch domain-containing protein 8a	Chromosome_1
FGRRES_17419		endoglucanase-4 precursor	Chromosome_1
FGRRES_10675		bacterial leucyl aminopeptidase	Chromosome_1
FGRRES_10676		6-hydroxy-d-nicotine oxidase	Chromosome_1
FGRRES_10677		feruloyl esterase b	Chromosome_1
FGRRES_17434		hypothetical protein FGSG_11046	Chromosome_1
FGRRES_07972		hypothetical protein FGSG_03521	Chromosome_2
FGRRES_07988		hypothetical protein FPSE_03486	Chromosome_2
FGRRES_07993		hypothetical protein FGSG_03531	Chromosome_2
FGRRES_13462		spore coat protein sp96 precursor	Chromosome_2
FGRRES_07996_M		xylanase 3	Chromosome_2
FGRRES_08002		hypothetical protein FGSG_03545	Chromosome_2
FGRRES_08003		related to glucan -beta-glucosidase	Chromosome_2
FGRRES_17119		murein transglycosylase	Chromosome_2
FGRRES_08011		related to glycosyl hydrolase family 43 protein	Chromosome_2
FGRRES_08021_M		unnamed protein product	Chromosome_2
FGRRES_08026		alkaline ceramidase	Chromosome_2
FGRRES_13450		triacylglycerol lipase	Chromosome_2
FGRRES_08041_M		alpha-l-arabinofuranosidase a precursor	Chromosome_2
FGRRES_08048		related to gpi anchored dioxygenase	Chromosome_2
FGRRES_08074_M		dna mismatch repair protein msh6	Chromosome_2
FGRRES_08085		related to hydrolases or acyltransferases (alpha beta hydrolase superfamily)	Chromosome_2
FGRRES_13443		hypothetical protein FGSG_04380	Chromosome_2
FGRRES_08094		alcohol dehydrogenase	Chromosome_2
FGRRES_08116		bnr asp-box repeat domain protein	Chromosome_2
FGRRES_08180		fatty acid transporter protein	Chromosome_2
FGRRES_08193_M		hydrolase or acyltransferase (alpha beta hydrolase superfamily)	Chromosome_2
FGRRES_08196		hypothetical protein FGSG_06497	Chromosome_2
FGRRES_15469		endoglucanase type k	Chromosome_2
FGRRES_08210		hypothetical protein FGSG_03601	Chromosome_2
FGRRES_08265		unnamed protein product	Chromosome_2
FGRRES_08282		het-c protein	Chromosome_2

FGRRES ID	Prediction	Annotation PH-1	Chromosome
FGRRES_17064		murein transglycosylase	Chromosome_2
FGRRES_17063		unnamed protein product	Chromosome_2
FGRRES_08387		related to hydrolases or acyltransferases (alpha beta hydrolase superfamily)	Chromosome_2
FGRRES_08423		hypothetical protein FGSG_08011	Chromosome_2
FGRRES_15481		xylanase 27	Chromosome_2
FGRRES_17031		unnamed protein product	Chromosome_2
FGRRES_08464		hypothetical protein FGSG_07728	Chromosome_2
FGRRES_08493		tannase and feruloyl esterase	Chromosome_2
FGRRES_08554		related to laccase precursor	Chromosome_2
FGRRES_17009		hypothetical protein FGSG_12792	Chromosome_2
FGRRES_08666		related to meiotically up-regulated gene 157 protein	Chromosome_2
FGRRES_08757		unnamed protein product	Chromosome_2
FGRRES_08765		hypothetical protein FGSG_05803	Chromosome_2
FGRRES_08824		glycoside hydrolase family 95 protein	Chromosome_2
FGRRES_08825		hypothetical protein FGSG_03609	Chromosome_2
FGRRES_08907		hypothetical protein FG05_03012	Chromosome_2
FGRRES_16394		hypothetical protein FGSG_10972	Chromosome_2
FGRRES_16392		hypothetical protein FGSG_04933	Chromosome_2
FGRRES_16381		alkali-sensitive linkage protein	Chromosome_2
FGRRES_02890		isoamyl alcohol	Chromosome_2
FGRRES_02893		hypothetical protein FGSG_07695	Chromosome_2
FGRRES_16372		hypothetical protein FGSG_10922	Chromosome_2
FGRRES_16371		alkaline protease	Chromosome_2
FGRRES_02909_M		hypothetical protein FGSG_10759	Chromosome_2
FGRRES_02910_M		unsaturated rhamnogalacturonyl hydrolase yter	Chromosome_2
FGRRES_12554		beta-hexosaminidase precursor	Chromosome_2
FGRRES_02914		pirin (iron-binding nuclear protein)	Chromosome_2
FGRRES_02918		hypothetical protein FGSG_06479	Chromosome_2
FGRRES_02935		hypothetical protein FGSG_01771	Chromosome_2
FGRRES_12551		hypothetical protein FGSG_03972	Chromosome_2
FGRRES_12548		hypothetical protein FG05_11097	Chromosome_2
FGRRES_12545_16364_M		endo-beta- -glucanase d	Chromosome_2
FGRRES_02961		polygalacturonase 1 precursor	Chromosome_2
FGRRES_02962		prc1-carboxypeptidase serine-type protease	Chromosome_2
FGRRES_02976		unnamed protein product	Chromosome_2
FGRRES_02977_M		unnamed protein product	Chromosome_2
FGRRES_02987		cell wall protein sed1	Chromosome_2
FGRRES_02999		conidial pigment biosynthesis oxidase arb2 brown2	Chromosome_2
FGRRES_03002		glycoside hydrolase family 2 protein	Chromosome_2
FGRRES_03003		glutamyl-trna amidotransferase subunit a	Chromosome_2
FGRRES_16353		murein transglycosylase	Chromosome_2
FGRRES_03013		hypothetical protein FGSG_01778	Chromosome_2
FGRRES_03034_M		hemoglobin and hemoglobin-haptoglobin-binding protein	Chromosome_2
FGRRES_03049		unnamed protein product	Chromosome_2
FGRRES_03052		hypothetical protein FGSG_02202	Chromosome_2
FGRRES_03058_M		endoglucanase type f	Chromosome_2
FGRRES_03072		hypothetical protein FGSG_09345	Chromosome_2
FGRRES_12514		hypothetical protein FGSG_11238	Chromosome_2

FGRRES ID	Prediction	Annotation PH-1	Chromosome
FGRRES_16334		hypothetical protein FGSG_10675	Chromosome_2
FGRRES_16333		amidohydrolase family protein	Chromosome_2
FGRRES_16328		hypothetical protein FGSG_09302	Chromosome_2
FGRRES_03096		cutinase	Chromosome_2
FGRRES_03109		beta-lactamase-like protein 2	Chromosome_2
FGRRES_03114		hypothetical protein FG05_30231	Chromosome_2
FGRRES_12504		hypothetical protein FGSG_03971	Chromosome_2
FGRRES_03121		hypothetical protein FGSG_06469	Chromosome_2
FGRRES_03122		hypothetical protein FGSG_02204	Chromosome_2
FGRRES_16324		hypothetical protein FGSG_02249	Chromosome_2
FGRRES_03130		sulphydryl oxidase protein	Chromosome_2
FGRRES_03131		unnamed protein product	Chromosome_2
FGRRES_03143		hypothetical protein FGSG_11156	Chromosome_2
FGRRES_15136_M		unnamed protein product	Chromosome_2
FGRRES_16312_M		6-hydroxy-d-nicotine oxidase	Chromosome_2
FGRRES_15175		chitin deacetylase 1	Chromosome_2
FGRRES_03209		hypothetical protein FGSG_09134	Chromosome_2
FGRRES_03211		hypothetical protein FGSG_02263	Chromosome_2
FGRRES_03217		unnamed protein product	Chromosome_2
FGRRES_03243		hypothetical protein FGSG_11350	Chromosome_2
FGRRES_03275		prepro-neutral protease	Chromosome_2
FGRRES_03304		isoamyl alcohol oxidase	Chromosome_2
FGRRES_03307		hypothetical protein FGSG_11493	Chromosome_2
FGRRES_03315		glucose-regulated protein	Chromosome_2
FGRRES_12461		fad linked oxidase-like protein	Chromosome_2
FGRRES_03334		probable acetylesterase	Chromosome_2
FGRRES_03343		glycosyl hydrolase	Chromosome_2
FGRRES_03344_M		hypothetical protein FGSG_02269	Chromosome_2
FGRRES_03348		hypothetical protein FGSG_09403	Chromosome_2
FGRRES_03365		lipase b	Chromosome_2
FGRRES_03371		probable alkaline protease	Chromosome_2
FGRRES_03384		hypothetical protein FG05_07934	Chromosome_2
FGRRES_03387_M		epl1 protein	Chromosome_2
FGRRES_03394		unnamed protein product	Chromosome_2
FGRRES_12445		hypothetical protein FGSG_04563	Chromosome_2
FGRRES_03402		fusarin c cluster-peptidase	Chromosome_2
FGRRES_15183		unnamed protein product	Chromosome_2
FGRRES_03406		unnamed protein product	Chromosome_2
FGRRES_12439		hypothetical protein FGSG_00576	Chromosome_2
FGRRES_03436		hypothetical protein FGSG_09109	Chromosome_2
FGRRES_12434		hypothetical protein FGSG_03969	Chromosome_2
FGRRES_03445		probable alpha beta fold family hydrolase	Chromosome_2
FGRRES_03463		cutinase precursor	Chromosome_2
FGRRES_03467		unnamed protein product	Chromosome_2
FGRRES_03483		hypothetical protein FGSG_06466	Chromosome_2
FGRRES_03507		endo- -beta-glucanase	Chromosome_2
FGRRES_03521		probable aspartic pepstatin-sensitive	Chromosome_2
FGRRES_03526		hypothetical protein FGSG_05838	Chromosome_2

FGRRES ID	Prediction	Annotation PH-1	Chromosome
FGRRES_03529		mitomycin radical oxidase	Chromosome_2
FGRRES_03531		probable beta-galactosidase	Chromosome_2
FGRRES_03532		hypothetical protein FGSG_09330	Chromosome_2
FGRRES_03544_M		hypothetical protein FGSG_10598	Chromosome_2
FGRRES_03545		hypothetical protein FGSG_02332	Chromosome_2
FGRRES_03570_M		hypothetical protein FGSG_06775	Chromosome_2
FGRRES_03574		unnamed protein product	Chromosome_2
FGRRES_03575		hypothetical protein FGSG_11310	Chromosome_2
FGRRES_03583		endo-beta- -glucanase d	Chromosome_2
FGRRES_03584		unnamed protein product	Chromosome_2
FGRRES_03585		probable beta-glucosidase 1 precursor	Chromosome_2
FGRRES_03599		probable catalase-3	Chromosome_2
FGRRES_03601		hypothetical protein FGSG_02337	Chromosome_2
FGRRES_20176		alpha-galactosidase b	Chromosome_2
FGRRES_03609		probable chitin binding protein	Chromosome_2
FGRRES_03612		hypothetical protein FGSG_02351	Chromosome_2
FGRRES_03614		hypothetical protein FGSG_00005	Chromosome_2
FGRRES_03616		feruloyl esterase b-2	Chromosome_2
FGRRES_12405_M		aspartic-type endopeptidase opsb	Chromosome_2
FGRRES_03624		l-asparaginase 3	Chromosome_2
FGRRES_03628		lipase 4	Chromosome_2
FGRRES_03629		glutamate carboxypeptidase 2	Chromosome_2
FGRRES_03640		probable chitosanase precursor	Chromosome_2
FGRRES_03673		probable cyb2-lactate dehydrogenase cytochrome b2	Chromosome_2
FGRRES_03674_M		extracellular lipase	Chromosome_2
FGRRES_03687_M		hypothetical protein FGSG_04781	Chromosome_2
FGRRES_03695		unnamed protein product	Chromosome_2
FGRRES_03708		hypothetical protein FGSG_12622	Chromosome_2
FGRRES_03713		hypothetical protein FGSG_06076	Chromosome_2
FGRRES_12390		hypothetical protein FGSG_07721	Chromosome_2
FGRRES_03742		hypothetical protein FPSE_07861	Chromosome_2
FGRRES_03748		hypothetical protein FGSG_02385	Chromosome_2
FGRRES_03750		acetylxylan esterase precursor	Chromosome_2
FGRRES_03762		fad binding domain-containing protein	Chromosome_2
FGRRES_03769		hypothetical protein FGSG_02448	Chromosome_2
FGRRES_03784		hypothetical protein FGSG_02721	Chromosome_2
FGRRES_03801		hypothetical protein FGSG_02841	Chromosome_2
FGRRES_03811		d-amino-acid oxidase	Chromosome_2
FGRRES_03813		glutamyl-trna amidotransferase subunit a	Chromosome_2
FGRRES_03820		hypothetical protein FGSG_11348	Chromosome_2
FGRRES_16196		aspartic proteinase yapsin-6	Chromosome_2
FGRRES_03846		hypothetical protein FGSG_04841	Chromosome_2
FGRRES_03858		glycosylhydrolase family 18-6	Chromosome_2
FGRRES_03865		trichothecene c-15 esterase	Chromosome_2
FGRRES_03867_M		exopolygalacturonase b	Chromosome_2
FGRRES_16186		hypothetical protein FGSG_07435	Chromosome_2
FGRRES_03883		d-arabinono- -lactone oxidase	Chromosome_2
FGRRES_03884		beta-lactamase-like 1	Chromosome_2

FGRRES ID	Prediction	Annotation PH-1	Chromosome
FGRRES_03894_M		probable endoglucanase iv precursor	Chromosome_2
FGRRES_03896		hypothetical protein FGSG_02888	Chromosome_2
FGRRES_03901		5 3 -nucleotidase	Chromosome_2
FGRRES_03905		probable endothiapepsin precursor	Chromosome_2
FGRRES_03914		unnamed protein product	Chromosome_2
FGRRES_03916		unnamed protein product	Chromosome_2
FGRRES_16182		fad-binding type 2	Chromosome_2
FGRRES_03922		tripeptidyl-peptidase i	Chromosome_2
FGRRES_03944		hypothetical protein FGSG_08666	Chromosome_2
FGRRES_03954		probable fusarubin cluster-esterase	Chromosome_2
FGRRES_03958		probable gegh 16 protein	Chromosome_2
FGRRES_03960		mannan endo- -beta-mannosidase b	Chromosome_2
FGRRES_03967		hypothetical protein FGSG_02914	Chromosome_2
FGRRES_03969		hypothetical protein FGSG_02933	Chromosome_2
FGRRES_03972		hypothetical protein FGSG_02961	Chromosome_2
FGRRES_03975		hypothetical protein FGSG_07772	Chromosome_2
FGRRES_03986		probable isoamyl alcohol oxidase	Chromosome_2
FGRRES_04014		l-ascorbate oxidase	Chromosome_2
FGRRES_04022		hypothetical protein FGSG_07993	Chromosome_2
FGRRES_04029		probable lysophospholipase	Chromosome_2
FGRRES_04074		alpha-amylase a type-1 2	Chromosome_2
FGRRES_04077		hypothetical protein FGSG_11645	Chromosome_2
FGRRES_16149_M		unnamed protein product	Chromosome_2
FGRRES_16148		hypothetical protein FPSE_00078	Chromosome_2
FGRRES_12300		siderophore biosynthesis protein	Chromosome_2
FGRRES_04146		gpi anchored serine-threonine rich protein	Chromosome_2
FGRRES_04230		carboxypeptidase y like protein a	Chromosome_2
FGRRES_04255		killer toxin subunits alpha beta	Chromosome_2
FGRRES_04345		hypothetical protein FGSG_02999	Chromosome_2
FGRRES_04380		probable metalloprotease mep1	Chromosome_2
FGRRES_04434		hypothetical protein FGSG_04739	Chromosome_2
FGRRES_20208		neurofilament medium polypeptide	Chromosome_2
FGRRES_12251		hypothetical protein FGSG_03967	Chromosome_2
FGRRES_04471		probable rasp f 9 allergen	Chromosome_2
FGRRES_04503		cellulase precursor	Chromosome_2
FGRRES_04504		cell wall glucanase	Chromosome_2
FGRRES_04527		beta-galactosidase b	Chromosome_2
FGRRES_04521		dipeptidyl-peptidase 4	Chromosome_2
FGRRES_04535		hypothetical protein FGSG_00006	Chromosome_2
FGRRES_04546		agglutinin-like protein 2	Chromosome_2
FGRRES_04583		hypothetical protein FGSG_09093	Chromosome_2
FGRRES_15251		n-acetylglucosaminylphosphatidylinositol deacetylase	Chromosome_2
FGRRES_04603		hypothetical protein FGSG_11206	Chromosome_2
FGRRES_04620		alkaline phosphatase	Chromosome_2
FGRRES_12214		transforming growth factor-beta-induced protein ig-h3	Chromosome_2
FGRRES_04624		protein disulfide-isomerase erp38	Chromosome_2
FGRRES_04646_M		anter-specific proline-rich protein apg	Chromosome_2
FGRRES_04647		carboxylesterase family protein	Chromosome_2

FGRRES ID	Prediction	Annotation PH-1	Chromosome
FGRRES_04652_M		endoglucanase type b	Chromosome_2
FGRRES_04656		gmc oxidoreductase	Chromosome_2
FGRRES_12206		serum paraoxonase lactonase 3	Chromosome_2
FGRRES_04678		tripeptidyl-peptidase i	Chromosome_2
FGRRES_04681_M		hypothetical protein FGSG_07207	Chromosome_2
FGRRES_16074		hypothetical protein FGSG_10495	Chromosome_2
FGRRES_04685		hypothetical protein FGSG_08003	Chromosome_2
FGRRES_04689		hypothetical protein FGSG_05719	Chromosome_2
FGRRES_16066		hypothetical protein FGSG_10435	Chromosome_2
FGRRES_14020_M		acetylxylan esterase 2	Chromosome_2
FGRRES_11559		glycosyl hydrolase family 17	Chromosome_2
FGRRES_11548		acetylxylan esterase 2	Chromosome_2
FGRRES_16051_M		hypothetical protein FGSG_10395	Chromosome_2
FGRRES_11528		hypothetical protein FGSG_09390	Chromosome_2
FGRRES_15658		oxalate decarboxylase	Chromosome_2
FGRRES_16047		hypothetical protein FGSG_08048	Chromosome_2
FGRRES_11516		hypothetical protein FG05_30605	Chromosome_2
FGRRES_11513_M		endoglucanase e1	Chromosome_2
FGRRES_12591		hypothetical protein FGSG_03986	Chromosome_3
FGRRES_04732		hypothetical protein FGSG_11379	Chromosome_3
FGRRES_04735		protein rds1	Chromosome_3
FGRRES_04739		acetylxylan esterase a	Chromosome_3
FGRRES_15123		endo- -beta-xylanase c	Chromosome_3
FGRRES_04740		hypothetical protein FGSG_03050	Chromosome_3
FGRRES_04743		glutamyl endopeptidase	Chromosome_3
FGRRES_04744		hypothetical protein FGSG_03052	Chromosome_3
FGRRES_04745		cell wall glycoprotein	Chromosome_3
FGRRES_16408		hypothetical protein FGSG_10341	Chromosome_3
FGRRES_04752_M		unnamed protein product	Chromosome_3
FGRRES_04756_M		6-hydroxy-d-nicotine oxidase	Chromosome_3
FGRRES_04758		enoyl- hydratase	Chromosome_3
FGRRES_04781		carboxypeptidase s1	Chromosome_3
FGRRES_04793		endothiapepsin precursor	Chromosome_3
FGRRES_04817		hypothetical protein FGSG_08554	Chromosome_3
FGRRES_04818		hypothetical protein FGSG_04521	Chromosome_3
FGRRES_04824		agmatinase 2	Chromosome_3
FGRRES_12622		hypothetical protein FGSG_04020	Chromosome_3
FGRRES_16431_M		carboxypeptidase cpds	Chromosome_3
FGRRES_04856		cellobiose dehydrogenase	Chromosome_3
FGRRES_04858		hypothetical protein FGSG_03122	Chromosome_3
FGRRES_04864		hypothetical protein FGSG_06036	Chromosome_3
FGRRES_04895		hypothetical protein FGSG_12938	Chromosome_3
FGRRES_04933		protein slg1	Chromosome_3
FGRRES_04953		glycosyl hydrolase family 10	Chromosome_3
FGRRES_04971		protein ycac	Chromosome_3
FGRRES_04972_M		hypothetical protein FGSG_08150	Chromosome_3
FGRRES_04980		unnamed protein product	Chromosome_3
FGRRES_05046		protein-arginine deiminase type ii	Chromosome_3

FGRRES ID	Prediction	Annotation PH-1	Chromosome
FGRRES_05050		unnamed protein product	Chromosome_3
FGRRES_05052		hypothetical protein FGSG_11496	Chromosome_3
FGRRES_05085		udp-glucose:glycoprotein glucosyltransferase	Chromosome_3
FGRRES_05163		pyridine nucleotide-disulfide oxidoreductase family protein	Chromosome_3
FGRRES_05245		triacylglycerol lipase fgl4	Chromosome_3
FGRRES_05292		tyrosinase	Chromosome_3
FGRRES_05341		rds1 protein	Chromosome_3
FGRRES_05446		hypothetical protein FGSG_12107	Chromosome_3
FGRRES_05458		related to 6-hydroxy-d-nicotine oxidase	Chromosome_3
FGRRES_05609		agmatinase 1	Chromosome_3
FGRRES_05628		related to acid sphingomyelinase	Chromosome_3
FGRRES_05637		hypothetical protein FGSG_03129	Chromosome_3
FGRRES_12792		hypothetical protein FGSG_04029	Chromosome_3
FGRRES_05763		hypothetical protein FG05_13864	Chromosome_3
FGRRES_16542		---NA---	Chromosome_3
FGRRES_16547		a chain native structure of the gh93 alpha-l-arabinofuranosidase of fusarium graminearum	Chromosome_3
FGRRES_05797		hypothetical protein FGSG_13876	Chromosome_3
FGRRES_05803		related to alcohol oxidase	Chromosome_3
FGRRES_05835		hypothetical protein FGSG_08094	Chromosome_3
FGRRES_05841		related to alkaline protease	Chromosome_3
FGRRES_05846		related to alpha-l-arabinofuranosidase ii precursor	Chromosome_3
FGRRES_05847		unnamed protein product	Chromosome_3
FGRRES_05851		tyrosinase	Chromosome_3
FGRRES_12835		aldose 1-epimerase	Chromosome_3
FGRRES_05906		hypothetical protein FG05_08007	Chromosome_3
FGRRES_05933		fungistatic metabolite	Chromosome_3
FGRRES_05947		hypothetical protein FGSG_00131	Chromosome_3
FGRRES_05970		related to aspartic-type signal peptidase	Chromosome_3
FGRRES_06010		unnamed protein product	Chromosome_3
FGRRES_06017		unnamed protein product	Chromosome_3
FGRRES_06023		hypothetical protein FGSG_11232	Chromosome_3
FGRRES_06036		alpha-l-arabinofuranosidase axha	Chromosome_3
FGRRES_06076		related to beta- exoglucanase	Chromosome_3
FGRRES_06110		lipase 4	Chromosome_3
FGRRES_06189		related to beta-galactosidase	Chromosome_3
FGRRES_06208		trypsin precursor	Chromosome_3
FGRRES_16623		guanyl-specific ribonuclease f1 precursor	Chromosome_3
FGRRES_16635		murein transglycosylase	Chromosome_3
FGRRES_06397		levanbiose-producing levanase	Chromosome_3
FGRRES_16645		dioxygenase	Chromosome_3
FGRRES_17524		n -(beta-n-acetylglucosaminyl)-l-asparaginase	Chromosome_3
FGRRES_10759		rhamnogalacturonate lyase c	Chromosome_3
FGRRES_10776_M		minor extracellular protease vpr	Chromosome_3
FGRRES_10922		hypothetical protein FGSG_03750	Chromosome_3
FGRRES_20306		---NA---	Chromosome_3
FGRRES_17494		hypothetical protein FGSG_10316	Chromosome_3
FGRRES_10972		hypothetical protein FGSG_03769	Chromosome_3

FGRRES ID	Prediction	Annotation PH-1	Chromosome
FGRRES_10982		hydrolase or acyltransferase (alpha beta hydrolase superfamily)	Chromosome_3
FGRRES_10985		hypothetical protein FGSG_04510	Chromosome_3
FGRRES_10986		hypothetical protein FGSG_12206	Chromosome_3
FGRRES_10998		unnamed protein product	Chromosome_3
FGRRES_10999		l-ascorbate peroxidase peroxisomal	Chromosome_3
FGRRES_13876		alpha-galactosidase 2	Chromosome_3
FGRRES_11008		hypothetical secretory lipase (family 3)	Chromosome_3
FGRRES_11033		rhamnogalacturonate lyase precursor	Chromosome_3
FGRRES_11035_M		hypothetical protein FGSG_10176	Chromosome_3
FGRRES_11036		manganese peroxidase 2	Chromosome_3
FGRRES_11037		hypothetical protein FGSG_05637	Chromosome_3
FGRRES_11046		ribonuclease t2 family protein	Chromosome_3
FGRRES_11047		ribonuclease trv	Chromosome_3
FGRRES_11048		glycoside hydrolase family 3 protein	Chromosome_3
FGRRES_11049		hypothetical protein FGSG_11715	Chromosome_3
FGRRES_11066		hypothetical protein FGSG_04971	Chromosome_3
FGRRES_11072		hypothetical protein FGSG_03784	Chromosome_3
FGRRES_11077		hypothetical protein FGSG_03801	Chromosome_3
FGRRES_11078		duf1237 domain protein	Chromosome_3
FGRRES_11095		hypothetical protein FGSG_13692	Chromosome_3
FGRRES_11097		murein transglycosylase	Chromosome_3
FGRRES_11101_M		hypothetical protein FGSG_09821	Chromosome_3
FGRRES_11106		hypothetical protein FGSG_08026	Chromosome_3
FGRRES_11112		hypothetical protein FG05_05947	Chromosome_3
FGRRES_17469		hypothetical protein FGSG_09742	Chromosome_3
FGRRES_17468		unnamed protein product	Chromosome_3
FGRRES_11136		alpha-glucuronidase precursor	Chromosome_3
FGRRES_13849		alkaline phosphatase	Chromosome_3
FGRRES_11156		hypothetical protein FGSG_03811	Chromosome_3
FGRRES_11163		hypothetical protein FGSG_06023	Chromosome_3
FGRRES_11164		unnamed protein product	Chromosome_3
FGRRES_11166		alpha-n-arabinofuranosidase b	Chromosome_3
FGRRES_17462		hypothetical protein FGSG_09650	Chromosome_3
FGRRES_11184		lipase 1	Chromosome_3
FGRRES_11190		mosc domain-containing protein mitochondrial	Chromosome_3
FGRRES_17459		hypothetical protein FG05_10357	Chromosome_3
FGRRES_17455		hypothetical protein FGSG_00569	Chromosome_3
FGRRES_11205		hypothetical protein FG05_07684	Chromosome_3
FGRRES_11206		hypothetical protein FGSG_03883	Chromosome_3
FGRRES_11208		xylosidase arabinosidase	Chromosome_3
FGRRES_11225		beta-glucosidase m	Chromosome_3
FGRRES_11227		hypothetical protein FGSG_04858	Chromosome_3
FGRRES_11229		hypothetical protein FGSG_03894	Chromosome_3
FGRRES_11231		hypothetical protein FGSG_05609	Chromosome_3
FGRRES_11232		hypothetical protein FGSG_03896	Chromosome_3
FGRRES_11238		duf1237 domain protein	Chromosome_3
FGRRES_11254		cel1 protein precursor	Chromosome_3
FGRRES_11257		feruloyl esterase b precursor	Chromosome_3

FGRRES ID	Prediction	Annotation PH-1	Chromosome
FGRRES_11276		aromatic peroxygenase	Chromosome_3
FGRRES_11280		endo- -beta-xylanase	Chromosome_3
FGRRES_11296		hypothetical protein FGSG_03901	Chromosome_3
FGRRES_11304		lipase 4	Chromosome_3
FGRRES_11310		salicylate hydroxylase	Chromosome_3
FGRRES_11315		exoglucanase type c precursor	Chromosome_3
FGRRES_11318		unnamed protein product	Chromosome_3
FGRRES_11333_M		berberine bridge enzyme	Chromosome_3
FGRRES_11348		secreted protein	Chromosome_3
FGRRES_11350		hypothetical protein FGSG_03905	Chromosome_3
FGRRES_17566		hypothetical protein FG05_12439	Chromosome_3
FGRRES_11360		cellobiose dehydrogenase	Chromosome_3
FGRRES_11361		hypothetical protein FGSG_03954	Chromosome_3
FGRRES_11366		hypothetical protein FGSG_08002	Chromosome_3
FGRRES_11373		serine protease	Chromosome_3
FGRRES_11379		bacterial-type extracellular deoxyribonuclease	Chromosome_3
FGRRES_13975_M		endoglucanase e	Chromosome_3
FGRRES_11386		hypothetical protein FGSG_08175	Chromosome_3
FGRRES_11399		hypothetical protein FG05_10335	Chromosome_3
FGRRES_11428		hypothetical protein FG05_11201	Chromosome_3
FGRRES_17545		hypothetical protein FGSG_05458	Chromosome_3
FGRRES_13947		gpi anchor protein	Chromosome_3
FGRRES_11468		FAD domain	Chromosome_3
FGRRES_11472		hypothetical protein FGSG_05163	Chromosome_3
FGRRES_11488		leucyl aminopeptidase	Chromosome_3
FGRRES_20325		hypothetical protein FGSG_09475	Chromosome_3
FGRRES_17535		endoglucanase c	Chromosome_3
FGRRES_11493		serine protease precursor	Chromosome_3
FGRRES_11496		serum paraoxonase arylesterase 1	Chromosome_3
FGRRES_20327		hypothetical protein FGSG_12551	Chromosome_3
FGRRES_06450_M		hypothetical protein FGSG_00072	Chromosome_4
FGRRES_06451		hypothetical protein FGSG_04744	Chromosome_4
FGRRES_06463		hypothetical protein FGSG_12547	Chromosome_4
FGRRES_06466		related to bromodomain protein bdf1	Chromosome_4
FGRRES_06479		carbonic anhydrase	Chromosome_4
FGRRES_06497		related to carboxypeptidase	Chromosome_4
FGRRES_16668		glycoside hydrolase family 5 protein	Chromosome_4
FGRRES_06506		hypothetical protein FGSG_03274	Chromosome_4
FGRRES_06549		unnamed protein product	Chromosome_4
FGRRES_12938		hypothetical protein FGSG_04345	Chromosome_4
FGRRES_06572		tripeptidyl-peptidase sed2	Chromosome_4
FGRRES_06597		related to cellobiose dehydrogenase	Chromosome_4
FGRRES_06612		unnamed protein product	Chromosome_4
FGRRES_16689		unnamed protein product	Chromosome_4
FGRRES_16697		hypothetical protein FGSG_11204	Chromosome_4
FGRRES_06712		hypothetical protein FGSG_03275	Chromosome_4
FGRRES_06730		related to cellulose-binding gdsl lipase acylhydrolase	Chromosome_4
FGRRES_06733		hypothetical protein FGSG_06780	Chromosome_4

FGRRES ID	Prediction	Annotation PH-1	Chromosome
FGRRES_06775		related to chitin binding protein	Chromosome_4
FGRRES_06780		related to cps1-gly-x carboxypeptidase yscs precursor	Chromosome_4
FGRRES_06888		laccase precursor	Chromosome_4
FGRRES_15396		n-sulfoglucosamine sulfohydrolase	Chromosome_4
FGRRES_06895		hypothetical protein FPSE_01352	Chromosome_4
FGRRES_13021		hypothetical protein FGSG_11276	Chromosome_4
FGRRES_06993		hypothetical protein FGSG_12835	Chromosome_4
FGRRES_16759		unnamed protein product	Chromosome_4
FGRRES_07010		unnamed protein product	Chromosome_4
FGRRES_07126_M		unnamed protein product	Chromosome_4
FGRRES_07180_M		carboxypeptidase a4	Chromosome_4
FGRRES_07207		hypothetical protein FGSG_03326	Chromosome_4
FGRRES_07238		unnamed protein product	Chromosome_4
FGRRES_07375		glucan endo- -beta-glucosidase	Chromosome_4
FGRRES_20368		2-amino-3-carboxymuconate-6-semialdehyde decarboxylase	Chromosome_4
FGRRES_07435		related to ecm14-involved in cell wall biogenesis and architecture	Chromosome_4
FGRRES_07539		malate dehydrogenase	Chromosome_4
FGRRES_16845		unnamed protein product	Chromosome_4
FGRRES_15437		chitinase	Chromosome_4
FGRRES_07629		related to endoglucanase iv precursor	Chromosome_4
FGRRES_07639		hypothetical protein FGSG_11166	Chromosome_4
FGRRES_07661		hypothetical protein FG05_08288	Chromosome_4
FGRRES_07678		fungal hydrophobin	Chromosome_4
FGRRES_07684_M		murein transglycosylase	Chromosome_4
FGRRES_16877		hypothetical protein FGSG_09445	Chromosome_4
FGRRES_13189		glycoside hydrolase family 39 protein	Chromosome_4
FGRRES_07695		hypothetical protein FGSG_03344	Chromosome_4
FGRRES_07698		hypothetical protein FGSG_03359	Chromosome_4
FGRRES_16883		alkaline proteinase	Chromosome_4
FGRRES_07721		hypothetical protein FGSG_03371	Chromosome_4
FGRRES_07728		hypothetical protein FGSG_03445	Chromosome_4
FGRRES_07755		hypothetical protein FGSG_05970	Chromosome_4
FGRRES_20377		hypothetical protein FGSG_09443	Chromosome_4
FGRRES_07775		hypothetical protein FG05_06332	Chromosome_4
FGRRES_07784		carbonic anhydrase	Chromosome_4
FGRRES_07797		bifunctional xylanase deacetylase	Chromosome_4
FGRRES_16898		hypothetical protein FG05_13925	Chromosome_4
FGRRES_16902		glycosidase crf2	Chromosome_4
FGRRES_07808		aspartic proteinase precursor	Chromosome_4
FGRRES_07829		related to extracellular gdsl-like lipase acylhydrolase	Chromosome_4
FGRRES_07838		unnamed protein product	Chromosome_4
FGRRES_13245_M		lipase 4	Chromosome_4
FGRRES_07921		related to glu asp-trna amidotransferase subunit a	Chromosome_4
FGRRES_16930		murein transglycosylase	Chromosome_4
FGRRES_07940		unnamed protein product	Chromosome_4
FGRRES_07944_M		hypothetical protein FPSE_02498	Chromosome_4
FGRRES_13655		triacylglycerol lipase fgl5	Chromosome_4

FGRRES ID	Prediction	Annotation PH-1	Chromosome
FGRRES_09821		related to triacylglycerol lipase ii precursor	Chromosome_4
FGRRES_09742		related to stress response protein rds1p	Chromosome_4
FGRRES_13628		subtilisin-like protease	Chromosome_4
FGRRES_09650_M		related to spr1-exo- -beta-glucanase precursor	Chromosome_4
FGRRES_09646		unnamed protein product	Chromosome_4
FGRRES_09586		hypothetical protein FGSG_06506	Chromosome_4
FGRRES_09522		feruloyl esterase b	Chromosome_4
FGRRES_09471		mannosyl-oligosaccharide alpha- -mannosidase	Chromosome_4
FGRRES_09445		related to spore coat protein sp96 precursor	Chromosome_4
FGRRES_09443		related to sam-dependent methyltransferases	Chromosome_4
FGRRES_17212_3_M		amidohydrolase ytcj-like	Chromosome_4
FGRRES_09390		carboxypeptidase s1	Chromosome_4
FGRRES_09403		related to s-adenosylmethionine:diacylglycerol 3-amino-3-carboxypropyl transferase	Chromosome_4
FGRRES_09382		hypothetical protein FGSG_11296	Chromosome_4
FGRRES_09345		hypothetical protein FGSG_03612	Chromosome_4
FGRRES_20390		unnamed protein product	Chromosome_4
FGRRES_09340		lysophospholipase 2	Chromosome_4
FGRRES_09330		related to protocatechuate -dioxygenase beta subunit	Chromosome_4
FGRRES_09302		related to paf acetylhydrolase family protein	Chromosome_4
FGRRES_09291		hypothetical protein FGSG_06189	Chromosome_4
FGRRES_17190		hypothetical protein FGSG_05628	Chromosome_4
FGRRES_20400		multicopper oxidase	Chromosome_4
FGRRES_09181		hypothetical protein FGSG_04824	Chromosome_4
FGRRES_09143_M		cell wall mannoprotein	Chromosome_4
FGRRES_09142		hypothetical protein FGSG_04620	Chromosome_4
FGRRES_09134		arabinoxylan arabinofuranohydrolase	Chromosome_4
FGRRES_09132		6-hydroxy-d-nicotine oxidase	Chromosome_4
FGRRES_09127		related to npp1 domain protein	Chromosome_4
FGRRES_09126		related to neutral proteinase	Chromosome_4
FGRRES_09109		alpha-n-arabinofuranosidase alpha-l-arabinofuranosidase	Chromosome_4
FGRRES_12214		6-hydroxy-d-nicotine oxidase	Chromosome_4
FGRRES_09094		related to monophenol monooxygenase	Chromosome_4
FGRRES_09093		related to monophenol monooxygenase	Chromosome_4
FGRRES_09085_M		hypothetical protein FPSE_06928	Chromosome_4
FGRRES_09066		arabinan endo- -alpha-l-arabinosidase	Chromosome_4
FGRRES_17151		cellobiose dehydrogenase	Chromosome_4
FGRRES_09032_M		hypothetical protein FGSG_11361	Chromosome_4
FGRRES_08987		triacylglycerol lipase v precursor	Chromosome_4
FGRRES_08978		galactose oxidase	Chromosome_4
FGRRES_08958		related to monophenol monooxygenase	Chromosome_4

Appendix 2: Statistical analysis outputs

Figure 4.1 Number of visibly diseased spikelets below the *F. graminearum* inoculation points in wheat ears at 12dpi from eight combined experiments.

Ear name	Treatment	Infected spikelets	Total spikelets	Batch	experiment
1	No Virus	6	12	2	1413
2	No Virus	7	12	2	1413
3	No Virus	5	12	2	1413
4	No Virus	7	12	2	1413
5	No Virus	7	12	3	1413
6	No Virus	5	12	3	1413
7	No Virus	8	12	4	1413
8	No Virus	7	12	4	1413
9	No Virus	2	12	4	1413
10	No Virus	8	12	4	1413
11	No virus	6	12	1	1414
12	No virus	5.5	12	1	1414
13	No virus	8.5	12	2	1414
14	No virus	6	12	2	1414
15	No virus	7.5	12	2	1414
16	No virus	5	12	2	1414
17	No virus	6	12	3	1414
18	No virus	6	12	3	1414
19	No virus	6.5	12	4	1414
20	No virus	9	12	4	1414
21	No virus	9	12	4	1414
22	No virus	6	12	5	1414
23	No Virus	7	13	1	1416
24	No Virus	5	12	1	1416
25	No Virus	5	12	1	1416
26	No Virus	8	12	1	1416
27	No Virus	7	13	1	1416
28	No Virus	4	14	2	1416
29	No Virus	7	12	2	1416
30	No Virus	6	11	2	1416
31	No Virus	5.5	12	2	1416
32	No Virus	4	12	2	1416
33	No Virus	2	13	2	1416
34	No Virus	8	11	3	1416
35	No Virus	8	12	1	1502
36	No Virus	6.5	12	1	1502
37	No Virus	5	12	1	1502
38	No Virus	4	12	1	1502
39	No Virus	8	12	1	1502
40	No Virus	7	12	1	1502
41	No Virus	7	12	2	1502
42	No Virus	8	12	2	1502
43	No Virus	7	12	3	1502
44	No Virus	9	12	3	1502
45	No Virus	6	12	1	1506
46	No Virus	8	12	1	1506
47	No Virus	9	12	2	1506
48	No Virus	6	12	2	1506

49	No Virus	11	12	2	1506
50	No Virus	11	12	2	1506
51	No Virus	8	12	3	1506
52	No Virus	6	12	3	1506
53	No Virus	8	12	3	1506
54	No Virus	6	12	3	1506
55	No Virus	8	12	1	1507
56	No Virus	8	12	2	1507
57	No Virus	8	12	2	1507
58	No Virus	11	12	3	1507
59	No Virus	8	12	4	1507
60	No Virus	11	12	4	1507
61	No Virus	9	12	5	1507
62	No Virus	9	12	5	1507
63	No Virus	7	12	5	1507
64	No Virus	7	12	1	1510
65	No Virus	7.5	12	1	1510
66	No Virus	8.5	12	1	1510
67	No Virus	8	12	2	1510
68	No Virus	7	12	2	1510
69	No Virus	7.5	12	2	1510
70	No Virus	7	12	2	1510
71	No Virus	8	12	2	1510
72	No Virus	7.5	12	2	1510
73	No Virus	2.5	12	2	1510
74	No Virus	6	12	1	1602
75	No Virus	7	12	1	1602
76	No Virus	8	12	1	1602
77	No Virus	6	12	1	1602
78	No Virus	7	12	1	1602
79	No Virus	8	12	1	1602
80	No Virus	8	12	1	1602
81	No Virus	7	12	2	1602
82	No Virus	7	12	2	1602
83	No Virus	8	12	2	1602
84	No Virus	9	12	2	1602
85	No Virus	4	12	2	1602
86	No Virus	9	12	2	1602
87	No Virus	8	12	2	1602
88	No Virus	4	12	2	1602
89	No Virus	7	12	2	1602
110	BSMV:MCS4D	12	12	1	1506
111	BSMV:MCS4D	12	12	2	1506
112	BSMV:MCS4D	12	12	2	1506
113	BSMV:MCS4D	12	12	2	1506
114	BSMV:MCS4D	12	12	2	1506
115	BSMV:MCS4D	12	12	2	1506
116	BSMV:MCS4D	12	12	2	1506
117	BSMV:MCS4D	12	12	2	1506

118	BSMV:MCS4D	12	12	3	1506
119	BSMV:MCS4D	9	12	3	1506
120	BSMV:MCS4D	4	12	3	1506
121	BSMV:MCS4D	12	12	1	1507
122	BSMV:MCS4D	12	12	1	1507
123	BSMV:MCS4D	10	12	2	1507
124	BSMV:MCS4D	12	12	3	1507
125	BSMV:MCS4D	7	12	3	1507
126	BSMV:MCS4D	8.5	12	3	1507
127	BSMV:MCS4D	12	12	4	1507
128	BSMV:MCS4D	5.5	12	4	1507
129	BSMV:MCS4D	8	12	4	1507
130	BSMV:MCS4D	9	12	5	1507
131	BSMV:MCS4D	11	12	5	1507
132	BSMV:MCS4D	10	12	1	1510
133	BSMV:MCS4D	11	12	1	1510
134	BSMV:MCS4D	12	12	1	1510
135	BSMV:MCS4D	10	12	1	1510
136	BSMV:MCS4D	11	12	1	1510
137	BSMV:MCS4D	12	12	1	1510
138	BSMV:MCS4D	12	12	1	1510
139	BSMV:MCS4D	10	12	2	1510
140	BSMV:MCS4D	8	12	2	1510
141	BSMV:MCS4D	10	12	2	1510
142	BSMV:MCS4D	12	12	2	1510
143	BSMV:MCS4D	9	12	2	1510
144	BSMV:MCS4D	12	12	1	1602
145	BSMV:MCS4D	10	12	1	1602
146	BSMV:MCS4D	8	12	1	1602
147	BSMV:MCS4D	11	12	1	1602
148	BSMV:MCS4D	7	12	1	1602
149	BSMV:MCS4D	11	12	2	1602
150	BSMV:MCS4D	10	12	2	1602
151	BSMV:MCS4D	7	12	2	1602
152	BSMV:MCS4D	12	12	2	1602
153	BSMV:MCS4D	12	12	2	1602
154	BSMV:MCS4D	8	12	2	1602
155	BSMV:MCS4D	8.5	12	3	1602
156	BSMV:MCS4D	8	12	3	1602
157	BSMV:MCS4D	12	12	3	1602
158	BSMV:MCS4D	10.5	12	3	1602
159	BSMV:MCS4D	10	12	3	1602
160	BSMV:MCS4D	9	12	4	1602
161	BSMV:MCS4D	10	12	4	1602
162	BSMV:MCS4D	10	12	4	1602
163	BSMV:MCS4D	6	12	5	1602
175	BSMV:MCS4D	12	12	1	1414
176	BSMV:MCS4D	9	12	1	1414
177	BSMV:MCS4D	11	12	1	1414

178	BSMV:MCS4D	6	12	1	1414
179	BSMV:MCS4D	5	12	2	1414
180	BSMV:MCS4D	5.5	12	2	1414
181	BSMV:MCS4D	9	12	2	1414
182	BSMV:MCS4D	12	12	3	1414
183	BSMV:MCS4D	8	12	3	1414
184	BSMV:MCS4D	12	12	3	1414
185	BSMV:MCS4D	7	12	4	1414
186	BSMV:MCS4D	12	12	4	1414
187	BSMV:MCS4D	10	12	5	1414
188	BSMV:MCS4D	10	12	1	1413
189	BSMV:MCS4D	8	12	1	1413
190	BSMV:MCS4D	8	12	3	1413
191	BSMV:MCS4D	6	12	3	1413
192	BSMV:MCS4D	2	12	3	1413
193	BSMV:MCS4D	5	12	3	1413
194	BSMV:MCS4D	6	12	3	1413
195	BSMV:MCS4D	7	12	4	1413
196	BSMV:MCS4D	8	9	3	1416
197	BSMV:MCS4D	5	10	3	1416
198	BSMV:MCS4D	2	10	3	1416
199	BSMV:MCS4D	5	15	4	1416
200	BSMV:MCS4D	9	12	4	1416
201	BSMV:MCS4D	2	12	4	1416
202	BSMV:MCS4D	6	12	4	1416
203	BSMV:MCS4D	6	12	4	1416
204	BSMV:MCS4D	0	12	5	1416
205	BSMV:MCS4D	10	12	2	1502
206	BSMV:MCS4D	9.5	12	2	1502
207	BSMV:MCS4D	6.5	12	3	1502
208	BSMV:MCS4D	5.5	12	3	1502
209	BSMV:MCS4D	9	12	4	1502
210	BSMV:MCS4D	4	12	4	1502
211	BSMV:MCS4D	5	12	4	1502
212	BSMV:MCS4D	6.5	12	4	1502
213	BSMV:MCS4D	9	12	1	1502
263	BSMV:FgSSP7	12	12	1	1413
264	BSMV:FgSSP7	12	12	3	1413
265	BSMV:FgSSP7	7	12	3	1413
266	BSMV:FgSSP7	7	12	3	1413
267	BSMV:FgSSP7	5	12	3	1413
268	BSMV:FgSSP7	11	12	4	1413
269	BSMV:FgSSP7	11	12	4	1413
270	BSMV:FgSSP7	12	12	4	1413
271	BSMV:FgSSP7	12	12	4	1413
272	BSMV:FgSSP7	6	10	3	1416
273	BSMV:FgSSP7	1	11	3	1416
274	BSMV:FgSSP7	6	14	3	1416
275	BSMV:FgSSP7	4.5	12	3	1416

276	BSMV:FgSSP7	7	12	3	1416
277	BSMV:FgSSP7	0	14	3	1416
278	BSMV:FgSSP7	6	12	4	1416
279	BSMV:FgSSP7	4	10	4	1416
280	BSMV:FgSSP7	5	12	4	1416
281	BSMV:FgSSP7	3	12	5	1416
282	BSMV:FgSSP7	7	12	6	1416
283	BSMV:FgSSP7	4	12	6	1416
284	BSMV:FgSSP7	12	12	1	1502
285	BSMV:FgSSP7	11	12	1	1502
286	BSMV:FgSSP7	10.5	12	2	1502
287	BSMV:FgSSP7	12	12	2	1502
288	BSMV:FgSSP7	11	12	3	1502
289	BSMV:FgSSP7	2	12	4	1502
290	BSMV:FgSSP7	7	12	4	1502
291	BSMV:FgSSP7	7	12	4	1502
292	BSMV:FgSSP7	5	12	4	1502
317	BSMV:FgSSP6	12	12	1	1413
318	BSMV:FgSSP6	12	12	1	1413
319	BSMV:FgSSP6	12	12	3	1413
320	BSMV:FgSSP6	12	12	3	1413
321	BSMV:FgSSP6	12	12	4	1413
322	BSMV:FgSSP6	12	12	4	1413
323	BSMV:FgSSP6	5	12	4	1413
324	BSMV:FgSSP6	11	12	4	1413
325	BSMV:FgSSP6	12	14	2	1416
326	BSMV:FgSSP6	9	12	3	1416
327	BSMV:FgSSP6	6.5	12	3	1416
328	BSMV:FgSSP6	8	12	3	1416
329	BSMV:FgSSP6	6	14	4	1416
330	BSMV:FgSSP6	4	13	4	1416
331	BSMV:FgSSP6	9	11	5	1416
332	BSMV:FgSSP6	10	12	5	1416
333	BSMV:FgSSP6	10	12	5	1416
334	BSMV:FgSSP6	4	12	5	1416
335	BSMV:FgSSP6	3	12	6	1416
336	BSMV:FgSSP6	10	12	6	1416
337	BSMV:FgSSP6	10	14	6	1416
338	BSMV:FgSSP6	11	12	1	1502
339	BSMV:FgSSP6	12	12	1	1502
340	BSMV:FgSSP6	10	12	1	1502
341	BSMV:FgSSP6	12	12	3	1502
342	BSMV:FgSSP6	9	12	4	1502
343	BSMV:FgSSP6	11	12	4	1502
344	BSMV:FgSSP6	6	12	4	1502
345	BSMV:FgSSP5	12	12	1	1506
346	BSMV:FgSSP5	12	12	1	1506
347	BSMV:FgSSP5	11	12	1	1506
348	BSMV:FgSSP5	12	12	2	1506

349	BSMV:FgSSP5	12	12	2	1506
350	BSMV:FgSSP5	12	12	2	1506
351	BSMV:FgSSP5	12	12	2	1506
352	BSMV:FgSSP5	10	12	3	1506
353	BSMV:FgSSP5	11	12	3	1506
354	BSMV:FgSSP5	10	12	3	1506
355	BSMV:FgSSP5	11	12	3	1506
356	BSMV:FgSSP5	10	12	1	1507
357	BSMV:FgSSP5	11	12	5	1507
358	BSMV:FgSSP5	11	12	5	1507
359	BSMV:FgSSP5	9	12	5	1507
360	BSMV:FgSSP5	9	12	5	1507
361	BSMV:FgSSP5	10	12	5	1507
362	BSMV:FgSSP5	11	12	5	1507
363	BSMV:FgSSP5	11	12	5	1507
364	BSMV:FgSSP5	9	12	5	1507
365	BSMV:FgSSP5	10	12	5	1507
366	BSMV:FgSSP5	12	12	1	1510
367	BSMV:FgSSP5	12	12	1	1510
368	BSMV:FgSSP5	12	12	1	1510
369	BSMV:FgSSP5	12	12	1	1510
370	BSMV:FgSSP5	12	12	1	1510
371	BSMV:FgSSP5	11	12	1	1510
372	BSMV:FgSSP5	11	12	1	1510
373	BSMV:FgSSP5	12	12	1	1510
374	BSMV:FgSSP5	12	12	1	1510
375	BSMV:FgSSP5	11	12	1	1510
376	BSMV:FgSSP5	8	12	1	1510
377	BSMV:FgSSP5	11	12	1	1602
378	BSMV:FgSSP5	12	12	2	1602
379	BSMV:FgSSP5	11	12	2	1602
380	BSMV:FgSSP5	9	12	2	1602
381	BSMV:FgSSP5	11	12	2	1602
382	BSMV:FgSSP5	12	12	2	1602
383	BSMV:FgSSP5	10	12	2	1602
384	BSMV:FgSSP5	12	12	2	1602
385	BSMV:FgSSP5	10	12	3	1602
386	BSMV:FgSSP5	12	12	3	1602
387	BSMV:FgSSP5	11	12	3	1602
388	BSMV:FgSSP5	9	12	3	1602
389	BSMV:FgSSP5	10	12	3	1602
390	BSMV:FgSSP5	11	12	3	1602
391	BSMV:FgSSP5	12	12	4	1602
392	BSMV:FgSSP5	8	12	4	1602
393	BSMV:FgSSP5	8	12	4	1602
394	BSMV:FgSSP5	11	12	4	1602
395	BSMV:FgSSP5	8	12	5	1602
396	BSMV:FgSSP5	7	12	5	1602
397	BSMV:FgSSP5	4	12	5	1602

398	BSMV:FgSSP4	11	12	1	1502
399	BSMV:FgSSP4	9	12	3	1502
400	BSMV:FgSSP4	10	12	3	1502
401	BSMV:FgSSP4	9	12	3	1502
402	BSMV:FgSSP4	4	12	4	1502
403	BSMV:FgSSP4	3	12	4	1502
404	BSMV:FgSSP4	6	12	4	1502
405	BSMV:FgSSP4	8	12	4	1502
406	BSMV:FgSSP4	3	12	4	1502
407	BSMV:FgSSP2	7	14	1	1416
408	BSMV:FgSSP2	7	12	3	1416
409	BSMV:FgSSP2	2	12	3	1416
410	BSMV:FgSSP2	2	13	3	1416
411	BSMV:FgSSP2	5	13	4	1416
412	BSMV:FgSSP2	2	10	4	1416
413	BSMV:FgSSP2	8	14	4	1416
414	BSMV:FgSSP2	0	12	4	1416
415	BSMV:FgSSP2	3	13	4	1416
416	BSMV:FgSSP2	2	12	4	1416
417	BSMV:FgSSP2	10	12	5	1416
418	BSMV:FgSSP1	9	12	1	1414
419	BSMV:FgSSP1	9	12	1	1414
420	BSMV:FgSSP1	6.5	12	2	1414
421	BSMV:FgSSP1	8	12	2	1414
422	BSMV:FgSSP1	6	12	2	1414
423	BSMV:FgSSP1	7	12	2	1414
424	BSMV:FgSSP1	7	12	3	1414
425	BSMV:FgSSP1	9	12	3	1414
426	BSMV:FgSSP1	5	12	3	1414
427	BSMV:FgSSP1	6	12	4	1414
428	BSMV:FgSSP1	7	12	5	1414
429	BSMV:FgSSP1	9	12	5	1414
430	BSMV:FgSSP1	9	12	5	1414

Generalized linear mixed model analysis

Method: c.f. Schall (1991) Biometrika
Response variate: Infected_spikelets
Binomial totals: Total_spikelets
Distribution: binomial
Link function: logit
Random model: experiment + experiment.Batch
Fixed model: Constant + Treatment

Dispersion parameter estimated

Monitoring information

Iteration	Gammas	Dispersion	Max change

1	0.1804	0.1592	1.687	2.5593E-01
2	0.1777	0.1514	1.753	6.6031E-02
3	0.1734	0.1480	1.813	5.9508E-02
4	0.1733	0.1479	1.815	2.4496E-03
5	0.1732	0.1478	1.815	5.7527E-05

Estimated variance components

Random term	component	s.e.
experiment	0.314	0.220
experiment.Batch	0.268	0.104

Residual variance model

Term	Model(order)	Parameter	Estimate	s.e.
Dispersn	Identity	Sigma2	1.815	0.152

Estimated variance matrix for variance components

experiment	1	0.04849		
experiment.Batch	2	-0.00203	0.01082	
Dispersn	3	-0.00026	-0.00135	0.02312
		1	2	3

Tests for fixed effects

Sequentially adding terms to fixed model

Fixed term	Wald statistic	n.d.f.	F statistic	d.d.f.	F pr
Treatment	101.07	7	14.44	307.2	<0.001

Dropping individual terms from full fixed model

Fixed term	Wald statistic	n.d.f.	F statistic	d.d.f.	F pr
Treatment	101.07	7	14.44	307.2	<0.001

Tables of means with standard errors

Table of predicted means for Treatment

Treatment	BSMV:FgSSP1	BSMV:FgSSP2	BSMV:FgSSP4	BSMV:FgSSP5	BSMV:FgSSP6
	0.508	0.804	1.006	1.700	2.064

Treatment	BSMV:FgSSP7	BSMV:MCS4D	No Virus
	1.309	1.117	0.244

Standard errors of differences

Average:	0.3077
Maximum:	0.4362
Minimum:	0.1412

Average variance of differences: 0.09980

Table of predicted means for Treatment

Treatment	BSMV:FgSSP1	BSMV:FgSSP2	BSMV:FgSSP4	BSMV:FgSSP5	BSMV:FgSSP6
	0.508	0.804	1.006	1.700	2.064

Treatment	BSMV:FgSSP7	BSMV:MCS4D	No Virus
	1.309	1.117	0.244

Standard errors

Average:	0.3096
Maximum:	0.3919
Minimum:	0.2388

Back-transformed Means (on the original scale)

Treatment	
BSMV:FgSSP1	0.6243
BSMV:FgSSP2	0.6909
BSMV:FgSSP4	0.7322
BSMV:FgSSP5	0.8456
BSMV:FgSSP6	0.8874
BSMV:FgSSP7	0.7874
BSMV:MCS4D	0.7535
No Virus	0.5608

```
118  vlsd Treatment
```

Approximate least significant differences (5% level) of REML means

Treatment

Treatment BSMV:FgSSP1	1	*			
Treatment BSMV:FgSSP2	2	0.8079	*		
Treatment BSMV:FgSSP4	3	0.8583	0.8446	*	
Treatment BSMV:FgSSP5	4	0.6895	0.7113	0.7681	*
Treatment BSMV:FgSSP6	5	0.7095	0.6376	0.7223	0.5975
Treatment BSMV:FgSSP7	6	0.6805	0.6129	0.6893	0.5626
Treatment BSMV:MCS4D	7	0.5787	0.5959	0.6642	0.4299
Treatment No Virus	8	0.5721	0.6076	0.6722	0.4318
		1	2	3	4

Treatment BSMV:FgSSP6	5	*			
Treatment BSMV:FgSSP7	6	0.4741	*		
Treatment BSMV:MCS4D	7	0.4586	0.4104	*	
Treatment No Virus	8	0.4658	0.4215	0.2779	*
		5	6	7	8

```
120  vdisp [pterm=Treatment; prin=mean; pse=alle]
```

Table of predicted means for Treatment

Treatment	BSMV:FgSSP1	BSMV:FgSSP2	BSMV:FgSSP4	BSMV:FgSSP5	BSMV:FgSSP6
	0.508	0.804	1.006	1.700	2.064

Treatment	BSMV:FgSSP7	BSMV:MCS4D	No Virus
	1.309	1.117	0.244

Standard errors

Treatment	BSMV:FgSSP1	BSMV:FgSSP2	BSMV:FgSSP4	BSMV:FgSSP5	BSMV:FgSSP6
	0.354	0.364	0.392	0.293	0.305

Treatment	BSMV:FgSSP7	BSMV:MCS4D	No Virus
	0.288	0.242	0.239

Standard errors

Average:	0.3096
Maximum:	0.3919
Minimum:	0.2388

Regression analysis

Response variate:	Inf_12_dpi
Binomial totals:	Total_infected_spiklets
Distribution:	Binomial
Link function:	Logit
Fitted terms:	Constant + batch + Treat

Summary of analysis

	mean	deviance	approx

Source	d.f.	deviance	deviance	ratio	F pr.
Regression	8	79.51	9.939	8.69	<.001
Residual	65	74.31	1.143		
Total	73	153.82	2.107		

Dispersion parameter is estimated to be 1.14 from the residual deviance.

Message: the following units have large standardized residuals.

Unit	Response	Residual
43	10.00	3.52
61	10.00	2.56

Message: the following units have high leverage.

Unit	Response	Leverage
42	6.00	0.30
43	10.00	0.30

Estimates of parameters

Parameter	estimate	s.e.	t(65)	t pr.	antilog of estimate
Constant	5.362	0.978	5.48	<.001	213.1
batch B	-1.354	0.680	-1.99	0.051	0.2583
batch C	-2.136	0.667	-3.20	0.002	0.1181
Treat BSMV:FgSSP6+7	-1.156	0.884	-1.31	0.196	0.3148
Treat BSMV:FgSSP6-SP	-1.899	0.815	-2.33	0.023	0.1498
Treat BSMV:FgSSP7	-0.893	0.873	-1.02	0.310	0.4094
Treat BSMV:FgSSP7-SP	-2.324	0.803	-2.89	0.005	0.09787
Treat BSMV:MCS4D	-2.239	0.822	-2.72	0.008	0.1065
Treat No Virus	-2.775	0.846	-3.28	0.002	0.06232

Message: s.e.s are based on the residual deviance.

Parameters for factors are differences compared with the reference level:

Factor	Reference level
batch	A
Treat	BSMV:FgSSP6

Accumulated analysis of deviance

Change	d.f.	deviance	mean deviance	deviance ratio	approx F pr.
+ batch + Treat	8	79.510	9.939	8.69	<.001
Residual	65	74.307	1.143		
Total	73	153.817	2.107		

```
  45  PREDICT [PRINT=description,predictions,se,sed,lsd; LSDLEVEL=5;
COMBINATIONS=present;\
  46    BACKTRANSFORM=link; ADJUST=marginal] Treat; LEVELS=*
```

Predictions from regression model

These predictions are estimated mean proportions, formed on the scale of the response variable, corresponding to one binomial trial, adjusted with respect to some factors as specified below.

The predictions have been formed only for those combinations of factor levels that are present in the data.

The predictions have been standardized by averaging over the levels of some factors:

Factor	Weighting policy	Status of weights
batch	Marginal weights	Adjusted to exclude combinations not present

The standard errors are appropriate for interpretation of the predictions as summaries of the data rather than as forecasts of new observations.

Response variate: Inf_12_dpi

Treat	Prediction	s.e.
BSMV:FgSSP6	0.9756	0.01815
BSMV:FgSSP6+7	0.9274	0.02942
BSMV:FgSSP6-SP	0.8360	0.03670
BSMV:FgSSP7	0.9429	0.02220
BSMV:FgSSP7-SP	0.7708	0.04007
BSMV:MCS4D	0.8177	0.04229
No Virus	0.7308	0.06531

Standard errors of differences of predictions

Treat BSMV:FgSSP6	1	*			
Treat BSMV:FgSSP6+7	2	0.03441	*		
Treat BSMV:FgSSP6-SP	3	0.04100	0.04744	*	
Treat BSMV:FgSSP7	4	0.02864	0.03670	0.04294	*
Treat BSMV:FgSSP7-SP	5	0.04419	0.05121	0.05370	0.04599
Treat BSMV:MCS4D	6	0.04599	0.05150	0.05596	0.04769
Treat No Virus	7	0.06775	0.07140	0.07501	0.06894
		1	2	3	4

Treat BSMV:FgSSP7-SP	5	*		
Treat BSMV:MCS4D	6	0.05813	*	
Treat No Virus	7	0.07699	0.07779	*
		5	6	7

Least significant differences of predictions (5% level)

Treat BSMV:FgSSP6	1	*			
Treat BSMV:FgSSP6+7	2	0.0687	*		
Treat BSMV:FgSSP6-SP	3	0.0819	0.0947	*	
Treat BSMV:FgSSP7	4	0.0572	0.0733	0.0858	*
Treat BSMV:FgSSP7-SP	5	0.0882	0.1023	0.1072	0.0918
Treat BSMV:MCS4D	6	0.0918	0.1029	0.1118	0.0953
Treat No Virus	7	0.1353	0.1426	0.1498	0.1377
		1	2	3	4

Treat BSMV:FgSSP7-SP	5	*	
Treat BSMV:MCS4D	6	0.1161	*

Treat No Virus	7	0.1538 5	0.1554 6	* 7

Figure 5.12. Average necrotic area of *N. benthamiana* leaves inoculated with *Fg*. A minimum of 6 leaves per virus treatment were analysed.

REML variance components analysis

Response variate: LOG10((area_mm2+1))
Fixed model: Constant + Treatment
Random model: Experiment + Experiment.Leaves
Number of units: 68

Experiment.Leaves used as residual term

Sparse algorithm with AI optimisation

Convergence monitoring

```
Cycle   Deviance   Current variance parameters: gammas, sigma2, others
    0   -21.4618   1.00000  0.200374
    1   -22.4616  0.492952  0.201381
    2   -23.4008  0.132817  0.205342
    3   -23.4117  0.120030  0.205777
    4   -23.4141  0.111314  0.206111
    5   -23.4141  0.111148  0.206117
    6   -23.4141  0.111137  0.206118
```

Estimated variance components

Random term	component	s.e.
Experiment	0.0229	0.0340

Residual variance model

Term	Model(order)	Parameter	Estimate	s.e.
Experiment.Leaves	Identity	Sigma2	0.206	0.0371

Deviance: -2*Log-Likelihood

Deviance	d.f.
-23.41	62

Note: deviance omits constants which depend on fixed model fitted.

Tests for fixed effects

Sequentially adding terms to fixed model

Fixed term	Wald statistic	n.d.f.	F statistic	d.d.f.	F pr
Treatment	3.94	3	1.31	62.7	0.278

Dropping individual terms from full fixed model

Fixed term	Wald statistic	n.d.f.	F statistic	d.d.f.	F pr
Treatment	3.94	3	1.31	62.7	0.278

Message: denominator degrees of freedom for approximate F-tests are calculated using algebraic derivatives ignoring fixed/boundary/singular variance parameters.

```
  99  VPREDICT [PRINT=description,prediction,se,avesed]
CLASSIFY=Treatment; LEVELS=*; PARALLEL=*
```

Predictions from REML analysis

Model terms included for prediction: Constant + Treatment
Model terms excluded for prediction: Experiment

Status of model variables in prediction:

Variable	Type	Status
Treatment	factor	Classifies predictions
Constant	factor	Included in prediction
Experiment	factor	Ignored

Response variate: LOG10((area_mm2+1))

Predictions

Treatment	FgSSP6	FgSSP7	Healthy	MCS
	1.388	1.348	1.155	1.138

Standard errors

Treatment	FgSSP6	FgSSP7	Healthy	MCS
	0.1376	0.1329	0.1545	0.1469

Approximate average standard error of difference: 0.1601 (calculated on variance scale)

Appedix 3: Western blot analysis of wheat ears infected with BSMV:FgSSP6 and BSMV:FgSSP7

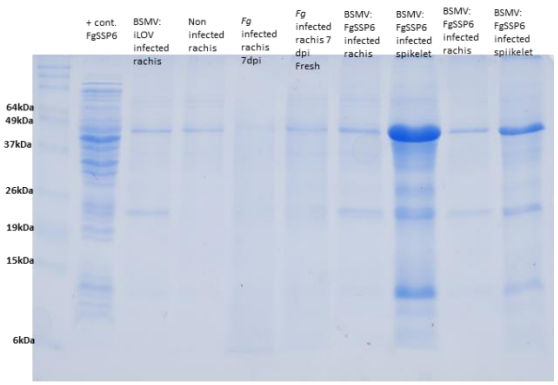
+ cont. FgSSP6
BSMV: iLOV infected rachis
Non infected rachis
Fg infected rachis 7dpi
Fg infected rachis 7 dpi Fresh
BSMV: FgSSP6 infected rachis
BSMV: FgSSP6 infected spikelet
BSMV: FgSSP6 infected rachis
BSMV: FgSSP6 infected spiikelet
64kDa
49kDa
37kDa
26kDa
19kDa
15kDa
6kDa

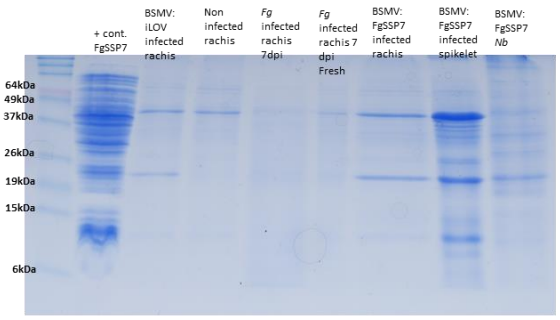
+ cont. FgSSP7
BSMV: iLOV infected rachis
Non infected rachis
Fg infected rachis 7dpi
Fg infected rachis 7 dpi Fresh
BSMV: FgSSP7 infected rachis
BSMV: FgSSP7 infected spikelet
BSMV: FgSSP7 Nb
64kDa
49kDa
37kDa
26kDa
19kDa
15kDa
6kDa

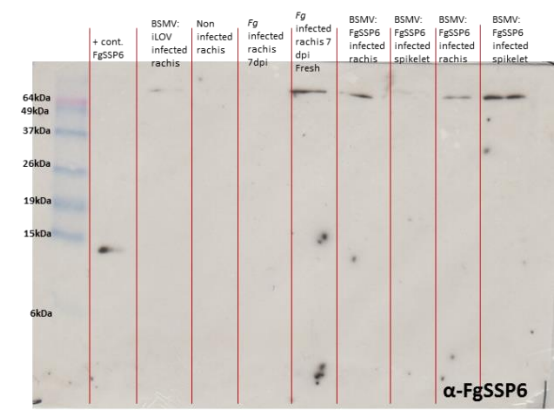
+ cont. FgSSP6
BSMV: iLOV infected rachis
Non infected rachis
Fg infected rachis 7dpi
Fg infected rachis 7 dpi Fresh
BSMV: FgSSP6 infected rachis
BSMV: FgSSP6 infected spikelet
BSMV: FgSSP6 infected rachis
BSMV: FgSSP6 infected spikelet
64kDa
49kDa
37kDa
26kDa
19kDa
15kDa
6kDa
α-FgSSP6

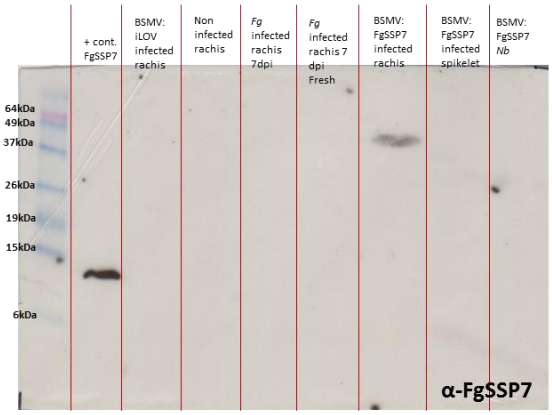
+ cont. FgSSP7
BSMV: iLOV infected rachis
Non infected rachis
Fg infected rachis 7dpi
Fg infected rachis 7 dpi Fresh
BSMV: FgSSP7 infected rachis
BSMV: FgSSP7 infected spikelet
BSMV: FgSSP7 Nb
64kDa
49kDa
37kDa
26kDa
19kDa
15kDa
6kDa
α-FgSSP7

Appendix 4: 24 hours post-infiltration of FgSSP6 and FgSSP7 heterologous proteins in 10 days-old wheat leaves cv. Bobwhite.

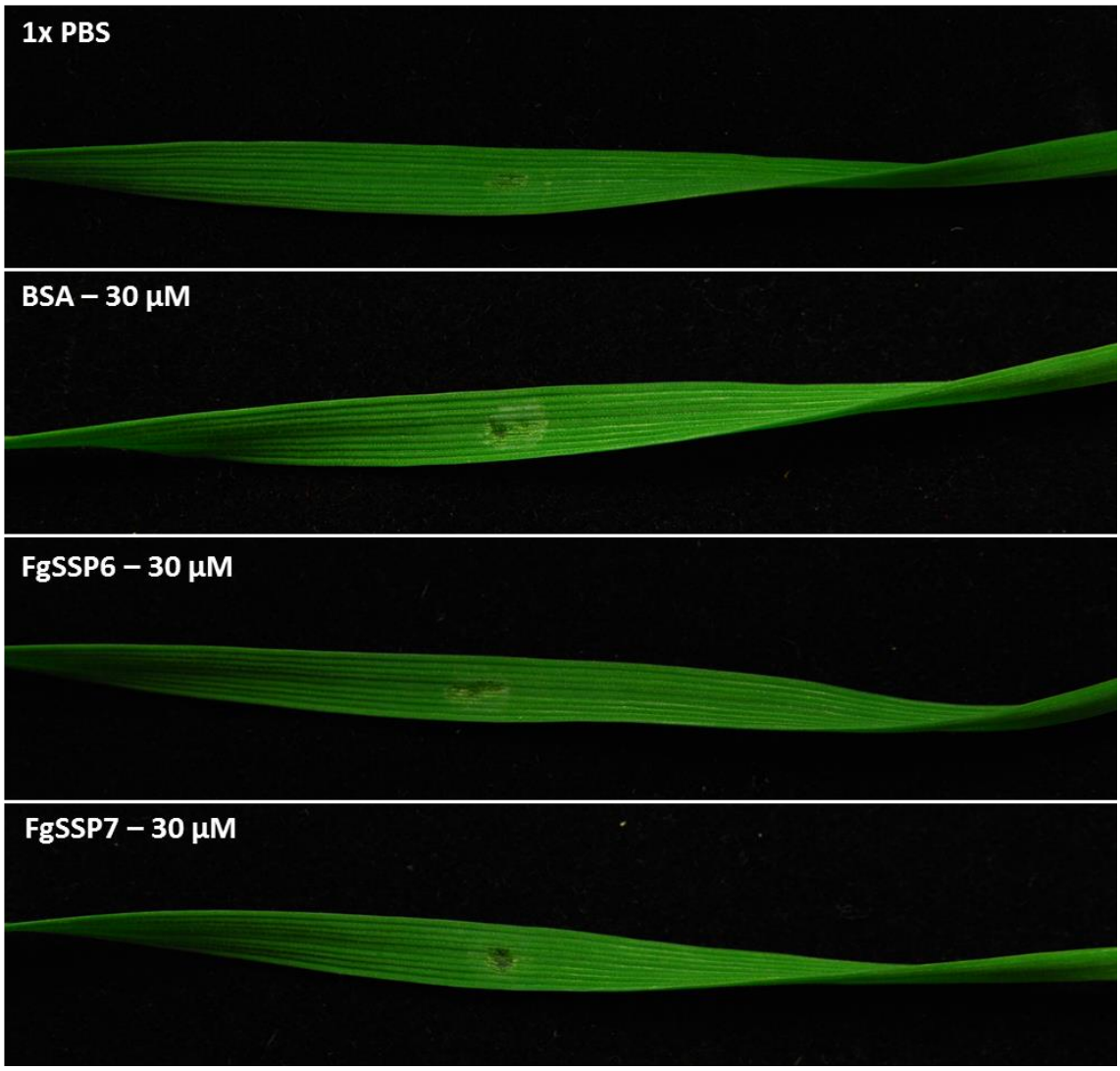

References

Agrios GN, 2005. *Plant Pathology*. Amsterdam ; Boston: Elsevier Academic Press.

Aguileta G, Lengelle J, Chiapello H*, et al.*, 2012. Genes under positive selection in a model plant pathogenic fungus, Botrytis. *Infection Genetics and Evolution* **12**, 987-96.

Alexander NJ, Hohn TM, Mccormick SP, 1998. The TRI11 gene of Fusarium sporotrichioides encodes a cytochrome P-450 monooxygenase required for C-15 hydroxylation in trichothecene biosynthesis. *Applied and Environmental Microbiology* **64**, 221-5.

Alexander NJ, Mccormick SP, Hohn TM, 1999. TRI12, a trichothecene efflux pump from Fusarium sporotrichioides: gene isolation and expression in yeast. *Molecular and General Genetics* **261**, 977-84.

Alexander NJ, Mccormick SP, Waalwijk C, Van Der Lee T, Proctor RH, 2011. The genetic basis for 3-ADON and 15-ADON trichothecene chemotypes in Fusarium. *Fungal Genetics and Biology* **48**, 485-95.

Alfaro M, Oguiza JA, Ramirez L, Pisabarro AG, 2014. Comparative analysis of secretomes in basidiomycete fungi. *J Proteomics* **102**, 28-43.

Alkhayyat F, Yu JH, 2014. Upstream Regulation of Mycotoxin Biosynthesis. *Advances in Applied Microbiology, Vol 86* **86**, 251-78.

Anders C, Niewoehner O, Duerst A, Jinek M, 2014. Structural basis of PAM-dependent target DNA recognition by the Cas9 endonuclease. *Nature* **513**, 569-73.

Anderson JA, Stack RW, Liu S*, et al.*, 2001. DNA markers for Fusarium head blight resistance QTLs in two wheat populations. *Theoretical and Applied Genetics* **102**, 1164-8.

Antoniw J, Beacham AM, Baldwin TK, Urban M, Rudd JJ, Hammond-Kosack KE, 2011. OmniMapFree: A unified tool to visualise and explore sequenced genomes. *Bmc Bioinformatics* **12**.

Arst HN, Penalva MA, 2003. pH regulation in Aspergillus and parallels with higher eukaryotic regulatory systems. *Trends in Genetics* **19**, 224-31.

Aslanidis C, Dejong PJ, 1990. Ligation-Independent Cloning of Pcr Products (Lic-Pcr). *Nucleic Acids Research* **18**, 6069-74.

Astolfi P, Reynoso MM, Ramirez ML*, et al.*, 2012. Genetic population structure and trichothecene genotypes of Fusarium graminearum isolated from wheat in southern Brazil. *Plant Pathology* **61**, 289-95.

Baccelli I, 2015. Cerato-platanin family proteins: one function for multiple biological roles? *Frontiers in Plant Science* **5**.

Baccelli I, Lombardi L, Luti S*, et al.*, 2014a. Cerato-Platanin Induces Resistance in Arabidopsis Leaves through Stomatal Perception, Overexpression of Salicylic Acid- and Ethylene-Signalling Genes and Camalexin Biosynthesis. *Plos One* **9**.

Baccelli I, Luti S, Bernardi R, Scala A, Pazzagli L, 2014b. Cerato-platanin shows expansin-like activity on cellulosic materials. *Applied Microbiology and Biotechnology* **98**, 175-84.

Baldwin TK, Urban M, Brown N, Hammond-Kosack KE, 2010. A Role for Topoisomerase I in Fusarium graminearum and F. culmorum Pathogenesis and Sporulation. *Molecular Plant-Microbe Interactions* **23**, 566-77.

Barsottini MRD, De Oliveira JF, Adamoski D*, et al.*, 2013. Functional Diversification of Cerato-Platanins in Moniliophthora perniciosa as Seen by Differential Expression and Protein Function Specialization. *Molecular Plant-Microbe Interactions* **26**, 1281-93.

Bassham DC, Brandizzi F, Otegui MS, Sanderfoot AA, 2008. The secretory system of Arabidopsis. *Arabidopsis Book* **6**, e0116.

Baulcombe DC, 2015. VIGS, HIGS and FIGS: small RNA silencing in the interactions of viruses or filamentous organisms with their plant hosts. *Current Opinion in Plant Biology* **26**, 141-6.

Beckerman JL, Ebbole DJ, 1996. MPG1, a gene encoding a fungal hydrophobin of Magnaporthe grisea, is involved in surface recognition. *Molecular Plant-Microbe Interactions* **9**, 450-6.

Bedell JA, Korf I, Gish W, 2000. MaskerAid: a performance enhancement to RepeatMasker. *Bioinformatics* **16**, 1040-1.

Berthiller F, Crews C, Dall'asta C*, et al.*, 2013. Masked mycotoxins: A review. *Molecular Nutrition & Food Research* **57**, 165-86.

Besemer J, Borodovsky M, 2005. GeneMark: web software for gene finding in prokaryotes, eukaryotes and viruses. *Nucleic Acids Research* **33**, W451-W4.

Bhadauria V, Banniza S, Wei Y, Peng YL, 2009. Reverse genetics for functional genomics of phytopathogenic fungi and oomycetes. *Comp Funct Genomics*, 380719.

Bickhart DM, Liu GE, 2014. The challenges and importance of structural variation detection in livestock. *Frontiers in Genetics* **5**.

Blumke A, Falter C, Herrfurth C*, et al.*, 2014. Secreted Fungal Effector Lipase Releases Free Fatty Acids to Inhibit Innate Immunity-Related Callose Formation during Wheat Head Infection. *Plant Physiology* **165**, 346-58.

Boenisch MJ, Schafer W, 2011. Fusarium graminearum forms mycotoxin producing infection structures on wheat. *Bmc Plant Biology* **11**.

Bolton MD, Van Esse HP, Vossen JH*, et al.*, 2008. The novel *Cladosporium fulvum* lysin motif effector Ecp6 is a virulence factor with orthologues in other fungal species. *Molecular Microbiology* **69**, 119-36.

Bonazza K, Gaderer R, Neudl S*, et al.*, 2015. The fungal cerato-platanin protein EPL1 forms highly ordered layers at hydrophobic/hydrophilic interfaces. *Soft Matter* **11**, 1723-32.

Bonnighausen J, Gebhard D, Kroger C*, et al.*, 2015. Disruption of the GABA shunt affects mitochondrial respiration and virulence in the cereal pathogen Fusarium graminearum. *Molecular Microbiology* **98**, 1115-32.

Bos JIB, Kanneganti TD, Young C*, et al.*, 2006. The C-terminal half of Phytophthora infestans RXLR effector AVR3a is sufficient to trigger R3a-mediated hypersensitivity and suppress INF1-induced cell death in Nicotiana benthamiana. *Plant Journal* **48**, 165-76.

Bottalico A, 1998. FUSARIUM DISEASES OF CEREALS: SPECIES COMPLEX AND RELATED MYCOTOXIN PROFILES, IN EUROPE. *Journal of Plant Pathology* **80**, 85-103.

Bottalico A, Perrone G, 2002. Toxigenic *Fusarium* species and mycotoxins associated with head blight in small-grain cereals in Europe. *European Journal of Plant Pathology* **108**, 611-24.

Bourras S, Mcnally KE, Ben-David R*, et al.*, 2015. Multiple Avirulence Loci and Allele-Specific Effector Recognition Control the Pm3 Race-Specific Resistance of Wheat to Powdery Mildew. *Plant Cell* **27**, 2991-3012.

Bouton C, King R, Chen H*, et al.*, 2017. Foxtail mosaic virus: A New Viral Vector for Heterologous Protein Expression in Wheat and Maize. *Plant Physiology* **submitted**.

Boyes DC, Zayed AM, Ascenzi R*, et al.*, 2001. Growth stage-based phenotypic analysis of arabidopsis: A model for high throughput functional genomics in plants. *Plant Cell* **13**, 1499-510.

Braaksma M, Martens-Uzunova ES, Punt PJ, Schaap PJ, 2010. An inventory of the Aspergillus niger secretome by combining in silico predictions with shotgun proteomics data. *Bmc Genomics* **11**.

Bradford MM, 1976. A rapid and sensitive method for the quantitation of microgram quantities of protein utilizing the principle of protein-dye binding. *Anal Biochem* **72**, 248-54.

Brewer HC, Hammond-Kosack KE, 2015. Host to a Stranger: Arabidopsis and Fusarium Ear Blight. *Trends in Plant Science* **20**, 651-63.

Brown DW, Mccormick SP, Alexander NJ, Proctor RH, Desjardins AE, 2001. A genetic and biochemical approach to study trichothecene diversity in Fusarium sporotrichioides and Fusarium graminearum. *Fungal Genetics and Biology* **32**, 121-33.

Brown DW, Mccormick SP, Alexander NJ, Proctor RH, Desjardins AE, 2002. Inactivation of a cytochrome P-450 is a determinant of trichothecene diversity in Fusarium species. *Fungal Genetics and Biology* **36**, 224-33.

Brown NA, 2011. *A comparison of the infection biology and transcriptome of wild-type and single gene deletion strains of Fusarium graminearum*: University of Edinburgh, Doctor of Phylosophy PhD thesis.

Brown NA, Antoniw J, Hammond-Kosack KE, 2012. The predicted secretome of the plant pathogenic fungus *Fusarium graminearum*: a refined comparative analysis. *Plos One* **7**, e33731.

Brown NA, Bass C, Baldwin TK*, et al.*, 2011. Characterisation of the *Fusarium graminearum*-wheat floral interaction. *J Pathog* **2011**, 626345.

Brown NA, Evans J, Mead A, Hammond-Kosack KE, 2017. A spatial temporal analysis of the Fusarium graminearum transcriptome during symptomless and symptomatic wheat infection. *Molecular Plant Pathology*.

Brown NA, Hammond-Kosack KE, 2015. Secreted biomolecules in fungal plant pathogenesis. In: Gupta VK, Mach RL, Sreenivasaprasad S, eds. *Fungal Biomolecules: Sources, Applications and Recent Developments.* Chichester, UK: John Wiley & Sons, Ltd.

Brown NA, Urban M, Van De Meene AML, Hammond-Kosack KE, 2010. The infection biology of *Fusarium graminearum*: defining the pathways of spikelet to spikelet colonisation in wheat ears. *Fungal Biology* **114**, 555-71.

Bryan GT, Wu KS, Farrall L*, et al.*, 2000. A single amino acid difference distinguishes resistant and susceptible alleles of the rice blast resistance gene Pi-ta. *Plant Cell* **12**, 2033-45.

Buerstmayr H, Lemmens M, 2015. Breeding healthy cereals: genetic improvement of Fusarium resistance and consequences for mycotoxins. *World Mycotoxin Journal* **8**, 591-602.

Buerstmayr H, Steiner B, Hartl L*, et al.*, 2003. Molecular mapping of QTLs for Fusarium head blight resistance in spring wheat. II. Resistance to fungal penetration and spread. *Theoretical and Applied Genetics* **107**, 503-8.

Burch-Smith TM, Anderson JC, Martin GB, Dinesh-Kumar SP, 2004. Applications and advantages of virus-induced gene silencing for gene function studies in plants. *Plant Journal* **39**, 734-46.

Burri L, Lithgow T, 2004. A complete set of SNAREs in yeast. *Traffic* **5**, 45-52.

Cantarel BL, Korf I, Robb SMC*, et al.*, 2008. MAKER: An easy-to-use annotation pipeline designed for emerging model organism genomes. *Genome Research* **18**, 188-96.

Cao J, Shi F, 2012. Evolution of the RALF Gene Family in Plants: Gene Duplication and Selection Patterns. *Evolutionary Bioinformatics* **8**, 271-92.

Catlett NL, Lee B-N, Yoder O, Turgeon BG, 2003. Split-marker recombination for efficient targeted deletion of fungal genes. *Fungal Genetics Reports* **50**, 9-11.

Chakraborty S, Tiedemann AV, Teng PS, 2000. Climate change: potential impact on plant diseases. *Environmental Pollution* **108**, 317-26.

Chang HX, Domier LL, Radwan O, Yendrek CR, Hudson ME, Hartman GL, 2016. Identification of Multiple Phytotoxins Produced by Fusarium virguliforme Including a Phytotoxic Effector (FvNIS1) Associated With Sudden Death Syndrome Foliar Symptoms. *Mol Plant Microbe Interact* **29**, 96-108.

Chen HX, Quintana J, Kovalchuk A, Ubhayasekera W, Asiegbu FO, 2015a. A cerato-platanin-like protein HaCPL2 from Heterobasidion annosum sensu stricto induces cell death in Nicotiana tabacum and Pinus sylvestris. *Fungal Genetics and Biology* **84**, 41-51.

Chen MJ, Zhang CZ, Zi Q, Qiu DW, Liu WX, Zeng HM, 2014. A novel elicitor identified from Magnaporthe oryzae triggers defense responses in tobacco and rice. *Plant Cell Reports* **33**, 1865-79.

Chen SB, Songkumarn P, Venu RC*, et al.*, 2013. Identification and Characterization of In planta-Expressed Secreted Effector Proteins from Magnaporthe oryzae That Induce Cell Death in Rice. *Molecular Plant-Microbe Interactions* **26**, 191-202.

Chen WX, Kastner C, Nowara D*, et al.*, 2016. Host-induced silencing of *Fusarium culmorum* genes protects wheat from infection. *Journal of Experimental Botany* **67**, 4979-91.

Chen Y, Gao QX, Huang MM*, et al.*, 2015b. Characterization of RNA silencing components in the plant pathogenic fungus *Fusarium graminearum*. *Scientific Reports* **5**, 12500.

Coakley SM, Scherm H, Chakraborty S, 1999. Climate change and plant disease management. *Annual Review of Phytopathology* **37**, 399-426.

Coleman JJ, Rounsley SD, Rodriguez-Carres M*, et al.*, 2009. The genome of Nectria haematococca: contribution of supernumerary chromosomes to gene expansion. *PLoS Genet* **5**, e1000618.

Costa V, Angelini C, De Feis I, Ciccodicola A, 2010. Uncovering the Complexity of Transcriptomes with RNA-Seq. *Journal of Biomedicine and Biotechnology*.

Covey PA, Subbaiah CC, Parsons RL*, et al.*, 2010. A pollen-specific RALF from tomato that regulates pollen tube elongation. *Plant Physiology* **153**, 703-15.

Cowger C, Patton-Ozkurt J, Brown-Guedira G, Perugini L, 2009. Post-Anthesis Moisture Increased Fusarium Head Blight and Deoxynivalenol Levels in North Carolina Winter Wheat. *Phytopathology* **99**, 320-7.

Cuellar WJ, Kreuze JF, Rajamaki ML, Cruzado KR, Untiveros M, Valkonen JPT, 2009. Elimination of antiviral defense by viral RNase III. *Proceedings of the National Academy of Sciences of the United States of America* **106**, 10354-8.

Cundliffe E, Cannon M, Davies J, 1974. Mechanism of Inhibition of Eukaryotic Protein-Synthesis by Trichothecene Fungal Toxins. *Proceedings of the National Academy of Sciences of the United States of America* **71**, 30-4.

Cuomo CA, Gueldener U, Xu JR*, et al.*, 2007. The Fusarium graminearum genome reveals a link between localized polymorphism and pathogen specialization. *Science* **317**, 1400-2.

Cuthbert PA, Somers DJ, Brule-Babel A, 2007. Mapping of Fhb2 on chromosome 6BS: a gene controlling Fusarium head blight field resistance in bread wheat (Triticum aestivum L.). *Theoretical and Applied Genetics* **114**, 429-37.

Cuthbert PA, Somers DJ, Thomas J, Cloutier S, Brule-Babel A, 2006. Fine mapping Fhb1, a major gene controlling fusarium head blight resistance in bread wheat (Triticum aestivum L.). *Theoretical and Applied Genetics* **112**, 1465-72.

Cuzick A, Urban M, Hammond-Kosack K, 2008. Fusarium graminearum gene deletion mutants map1 and tri5 reveal similarities and differences in the pathogenicity requirements to cause disease on Arabidopsis and wheat floral tissue. *New Phytologist* **177**, 990-1000.

Dash S, Van Hemert J, Hong L, Wise RP, Dickerson JA, 2012. PLEXdb: gene expression resources for plants and plant pathogens. *Nucleic Acids Research* **40**, D1194-D201.

De Guillen K, Ortiz-Vallejo D, Gracy J, Fournier E, Kroj T, Padilla A, 2015. Structure Analysis Uncovers a Highly Diverse but Structurally Conserved Effector Family in Phytopathogenic Fungi. *Plos Pathogens* **11**, e1005228.

De Jonge R, Bolton MD, Kombrink A, Van Den Berg GCM, Yadeta KA, Thomma BPHJ, 2013. Extensive chromosomal reshuffling drives evolution of virulence in an asexual pathogen. *Genome Research* **23**, 1271-82.

De Jonge R, Bolton MD, Thomma BPHJ, 2011. How filamentous pathogens co-opt plants: the ins and outs of fungal effectors. *Current Opinion in Plant Biology* **14**, 400-6.

De Jonge R, Thomma BPHJ, 2009. Fungal LysM effectors: extinguishers of host immunity? *Trends in Microbiology* **17**, 151-7.

De Oliveira AL, Gallo M, Pazzagli L*, et al.*, 2011. The Structure of the Elicitor Cerato-platanin (CP), the First Member of the CP Fungal Protein Family, Reveals a Double psi beta-Barrel Fold and Carbohydrate Binding. *Journal of Biological Chemistry* **286**, 17560-8.

De Wit PJ, 2016. Apoplastic fungal effectors in historic perspective; a personal view. *New Phytologist* **212**, 805-13.

Dean R, Van Kan JaL, Pretorius ZA*, et al.*, 2012. The Top 10 fungal pathogens in molecular plant pathology. *Molecular Plant Pathology* **13**, 414-30.

Dean RA, Talbot NJ, Ebbole DJ*, et al.*, 2005. The genome sequence of the rice blast fungus Magnaporthe grisea. *Nature* **434**, 980-6.

Del Ponte EM, Fernandes JMC, Pavan W, Baethgen WE, 2009. A model-based assessment of the impacts of climate variability on Fusarium head blight seasonal risk in southern Brazil. *Journal of Phytopathology* **157**, 675-81.

Del Ponte EM, Spolti P, Ward TJ*, et al.*, 2015. Regional and field-specific factors affect the composition of Fusarium head blight pathogens in subtropical no-till wheat agroecosystem of Brazil. *Phytopathology* **105**, 246-54.

Derbise A, Song YP, Parikh S, Fischetti VA, Pancholi V, 2004. Role of the C-terminal lysine residues of streptococcal surface enolase in Glu- and Lys-plasminogen-binding activities of group A streptococci. *Infection and Immunity* **72**, 94-105.

Desjardins AE, Proctor RH, 2007. Molecular biology of *Fusarium* mycotoxins. *International Journal of Food Microbiology* **119**, 47-50.

Desmond OJ, Manners JM, Stephens AE*, et al.*, 2008. The Fusarium mycotoxin deoxynivalenol elicits hydrogen peroxide production, programmed cell death and defence responses in wheat. *Molecular Plant Pathology* **9**, 435-45.

Dill-Macky R, Jones RK, 2000. The effect of previous crop residues and tillage on Fusarium head blight of wheat. *Plant Disease* **84**, 71-6.

Ding LN, Xu HB, Yi HY*, et al.*, 2011. Resistance to Hemi-Biotrophic F-graminearum Infection Is Associated with Coordinated and Ordered Expression of Diverse Defense Signaling Pathways. *Plos One* **6**.

Djamei A, Schipper K, Rabe F*, et al.*, 2011. Metabolic priming by a secreted fungal effector. *Nature* **478**, 395-400.

Djonovic S, Pozo MJ, Dangott LJ, Howell CR, Kenerley CM, 2006. Sm1, a proteinaceous elicitor secreted by the biocontrol fungus Trichoderma virens induces plant defense responses and systemic resistance. *Molecular Plant-Microbe Interactions* **19**, 838-53.

Djonovic S, Vargas WA, Kolomiets MV, Horndeski M, Wiest A, Kenerley CM, 2007. A proteinaceous elicitor Sm1 from the beneficial fungus Trichoderma virens is required for induced systemic resistance in maize. *Plant Physiology* **145**, 875-89.

Do Canto AM, Ceciliato PHO, Ribeiro B*, et al.*, 2014. Biological activity of nine recombinant AtRALF peptides: Implications for their perception and function in Arabidopsis. *Plant Physiology and Biochemistry* **75**, 45-54.

Doehlemann G, Reissmann S, Assmann D, Fleckenstein M, Kahmann R, 2011. Two linked genes encoding a secreted effector and a membrane protein are essential for Ustilago maydis-induced tumour formation. *Molecular Microbiology* **81**, 751-66.

Dou DL, Kale SD, Wang X*, et al.*, 2008. RXLR-mediated entry of Phytophthora sojae effector Avr1b into soybean cells does not require pathogen-encoded machinery. *Plant Cell* **20**, 1930-47.

Duan QH, Kita D, Li C, Cheung AY, Wu HM, 2010. FERONIA receptor-like kinase regulates RHO GTPase signaling of root hair development. *Proceedings of the National Academy of Sciences of the United States of America* **107**, 17821-6.

Dufresne M, Van Der Lee T, Ben M'barek S*, et al.*, 2008. Transposon-tagging identifies novel pathogenicity genes in Fusarium graminearum. *Fungal Genetics and Biology* **45**, 1552-61.

Dunn B, Richter C, Kvitek DJ, Pugh T, Sherlock G, 2012. Analysis of the Saccharomyces cerevisiae pan-genome reveals a pool of copy number variants distributed in diverse yeast strains from differing industrial environments. *Genome Research* **22**, 908-24.

Duveiller E, 2004. Controlling foliar blights of wheat in the rice-wheat systems of Asia. *Plant Disease* **88**, 552-6.

Duveiller E, Singh P, Mezzalama M, Singh R, Dababat A, 2012. Wheat diseases and pests: a guide for field identification.

Duveiller E, Singh RP, Nicol JM, 2007. The challenges of maintaining wheat productivity: pests, diseases, and potential epidemics. *Euphytica* **157**, 417-30.

Dweba CC, Figlan S, Shimelis HA*, et al.*, 2017. Fusarium head blight of wheat: Pathogenesis and control strategies. *Crop Protection* **91**, 114-22.

Dyer RB, Plattner RD, Kendra DF, Brown DW, 2005. Fusarium graminearum TRI14 is required for high virulence and DON production on wheat but not for DON synthesis in vitro. *Journal of Agricultural and Food Chemistry* **53**, 9281-7.

Egan MJ, Wang ZY, Jones MA, Smirnoff N, Talbot NJ, 2007. Generation of reactive oxygen species by fungal NADPH oxidases is required for rice blast disease. *Proceedings of the National Academy of Sciences of the United States of America* **104**, 11772-7.

Eisenhaber B, Schneider G, Wildpaner M, Eisenhaber F, 2004. A sensitive predictor for potential GPI lipid modification sites in fungal protein sequences and its application to genome-wide studies for Aspergillus nidulans, Candida albicans Neurospora crassa, Saccharomyces cerevisiae and Schizosaccharomyces pombe. *Journal of Molecular Biology* **337**, 243-53.

El Amrani A, Barakate A, Askari BM*, et al.*, 2004. Coordinate expression and independent subcellular targeting of multiple proteins from a single transgene. *Plant Physiology* **135**, 16-24.

Ellis JG, Rafiqi M, Gan P, Chakrabarti A, Dodds PN, 2009. Recent progress in discovery and functional analysis of effector proteins of fungal and oomycete plant pathogens. *Current Opinion in Plant Biology* **12**, 399-405.

Ellner FM, 2005. Results of long-term field studies into the effect of strobilurin containing fungicides on the production of mycotoxins in several winter wheat varieties. *Mycotoxin Research* **21**, 112-5.

Emanuelsson O, Nielsen H, Brunak S, Von Heijne G, 2000. Predicting subcellular localization of proteins based on their N-terminal amino acid sequence. *Journal of Molecular Biology* **300**, 1005-16.

Espino JJ, Gutierrez-Sanchez G, Brito N, Shah P, Orlando R, Gonzalez C, 2010. The Botrytis cinerea early secretome. *Proteomics* **10**, 3020-34.

Fairhead C, Llorente B, Denis F, Soler M, Dujon B, 1996. New vectors for combinatorial deletions in yeast chromosomes and for gap-repair cloning using 'split-marker' recombination. *Yeast* **12**, 1439-58.

Fairhead C, Thierry A, Denis F, Eck M, Dujon B, 1998. 'Mass-murder' of ORFs from three regions of chromosome XI from Saccharomyces cerevisiae. *Gene* **223**, 33-46.

Fan JR, Urban M, Parker JE*, et al.*, 2013. Characterization of the sterol 14 alpha-demethylases of *Fusarium graminearum* identifies a novel genus-specific CYP51 function. *New Phytologist* **198**, 821-35.

Fao, 2009. How to Feed the World in 2050. In.: Food and Agriculture Organization of the United Nations.

Fao, 2016. Cereal Supply and Demand Brief. In.: Food and Agriculture Organization of United Nations.

Ferrari S, Sella L, Janni M, De Lorenzo G, Favaron F, D'ovidio R, 2012. Transgenic expression of polygalacturonase-inhibiting proteins in Arabidopsis and wheat increases resistance to the flower pathogen Fusarium graminearum. *Plant Biology* **14**, 31-8.

Ferre F, Clote P, 2005. DiANNA: a web server for disulfide connectivity prediction. *Nucleic Acids Research* **33**, W230-W2.

Finn RD, Attwood TK, Babbitt PC*, et al.*, 2017. InterPro in 2017-beyond protein family and domain annotations. *Nucleic Acids Research* **45**, D190-D9.

Finn RD, Coggill P, Eberhardt RY*, et al.*, 2016. The Pfam protein families database: towards a more sustainable future. *Nucleic Acids Research* **44**, D279-D85.

Fitzgerald TL, Powell JJ, Schneebeli K*, et al.*, 2015. Brachypodium as an emerging model for cereal-pathogen interactions. *Annals of Botany* **115**, 717-31.

Fontan PA, Pancholi V, Nociari MM, Fischetti VA, 2000. Antibodies to streptococcal surface enolase react with human alpha-enolase: Implications in poststreptococcal sequelae. *Journal of Infectious Diseases* **182**, 1712-21.

Fontana F, Santini A, Salvini M*, et al.*, 2008. Cerato-platanin treated plane leaves restrict Ceratocystis platani growth and overexpress defence-related genes. *Journal of Plant Pathology* **90**, 295-306.

Foroud NA, Mccormick SP, Macmillan T*, et al.*, 2012. Greenhouse studies reveal increased aggressiveness of emergent Canadian *Fusarium graminearum* chemotypes in wheat. *Plant Disease* **96**, 1271-9.

Franceschetti M, Maqbool A, Jiménez-Dalmaroni MJ, Pennington HG, Kamoun S, Banfield MJ, 2017. Effectors of Filamentous Plant Pathogens: Commonalities amid Diversity. *Microbiol Mol Biol Rev* **81**.

Frias M, Brito N, Gonzalez C, 2013. The Botrytis cinerea cerato-platanin BcSpl1 is a potent inducer of systemic acquired resistance (SAR) in tobacco and generates a wave of salicylic acid expanding from the site of application. *Molecular Plant Pathology* **14**, 191-6.

Frias M, Brito N, Gonzalez M, Gonzalez C, 2014. The phytotoxic activity of the cerato-platanin BcSpl1 resides in a two-peptide motif on the protein surface. *Molecular Plant Pathology* **15**, 342-51.

Frias M, Gonzalez C, Brito N, 2011. BcSpl1, a cerato-platanin family protein, contributes to Botrytis cinerea virulence and elicits the hypersensitive response in the host. *New Phytologist* **192**, 483-95.

Frías M, González C, Brito N, 2011. BcSpl1, a cerato-platanin family protein, contributes to Botrytis cinerea virulence and elicits the hypersensitive response in the host. *New Phytologist* **192**, 483-95.

Friesen TL, Meinhardt SW, Faris JD, 2007. The Stagonospora nodorum-wheat pathosystem involves multiple proteinaceous host-selective toxins and corresponding host sensitivity genes that interact in an inverse gene-for-gene manner. *Plant Journal* **51**, 681-92.

Friesen TL, Stukenbrock EH, Liu Z*, et al.*, 2006. Emergence of a new disease as a result of interspecific virulence gene transfer. *Nat Genet* **38**, 953-6.

Frischmann A, Neudl S, Gaderer R*, et al.*, 2013. Self-assembly at Air/Water Interfaces and Carbohydrate Binding Properties of the Small Secreted Protein EPL1 from the fungus Trichoderma atroviride. *Journal of Biological Chemistry* **288**, 4278-87.

Fu J, Hettler E, Wickes BL, 2006. Split marker transformation increases homologous integration frequency in Cryptococcus neoformans. *Fungal Genetics and Biology* **43**, 200-12.

Gaderer R, Bonazza K, Seidl-Seiboth V, 2014. Cerato-platanins: a fungal protein family with intriguing properties and application potential. *Applied Microbiology and Biotechnology* **98**, 4795-803.

Gaderer R, Lamdan NL, Frischmann A*, et al.*, 2015. Sm2, a paralog of the Trichoderma cerato-platanin elicitor Sm1, is also highly important for plant protection conferred by the fungal-root interaction of Trichoderma with maize. *Bmc Microbiology* **15**.

Gage MJ, Bruenn J, Fischer M, Sanders D, Smith TJ, 2001. KP4 fungal toxin inhibits growth in Ustilago maydis by blocking calcium uptake. *Molecular Microbiology* **41**, 775-85.

Gage MJ, Rane SG, Hockerman GH, Smith TJ, 2002. The virally encoded fungal toxin KP4 specifically blocks L-type voltage-gated calcium channels. *Molecular Pharmacology* **61**, 936-44.

Gale LR, Bryant JD, Calvo S*, et al.*, 2005. Chromosome complement of the fungal plant pathogen Fusarium graminearum based on genetic and physical mapping and cytological observations. *Genetics* **171**, 985-1001.

Gardiner DM, Kazan K, Manners JM, 2009. Novel genes of Fusarium graminearum that negatively regulate deoxynivalenol production and virulence. *Mol Plant Microbe Interact* **22**, 1588-600.

Gardiner DM, Mcdonald MC, Covarelli L*, et al.*, 2012. Comparative pathogenomics reveals horizontally acquired novel virulence genes in fungi infecting cereal hosts. *Plos Pathogens* **8**, e1002952.

Gardiner DM, Stiller J, Kazan K, 2014. Genome Sequence of Fusarium graminearum Isolate CS3005. *Genome Announc* **2**.

Georgelis N, Nikolaidis N, Cosgrove DJ, 2015. Bacterial expansins and related proteins from the world of microbes. *Applied Microbiology and Biotechnology* **99**, 3807-23.

Gilbert J, Brule-Babel A, Guerrieri AT*, et al.*, 2014. Ratio of 3-ADON and 15-ADON isolates of *Fusarium graminearum* recovered from wheat kernels in Manitoba from 2008 to 2012. *Canadian Journal of Plant Pathology* **36**, 54-63.

Gilbert J, Haber S, 2013. Overview of some recent research developments in Fusarium head blight of wheat. *Canadian Journal of Plant Pathology* **35**, 149-74.

Giraldo MC, Dagdas YF, Gupta YK*, et al.*, 2013. Two distinct secretion systems facilitate tissue invasion by the rice blast fungus Magnaporthe oryzae. *Nature Communications* **4**.

Giraldo MC, Valent B, 2013. Filamentous plant pathogen effectors in action. *Nature Reviews Microbiology* **11**, 800-14.

Godfrey D, Bohlenius H, Pedersen C, Zhang ZG, Emmersen J, Thordal-Christensen H, 2010. Powdery mildew fungal effector candidates share N-terminal Y/F/WxC-motif. *Bmc Genomics* **11**.

Golicz AA, Batley J, Edwards D, 2016a. Towards plant pangenomics. *Plant Biotechnology Journal* **14**, 1099-105.

Golicz AA, Bayer PE, Barker GC*, et al.*, 2016b. The pangenome of an agronomically important crop plant Brassica oleracea. *Nature Communications* **7**, 13390.

Goodwin S, Mcpherson JD, Mccombie WR, 2016. Coming of age: ten years of next-generation sequencing technologies. *Nat Rev Genet* **17**, 333-51.

Goswami RS, Kistler HC, 2005. Pathogenicity and in planta mycotoxin accumulation among members of the Fusarium graminearum species complex on wheat and rice. *Phytopathology* **95**, 1397-404.

Govrin EM, Levine A, 2000. The hypersensitive response facilitates plant infection by the necrotrophic pathogen Botrytis cinerea. *Curr Biol* **10**, 751-7.

Graham S, Browne RA, 2009. Anther Extrusion and Fusarium Head Blight Resistance in European Wheat. *Journal of Phytopathology* **157**, 580-2.

Greenshields DL, Liu G, Feng J, Selvaraj G, Wei Y, 2007. The siderophore biosynthetic gene SID1, but not the ferroxidase gene FET3, is required for full Fusarium graminearum virulence. *Molecular Plant Pathology* **8**, 411-21.

Guenther JC, Hallen-Adams HE, Bücking H, Shachar-Hill Y, Trail F, 2009. Triacylglyceride metabolism by Fusarium graminearum during colonization and sexual development on wheat. *Mol Plant Microbe Interact* **22**, 1492-503.

Guldener U, Seong KY, Boddu J*, et al.*, 2006. Development of a Fusarium graminearum Affymetrix GeneChip for profiling fungal gene expression in vitro and in planta. *Fungal Genetics and Biology* **43**, 316-25.

Guo L, Zhao GY, Xu JR, Kistler HC, Gao LX, Ma LJ, 2016. Compartmentalized gene regulatory network of the pathogenic fungus Fusarium graminearum. *New Phytologist* **211**, 527-41.

Guyon K, Balague C, Roby D, Raffaele S, 2014. Secretome analysis reveals effector candidates associated with broad host range necrotrophy in the fungal plant pathogen Sclerotinia sclerotiorum. *Bmc Genomics* **15**, 336.

Haas H, Eisendle M, Turgeon BG, 2008. Siderophores in fungal physiology and virulence. *Annual Review of Phytopathology* **46**, 149-87.

Hall N, Keon JPR, Hargreaves JA, 1999. A homologue of a gene implicated in the virulence of human fungal diseases is present in a plant fungal pathogen and is expressed during infection. *Physiological and Molecular Plant Pathology* **55**, 69-73.

Hallen HE, Huebner M, Shiu SH, Giildener U, Trail F, 2007. Gene expression shifts during perithecium development in Gibberella zeae (anamorph Fusarium graminearum), with particular emphasis on ion transport proteins. *Fungal Genetics and Biology* **44**, 1146-56.

Hallen HE, Trail F, 2008. The L-type calcium ion channel cch1 affects ascospore discharge and mycelial growth in the filamentous fungus Gibberella zeae (anamorph Fusarium graminearum). *Eukaryot Cell* **7**, 415-24.

Han YK, Lee T, Han KH, Yun SH, Lee YW, 2004. Functional analysis of the homoserine O-acetyltransferase gene and its identification as a selectable marker in Gibberella zeae. *Current Genetics* **46**, 205-12.

Harris LJ, Balcerzak M, Johnston A, Schneiderman D, Ouellet T, 2016. Host-preferential Fusarium graminearum gene expression during infection of wheat, barley, and maize. *Fungal Biology* **120**, 111-23.

Harris LJ, Desjardins AE, Plattner RD*, et al.*, 1999. Possible role of trichothecene mycotoxins in virulence of Fusarium graminearum on maize. *Plant Disease* **83**, 954-60.

Hartley JL, Temple GF, Brasch MA, 2000. DNA cloning using in vitro site-specific recombination. *Genome Research* **10**, 1788-95.

Haruta M, Sabat G, Stecker K, Minkoff BB, Sussman MR, 2014. A Peptide Hormone and Its Receptor Protein Kinase Regulate Plant Cell Expansion. *Science* **343**, 408-11.

Haupt S, Oparka KJ, Sauer N, Neumann S, 2001. Macromolecular trafficking between Nicotiana tabacum and the holoparasite Cuscuta reflexa. *Journal of Experimental Botany* **52**, 173-7.

Heard S, Brown NA, Hammond-Kosack K, 2015. An Interspecies Comparative Analysis of the Predicted Secretomes of the Necrotrophic Plant Pathogens Sclerotinia sclerotiorum and Botrytis cinerea. *Plos One* **10**, e0130534.

Heese A, Hann DR, Gimenez-Ibanez S*, et al.*, 2007. The receptor-like kinase SERK3/BAK1 is a central regulator of innate immunity in plants. *Proceedings of the National Academy of Sciences of the United States of America* **104**, 12217-22.

Hemetsberger C, Herrberger C, Zechmann B, Hillmer M, Doehlemann G, 2012. The Ustilago maydis Effector Pep1 Suppresses Plant Immunity by Inhibition of Host Peroxidase Activity. *Plos Pathogens* **8**.

Hohn TM, Desjardins AE, 1992. Isolation and Gene Disruption of the Tox5 Gene Encoding Trichodiene Synthase in Gibberella-Pulicaris. *Molecular Plant-Microbe Interactions* **5**, 249-56.

Hohn TM, Mccormick SP, Alexander NJ, Desjardins AE, Proctor RH, 1998. Function and biosynthesis of trichothecenes produced by *Fusarium* species. *Molecular Genetics of Host-Specific Toxins in Plant Diseases* **13**, 17-24.

Hong YB, Yang YY, Zhang HJ, Huang L, Li DY, Song FM, 2017. Overexpression of MoSM1, encoding for an immunity-inducing protein from Magnaporthe oryzae, in rice confers broad-spectrum resistance against fungal and bacterial diseases. *Scientific Reports* **7**.

Horton P, Park KJ, Obayashi T*, et al.*, 2007. WoLF PSORT: protein localization predictor. *Nucleic Acids Research* **35**, W585-W7.

Horvath P, Barrangou R, 2010. CRISPR/Cas, the immune system of bacteria and archaea. *Science* **327**, 167-70.

Houterman PM, Cornelissen BJC, Rep M, 2008. Suppression of plant resistance gene-based immunity by a fungal effector. *Plos Pathogens* **4**.

Houterman PM, Ma L, Van Ooijen G*, et al.*, 2009. The effector protein Avr2 of the xylem-colonizing fungus Fusarium oxysporum activates the tomato resistance protein I-2 intracellularly. *Plant Journal* **58**, 970-8.

Huang CC, Lindhout P, 1997. Screening for resistance in wild Lycopersicon species to Fusarium oxysporum f sp lycopersici race 1 and race 2. *Euphytica* **93**, 145-53.

Iliakis G, Wang H, Perrault AR*, et al.*, 2004. Mechanisms of DNA double strand break repair and chromosome aberration formation. *Cytogenetic and Genome Research* **104**, 14-20.

Itzek A, Gillen CM, Fulde M*, et al.*, 2010. Contribution of Plasminogen Activation towards the Pathogenic Potential of Oral Streptococci. *Plos One* **5**.

Jansen C, Von Wettstein D, Schafer W, Kogel KH, Felk A, Maier FJ, 2005. Infection patterns in barley and wheat spikes inoculated with wild-type and trichodiene synthase gene disrupted Fusarium graminearum. *Proceedings of the National Academy of Sciences of the United States of America* **102**, 16892-7.

Jenczmionka NJ, Schafer W, 2005. The Gpmk1 MAP kinase of Fusarium graminearum regulates the induction of specific secreted enzymes. *Current Genetics* **47**, 29-36.

Jennings P, Coates ME, Turner JA, Nicholson P, 2003. Distribution, toxin production and control of fusarium head blight pathogens in the UK. *Mycotoxins* **2003**, 69-75.

Jeong H, Lee S, Choi GJ, Lee T, Yun SH, 2013. Draft Genome Sequence of Fusarium fujikuroi B14, the Causal Agent of the Bakanae Disease of Rice. *Genome Announc* **1**.

Jeong JS, Mitchell TK, Dean RA, 2007. The Magnaporthe grisea snodprot1 homolog, MSPI, is required for virulence. *Fems Microbiology Letters* **273**, 157-65.

Ji F, Xu JH, Liu X, Yin XC, Shi JR, 2014. Natural occurrence of deoxynivalenol and zearalenone in wheat from Jiangsu province, China. *Food Chemistry* **157**, 393-7.

Jones JDG, Dangl JL, 2006. The plant immune system. *Nature* **444**, 323-9.

Jonkers W, Dong YH, Broz K, Kistler HC, 2012. The Wor1-like Protein Fgp1 Regulates Pathogenicity, Toxin Synthesis and Reproduction in the Phytopathogenic Fungus Fusarium graminearum. *Plos Pathogens* **8**.

Kachroo P, Lee KH, Schwerdel C, Bailey JE, Chattoo BB, 1997. Analysis of host-induced response in the rice blast fungus Magnaporthe grisea using two-dimensional polyacrylamide gel electrophoresis. *Electrophoresis* **18**, 163-9.

Kamper J, Kahmann R, Bolker M*, et al.*, 2006. Insights from the genome of the biotrophic fungal plant pathogen Ustilago maydis. *Nature* **444**, 97-101.

Kang SC, Sweigard JA, Valent B, 1995. The PWL host specificity gene family in the blast fungus Magnaporthe grisea. *Molecular Plant-Microbe Interactions* **8**, 939-48.

Kazan K, Gardiner DM, 2017. Transcriptomics of cereal-Fusarium graminearum interactions: what we have learned so far. *Molecular Plant Pathology*.

Kazan K, Gardiner DM, Manners JM, 2012. On the trail of a cereal killer: recent advances in Fusarium graminearum pathogenomics and host resistance. *Molecular Plant Pathology* **13**, 399-413.

Kearse M, Moir R, Wilson A*, et al.*, 2012. Geneious Basic: An integrated and extendable desktop software platform for the organization and analysis of sequence data. *Bioinformatics* **28**, 1647-9.

Kelley LA, Mezulis S, Yates CM, Wass MN, Sternberg MJ, 2015a. The Phyre2 web portal for protein modeling, prediction and analysis. *Nat Protoc* **10**, 845-58.

Kelley LA, Mezulis S, Yates CM, Wass MN, Sternberg MJE, 2015b. The Phyre2 web portal for protein modeling, prediction and analysis. *Nat. Protocols* **10**, 845-58.

Kelley LA, Sternberg MJE, 2009. Protein structure prediction on the Web: a case study using the Phyre server. *Nat Protoc* **4**, 363-71.

Kettles GJ, Bayon C, Sparks C, Canning G, Kanyuka K, Rudd JJ, 2017. Characterisation of an antimicrobial and phytotoxic ribonuclease secreted by the fungal wheat pathogen Zymoseptoria tritici. *bioRxiv*.

Khang CH, Berruyer R, Giraldo MC*, et al.*, 2010. Translocation of Magnaporthe oryzae Effectors into Rice Cells and Their Subsequent Cell-to-Cell Movement. *Plant Cell* **22**, 1388-403.

Khang CH, Park SY, Lee YH, Valent B, Kang S, 2008. Genome organization and evolution of the AVR-Pita avirulence gene family in the Magnaporthe grisea species complex. *Molecular Plant-Microbe Interactions* **21**, 658-70.

Kim KS, Min JY, Dickman MB, 2008. Oxalic acid is an elicitor of plant programmed cell death during Sclerotinia sclerotiorum disease development. *Mol Plant Microbe Interact* **21**, 605-12.

Kim KT, Jeon J, Choi J*, et al.*, 2016. Kingdom-Wide Analysis of Fungal Small Secreted Proteins (SSPs) Reveals their Potential Role in Host Association. *Frontiers in Plant Science* **7**, 186.

Kimura M, Tokai T, O'donnell K*, et al.*, 2003. The trichothecene biosynthesis gene cluster of Fusarium graminearum F15 contains a limited number of essential pathway genes and expressed non-essential genes. *Febs Letters* **539**, 105-10.

King R, Brown NA, Urban M, Hammond-Kosack KE, 2017a. Inter-genome comparison of the Quorn fungus, *Fusarium venenatum*, and the closely related plant infecting pathogen *Fusarium graminearum*. *Bmc Genomics* **submitted**.

King R, Urban M, Hammond-Kosack KE, 2017b. Annotation of *Fusarium graminearum* (PH-1) Version 5.0. *Genome Announc* **5**, e01479-16.

King R, Urban M, Hammond-Kosack MCU, Hassani-Pak K, Hammond-Kosack KE, 2015. The completed genome sequence of the pathogenic ascomycete fungus *Fusarium graminearum*. *Bmc Genomics* **16**, 544.

Koch A, Biedenkopf D, Furch A*, et al.*, 2016. An RNAi-based control of *Fusarium graminearum* infections through spraying of long dsRNAs involves a plant passage and is controlled by the fungal silencing machinery. *Plos Pathogens* **12**, e1005901.

Koch A, Kumar N, Weber L, Keller H, Imani J, Kogel KH, 2013. Host-induced gene silencing of cytochrome P450 lanosterol C14 alpha-demethylase-encoding genes confers strong resistance to *Fusarium* species. *Proceedings of the National Academy of Sciences of the United States of America* **110**, 19324-9.

Koharudin LMI, Viscomi AR, Montanini B*, et al.*, 2011. Structure-Function Analysis of a CVNH-LysM Lectin Expressed during Plant Infection by the Rice Blast Fungus Magnaporthe oryzae. *Structure* **19**, 662-74.

Koressaar T, Remm M, 2007. Enhancements and modifications of primer design program Primer3. *Bioinformatics* **23**, 1289-91.

Kriel WM, Pretorius ZA, 2008. The FHB challenge to irrigation wheat production in South Africa. *Cereal Research Communications* **36**, 569-71.

Kubo K, Kawada N, Fujita M, Hatta K, Oda S, Nakajima T, 2010. Effect of cleistogamy on Fusarium head blight resistance in wheat. *Breeding Science* **60**, 405-11.

Kulkarni RD, Kelkar HS, Dean RA, 2003. An eight-cysteine-containing CFEM domain unique to a group of fungal membrane proteins. *Trends in Biochemical Sciences* **28**, 118-21.

Kulkarni RD, Thon MR, Pan HQ, Dean RA, 2005. Novel G-protein-coupled receptor-like proteins in the plant pathogenic fungus Magnaporthe grisea. *Genome Biology* **6**.

Kusch S, Ahmadinejad N, Panstruga R, Kuhn H, 2014. In silico analysis of the core signaling proteome from the barley powdery mildew pathogen (Blumeria graminis f.sp hordei). *Bmc Genomics* **15**.

Lacadena J, Alvarez-Garcia E, Carreras-Sangra N*, et al.*, 2007. Fungal ribotoxins: molecular dissection of a family of natural killers. *Fems Microbiology Reviews* **31**, 212-37.

Lawrence DM, Jackson AO, 2001. Requirements for cell-to-cell movement of Barley stripe mosaic virus in monocot and dicot hosts. *Molecular Plant Pathology* **2**, 65-75.

Lee T, Han YK, Kim KH, Yun SH, Lee YW, 2002. Tri13 and Tri7 determine deoxynivalenol- and nivalenol-producing chemotypes of Gibberella zeae. *Applied and Environmental Microbiology* **68**, 2148-54.

Lee WS, Hammond-Kosack KE, Kanyuka K, 2012. Barley stripe mosaic virus-mediated tools for investigating gene function in cereal plants and their pathogens: virus-induced gene silencing, host-mediated gene silencing, and virus-mediated overexpression of heterologous protein. *Plant Physiology* **160**, 582-90.

Lemmens M, Scholz U, Berthiller F*, et al.*, 2005. The ability to detoxify the mycotoxin deoxynivalenol colocalizes with a major quantitative trait locus for fusarium head blight resistance in wheat. *Molecular Plant-Microbe Interactions* **18**, 1318-24.

Lepesheva GI, Waterman MR, 2007. Sterol 14 alpha-demethylase cytochrome P450 (CYP51), a P450 in all biological kingdoms. *Biochimica Et Biophysica Acta-General Subjects* **1770**, 467-77.

Leslie JF, Summerell BA, 2008. *The Fusarium laboratory manual*. John Wiley & Sons.

Li C, Wu HM, Cheung AY, 2016. FERONIA and Her Pals: Functions and Mechanisms. *Plant Physiology* **171**, 2379-92.

Li C, Yeh FL, Cheung AY*, et al.*, 2015. Glycosylphosphatidylinositol-anchored proteins as chaperones and co-receptors for FERONIA receptor kinase signaling in Arabidopsis. *Elife* **4**.

Li YH, Zhou GY, Ma JX*, et al.*, 2014. De novo assembly of soybean wild relatives for pan-genome analysis of diversity and agronomic traits. *Nature Biotechnology* **32**, 1045-+.

Liang LQ, Li JQ, Cheng L*, et al.*, 2014. A high efficiency gene disruption strategy using a positive-negative split selection marker and electroporation for Fusarium oxysporum. *Microbiological Research* **169**, 835-43.

Liu G, Greenshields DL, Sammynaiken R, Hirji RN, Selvaraj G, Wei Y, 2007. Targeted alterations in iron homeostasis underlie plant defense responses. *J Cell Sci* **120**, 596-605.

Lo Presti L, Lanver D, Schweizer G*, et al.*, 2015. Fungal Effectors and Plant Susceptibility. *Annual Review of Plant Biology, Vol 66* **66**, 513-45.

Lo Presti L, Zechmann B, Kumlehn J*, et al.*, 2017. An assay for entry of secreted fungal effectors into plant cells. *New Phytologist* **213**, 956-64.

Luti S, Martellini F, Bemporad F, Mazzoli L, Paoli P, Pazzagli L, 2017. A single amino acid mutation affects elicitor and expansins-like activities of cerato-platanin, a non-catalytic fungal protein. *Plos One* **12**, e0178337.

Lysoe E, Seong KY, Kistler HC, 2011. The Transcriptome of Fusarium graminearum During the Infection of Wheat. *Molecular Plant-Microbe Interactions* **24**, 995-1000.

Ma LJ, Geiser DM, Proctor RH*, et al.*, 2013. Fusarium Pathogenomics. *Annual Review of Microbiology, Vol 67* **67**, 399-416.

Ma LJ, Van Der Does HC, Borkovich KA*, et al.*, 2010. Comparative genomics reveals mobile pathogenicity chromosomes in Fusarium. *Nature* **464**, 367-73.

Ma Z, Li G, Zhou J*, et al.* Map-based cloning of *Fhb1* revealed unique mutation of a well-conserved gene resulting in resistance to wheat Fusarium head blight. In: Buerstmayr H, Lang-Mladek C, Steiner B, et al., eds. *Proceedings of the 13th International Wheat Genetics Symposium*, *2017*. Tulln, Austria: BOKU - Univeristy of Natural Resources and Life Sciences, Vienna.

Machado AK, Brown NA, Urban M, Kanyuka K, Hammond-Kosack K, 2017. RNAi as an emerging approach to control Fusarium Head Blight disease and mycotoxin contamination in cereals. *Pest Management Science* **submitted**.

Magan N, Aldred D, Mylona K, Lambert RJW, 2010. Limiting mycotoxins in stored wheat. *Food Additives and Contaminants Part a-Chemistry Analysis Control Exposure & Risk Assessment* **27**, 644-50.

Maier FJ, Miedaner T, Hadeler B*, et al.*, 2006. Involvement of trichothecenes in fusarioses of wheat, barley and maize evaluated by gene disruption of the trichodiene synthase (Tri5) gene in three field isolates of different chemotype and virulence. *Molecular Plant Pathology* **7**, 449-61.

Manning VA, Chu AL, Scofield SR, Ciuffetti LM, 2010. Intracellular expression of a host-selective toxin, ToxA, in diverse plants phenocopies silencing of a ToxA-interacting protein, ToxABP1. *New Phytologist* **187**, 1034-47.

Manning VA, Hardison LK, Ciuffetti LM, 2007. Ptr ToxA interacts with a chloroplast-localized protein. *Molecular Plant-Microbe Interactions* **20**, 168-77.

Mao CG, Obeid LM, 2008. Ceramidases: regulators of cellular responses mediated by ceramide, sphingosine, and sphingosine-1-phosphate. *Biochimica Et Biophysica Acta-Molecular and Cell Biology of Lipids* **1781**, 424-34.

Maqbool A, Saitoh H, Franceschetti M*, et al.*, 2015. Structural basis of pathogen recognition by an integrated HMA domain in a plant NLR immune receptor. *Elife* **4**.

Marmeisse R, Vandenackerveken GFJM, Goosen T, Dewit PJGM, Vandenbroek HWJ, 1993. Disruption of the Avirulence Gene Avr9 in 2 Races of the Tomato Pathogen Cladosporium-Fulvum Causes Virulence on Tomato Genotypes with the Complementary Resistance Gene Cf9. *Molecular Plant-Microbe Interactions* **6**, 412-7.

Marshall R, Kombrink A, Motteram J*, et al.*, 2011. Analysis of Two in Planta Expressed LysM Effector Homologs from the Fungus Mycosphaerella graminicola Reveals Novel Functional Properties and Varying Contributions to Virulence on Wheat. *Plant Physiology* **156**, 756-69.

Martin F, Aerts A, Ahren D*, et al.*, 2008. The genome of Laccaria bicolor provides insights into mycorrhizal symbiosis. *Nature* **452**, 88-U7.

Marx V, 2013. The Genome Jigsaw. *Nature* **501**, 263-8.

Masachis S, Segorbe D, Turra D*, et al.*, 2016. A fungal pathogen secretes plant alkalinizing peptides to increase infection. *Nature Microbiology* **1**.

Mccormick SP, Alexander NJ, 2002. Fusarium Tri8 encodes a trichothecene C-3 esterase. *Applied and Environmental Microbiology* **68**, 2959-64.

Mcmullen M, Bergstrom G, De Wolf E*, et al.*, 2012. A unified effort to fight an enemy of wheat and barley: Fusarium head blight. *Plant Disease* **96**, 1712-28.

Mentlak TA, Kombrink A, Shinya T*, et al.*, 2012. Effector-Mediated Suppression of Chitin-Triggered Immunity by Magnaporthe oryzae Is Necessary for Rice Blast Disease. *Plant Cell* **24**, 322-35.

Mesterhazy A, 1995. Types and components of resistance to Fusarium head blight of wheat. *Plant Breeding* **114**, 377-86.

Minenko E, Vogel RF, Niessen L, 2014. Significance of the class II hydrophobin FgHyd5p for the life cycle of Fusarium graminearum. *Fungal Biology* **118**, 385-93.

Mingossi FB, Matos JL, Rizzato AP*, et al.*, 2010. SacRALF1, a peptide signal from the grass sugarcane (Saccharum spp.), is potentially involved in the regulation of tissue expansion. *Plant Molecular Biology* **73**, 271-81.

Moolhuijzen PM, Manners JM, Wilcox SA, Bellgard MI, Gardiner DM, 2013. Genome sequences of six wheat-infecting fusarium species isolates. *Genome Announc* **1**.

Moreland N, Ashton R, Baker HM*, et al.*, 2005. A flexible and economical medium-throughput strategy for protein production and crystallization. *Acta Crystallographica Section D-Biological Crystallography* **61**, 1378-85.

Mueller AN, Ziemann S, Treitschke S, Assmann D, Doehlemann G, 2013. Compatibility in the Ustilago maydis-Maize Interaction Requires Inhibition of Host Cysteine Proteases by the Fungal Effector Pit2. *Plos Pathogens* **9**.

Mueller O, Kahmann R, Aguilar G, Trejo-Aguilar B, Wu A, De Vries RP, 2008. The secretome of the maize pathogen Ustilago maydis. *Fungal Genetics and Biology* **45**, S63-S70.

Muller O, Schreier PH, Uhrig JF, 2008. Identification and characterization of secreted and pathogenesis-related proteins in Ustilago maydis. *Molecular Genetics and Genomics* **279**, 27-39.

Murphy E, De Smet I, 2014. Understanding the RALF family: a tale of many species. *Trends in Plant Science* **19**, 664-71.

Naquin D, D'aubenton-Carafa Y, Thermes C, Silvain M, 2014. CIRCUS: a package for Circos display of structural genome variations from paired-end and mate-pair sequencing data. *Bmc Bioinformatics* **15**.

Niwa S, Kubo K, Lewis J, Kikuchi R, Alagu M, Ban T, 2014. Variations for Fusarium head blight resistance associated with genomic diversity in different sources of the resistant wheat cultivar 'Sumai 3'. *Breeding Science* **64**, 90-6.

Nodvig CS, Nielsen JB, Kogle ME, Mortensen UH, 2015. A CRISPR-Cas9 System for Genetic Engineering of Filamentous Fungi. *Plos One* **10**.

Nowara D, Gay A, Lacomme C*, et al.*, 2010. HIGS: Host-induced gene silencing in the obligate biotrophic fungal pathogen *Blumeria graminis*. *Plant Cell* **22**, 3130-41.

Nunes CC, Dean RA, 2012. Host-induced gene silencing: a tool for understanding fungal host interaction and for developing novel disease control strategies. *Molecular Plant Pathology* **13**, 519-29.

O'donnell K, Rooney AP, Proctor RH*, et al.*, 2013. Phylogenetic analyses of RPB1 and RPB2 support a middle Cretaceous origin for a clade comprising all agriculturally and medically important fusaria. *Fungal Genetics and Biology* **52**, 20-31.

O'donnell K, Ward TJ, Aberra D*, et al.*, 2008. Multilocus genotyping and molecular phylogenetics resolve a novel head blight pathogen within the Fusarium graminearum species complex from Ethiopia. *Fungal Genetics and Biology* **45**, 1514-22.

O'donnell K, Ward TJ, Geiser DM, Kistler HC, Aoki T, 2004. Genealogical concordance between the mating type locus and seven other nuclear genes supports formal recognition of nine phylogenetically distinct species within the Fusarium graminearum clade. *Fungal Genetics and Biology* **41**, 600-23.

O'leary BM, Rico A, Mccraw S, Fones HN, Preston GM, 2014. The Infiltration-centrifugation Technique for Extraction of Apoplastic Fluid from Plant Leaves Using Phaseolus vulgaris as an Example. *Journal of Visualized Experiments : JoVE*, 52113.

Oerke EC, 2006. Crop losses to pests. *Journal of Agricultural Science* **144**, 31-43.

Oerke EC, Dehne HW, 1997. Global crop production and the efficacy of crop protection - Current situation and future trends. *European Journal of Plant Pathology* **103**, 203-15.

Oide S, Moeder W, Krasnoff S*, et al.*, 2006. NPS6, encoding a nonribosomal peptide synthetase involved in siderophore-mediated iron metabolism, is a conserved virulence determinant of plant pathogenic ascomycetes. *Plant Cell* **18**, 2836-53.

Okmen B, Doehlemann G, 2014. Inside plant: biotrophic strategies to modulate host immunity and metabolism. *Current Opinion in Plant Biology* **20**, 19-25.

Oliver R, 2012. Genomic tillage and the harvest of fungal phytopathogens. *New Phytologist* **196**, 1015-23.

Oliver RP, Solomon PS, 2010. New developments in pathogenicity and virulence of necrotrophs. *Current Opinion in Plant Biology* **13**, 415-9.

Olsen KM, Womack A, Garrett AR, Suddith JI, Purugganan MD, 2002. Contrasting evolutionary forces in the Arabidopsis thaliana floral developmental pathway. *Genetics* **160**, 1641-50.

Orbach MJ, Farrall L, Sweigard JA, Chumley FG, Valent B, 2000. A telomeric avirulence gene determines efficacy for the rice blast resistance gene Pi-ta. *Plant Cell* **12**, 2019-32.

Paper JM, Scott-Craig JS, Adhikari ND, Cuomo CA, Walton JD, 2007. Comparative proteomics of extracellular proteins in vitro and in planta from the pathogenic fungus Fusarium graminearum. *Proteomics* **7**, 3171-83.

Parlange F, Roffler S, Menardo F*, et al.*, 2015. Genetic and molecular characterization of a locus involved in avirulence of Blumeria graminis f. sp. tritici on wheat Pm3 resistance alleles. *Fungal Genetics and Biology* **82**, 181-92.

Parry DW, Jenkinson P, Mcleod L, 1995. Fusarium ear blight (scab) in small-grain cereals - a review. *Plant Pathology* **44**, 207-38.

Paul PA, Mcmullen MP, Hershman DE, Madden LV, 2010. Meta-Analysis of the Effects of Triazole-Based Fungicides on Wheat Yield and Test Weight as Influenced by Fusarium Head Blight Intensity. *Phytopathology* **100**, 160-71.

Pazzagli L, Cappugi G, Manao G, Camici G, Santini A, Scala A, 1999. Purification, characterization, and amino acid sequence of cerato-platanin, a new phytotoxic protein from Ceratocystis fimbriata f. sp platani. *Journal of Biological Chemistry* **274**, 24959-64.

Pazzagli L, Pantera B, Carresi L*, et al.*, 2006. Cerato-platanin, the first member of a new fungal protein family - Cloning, expression, and characterization. *Cell Biochemistry and Biophysics* **44**, 512-21.

Pazzagli L, Seidl-Seiboth V, Barsottini M, Vargas WA, Scala A, Mukherjee PK, 2014. Cerato-platanins: Elicitors and effectors. *Plant Science*.

Pazzagli L, Zoppi C, Carresi L*, et al.*, 2009. Characterization of ordered aggregates of cerato-platanin and their involvement in fungus-host interactions. *Biochimica Et Biophysica Acta-General Subjects* **1790**, 1334-44.

Pearce G, Yamaguchi Y, Munske G, Ryan CA, 2010. Structure-activity studies of RALF, Rapid Alkalinization Factor, reveal an essential - YISY - motif. *Peptides* **31**, 1973-7.

Pennington HG, Gheorghe DM, Damerum A*, et al.*, 2016. Interactions between the Powdery Mildew Effector BEC1054 and Barley Proteins Identify Candidate Host Targets. *Journal of Proteome Research* **15**, 826-39.

Petersen TN, Brunak S, Von Heijne G, Nielsen H, 2011. SignalP 4.0: discriminating signal peptides from transmembrane regions. *Nature Methods* **8**, 785-6.

Phalip V, Delalande F, Carapito C*, et al.*, 2005. Diversity of the exoproteome of Fusarium graminearum grown on plant cell wall. *Current Genetics* **48**, 366-79.

Pliego C, Nowara D, Bonciani G*, et al.*, 2013. Host-induced gene silencing in barley powdery mildew reveals a class of ribonuclease-like effectors. *Molecular Plant-Microbe Interactions* **26**, 633-42.

Prasad BVLS, Suguna K, 2002. Role of water molecules in the structure and function of aspartic proteinases. *Acta Crystallographica Section D-Biological Crystallography* **58**, 250-9.

Praz CR, Bourras S, Zeng F*, et al.*, 2017. AvrPm2 encodes an RNase-like avirulence effector which is conserved in the two different specialized forms of wheat and rye powdery mildew fungus. *New Phytologist* **213**, 1301-14.

Prelich G, 2012. Gene Overexpression: Uses, Mechanisms, and Interpretation. *Genetics* **190**, 841-54.

Proctor RH, Hohn TM, Mccormick SP, 1995. Reduced Virulence of Gibberella-Zeae Caused by Disruption of a Trichothecene Toxin Biosynthetic Gene. *Molecular Plant-Microbe Interactions* **8**, 593-601.

Proctor RH, Hohn TM, Mccormick SP, 1997. Restoration of wild-type virulence to Tri5 disruption mutants of Gibberella zeae via gene reversion and mutant complementation. *Microbiology-Uk* **143**, 2583-91.

Protcomp S, 2011. 9.0: Predict the sub-cellular localization for plant proteins. *Retrieved May*.

Prusky D, Mcevoy JL, Leverentz B, Conway WS, 2001. Local modulation of host pH by Colletotrichum species as a mechanism to increase virulence. *Molecular Plant-Microbe Interactions* **14**, 1105-13.

Prusky D, Yakoby N, 2003. Pathogenic fungi: leading or led by ambient pH? *Molecular Plant Pathology* **4**, 509-16.

Quarantin A, Glasenapp A, Schafer W, Favaron F, Sella L, 2016. Involvement of the Fusarium graminearum cerato-platanin proteins in fungal growth and plant infection. *Plant Physiol Biochem* **109**, 220-9.

Quiroz-Castaneda RE, Martinez-Anaya C, Cuervo-Soto LI, Segovia L, Folch-Mallol JL, 2011. Loosenin, a novel protein with cellulose-disrupting activity from Bjerkandera adusta. *Microbial Cell Factories* **10**.

Raffaele S, Kamoun S, 2012. Genome evolution in filamentous plant pathogens: why bigger can be better. *Nature Reviews Microbiology* **10**, 417-30.

Rafiqi M, Ellis JG, Ludowici VA, Hardham AR, Dodds PN, 2012. Challenges and progress towards understanding the role of effectors in plant-fungal interactions. *Current Opinion in Plant Biology* **15**, 477-82.

Ramamoorthy V, Zhao XH, Snyder AK, Xu JR, Shah DM, 2007. Two mitogen-activated protein kinase signalling cascades mediate basal resistance to antifungal plant defensins in Fusarium graminearum. *Cellular Microbiology* **9**, 1491-506.

Rao ZM, Dong HT, Zhuang JY*, et al.*, 2002. [Analysis of gene expression profiles during host-Magnaporthe grisea interactions in a pair of near isogenic lines of rice]. *Yi Chuan Xue Bao* **29**, 887-93.

Rastogi S, Rost B, 2011. LocDB: experimental annotations of localization for Homo sapiens and Arabidopsis thaliana. *Nucleic Acids Research* **39**, D230-D4.

Rawat N, Pumphrey MO, Liu SX*, et al.*, 2016. Wheat *Fhb1* encodes a chimeric lectin with agglutinin domains and a pore-forming toxin-like domain conferring resistance to Fusarium head blight. *Nature Genetics* **48**, 1576-80.

Redman M, King A, Watson C, King D, 2016. What is CRISPR/Cas9? *Arch Dis Child Educ Pract Ed* **101**, 213-5.

Reis EM, Carmona MA, 2013. Integrated disease management of Fusarium head blight. In: Alconada Magliano TM, Chulze SN, eds. *Fusarium Head Blight in Latin America.* Dordrecht: Springer Netherlands, 159-73.

Rep M, Kistler HC, 2010. The genomic organization of plant pathogenicity in Fusarium species. *Current Opinion in Plant Biology* **13**, 420-6.

Rep M, Meijer M, Houterman PM, Van Der Does HC, Cornelissen BJC, 2005. Fusarium oxysporum evades I-3-mediated resistance without altering the matching avirulence gene. *Molecular Plant-Microbe Interactions* **18**, 15-23.

Rep M, Van Der Does HC, Meijer M*, et al.*, 2004. A small, cysteine-rich protein secreted by Fusarium oxysporum during colonization of xylem vessels is required for I-3-mediated resistance in tomato. *Molecular Microbiology* **53**, 1373-83.

Rolke Y, Liu S, Quidde T*, et al.*, 2004. Functional analysis of H(2)O(2)-generating systems in Botrytis cinerea: the major Cu-Zn-superoxide dismutase (BCSOD1) contributes to virulence on French bean, whereas a glucose oxidase (BCGOD1) is dispensable. *Molecular Plant Pathology* **5**, 17-27.

Rollins JA, Dickman MB, 2001. pH signaling in Sclerotinia sclerotiorum: identification of a pacC/RIM1 homolog. *Appl Environ Microbiol* **67**, 75-81.

Ruhanen H, Hurley D, Ghosh A, O'brien KT, Johnston CR, Shields DC, 2014. Potential of known and short prokaryotic protein motifs as a basis for novel peptide-based antibacterial therapeutics: a computational survey. *Front Microbiol* **5**.

Sainsbury F, Thuenemann EC, Lomonossoff GP, 2009. pEAQ: versatile expression vectors for easy and quick transient expression of heterologous proteins in plants. *Plant Biotechnology Journal* **7**, 682-93.

Saitoh H, Fujisawa S, Mitsuoka C*, et al.*, 2012. Large-Scale Gene Disruption in Magnaporthe oryzae Identifies MC69, a Secreted Protein Required for Infection by Monocot and Dicot Fungal Pathogens. *Plos Pathogens* **8**.

Salas-Marina MA, Isordia-Jasso MI, Islas-Osuna MA*, et al.*, 2015. The Epl1 and Sm1 proteins from Trichoderma atroviride and Trichoderma virens differentially modulate systemic disease resistance against different life style pathogens in Solanum lycopersicum. *Frontiers in Plant Science* **6**, 77.

Salgado JD, Madden LV, Paul PA, 2015. Quantifying the Effects of Fusarium Head Blight on Grain Yield and Test Weight in Soft Red Winter Wheat. *Phytopathology* **105**, 295-306.

Sambrook J, Russell DW, Sambrook J, 2006. *The condensed protocols from Molecular cloning : a laboratory manual*. Cold Spring Harbor, N.Y.: Cold Spring Harbor Laboratory Press.

Sampedro J, Cosgrove DJ, 2005. The expansin superfamily. *Genome Biology* **6**.

Sampietro DA, Diaz CG, Gonzalez V*, et al.*, 2011. Species diversity and toxigenic potential of Fusarium graminearum complex isolates from maize fields in northwest Argentina. *International Journal of Food Microbiology* **145**, 359-64.

Sansen S, De Ranter CJ, Gebruers K*, et al.*, 2004. Structural basis for inhibition of Aspergillus niger xylanase by Triticum aestivum xylanase inhibitor-I. *Journal of Biological Chemistry* **279**, 36022-8.

Sarver BaJ, Ward TJ, Gale LR*, et al.*, 2011. Novel Fusarium head blight pathogens from Nepal and Louisiana revealed by multilocus genealogical concordance. *Fungal Genetics and Biology* **48**, 1096-107.

Sasso S, Ramakrishnan C, Gamper M, Hilvert D, Kast P, 2005. Characterization of the secreted chorismate mutase from the pathogen Mycobacterium tuberculosis. *Febs Journal* **272**, 375-89.

Savary S, Ficke A, Aubertot JN, Hollier C, 2012. Crop losses due to diseases and their implications for global food production losses and food security. *Food Security* **4**, 519-37.

Schaafsma AW, Tamburic-Ilincic L, Hooker DC, 2005. Effect of previous crop, tillage, field size, adjacent crop, and sampling direction on airborne propagules of *Gibberella zeae/Fusarium graminearum*, Fusarium head blight severity, and deoxynivalenol accumulation in winter wheat. *Canadian Journal of Plant Pathology-Revue Canadienne De Phytopathologie* **27**, 217-24.

Schafer W, 1994. Molecular Mechanisms of Fungal Pathogenicity to Plants. *Annual Review of Phytopathology* **32**, 461-77.

Schenk PM, Kazan K, Wilson I*, et al.*, 2000. Coordinated plant defense responses in Arabidopsis revealed by microarray analysis. *Proceedings of the National Academy of Sciences of the United States of America* **97**, 11655-60.

Schroeder HW, Christensen JJ, 1963. Factors Affecting Resistance of Wheat to Scab Caused by Gibberella Zeae. *Phytopathology* **53**, 831-&.

Schumann GL, D'arcy CJ, 2006. *Essential plant pathology*. St. Paul, USA: American Phytopathological Society (APS Press).

Scofield SR, Nelson RS, 2009. Resources for Virus-Induced Gene Silencing in the Grasses. *Plant Physiology* **149**, 152-7.

Scoz LB, Astolfi P, Reartes DS, Schmale DG, Moraes MG, Del Ponte EM, 2009. Trichothecene mycotoxin genotypes of Fusarium graminearum sensu stricto and Fusarium meridionale in wheat from southern Brazil. *Plant Pathology* **58**, 344-51.

Segerman B, 2012. The genetic integrity of bacterial species: the core genome and the accessory genome, two different stories. *Frontiers in Cellular and Infection Microbiology* **2**.

Seidl MF, Thomma BPHJ, 2014. Sex or no sex: Evolutionary adaptation occurs regardless. *Bioessays* **36**, 335-45.

Seidl V, Marchetti M, Schandl R, Allmaier G, Kubicek CP, 2006. Epl1, the major secreted protein of Hypocrea atroviridis on glucose, is a member of a strongly conserved protein family comprising plant defense response elicitors. *Febs Journal* **273**, 4346-59.

Senthil-Kumar M, Mysore KS, 2011. New dimensions for VIGS in plant functional genomics. *Trends in Plant Science* **16**, 656-65.

Seong K, Hou Z, Tracy M, Kistler HC, Xu JR, 2005. Random Insertional Mutagenesis Identifies Genes Associated with Virulence in the Wheat Scab Fungus Fusarium graminearum. *Phytopathology* **95**, 744-50.

Seong KY, Pasquali M, Zhou X*, et al.*, 2009. Global gene regulation by Fusarium transcription factors Tri6 and Tri10 reveals adaptations for toxin biosynthesis. *Molecular Microbiology* **72**, 354-67.

Seong KY, Zhao X, Xu JR, Guldener U, Kistler HC, 2008a. Conidial germination in the filamentous fungus Fusarium graminearum. *Fungal Genetics and Biology* **45**, 389-99.

Seong KY, Zhao X, Xu JR, Güldener U, Kistler HC, 2008b. Conidial germination in the filamentous fungus Fusarium graminearum. *Fungal Genetics and Biology* **45**, 389-99.

Shah P, Atwood JA, Orlando R, El Mubarek H, Podila GK, Davis MR, 2009. Comparative Proteomic Analysis of Botrytis cinerea Secretome. *Journal of Proteome Research* **8**, 1123-30.

Shaner G, 2003. Epidemiology of Fusarium head blight of small grain cereals in North America. In: Leonard KJ, Bushnell WR, eds. *Fusarium Head Blight of Wheat and Barley.* St. Paul, MN: APS Press, 84-119.

Simms D, Cizdziel PE, Chomczynski P, 1993. TRIzol: A new reagent for optimal single-step isolation of RNA. *Focus* **15**, 532-5.

Siou D, Gelisse S, Laval V*, et al.*, 2014. Effect of wheat spike infection timing on fusarium head blight development and mycotoxin accumulation. *Plant Pathology* **63**, 390-9.

Skinnes H, Semagn K, Tarkegne Y, Maroy AG, Bjornstad A, 2010. The inheritance of anther extrusion in hexaploid wheat and its relationship to Fusarium head blight resistance and deoxynivalenol content. *Plant Breeding* **129**, 149-55.

Skonier J, Bennett K, Rothwell V*, et al.*, 1994. Beta-Ig-H3 - a Transforming Growth Factor-Beta-Responsive Gene Encoding a Secreted Protein That Inhibits Cell Attachment in-Vitro and Suppresses the Growth of Cho Cells in Nude-Mice. *DNA and Cell Biology* **13**, 571-84.

Soanes DM, Richards TA, Talbot NJ, 2007. Insights from sequencing fungal and oomycete genomes: What can we learn about plant disease and the evolution of pathogenicity? *Plant Cell* **19**, 3318-26.

Sobrova P, Adam V, Vasatkova A, Beklova M, Zeman L, Kizek R, 2010. Deoxynivalenol and its toxicity. *Interdiscip Toxicol* **3**, 94-9.

Son H, Seo YS, Min K*, et al.*, 2011. A phenome-based functional analysis of transcription factors in the cereal head blight fungus, Fusarium graminearum. *Plos Pathogens* **7**, e1002310.

Sperschneider J, Gardiner DM, Dodds PN*, et al.*, 2016. EffectorP: predicting fungal effector proteins from secretomes using machine learning. *New Phytologist* **210**, 743-61.

Spolti P, Del Ponte EM, Dong YH, Cummings JA, Bergstrom GC, 2014. Triazole sensitivity in a contemporary population of *Fusarium graminearum* from New York wheat and competitiveness of a tebuconazole-resistant isolate. *Plant Disease* **98**, 607-13.

Spolti P, Shah DA, Fernandes JMC, Bergstrom GC, Del Ponte EM, 2015. Disease risk, spatial patterns, and incidence-severity relationships of Fusarium head blight in no-till spring wheat following maize or soybean. *Plant Disease* **99**, 1360-6.

Srivastava R, Liu JX, Guo HQ, Yin YH, Howell SH, 2009. Regulation and processing of a plant peptide hormone, AtRALF23, in Arabidopsis. *Plant Journal* **59**, 930-9.

Stack JP, 2003. Recurring and emerging sorghum diseases in North America. *Sorghum and Millets Diseases*, 449-56.

Stanke M, Steinkamp R, Waack S, Morgenstern B, 2004. AUGUSTUS: a web server for gene finding in eukaryotes. *Nucleic Acids Research* **32**, W309-W12.

Starkey DE, Ward TJ, Aoki T*, et al.*, 2007. Global molecular surveillance reveals novel Fusarium head blight species and trichothecene toxin diversity. *Fungal Genetics and Biology* **44**, 1191-204.

Stegmann M, Monaghan J, Smakowska-Luzan E*, et al.*, 2017. The receptor kinase FER is a RALF-regulated scaffold controlling plant immune signaling. *Science* **355**, 287-+.

Steiner B, Zimmerl S, Polzer R*, et al.* Functional identification of the wheat gene enhancing mycotoxin detoxification of the major *Fusarium* resistance QTL *Fhb1*. In: Buerstmayr H, Lang-Mladek C, Steiner B, et al., eds. *Proceedings of the 13th*

International Wheat Genetics Symposium, *2017*. Tulln, Austria: BOKU - Univeristy of Natural Resources and Life Sciences, Vienna.

Stephens AE, Gardiner DM, White RG, Munn AL, Manners JM, 2008. Phases of Infection and Gene Expression of Fusarium graminearum During Crown Rot Disease of Wheat. *Molecular Plant-Microbe Interactions* **21**, 1571-81.

Stergiopoulos I, Collemare J, Mehrabi R, De Wit PJGM, 2013. Phytotoxic secondary metabolites and peptides produced by plant pathogenic Dothideomycete fungi. *Fems Microbiology Reviews* **37**, 67-93.

Stergiopoulos I, De Wit PJGM, 2009. Fungal Effector Proteins. *Annual Review of Phytopathology* **47**, 233-63.

Studier FW, Moffatt BA, 1986. Use of Bacteriophage-T7 Rna-Polymerase to Direct Selective High-Level Expression of Cloned Genes. *Journal of Molecular Biology* **189**, 113-30.

Su Z, Bernardo A, Li C, Lu P, Cai S, Bai G. *TaHRC* is the key gene underlying *Fhb1* resistance to Fusarium head blight in wheat In: Buerstmayr H, Lang-Mladek C, Steiner B, et al., eds. *Proceedings of the 13th International Wheat Genetics Symposium*, *2017*. Tulln, Austria: BOKU - Univeristy of Natural Resources and Life Sciences, Vienna.

Sweigard JA, Carroll AM, Kang S, Farrall L, Chumley FG, Valent B, 1995. Identification, Cloning, and Characterization of Pwl2, a Gene for Host Species-Specificity in the Rice Blast Fungus. *Plant Cell* **7**, 1221-33.

Tag A, Hicks J, Garifullina G*, et al.*, 2000. G-protein signalling mediates differential production of toxic secondary metabolites. *Molecular Microbiology* **38**, 658-65.

Takano Y, Choi W, Mitchell TK, Okuno T, Dean RA, 2003. Large scale parallel analysis of gene expression during infection-related morphogenesis of Magnaporthe grisea. *Molecular Plant Pathology* **4**, 337-46.

Takken F, Rep M, 2010. The arms race between tomato and Fusarium oxysporum. *Molecular Plant Pathology* **11**, 309-14.

Talas F, Kalih R, Miedaner T, Mcdonald BA, 2016. Genome-Wide Association Study Identifies Novel Candidate Genes for Aggressiveness, Deoxynivalenol Production, and Azole Sensitivity in Natural Field Populations of Fusarium graminearum. *Molecular Plant-Microbe Interactions* **29**, 417-30.

Talbot NJ, 2003. On the trail of a cereal killer: Exploring the biology of Magnaporthe grisea. *Annual Review of Microbiology* **57**, 177-202.

Talbot NJ, Ebbole DJ, Hamer JE, 1993. Identification and Characterization of Mpg1, a Gene Involved in Pathogenicity from the Rice Blast Fungus Magnaporthe-Grisea. *Plant Cell* **5**, 1575-90.

Talbot NJ, Kershaw MJ, Wakley GE, Devries OMH, Wessels JGH, Hamer JE, 1996. MPG1 encodes a fungal hydrophobin involved in surface interactions during infection-related development of Magnaporthe grisea. *Plant Cell* **8**, 985-99.

Taylor RD, Saparno A, Blackwell B*, et al.*, 2008. Proteomic analyses of Fusarium graminearum grown under mycotoxin-inducing conditions. *Proteomics* **8**, 2256-65.

Tettelin H, Masignani V, Cieslewicz MJ*, et al.*, 2005. Genome analysis of multiple pathogenic isolates of Streptococcus agalactiae: Implications for the microbial "pan-

genome". *Proceedings of the National Academy of Sciences of the United States of America* **102**, 13950-5.

Tettelin H, Riley D, Cattuto C, Medini D, 2008. Comparative genomics: the bacterial pan-genome. *Current Opinion in Microbiology* **11**, 472-7.

Thatcher LF, Gardiner DM, Kazan K, Manners JM, 2012. A Highly Conserved Effector in Fusarium oxysporum Is Required for Full Virulence on Arabidopsis. *Molecular Plant-Microbe Interactions* **25**, 180-90.

Thomma BPHJ, Seidl MF, Shi-Kunne X*, et al.*, 2016. Mind the gap; seven reasons to close fragmented genome assemblies. *Fungal Genetics and Biology* **90**, 24-30.

Thomma BPHJ, Van Esse HP, Crous PW, De Wit PJGM, 2005. Cladosporium fulvum (syn. Passalora fulva), a highly specialized plant pathogen as a model for functional studies on plant pathogenic Mycosphaerellaceae. *Molecular Plant Pathology* **6**, 379-93.

Thorisson GA, Lancaster O, Free RC*, et al.*, 2009. HGVbaseG2P: a central genetic association database. *Nucleic Acids Research* **37**, D797-D802.

Thynne E, Saur IML, Simbaqueba J*, et al.*, 2017. Fungal phytopathogens encode functional homologues of plant rapid alkalinization factor (RALF) peptides. *Molecular Plant Pathology* **18**, 811-24.

Tilburn J, Sarkar S, Widdick DA*, et al.*, 1995. The Aspergillus Pacc Zinc-Finger Transcription Factor Mediates Regulation of Both Acid-Expressed and Alkaline-Expressed Genes by Ambient Ph. *Embo Journal* **14**, 779-90.

Tinoco MLP, Dias BBA, Dall'astta RC, Pamphile JA, Aragao FJL, 2010. *In vivo* trans-specific gene silencing in fungal cells by *in planta* expression of a double-stranded RNA. *BMC Biology* **8**, 27.

Trail F, Common R, 2000. Perithecial development by Gibberella zeae: a light microscopy study. *Mycologia* **92**, 130-8.

Umpierrez-Failache M, Garmendia G, Pereyra S, Rodriguez-Haralambides A, Ward TJ, Vero S, 2013. Regional differences in species composition and toxigenic potential among Fusarium head blight isolates from Uruguay indicate a risk of nivalenol contamination in new wheat production areas. *International Journal of Food Microbiology* **166**, 135-40.

Untergasser A, Cutcutache I, Koressaar T*, et al.*, 2012. Primer3-new capabilities and interfaces. *Nucleic Acids Research* **40**.

Urban M, Daniels S, Mott E, Hammond-Kosack K, 2002. Arabidopsis is susceptible to the cereal ear blight fungal pathogens Fusarium graminearum and Fusarium culmorum. *Plant Journal* **32**, 961-73.

Urban M, Hammond-Kosack KE, 2013. Molecular genetics and genomic approaches to explore Fusarium infection of wheat floral tissue. In: Proctor RH, Brown D, eds. *Fusarium genomics and molecular and cellular biology (Proctor, RH and Brown, D., eds).* 43-79.

Urban M, Irvine AG, Cuzick A, Hammond-Kosack KE, 2015a. Using the pathogen-host interactions database (PHI-base) to investigate plant pathogen genomes and genes implicated in virulence. *Frontiers in Plant Science* **6**.

Urban M, King R, Andongabo A*, et al.*, 2016. First Draft Genome Sequence of a UK Strain (UK99) of Fusarium culmorum. *Genome Announc* **4**.

Urban M, King R, Hassani-Pak K, Hammond-Kosack KE, 2015b. Whole-genome analysis of Fusarium graminearum insertional mutants identifies virulence associated genes and unmasks untagged chromosomal deletions. *Bmc Genomics* **16**.

Urban M, Mott E, Farley T, Hammond-Kosack K, 2003. The Fusarium graminearum MAP1 gene is essential for pathogenicity and development of perithecia. *Molecular Plant Pathology* **4**, 347-59.

Valent B, Giraldo MC, Khang CH, Mosquera G, Dalby M, 2013. Hemibiotrophy: The Magnaporthe oryzae-rice interaction. *Phytopathology* **103**, 186-.

Van Den Burg HA, Harrison SJ, Joosten MHaJ, Vervoort J, De Wit PJGM, 2006. Cladosporium fulvum Avr4 protects fungal cell walls against hydrolysis by plant chitinases accumulating during infection. *Molecular Plant-Microbe Interactions* **19**, 1420-30.

Van Der Lee T, Zhang H, Van Diepeningen A, Waalwijk C, 2015. Biogeography of *Fusarium graminearum* species complex and chemotypes: a review. *Food Additives and Contaminants Part a-Chemistry Analysis Control Exposure & Risk Assessment* **32**, 453-60.

Van Egmond HP, Schothorst RC, Jonker MA, 2007. Regulations relating to mycotoxins in food. *Analytical and Bioanalytical Chemistry* **389**, 147-57.

Van Esse HP, Bolton MD, Stergiopoulos I, De Wit PJGM, Thomma BPHJ, 2007. The chitin-binding Cladosporium fulvum effector protein Avr4 is a virulence factor. *Molecular Plant-Microbe Interactions* **20**, 1092-101.

Van Esse HP, Van't Klooster JW, Bolton MD*, et al.*, 2008. The Cladosporium fulvum virulence protein Avr2 inhibits host proteases required for basal defense. *Plant Cell* **20**, 1948-63.

Vandenackerveken GFJM, Vossen P, Dewit PJGM, 1993. The Avr9 Race-Specific Elicitor of Cladosporium-Fulvum Is Processed by Endogenous and Plant Proteases. *Plant Physiology* **103**, 91-6.

Varden FA, De La Concepcion JC, Maidment JHR, Banfield MJ, 2017. Taking the stage: effectors in the spotlight. *Current Opinion in Plant Biology* **38**, 25-33.

Varga E, Wiesenberger G, Hametner C*, et al.*, 2015. New tricks of an old enemy: isolates of *Fusarium graminearum* produce a type A trichothecene mycotoxin. *Environ Microbiol* **17**, 2588-600.

Vargas WA, Djonovic S, Sukno SA, Kenerley CM, 2008. Dimerization controls the activity of fungal elicitors that trigger systemic resistance in plants. *Journal of Biological Chemistry* **283**, 19804-15.

Vernikos G, Medini D, Riley DR, Tettelin H, 2015. Ten years of pan-genome analyses. *Current Opinion in Microbiology* **23**, 148-54.

Vleeshouwers VGaA, Raffaele S, Vossen JH*, et al.*, 2011. Understanding and Exploiting Late Blight Resistance in the Age of Effectors. *Annual Review of Phytopathology, Vol 49* **49**, 507-31.

Voigt CA, Schafer W, Salomon S, 2005. A secreted lipase of Fusarium graminearum is a virulence factor required for infection of cereals. *Plant Journal* **42**, 364-75.

Walhout AJM, Temple GF, Brasch MA*, et al.*, 2000. GATEWAY recombinational cloning: Application to the cloning of large numbers of open reading frames or ORFeomes. *Applications of Chimeric Genes and Hybrid Proteins, Pt C* **328**, 575-92.

Walkowiak S, Bonner CT, Wang L, Blackwell B, Rowland O, Subramaniam R, 2015. Intraspecies Interaction of Fusarium graminearum Contributes to Reduced Toxin Production and Virulence. *Molecular Plant-Microbe Interactions* **28**, 1256-67.

Walkowiak S, Rowland O, Rodrigue N, Subramaniam R, 2016. Whole genome sequencing and comparative genomics of closely related Fusarium Head Blight fungi: Fusarium graminearum, F-meridionale and F-asiaticum. *Bmc Genomics* **17**.

Walton JD, Avis TJ, Alfano JR*, et al.*, 2009. Effectors, Effectors et encore des Effectors: The XIV International Congress on Molecular-Plant Microbe Interactions, Quebec. *Molecular Plant-Microbe Interactions* **22**, 1479-83.

Wang GX, Wang L, Cui Y*, et al.*, 2017. RNA-seq analysis of Brachypodium distachyon responses to Barley stripe mosaic virus infection. *Crop Journal* **5**, 1-10.

Wang M, Jin HL, 2017. Spray-Induced Gene Silencing: a Powerful Innovative Strategy for Crop Protection. *Trends in Microbiology* **25**, 4-6.

Wang M, Weiberg A, Lin FM, Thomma BP, Huang HD, Jin H, 2016a. Bidirectional cross-kingdom RNAi and fungal uptake of external RNAs confer plant protection. *Nat Plants* **2**, 16151.

Wang Y, Wu J, Kim SG*, et al.*, 2016b. Magnaporthe oryzae-Secreted Protein MSP1 Induces Cell Death and Elicits Defense Responses in Rice. *Molecular Plant-Microbe Interactions* **29**, 299-312.

Wang Y, Yang L, Xu H, Li Q, Ma Z, Chu C, 2005. Differential proteomic analysis of proteins in wheat spikes induced by Fusarium graminearum. *Proteomics* **5**, 4496-503.

Ward TJ, Clear RM, Rooney AP*, et al.*, 2008. An adaptive evolutionary shift in Fusarium head blight pathogen populations is driving the rapid spread of more toxigenic *Fusarium graminearum* in North America. *Fungal Genetics and Biology* **45**, 473-84.

Watson RJ, Burchat S, Bosley J, 2008. A model for integration of DNA into the genome during transformation of Fusarium graminearum. *Fungal Genetics and Biology* **45**, 1348-63.

Wegulo SN, Baenziger PS, Nopsa JH, Bockus WW, Hallen-Adams H, 2015. Management of Fusarium head blight of wheat and barley. *Crop Protection* **73**, 100-7.

Weiberg A, Wang M, Lin FM*, et al.*, 2013. Fungal small RNAs suppress plant immunity by hijacking host RNA interference pathways. *Science* **342**, 118-23.

West JS, Holdgate S, Townsend JA, Edwards SG, Jennings P, Fitt BDL, 2012. Impacts of changing climate and agronomic factors on fusarium ear blight of wheat in the UK. *Fungal Ecology* **5**, 53-61.

Wiemann P, Sieber CMK, Von Bargen KW*, et al.*, 2013. Deciphering the cryptic genome: Genome-wide analyses of the rice pathogen *Fusarium fujikuroi* reveal

complex regulation of secondary metabolism and novel metabolites. *Plos Pathogens* **9**, e1003475.

Wilson LM, Idnurm A, Howlett BJ, 2002. Characterization of a gene (sp1) encoding a secreted protein from Leptosphaeria maculans, the blackleg pathogen of Brassica napus. *Molecular Plant Pathology* **3**, 487-93.

Win J, Krasileva KV, Kamoun S, Shirasu K, Staskawicz BJ, Banfield MJ, 2012. Sequence Divergent RXLR Effectors Share a Structural Fold Conserved across Plant Pathogenic Oomycete Species. *Plos Pathogens* **8**.

Wingfield BD, Steenkamp ET, Santana QC*, et al.*, 2012. First fungal genome sequence from Africa: A preliminary analysis. *South African Journal of Science* **108**, 104-12.

Wong P, Walter M, Lee W*, et al.*, 2011. FGDB: revisiting the genome annotation of the plant pathogen *Fusarium graminearum*. *Nucleic Acids Research* **39**, D637-D9.

Wu BP, Tao QF, Lyle S, 2005. Autofluorescence in the stem cell region of the hair follicle bulge. *Journal of Investigative Dermatology* **124**, 860-2.

Xiong K, Hu W, Wang M, Wei H, Cheng B, 2009. A survey on contamination of deoxynivalenol and zearalenol in maize and wheat from Anhui and Henan Province. *Food Science* **30**, 265-8.

Xu JR, Leslie JF, 1996. A genetic map of Gibberella fujikuroi mating population A (Fusarium moniliforme). *Genetics* **143**, 175-89.

Yakoby N, Kobiler I, Dinoor A, Prusky D, 2000. pH regulation of pectate lyase secretion modulates the attack of Colletotrichum gloeosporioides on avocado fruits. *Applied and Environmental Microbiology* **66**, 1026-30.

Yang YY, Zhang HJ, Li GJ, Li W, Wang XE, Song FM, 2009. Ectopic expression of MgSM1, a Cerato-platanin family protein from Magnaporthe grisea, confers broad-spectrum disease resistance in Arabidopsis. *Plant Biotechnology Journal* **7**, 763-77.

Yli-Mattila T, Gagkaeva T, Ward TJ, Aoki T, Kistler HC, O'donnell K, 2009. A novel Asian clade within the Fusarium graminearum species complex includes a newly discovered cereal head blight pathogen from the Russian Far East. *Mycologia* **101**, 841-52.

Yuan C, Li C, Yan LJ*, et al.*, 2011. A High Throughput Barley Stripe Mosaic Virus Vector for Virus Induced Gene Silencing in Monocots and Dicots. *Plos One* **6**.

Zadoks JC, 1985. Citation Classic - a Decimal Code for the Growth-Stages of Cereals. *Current Contents/Agriculture Biology & Environmental Sciences*, 14-.

Zadoks JC, 2008. The 'Continental Famine' of Europe, 1846/7; Causes and consequences. *Phytopathology* **98**, S187-S8.

Zain ME, Bahkali AH, Al-Othman MR, 2012. Effect of chemical compounds on amino acid content of some Fusarium species and its significance to fungal chemotaxonomy. *Journal of Saudi Chemical Society* **16**, 183-92.

Zhang C, Meng XH, Wei XL, Lu L, 2016a. Highly efficient CRISPR mutagenesis by microhomology-mediated end joining in Aspergillus fumigatus. *Fungal Genetics and Biology* **86**, 47-57.

Zhang F, 2015. Development and Applications of CRISPR-Cas9 for Genome Manipulations. *Faseb Journal* **29**.

Zhang F, Wen Y, Guo X, 2014. CRISPR/Cas9 for genome editing: progress, implications and challenges. *Hum Mol Genet* **23**, R40-6.

Zhang HF, Li B, Fang Q, Li Y, Zheng XB, Zhang ZG, 2016b. SNARE protein FgVam7 controls growth, asexual and sexual development, and plant infection in Fusarium graminearum. *Molecular Plant Pathology* **17**, 108-19.

Zhang XW, Jia LJ, Zhang Y*, et al.*, 2012. In Planta Stage-Specific Fungal Gene Profiling Elucidates the Molecular Strategies of Fusarium graminearum Growing inside Wheat Coleoptiles. *Plant Cell* **24**, 5159-76.

Zhang Y, Liang Y, Qiu D, Yuan J, Yang X, 2017. Comparison of cerato-platanin family protein BcSpl1 produced in Pichia pastoris and Escherichia coli. *Protein Expr Purif* **136**, 20-6.

Zhang YJ, Fan PS, Zhang X, Chen CJ, Zhou MG, 2009. Quantification of Fusarium graminearum in Harvested Grain by Real-Time Polymerase Chain Reaction to Assess Efficacies of Fungicides on Fusarium Head Blight, Deoxynivalenol Contamination, and Yield of Winter Wheat. *Phytopathology* **99**, 95-100.

Zhao CZ, Waalwijk C, De Wit PJGM, Tang DZ, Van Der Lee T, 2014. Relocation of genes generates non-conserved chromosomal segments in Fusarium graminearum that show distinct and co-regulated gene expression patterns. *Bmc Genomics* **15**.